Investigating the role of Tyrosyl-DNA Phosphodiesterase 1 in nuclear and mitochondrial DNA repair

A thesis submitted to the University of Sussex

for the degree of Doctor of Philosophy

By

Shih-Chieh Chiang

September 2016

ACKNOWLEDGEMENTS

Firstly, I would like to thank the Wellcome Trust for funding my research. I am greatly indebted to my supervisor Prof. Sherif El-Khamisy, whose exemplary enthusiasm and dedication inspired and propelled me throughout my PhD. I am most grateful for all the help and support from members of the El-Khamisy lab, as well as researchers at the Genome Damage and Stability Centre of the University of Sussex, and at the Department of Molecular Biology & Biotechnology of the University of Sheffield. I would like extend my sincerest thanks to Jean Carroll, Jessica Hudson, Owen Wells, Meryem Alagoz, Christopher Rookyard, and Abhishek Sharma, without whom publication of my work would not have been possible.

Furthermore, I would also like to thank the following people for their generous help during my PhD: Prof. Keith Caldecott (GDSC, University of Sussex) for the yeast two-hybrid plasmids; Dr Roger Phillips (Department of Biochemistry, University of Sussex) for training on confocal microscopy; Drs Sarah Walker and Conny Meisenberg for optimising the TDP1 enzymatic activity assays; Dr Majid Hafezparast (University of Sussex) for the SOD1^{G93A} transgenic mice, helpful discussions and feedback on the manuscripts; Mrs Limei Ju (GDSC) for her meticulous work on maintaining and crossing the *Tdp1* and *SOD1*^{G93A} mice strains; Drs Nick Kassouf and Rachel Haywood (RAFT, Mount Vernon Hospital) for the ESR experiments; Dr Martin Meagher and Prof. Rob Lightowlers (Wellcome Trust Centre for Mitochondrial Research, University of Newcastle) for the mitochondrial studies and feedback on the manuscripts; Dr Nicolas Viphakone and Prof. Stuart Wilson (Department of Molecular Biology & Biotechnology, University of Sheffield) for their expertise on generating the Flp-In T-Rex cell lines; Dr Heather Mortiboys (Sheffield Institute for Translational Neuroscience, University of Sheffield) for training on the Seahorse Bioanalyzer and helpful discussions; Dr Anoushka Dave (GDSC) and Dr Bin Hu (Department of Molecular Biology & Biotechnology, University of Sheffield) for training on RT-qPCR; and my lab colleague Dr Swagat Ray for his expertise on ChIP-qPCR. Last but not least, I would like to thank Conny, Owen and Swagat for proofreading this thesis.

Finally, I would like to thank my family and friends for their support and sacrifice over the past few years.

ABSTRACT

Damages to the genetic materials arise throughout the lifespan of a cell, and elicit upregulation of DNA repair factors. Tyrosyl-DNA phosphodiesterase 1 (TDP1) is part of a DNA repair protein complex that specialises in the repair of DNA base modifications and single-strand breaks (SSBs). TDP1 removes a broad spectrum of chemical adducts from the 3' end of a DNA strand break, including topoisomerase 1 (TOP1) peptide, during DNA transcription and replication. Inactivation or deletion of TDP1 is associated with cerebellar dysfunction and degeneration, with remarkably little extra-neurological manifestation. The reason for the selective dependence of the cerebellar neurons on TDP1 activity is not clear. It was hypothesised that the TDP1 activity is upregulated in tissues with high levels of SSBs, either from DNA transcriptional activity, or reactive oxygen species (ROS)-induced damage.

The aim of this doctoral project was therefore to identify and characterise the cellular mechanisms that regulate TDP1 activity. Our lab has previously shown that the N-terminus domain (NTD) of TDP1 covalently interacts with DNA ligase 3α. In this thesis, evidence has been presented to show that this interaction is regulated by the putative ATM/ATR/DNA-PK phosphorylation site, serine 81, to prolong TDP1 half-life, and enhance cellular survival after genotoxic stress. A second post-translational modification in the NTD by SUMOylation of the K111 residue was identified, enlightening a mechanism by which TDP1 is recruited to sites of transcription-mediated SSBs.

To investigate the requirement for TDP1 in cells under high levels of oxidative stress, I have developed a mouse cellular model whereby the levels of endogenous ROS can be modulated by overexpression of the human anti-oxidant enzyme superoxide dismutase 1 (SOD1) or its toxic mutant $SOD1^{G93A}$. Overexpression of $SOD1^{G93A}$ in *Tdp1*$^{-/-}$ MEFs induces accumulation of chromosomal SSBs and decreases survival after H_2O_2 challenge, while overexpression of SOD1 has a protective effect. Besides repair of ROS-induced TOP1-cc in the nucleus, TDP1 also repairs mitochondrial topoisomerase 1-mediated DNA breaks. This role is required during transcription and assembly of mitochondrial subunits of the electron transfer chain complexes, and has direct impact on mitochondrial respiration and ROS production. Collectively, these data provide mechanistic insights into regulation of TDP1-mediated chromosomal and mitochondrial DNA repair.

TABLE OF CONTENTS

LIST OF FIGURES

After page

LIST OF TABLES

After page

ABBREVIATIONS

8-oxo-G	8-hydroxyguanine
53BP1	p53-binding protein 1
A549	adenocarcinomic human alveolar epithelial 549 cells
A-T	ataxia-telangiectasia
a.a.	amino acid
ALS	amyotrophic lateral sclerosis
AP	apurine/apyrimidine
APE1	apurinic/apyrimidinic endonuclease 1
APS	ammonium persulphate
APS	ammonium persulphate
APTX	aprataxin
ATM	ataxia-telangiectasia mutated
ATP	adenosine triphosphate
ATR	ataxia-telangiectasia mutated and Rad3-related
ATRIP	ATR interacting protein
AU	artificial unit
β-gal	β-galactosidase
BER	base excision repair
bp	base pairs
BLM	Bloom’s syndrome protein
BRCA	breast cancer associated protein
BSA	bovine serum albumin
CDK	cyclin-dependent kinase
cDNA	complementary DNA
CHK1	checkpoint kinase 1
CHK2	checkpoint kinase 2
CHX	cycloheximide
Co-IP	co-immunoprecipitation
CPT	camptothecin
CPRG	chlorophenol red galactopyranoside
CSA	Cockayne syndrome protein A

CSB	Cockayne syndrome protein B
CsCl	caesium chloride
CtIP	C-terminal binding protein-interacting protein
D-loop	displacement loop
DAPI	4'-6-diamino-2-phenylindole
DDR	DNA damage response
DMEM	Dulbecco's modified Eagle's medium
DMSO	dimethylsulphoxide
DNA	deoxyribonucleic acid
DNA-PK	DNA-dependent protein kinase
DNAse	deoxyribonuclease
dNTP	deoxynucleotide triphosphate
dRP	deoxyribose phosphate
DSB	double-strand DNA break
DSBR	double-strand break repair
DRB	5,6-Dichloro-1-β-D-ribofuranosylbenzimidazole
DTT	dithiothreitol
E. coli	*Escherichia coli*
ECL	enhanced chemiluminescence
EDTA	ethylenediaminetetracetic acid
EGTA	ethylene glycol-bis(2-aminoethylether)-*N,N,N',N'*-tetraacetic acid
EmGFP	emerald green fluorescent protein
ERCC1	excision repair cross-complementing 1
EtBr	ethidium bromide
ETC	electron transfer chain
FCS	foetal calf serum
FEN1	flap endonuclease 1
FITC	fluorescein isothiocyanate
g	relative centrifugal force
G93A	glycine at position 93 converted to alanine
GAPDH	glyceraldehyde 3-phosphate dehydrogenase
Gy	Gray
γH2AX	phosphorylated histone H2A variant H2AX
H_2O_2	hydrogen peroxide
HCl	hydrochloric acid
HEK293	human embryonic kidney 293 cells
His	histidine

HR	homologous recombination
HRP	horse radish peroxidase
hrs	hours
IF	immunofluorescence
IR	ionising radiation
K111R	lysine at position 111 converted to arginine
Kb	kilobase
kDa	kilodalton
LB	Luria-Bertani bacterial medium
LCL	lymphoblastoid cell line
Leu	leucine
LiAc	lithium acetate
Lig3α	DNA ligase 3α
MCS	multiple cloning site
MEF	mouse embryonic fibroblasts
MEM	minimum essential media
MG132	carbobenzoxy-Leu-Leu-leucinal (proteasome inhibitor)
MMS	methyl methanesulfonate
MRN	Mre11-Rad50-Nbs1
mRNA	messenger RNA
mtDNA	mitochondrial DNA
mtTDP1	mitochondrial tyrosyl DNA phosphodiesterase 1
MUS81	MUS81structure-specific endonuclease subunit
N558H	asparagine at position 558 converted to histidine
NAD(P)H	nicotinamide adenine dinucleotide phosphate
NEIL	endonuclease VIII-like
NEM	N-ethylmaleimide
NER	nucleotide excision repair
NHEJ	non-homologous end-joining
NBS	Nijmegen Breakage syndrome
NLS	nuclear localisation signal
N-terminus	amino terminus
OD	optic density
OGG1	8-oxoguanine DNA glycosylase
OH	hydroxyl
OXPHOS	oxidative phosphorylation
p53	tumour protein 53

PARP	Poly (ADP-ribose) polymerase
PBS	phosphate buffered saline
PCR	polymerase chain reaction
PCNA	proliferating cell nuclear antigen
PEG	Poly(ethylene glycol)
PFA	paraformaldehyde
PG	phosphoglycolate
PIKK	phosphatidylinositol 3-kinase like kinase
PMSF	phenylmethylsulfonyl fluoride
PNK	polynucleotide kinase
Pol	polymerase
PY	phosphotyrosyl
R-loop	DNA/RNA hybrid
RAD51	DNA repair protein RAD51 homolog 1
RFC	replication factor c
RNA	ribonucleic acid
RNAi	RNA interference
ROS	reactive oxygen species
RPA	replication protein A
rpm	revolution per minute
RPMI	Roswell Park Memorial Institute media
RT	Room temperature
RT-qPCR	real-time quantitative PCR
S81A	serine at position 81 converted to alanine
S81E	serine at position 81 converted to glutamic acid
SAE1	SUMO-activating enzyme subunit 1
SAE2	SUMO-activating enzyme subunit 2
SCAN1	spinocerebellar ataxia with axonal neuropathy 1
SDS-PAGE	sodium dodecyl sulphate polyacrylamide gel electrophoresis
S.E.M	standard error of the mean
siRNA	small interfering RNA
SOC	super optimal broth with catabolic repression
Spo11	sporulation 11
SSB	single-strand DNA break
SSBR	single-strand DNA break repair
ssDNA	single-stranded DNA
T554A	threonine at position 554 converted to alanine

TBH	tert-butyl-hydroperoxide
TBS	tris-buffered saline
TDP1	tyrosyl DNA phosphodiesterase 1
TEMED	N,N,N',N'- tetramethylethylendiamine
TMRM	tetramethylrhodamine, methyl ester, perchlorate
TOP1	topoisomerase 1
TOP1-cc	topoisomerase 1-DNA cleavage complexes
TOP1mt	mitochondrial topoisomerase 1
TOP1mt-cc	mitochondrial topoisomerase 1-DNA cleavage complexes
Tris	trishydroxyaminomethane
Trp	tryptophan
Tween-20	polyoxyethylene sorbitanmonolaurate
Triton X-100	polyethylene glycol octylphenyl ether
U	unit
Ub	ubiquitin
UBC9	ubiquitin conjugating enzyme 9
UBE2I	ubiquitin conjugating enzyme E2I
UV	ultra-violet
V(D)J	Variable (V), Diversity (D) and Joining (J) genes
WCE	whole cell extract
WT	wildtype
XLF	XRCC4-like factor
XP	xeroderma pigmentosum
XRCC1	X-ray repair cross-complementing protein 1
YMM	yeast minimum media
YPD	yeast extract peptone dextrose
$ZnCl_2$	zinc chloride

CHAPTER 1

Introduction

1.1 Genome stability

Inside each living cell, the genetic material is constantly being altered everyday (Lindahl, 1993), either by programmed biological processes, or by environmental stimuli. Programmed biological processes that introduce genetic alterations include DNA transcription and replication, mitosis and meiosis. The intracellular environment can generate molecules that lead to spontaneous DNA damage, such as reactive oxygen and nitrogen species. Environmental stimuli originate from outside the organism, such as UV radiation, chemical compounds with high-energy state or high nucleic acid binding affinity, and reprogramming by viral species.

The process of permanent alteration of genetic material is a driving force of biological evolution. However, in multicellular organisms, particularly those with highly specialised organ-systems, genetic mutations must be kept under check during the reproductive lifespan of the particular organism, to ensure transfer of accurate genetic information to the next generation. Otherwise, it may result in deleterious outcomes to the somatic cells such as developmental failure (loss of programmed developmental stages), premature aging (loss of cellular functions), and tumourigenesis (loss of cellular specialisation and co-ordination), to name but a few.

The importance of maintaining genome stability is apparent in the array of DNA damage response and repair pathways conserved in all living cells. As our understanding of each pathway expands, new players and layers of regulation will emerge and challenge our assumptions. But for the purpose of this introduction, a broad classification of the DNA repair pathways according to the types of DNA lesions is described below, with an emphasis placed on higher eukaryotic model organisms. But first, a classification of the types of DNA damage is required.

1.2 Types of DNA damage

The types of DNA damage can be classified according to the site and nature of the alteration to the molecule. For example, 1) the nucleobases, 2) the glycosidic bonds between a base and the deoxyribose sugar, or 3) the sugar phosphate backbone. Lesions on the backbone can further be classified into single-stranded breaks, and double-stranded breaks (**Fig. 1.1**). In reality, one form of DNA lesion is often transformed into another over time either spontaneously, or in concert with DNA replication, transcription or repair.

1.2.1 Base modifications/loss

1.2.1.1 Oxidation

In aerobic organisms, the most abundant source of base damaging agent is from reactive oxygen species (ROS), a by-product of oxidative phosphorylation in the mitochondria. About 10^9 ROS species are generated per human cell per hour, a proportion of the more stable species can cross the nuclear pore and damage chromosomal DNA (Lieber, 2010). Other endogenous sources of ROS include lipid peroxidation and the Fenton reaction through ferrous ions (Haber and Weiss, 1934; Goldstein *et al*., 1993). Exogenous sources of ROS include UV and ionising radiation. ROS include hydrogen peroxide (H_2O_2), hydroxyl radical (•OH), hydroxide ($^-$OH), superoxide (O_2^-) and singlet O_2 ($^1O_2$). Numerous forms of oxidised bases have been documented (Evans *et al*., 2004), the most well-characterised being 8-hydroxyguanine (8-oxo-G). It has been estimated that ~ 180 8-oxo-G lesions are generated per mammalian cell per day (Lindahl, 1993). 8-oxo-G is mutagenic as it can pair with adenine or cytosine during DNA replication, and potentially introduce permanent mutation to thymine in the next round of replication (G->T transversion) (Shibutani *et al*., 1991; Maki and Sekiguchi, 1992). DNA oxidation is associated with aging, neurodegeneration, cardiovascular diseases, and cancers (Cooke *et al*., 2003).

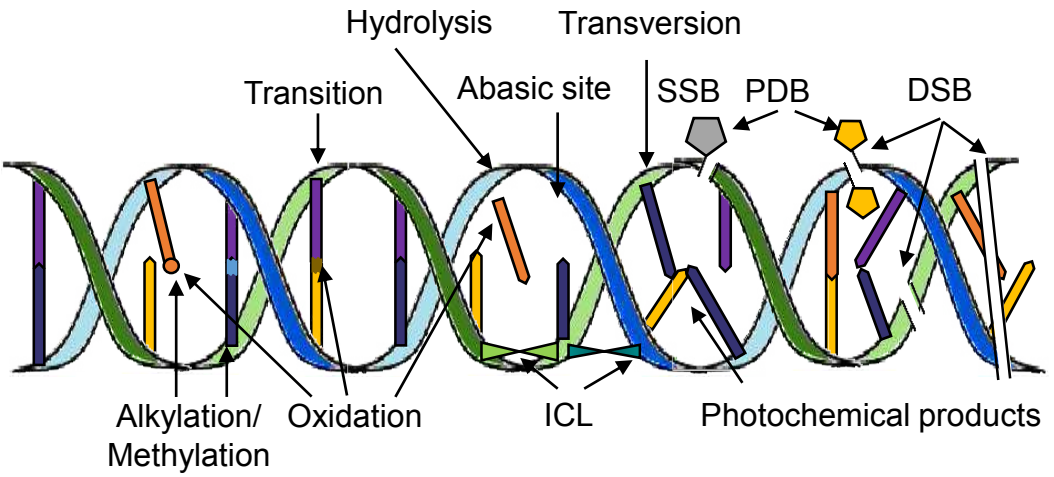

Figure 1.1 Types of common DNA damage. Modifications to the bases include alkylation, methylation, oxidation most commonly due to ROS or toxic chemicals. Non-Watson-Crick pairing of bases (transversions, transitions) can occur during translesion synthesis. Hydrolysis of a base from the phosphate backbone can occur due to physical stress (heat, low pH), oxidation, or action of a glycosidase, leading to an abasic site. Intercalating agents such as cisplatin causes intra- and inter-strand crosslinks ("ICL"). UVB and UVC radiation induce binding of adjacent bases, forming stable photochemical products. Spontaneous or enzymatic degradation of the sugar phosphate backbone generates single-strand breaks ("SSBs"). Abortive topoisomerase reactions lead to protein-DNA breaks ("PDBs"). Double-strand breaks ("DSBs") occur when two SSBs on anti-parallel strands occur in proximity to each other, or when high energy electromagnetic waves disrupt right across the DNA double helix structure. Adapted from Hoeijmakers, 2001.

1.2.1.2 Alkylation/methylation

Covalent modifications of bases by alkyl/methyl carbon groups can disrupt base pairing thereby promote mutagenesis, block DNA replication and transcription. Alkylating agents are ubiquitous, including environmental pollutants (fuel combustion wastes and tobacco smoke), biological by-products (methyl chloride from algae, bacterial nitrosation), or endogenously from oxidative damage or aberrant methylation by *S*-adensylmethione, 30 % of which originate in the mitochondria (Fu *et al*., 2012).

Two common products of DNA alkylation are 7-methylguanine (7meG) and 3-methyladenine (3meA) (Fu *et al*., 2012). The N-glycosidic bond between the deoxyribose backbone and 7meG is unstable and spontaneously transforms into potentially mutagenic abasic site (Park and Ames, 1988), while 3meA is a bulky adduct that can block replication. (Rydberg and Lindahl, 1982; Sedgwick *et al*., 2006). Both 7meG and 3meA have been associated methyl methanesulfonate (MMS)-induced transversions in mouse model lacking Alkylpurine-DNA-*N*-glycosylase (APNG) (Elder *et al*., 1998). O^6-methylguanine (O^6meG) can cause G->A transition, activate DNA recombination, and induce apoptosis (Margison *et al*., 2002).

Alkylating agents therefore have been widely used as anti-cancer drugs. 7meG, 3meA and O^6meG are the primary lesions induced by the monofunctional type of alkylating agents such as dacarbazone and temozolomide; while bifunctional alkylating agents such as nitrogen mustards, mitomycin C and cisplatin induce crosslinks between two alkylated bases from two DNA strands (inter-strand crosslinks) (Fu *et al*., 2012).

1.2.1.3 Hydrolysis

The N-glycosidic bond between a base and the sugar backbone can be enzymatically cleaved by glycosylases as part of the process to repair damaged bases, or non-enzymatically by alkylation or heat, leaving an intermediate abasic site (AP-site) (Lindahl and Nyberg, 1972; Lindahl and Karlström, 1973). The lesion can be

potentially mutagenic or block DNA replication and transcription (Loeb *et al*., 1986; Guillet and Boiteux, 2002; Yu *et al*., 2003).

Spontaneous or ROS-induced hydrolysis of the $-NH_2$ group of cytosine forms 5-hydroxycytosine, 5-hydroyxuracil and uracil glycol, the latter two can cause C->T transitions (Duncan and Miller, 1980). Activation-induced deaminase (AID)-mediated deamination of cytosine is physiologically important in B-cell antibody diversification through somatic hypermutation (SHM), but can also induce oncogenic transformation (Liu and Schatz, 2009). Deamination of thymine to thymine glycol can give rise to T->C transitions (Basu *et al*., 1989); the bulky thymine glycol also distorts the DNA structure and can stall replication (Ide *et al*., 1985; Clark and Beardsley, 1986; Clark *et al*., 1987).

1.2.1.4 Photochemical products

Characteristic of UV irradiation, UV-photoproducts are formed when two opposing pyrimidines on anti-parallel strands of the DNA absorb the electromagnetic energy from the UV ray and form a 4-ring structure with stabilised bonds between C5 and C6 (in the case of cyclobutane pyrimidine dimers, or CPD), or between adjacent C6 and C4 of the same strand (in the case of (6-4) photoproducts, or (6-4) PP) (Pfeifer, 1997). Besides distorting the DNA helical structure and inhibiting DNA replication, UV-photoproducts can spontaneously deaminate, causing transitions and transversions (Ikehata and Ono, 2011).

1.2.1.5 Spontaneous base substitution

In the eukaryotes, replicative DNA polymerases (Polα, Polδ and Polε) have high selectivity for the Watson-Crick pairing of complementary bases. However, it is estimated that one in 3.3×10^8 bases can undergo spontaneous misincorporation per cell division (Lynch *et al*., 2008). Polδ and Polε have additional exonuclease activity to excise mismatched bases, and mice lacking the Polδ and Polε exonuclease activity

have 10-fold higher mutation rates and develop cancers prematurely (Goldsby *et al*., 2002; Uchimura *et al*., 2009; Albertson *et al*., 2009).

1.2.2 Single-stranded breaks (SSBs)

SSBs occur on the phosphate backbone of one strand of the DNA, and an estimated 10,000 SSBs are formed per cell per day (Lindahl and Nyberg, 1972; Lindahl, 1993; Beckman and Ames, 1997; Ward, 1998). SSBs can arise directly from oxidised sugars that spontaneously degrade, leaving a one-base gap with damaged 3' termini; or as an intermediate product of base excision repair, which can form either a one- or multiple-base gap. Most SSBs from ROS damage have 3'-phosphate or 3'-phosphoglycolate ends, with intact 5' ends (Ward, 1998; Caldecott, 2008). A small proportion has 5' hydroxyl group (Nakamura *et al*., 2000). Additionally, transient SSBs with no gaps are generated in the phosphodiester bond linking the sugar phosphate backbone by type I topoisomerases to facilitate unwinding of the DNA duplex, as well as to remove torsional stress built-up during replication and transcription (Wang, 2002).

Although SSBs are not mutagenic *per se*, they can inhibit transcription or transform into unstable double-stranded breaks (DSBs) during replication, or deplete NAD+ by excessive PARP1 activation, leading to mitochondria-mediated apoptosis (Caldecott, 2008) (**Fig. 1.2**). Defective repair of SSBs have been linked to several neurodegenerative diseases, which will be discussed in **Section 1.3.2.5**.

1.2.3 Double-stranded breaks (DSBs)

DSBs occur when two SSBs are closely spaced on antiparallel strands so that the strands are not sufficiently held together by base-pairing and the nucleosome structure. It has been estimated that ten DSBs arise per cell per day in mammalian fibroblasts (Martin *et al*., 1985; Lieber *et al*., 2003; Lieber and Karanjawala, 2004). DNA replication across an unrepaired SSB nick or an inter-strand crosslink lesion is a major source of endogenous DSBs (Pfeiffer *et al*., 2000); while programmed DSBs arise in germline cells during meiosis (Keeney and Neale, 2006), and in early development

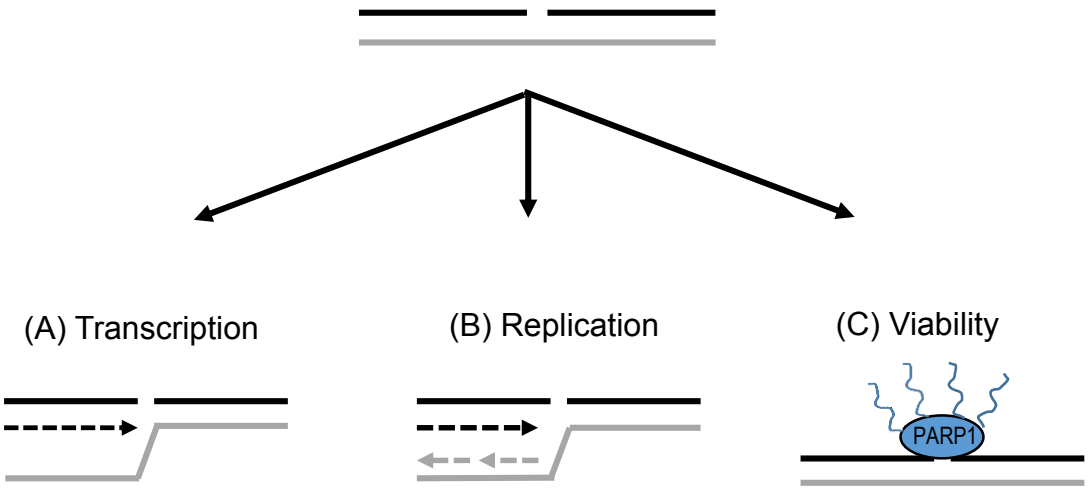

Figure 1.2 Consequences unrepaired SSBs. (A) Persistent SSBs can stall transcription elongation, triggering transcription-coupled repair (TCR). Failing that, premature termination of transcription may result, while annealing of the nascent mRNA to the DNA template exposes the single-stranded anti-sense strand (forming a R-loop) susceptible to genotoxic stressors. **(B)** In replicating cells, a persistent SSB or R-loop can impede progression of the replication fork, causing a one-sided DSB which may cause fork reversal if not repaired, or eventually collapse into frank DSB, a strong trigger for checkpoint activation. **(C)** In non-replicating cells, persistent or excessive SSBs following oxidative stress can deplete mitochondrial NAD+ by excessive activation of PARP1, leading to reduced ATP production and cell death. Adapted from Caldecott, 2008.

lymphocytes for immunoglobulin class switch recombination (CSR) and somatic hypermutation (SHM) (Dudley *et al*., 2005). DSBs can also be generated from the activity of type II topoisomerases (Adachi *et al*., 2003; Haffner *et al*., 2011). TOP2B-induced DSBs have been found to play a critical role in transcription initiation of a subset of oestrogen and androgen responsive transcription factors (Ju *et al*., 2006; Wong *et al*., 2009; Haffner *et al*., 2010).

Reactive oxygen species (ROS) is another major source of DSBs. It is estimated that ~ 10^9 ROS are generated per hour per cell (Lieber, 2010). Mitochondrial genome sustains more DNA damage than the nuclear genome due to its close proximity to the source of ROS production (Yakes and Van Houten, 1997; Salazar and Van Houten, 1997; Ballinger *et al*., 1999; Ballinger *et al*., 2000; Mandavilli *et al*., 2000; Jin *et al*., 2001; Sawyer *et al*., 2001). Exogenous source of ROS can come in the form of ionising radiation (IR), when the electromagnetic energy is transferred to the water molecules surrounding the DNA (Riley, 1994). DSBs account for only < 5 % of the lesions caused by IR (Ward, 1990; Friedberg *et al*., 2006). However, persistent DSBs are highly cytotoxic due to their potential to cause gross chromosomal aberrations, such as deletions, translocations, and mis-segregations during mitosis, or activation of apoptosis (Hoeijmakers, 2001).

1.3 The DNA Damage Response (DDR)

Given the amount of DNA damage that continually arises from exogenous and endogenous sources, a cell must be well-equipped with an array of coordinated responses to preserve genome stability and prevent passing on deleterious genetic material to future generations. In a eukaryotic cell, these responses entail activation of cell cycle checkpoints, DNA repair, and apoptosis or senescence when repair is not possible. Defective DDR factors are associated with developmental defects,

neurodegeneration, immunodeficiency, radiosensitivity, sterility, and cancer predisposition (Jackson and Bartek, 2009).

1.3.1 Cell cycle checkpoints

Eukaryotic cells undergo four phases of cell cycle: G1, whereby all cell contents, except the chromosomes, are duplicated; S, whereby the chromosomes are duplicated (forming sister chromatids); G2, whereby cytoplasmic contents are assembled and errors in duplicated DNA are checked; and M, whereby chromosomes are divided between daughter cells during mitosis. After mitosis a cell returns to G1-phase, or exits the cell cycle (G0-phase) (Sclafani and Holzen, 2007).

Progression through the cell cycle is dependent on expression of cyclin-dependent kinases (CDKs) (Norbury and Nurse, 1992). Arrest of cell cycle progression can occur at four checkpoints: G1 (which prevents initiation of DNA replication), intra-S (which prevents firing of late replication origins and activates DNA repair), G2/M (which prevents entry into mitosis) (Vermeulen *et al*., 2003), and M-phase (also known as the "spindle assembly checkpoint", which prevents progression of cytokinesis). Inhibition of activities of CDKs is achieved through highly interlinked but cell cycle-dependent signalling cascades via DNA damage sensors, signal transducers, and downstream effectors. The major factors in cell cycle checkpoint activation are described below.

1.3.1.1 Phosphaditylinositol 3-kinase-like kinases (PIKKs)

The phosphaditylinositol 3-kinase-like kinases (PIKKs) – ATM, ATR and DNA-PK, are the central signal transducers in the DDR pathways. ATM and DNA-PK are primarily recruited to sites of IR-induced DSBs, while ATR is primarily activated at sites of ssDNA associated with replication fork stalling by bulky base lesions and UV photoproducts, as well as resected DSBs during homologous recombination (HR) (Wright *et al*., 1998; Hekmat-Nejad *et al*., 2000; Lowndes and Murguia, 2000; Pandita *et al*., 2000; Abraham, 2001; Andegeko *et al*., 2001; Cortez *et al*., 2001). Recruitment of the PIKKs is mediated by interactions with DNA repair factors with affinity for

damaged DNA. Recruitment of ATM to DSBs is mediated by the MRN complex (MRE11, RAD50 and NBS1) (**Section 1.3.2.9**); and recruitment of DNK-PK is dependent on Ku70/Ku80 (**Section 1.3.2.8**); while ATR is recruited to RPA-coated ssDNA via its interacting partner ATRIP (Cortez *et al*., 2001; Unsal-Kaçmaz *et al*., 2002; Zou and Elledge, 2003; Unsal-Kaçmaz and Sancar, 2004; Ball *et al*., 2005).

Through phosphorylation of a vast number of downstream effectors, the PIKKs initiate multiple responses to DNA damage, including cell cycle arrest, chromatin remodelling, upregulation of DNA repair, and apoptosis (Shiloh, 2003). ATM, ATR and DNA-PK preferentially phosphorylate their target substrates at a serine or a threonine residue followed by a glutamine (SQ or TQ motif), and there is considerable overlap in their substrates (Anderson and Lees-Miller, 1992; Bannister *et al*., 1993; Kim *et al*., 1999; Rathbun *et al*., 1999; Kastan and Lim, 2000). CHK1 and CHK2 are two substrates of ATM and ATR with prominent roles in the checkpoint pathways

1.3.1.2 G1 checkpoint

DNA damage sustained in G1-phase cells induces phosphorylation of tumour suppressor protein, p53, by ATM, CHK2 and ATR (Abraham, 2001). p53 phosphorylation stabilises the protein (Chehab *et al*., 2000; Hirao *et al*., 2000; Shieh *et al*., 2000; Maya *et al*., 2001), and promotes transcription of p21 (el-Deiry *et al*., 1994; Dumaz and Meek, 1999), which inhibits cyclin E and cyclin A-associated CDK2 activities required for initiation of replication (Xiong *et al*., 1993; Waga *et al*., 1994; Brugarolas *et al*., 1999; Donaldson and Blow, 1999)

1.3.1.3 Intra-S checkpoint

In S-phase cells, to ensure timely repair of DSBs during DNA replication, and to prevent stalled replication forks from collapsing into DSBs, there are multiple pathways in operation. In addition to the ATM, CHK2 and ATR mediated upregulation of p53 stability and transcription activity, there are several pathways that inhibit DNA

synthesis. Firstly, ATM, ATR, CHK2 and CHK1 phosphorylate the cdc25A phosphatase (Sanchez *et al*., 1997; Falck *et al*., 2001) which in turn downregulates the activity of cyclin A/CDK2 and inhibits progression of replication (Falck *et al*., 2001). Secondly, ATM also phosphorylates SMC1 (Kim *et al*., 2002; Yazdi *et al*., 2002; Kitagawa *et al*., 2004), NBS1 (Gatei *et al*., 2000b; Lim *et al*., 2000; Wu *et al*., 2000) and BRCA1 (Cortez *et al*., 1999; Gatei *et al*., 2000a; Xu *et al*., 2001). This pathway has been shown to promote proper activation of the intra-S checkpoint, DSBR by HR (**Section 1.3.2.9**), and genome stability (Falck *et al*., 2002; Wakeman *et al*., 2004; Kitagawa and Kastan; Antoccia *et al*., 2008; Bauerschmidt *et al*., 2011). In response to replication-blocking lesions, ATR-ATRIP, together with the checkpoint clamp loader Rad17, recruits the 9-1-1 complex (Rad9-Hus1-Rad1) (Kondo *et al*., 2001; Melo *et al*., 2001; Zou *et al*., 2002; Jones *et al*., 2003), which phosphorylates and activates CHK1 (Weiss *et al*., 2002; Jones *et al*., 2003; Roos-Mattjus *et al*., 2003).

1.3.1.4 G2/M checkpoint

The G2/M checkpoint is the final point whereby unrepaired or newly-arisen DNA damage can be resolved before mitosis, therefore is especially important in preventing genomic instability. Activation of the ATM/CHK2 and ATR/CHK1 pathways results in degradation of Cdc25A and upregulation of Wee1, which together inhibit Cdc2/Cyclin B activity required for entry into mitosis (Zhao and Piwnica-Worms, 2001; Xu *et al*., 2001; Yarden *et al*., 2002; Zhao *et al*., 2002; Brown and Baltimore, 2003). The ATM/CHK2 pathway also contributes to the maintenance of the G2/M checkpoint by p53-mediated transcriptional activation of GADD45 (Papathanasiou *et al*., 1991; Artuso *et al*., 1995; Wang *et al*., 1999) and 14-3-3 (Hermeking *et al*., 1997), both of which inhibit cdc25A and Cyclin B activities (Kumagai and Dunphy, 1999; Wang *et al*., 1999; Zhan *et al*., 1999; Forrest and Gabrielli, 2001; Jin *et al*., 2002; Chen *et al*., 2003; Dalal *et al*., 2004).

1.3.2 DNA repair

Based on the type of DNA damage sustained and the cell cycle stage it is in, a cell will attempt to repair the damage using a multitude of repair pathways. For each pathway, the mechanism of lesion detection, removal and repair are described, followed by the consequences of in case of dysfunction.

1.3.2.1 Direct reversal

There is a small proportion of DNA lesions that can be directly repaired without altering the structure of the molecule, simply by cleaving off the aberrant bond(s). For example, photolyases utilise the energy from light to break the bonds between the pyrimidines in UV products CPDs and (6-4) PPs (Weber, 2005). Another example is the O6-methylguanine-DNA methyltransferase (*MGMT*)-encoded protein, O6-alkylguinine-DNA alkyltransferase (AGT), which removes the alkyl groups from O6-methylguanine and O4-methylthymine to restore the normal guanine structure (Gerson, 2004).

Methylation of the *MGMT* promoter is associated with both tumourigenesis and sensitization to anti-tumour alkylating agents such as temozolamide, while overexpression in normal tissues confers protection against the cytotoxic effects of these alkylating agents (Soejima *et al*., 2005).

1.3.2.2 Mismatch repair (MMR)

DNA mismatches can arise through modification of bases (**Section 1.2.1**) or slippage of the DNA replication machinery at regions of tandem repeats (microsatellite instability). The mutagenic nature of these lesions requires prompt removal before completion of DNA replication, this pathway is therefore highly conserved from bacteria to human (Li, 2008).

In mammals, detection and binding of structure-distorting lesions by the MutS heterodimer MutSα (MSH2/MSH6) or MutSβ (MSH2/MSH3) (Drummond *et al*., 1995; Palombo *et al*., 1995; Palombo *et al*., 1996) results in the recruitment of MutL

heterodimer MutLα (MLH1/PMS2) (Li and Modrich, 1995), MutLβ (MLH1/PMS1) (Räschle *et al*., 1999) or MutLγ (MLH1/MLH3) (Cannavo *et al*., 2005). The replication clamp PCNA and clamp loader replication factor C (RFC) physically interact with MSH2 (Clark *et al*., 2000; Flores-Rozas *et al*., 2000; Lau and Kolodner, 2003) and MLH1 to promote localisation of MutSα to the mismatch site (Umar *et al*., 1996; Gu *et al*., 1998) and activation of the endonuclease activity of MutLα (Kadyrov *et al*., 2006; Pluciennik *et al*., 2010). MutLα then makes a nick on the discontinuous daughter strand, either 5' or 3' of the mismatch site (Kadyrov *et al*., 2006). 5' to 3' excision of the daughter strand from the nick to past the mismatch site is dependent on the activity of Exo1 (Umar *et al*., 1996; Gu *et al*., 1998), while 3' to 5' excision requires both Exo1 and PCNA (Guo *et al*., 2004). The resected DNA is then coated with single-stranded DNA binding protein RPA, which displaces MutSα and MutLα and promote gap-filling by DNA polymerase δ (Polδ) (Ramilo *et al*., 2002; Zhang *et al*., 2005; Guo *et al*., 2006). The nick is then sealed by DNA ligase 1 (Lig1) (Zhang *et al*., 2005).

The MMR factors play a significant role in the DDR pathways through interactions with ATM (Brown *et al*., 2003; Adamson *et al*., 2005), ATR (Wang and Qin, 2003) CHK1 and CHK2 (Adamson *et al*., 2005), p53 (Chen and Sadowski, 2005), and p73 (Shimodaira *et al*., 2003). MMR factors also play a role in antibody diversification by class switch recombination (CSR) of immunoglobulin genes (Martin and Scharff, 2002).

In humans, defective MMR is associated with increased risk of tumourigenesis, typified by Lynch syndrome (Sijmons and Hofstra, 2016), which is characterised by hereditary non-polyposis colorectal cancer (HNPCC), amongst other cancers (OMIM #120435).

1.3.2.3 Nuclear excision Repair (NER)

The NER pathway repairs a wide range of bulky DNA distorting lesions that impede replication and transcription, such as UV photoproducts CPDs, (6-4) PPs, inter-strand crosslinks induced by cisplatin, or ROS-induced bulky base modifications such as cyclopurines (Gillet and Schärer, 2006).

There are two pathways in NER: global genome NER (GG-NER) and transcription-coupled NER (TC-NER) (**Fig. 1.3**). They differ in that TC-NER is specialised in detection of lesions within the proximity of a stalled transcription machinery, while GG-NER can detect lesions in the whole genome irrespective of the transcription status. In GG-NER, the XPC-RAD23B-Centrin2 complex (Masutani *et al*., 1994; Shivji *et al*., 1994; Nishi *et al*., 2005) scans the genome (Sugasawa *et al*., 1998; Wood, 1999) and binds the strand opposite the lesion (Min and Pavletich, 2007; Maillard *et al*., 2007; Schärer, 2007), then recruits the transcription factor II H (TFIIH) complex (Coin *et al*., 2007; Oksenych *et al*., 2009). Within the complex, the helicase activity by subunits XPB (3' – 5') and XPD (5' – 3') forms a bubble ~ 30 nucleotides around the lesion (Evans *et al*., 1997; Coin *et al*., 2007; Mathieu *et al*., 2010), which is coated and stabilised by RPA (De Laat *et al*., 1998; Hermanson-Miller and Turchi, 2002). XPA, which is also recruited to the bubble platform, displaces the TFIIH and RPA (Coin *et al*., 2008), and promotes recruitment of the endonuclease complexes XPF-ERCC1 and XPG to resect the 5' and 3' ends, respectively, of the strand containing the bulky lesion (De Laat *et al*., 1998; Fagbemi *et al*., 2011). The gap is then filled by replicative DNA polymerases δ, ε, or κ with the aid of PCNA and RFC (Ogi and Lehmann, 2006; Mocquet *et al*., 2008; Ogi *et al*., 2010). Finally, the nick is repaired by XRCC1-Lig3α (Moser *et al*., 2007; Paul-Konietzko *et al*., 2015) or FEN1-Lig1 during S-phase (Mocquet *et al*., 2008).

In TC-NER, the lesion detection step is carried out by Cockayne syndrome proteins CSA and CSB by interaction with stalled RNA polymerase II (RNAP II) (Henning *et al*., 1995; Van Gool *et al*., 1997; Lee *et al*., 2002). CSA and CSB promote recruitment of the NER machinery (Fousteri *et al*., 2006), and further repair is thought to proceed similar to the GG-NER pathway (Hanawalt and Spivak, 2008).

In humans, defective NER has been historically associated with xeroderma pigmentosum (XP) (Cleaver, 1978), Cockayne syndrome (CS) (Schmickel *et al*., 1977;

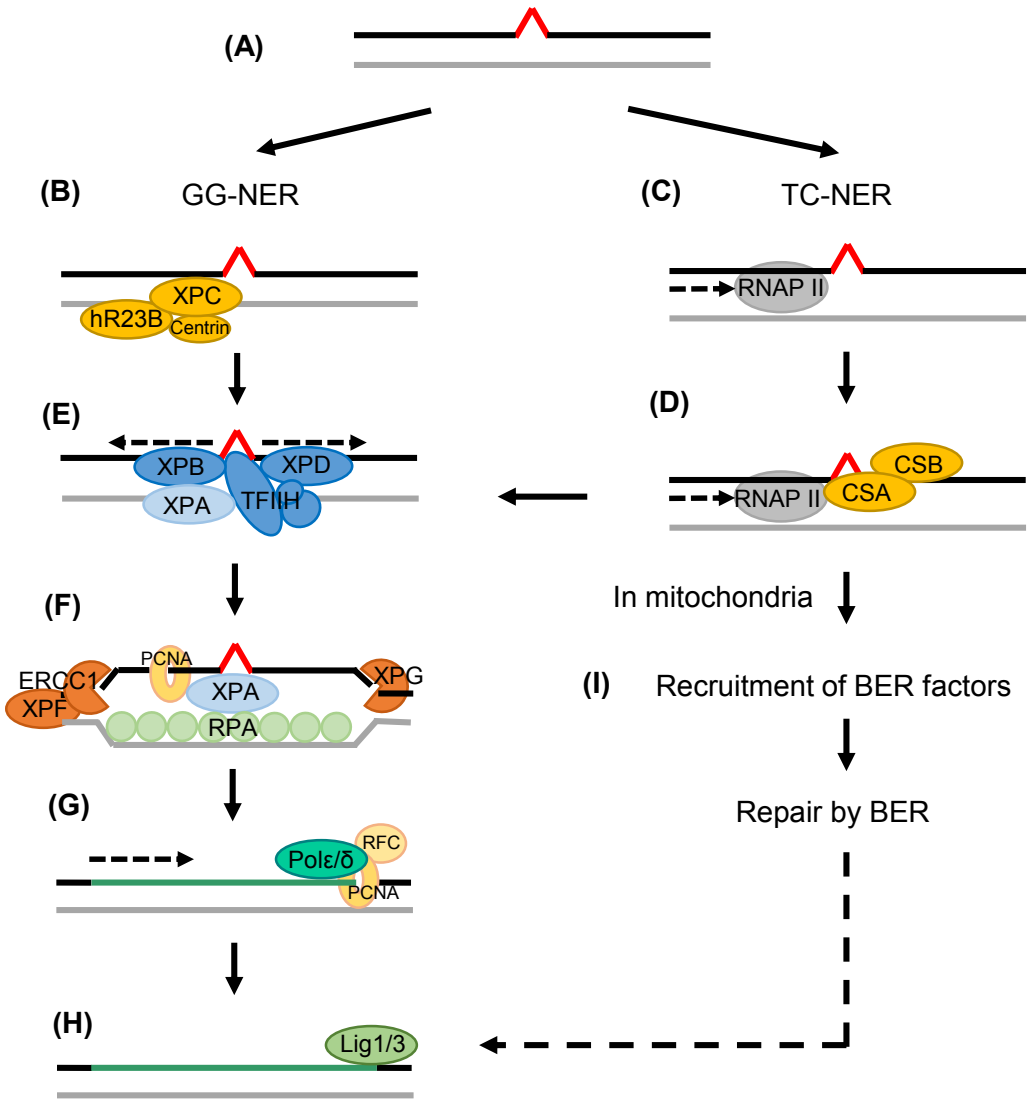

Figure 1.3 The nucleotide excision repair pathway. (A) A bulky lesion that distorts the DNA helix is **(B)** detected by the XPC-RAD23B-Centrin complex, or **(C)** stalls an elongating RNAP II transcription complex, which **(D)** recruits the CSA/CSB complex that recognises the lesion. **(E)** Both XPC and CSA/B can recruit the multiprotein transcription factor TFIIH. The XPB and XPD helicase subunits separate the strands surrounding the lesion, **(F)** forming a ~ 30-nucleotide bubble, which is stabilised by coating with RPA. XPA then displaces TFIIH and RPA, recruits exonucleases XPF/ERCC1 and XPG to excise the lesion-containing strand, and PCNA, which mediates the polymerase switch for subsequent gap repair. **(G)** Gap-filling is carried out by DNA Pol ε and δ, with the help of PCNA and RFC. **(H)** Ligase 1 or 3 seals the nick to complete the repair. **(I)** Notably, in the mitochondria, where GG-NER factors are absent, repair is carried out through the BER pathway. Adapted from Diderich *et al.,* 2011.

Andrews *et al*., 1978; Mayne and Lehmann, 1982; Venema *et al*., 1990), and trichothiodystrophy (TTD) (Stefanini *et al*., 1993a; Stefanini *et al*., 1993b; Vermeulen *et al*., 1994). Clinical symptoms of these syndromes are diverse, characterised by skin and eye manifestations of UV hypersensitivity, cancers of the skin and internal organs, neurological and skeletal abnormalities and premature aging (Lehmann, 2003). The variability in symptoms likely reflects the wide spectrum of lesions that accumulate in NER-deficient individuals.

Notably, XP patients with defective TC-NER display more severe neurological symptoms (Lehmann, 2003), which possibly reflect the role of TC-NER in repair of oxidised bases such as thymine glycols (Cooper *et al*., 1997) and 8-oxo-G, 8-oxo-A (Reardon *et al*., 1997; Le Page *et al*., 1999). Increasing evidence suggests an overlap in the TC-NER and BER pathways for repair of oxidative DNA damage, which will be discussed in **Section 1.3.2.6**.

1.3.2.4 Base excision repair (BER)

Non-bulky base modifications and AP-site lesions (**Section 1.2.1**) are generally repaired by the BER pathway (Lindahl and Wood, 1999). Given the frequent occurrence of these lesions, BER is another crucial pathway for maintaining genome stability.

The steps involved in BER are: damage recognition, base excision, end processing, gap filling, and ligation (**Fig. 1.4**).

Recognition of damaged bases depends on the glycosylases. There are 11 known glycosylases, each specific to the altered base structure that it recognises (Jacobs and Schär, 2012). For example, OGG1 recognises 8-oxo-G and Fapy-G (Boiteux and Radicella, 2000). They can be classified as monofunctional or bifunctional. Monofunctional glycosylases simply excise the base to be repaired, while bifunctional glycosylases also generate a nick in the phosphodiester bond in the backbone (Jacobs

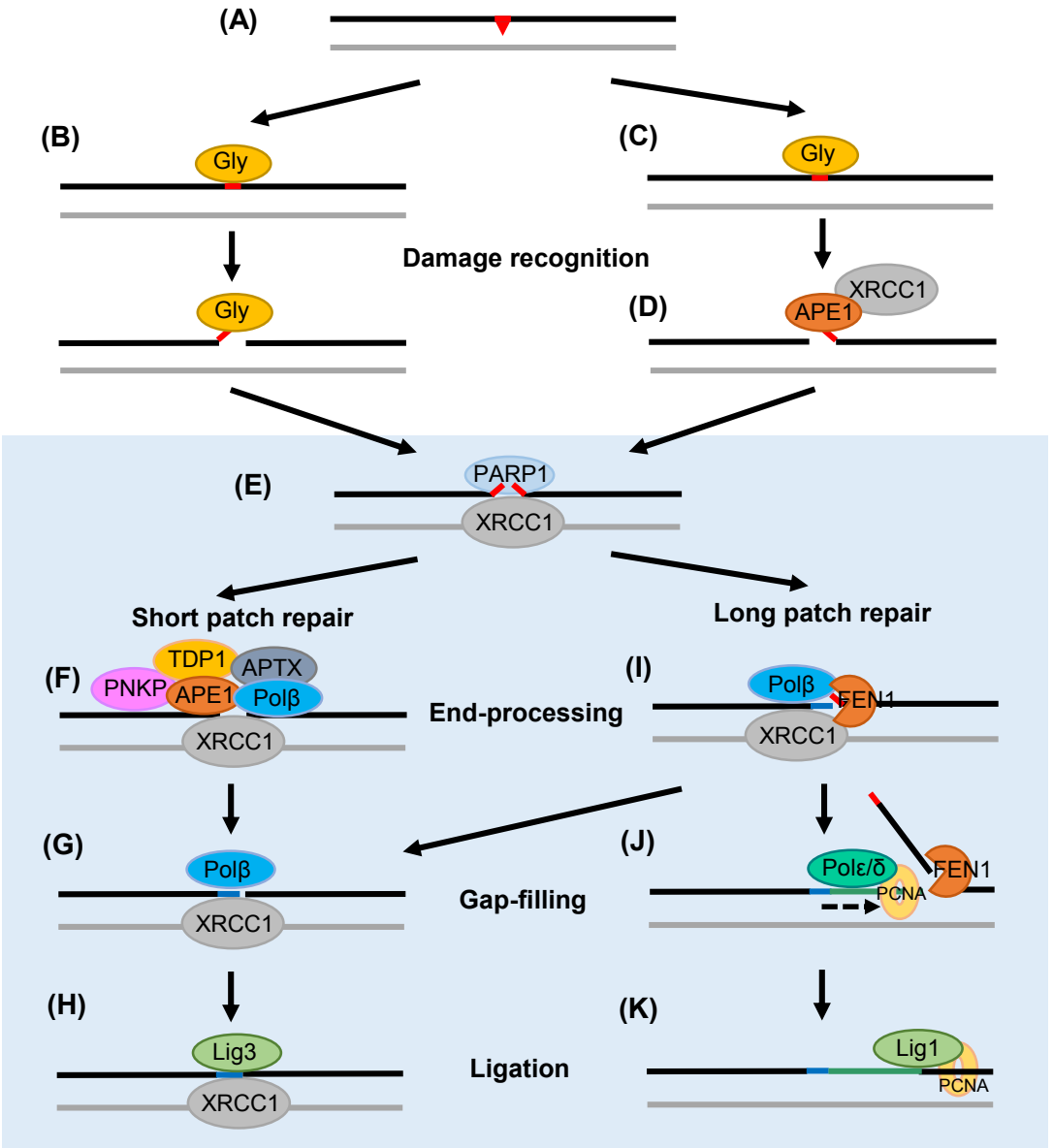

Figure 1.4 The base excision repair and SSB repair pathways. (A) A non-bulky base lesion is **(B)** excised by a bifunctional glycosylase, or **(C)** a monofunctional glycosylase, followed by **(D)** cleavage of the phosphodiester backbone by APE1. APE1 associates with the scaffold protein XRCC1, **(E)** which recruits PARP1 to stabilise the break ends and activate downstream repair factors. **(F)** The end-processing factors restore the chemistry around the nick. **(G)** In SP-BER, Pol β fills in the missing nucleotide and **(H)** Lig3 seals the nick. **(I)** If the 5'-dRP end is oxidised, repair is carried out by LP-BER. Outside S-phase, repair is achieved through coordinated gap filling and strand displacement up to 2 nt by Polβ and FEN1, followed by steps (G) to (H). **(J)** During S-phase, switching to replicative polymerase allows insertion 2 – 10 nucleotides past the break end, generating a short flap, which is excised by FEN1. **(K)** Lig1 seals the nick to complete the repair. Part highlighted in blue indicates overlap with the single-strand break repair pathway. Adapted from Caldecott, 2008.

and Schär, 2012). Upon binding with the damaged base, the glycosylase cleaves the C1-N-glycosidic bond, leaving an AP-site (Brooks *et al*., 2013). AP-sites arising from spontaneous deamination of bases are further processed in an identical manner.

To initiate repair of the AP-site, the phosphodiester bond is hydrolysed either by a bifunctional glycosylase (Sun *et al*., 1995; Nash *et al*., 1997; Takao *et al*., 2002), or by apurine/apyrimidine endonuclease 1 (APE1) (Demple *et al*., 1991; Robson and Hickson, 1991). APE1 is recruited to the AP-site by a monofunctional glycosylase, along with x-ray cross complementing protein 1 (XRCC1), a scaffold protein required for assembly of the repair machinery (Parikh *et al*., 1998; Waters *et al*., 1999; Hardeland *et al*., 2000; Hill *et al*., 2001; Pope *et al*., 2002; Marsin *et al*., 2003; Campalans *et al*., 2005). APE1 cleaves the phosphodiester bond 5' to the AP-site to generate a 5'-deoxyribosephosphate (5-dRP) end and 3'-hydroxyl (3'-OH) end (Demple and Harrison, 1994; Barzilay and Hickson, 1995; Parikh *et al*., 1998; Waters *et al*., 1999; Hill *et al*., 2001). This lesion is then rapidly detected by Poly(ADP-ribose) polymerase 1 (PARP1), which forms poly(ADP-ribose) chains on itself (to amplify the signal) (Ogata *et al*., 1981; Huletsky *et al*., 1989; D'Amours *et al*., 1999), as well as surrounding histones (to promote chromatin relaxation) (Beneke, 2012) and BER scaffold protein XRCC1 (Masson *et al*., 1998; Pleschke *et al*., 2000; El-Khamisy *et al*., 2003). XRCC1 provides a platform for the assembly of downstream BER factors such as PNKP, DNA polymerase β (Polβ) and DNA ligase 3α (Lig3α) required for further processing of the base lesion (Caldecott, 2001).

To insert a new nucleotide into the gap, the 5' and 3' ends of the phosphodiester bond must be restored to a 5'-phosphate and 3'-hydroxyl moiety, which are often altered by the actions of glycosylases and APE1. Bifunctional glycosylases with β-lyase activity generate 3'-α,β unsaturated aldehyde ends (Mazumder *et al*., 1991) that are repaired by APE1 (Izumi *et al*., 2000). Bifunctional glycosylases with β,σ-lyase activity such as NEIL1, NEIL2 and NEIL3 generate 3'-phosphate ends that are repaired by

polynucleotide kinase-phosphatase (PNKP) or APE1 (Habraken and Verly, 1988; Jilani *et al*., 1999; Wiederhold *et al*., 2004). The 5'-dRP ends generated by APE1 is removed by Polβ (Allinson *et al*., 2001; Podlutsky *et al*., 2001).

Further repair of the nick on the DNA backbone proceeds as in the case of single-strand break repair (SSBR), with modifications in the steps of damage recognition and DNA end-processing.

1.3.2.5 Single-strand break repair (SSBR)

The recognition step of SSBs starts with binding and PARylation by PARP1, which protects the site from further damage (Parsons *et al*., 2005), and recruits downstream repair machinery (Caldecott *et al*., 1996; Pleschke *et al*., 2000; El-Khamisy *et al*., 2003; Okano *et al*., 2003; Das *et al*., 2014). The steady-state of PARylation/dePARylation is regulated by poly(ADP-ribose) glycohydrolase (PARG) and terminal ADP-ribose protein glycohydrolase (TARG1), which catabolise the PAR chains to allow access of the repair factors (Zahradka and Ebisuzaki, 1982; Oka *et al*., 1984; Lin *et al*., 1997; Davidovic *et al*., 2001; Fisher *et al*., 2007; Gao *et al*., 2007; Chen *et al*., 2011; Slade *et al*., 2011; Zaja *et al*., 2012).

The end-processing factors in BER can also repair similar ends generated by other means (**Fig. 1.4**). For example, 3'-phosphate termini arising from spontaneous disintegration of oxidised bases or processing of TOP1-cc are repaired by PNKP (Jilani *et al*., 1999; Karimi-Busheri *et al*., 1998; Inamdar *et al*., 2002). 3'-phosphoglycolate termini from ROS damage are efficiently repaired by APE1 (Suh *et al*., 1997; Parsons *et al*., 2004). However, there are several additional SSBR end-processing factors to fine-tune the repair. For example, tyrosyl-DNA-phosphodiesterase 1 (TDP1) can accurately remove 3' moieties such as phosphoglycolate (Zhou *et al*., 2005), dRP (Lebedeva *et al*., 2011), or a tyrosyl group (from the active site of TOP1) (Davies *et al*., 2003; Interthal *et al*., 2005a), leaving an ungapped nick with 5'-OH and 3'-phosphate terminus for further processing by PNKP (Inamdar *et al*., 2002). Similarly, 5'-AMP

termini (resulting from abortive DNA ligase activity near 5'-phosphate ends) can be accurately removed by aprataxin (APTX), leaving a 5'-phosphate terminus (Ahel *et al*., 2006). Several DNA polymerases besides Polβ have also been shown to process dRP termini from oxidative damage, such as Polλ and Polι (García-Díaz *et al*., 2001; Bebenek *et al*., 2001; Braithwaite *et al*., 2005a; Braithwaite *et al*., 2005b). When a 5'-dRP or 5' sugar phosphate is oxidised, it becomes resistant to the lyase activity of Polβ. These lesions need to be repaired by the long-patch BER (LP-BER) pathway.

The next step is to fill in the missing nucleotide(s) by DNA polymerases. Depending on the efficiency of the end-processing step, and the cell cycle status, short-patch BER (SP-BER) or long-patch BER (LP-BER) (during S-phase, or if either of the nicked termini cannot be correctly restored) may be chosen. In SP-BER, Polβ inserts one nucleotide in the gap (if necessary) and Lig3α seals the nick to complete the repair (Caldecott, 2008).

LP-BER, in its most efficient form, entails one nucleotide gap filling by Polβ, followed by excision of one nucleotide flap at the 5' end containing the oxidised lesion by Flap endonuclease 1 (FEN1) (Liu *et al*., 2005). Lig3α seals the nick and completes the repair. Alternatively, during DNA replication, polymerase switching can occur when a replisome approaches, resulting in Polε and Polδ mediated extension past the break point and generation of 5' flap of a 3 – 10 nucleotides. The 5' flap is excised by the concerted action of flap endonuclease 1 (FEN1), PCNA and PARP1 (Prasad *et al*., 2000). Lig1 reseals the nick between the newly synthesised strand and the 5' end to complete the repair (Mortusewicz *et al*., 2006).

As the "housekeeping" DNA repair pathway, deficiency of the BER pathway is associated with tumourigenesis, neurodegeneration and aging, and in some cases, is incompatible with life (Wilson and Bohr, 2007; Caldecott, 2008; Maynard *et al*., 2009). Both reduction and overexpression of some BER factors have been associated with cancers (Mohan and Madhusudan, 2013). As BER plays a role in preventing

mutagenesis, as well as promoting tumour resistance to radio- and chemotherapeutic agents, it is unclear whether the aberrant expression patterns reflect the cause or the consequence of tumourigenesis. Regulation of BER factors is therefore an important area of cancer research.

Intriguingly, defects in three of the SSBR-specific end-processing factors, APTX, TDP1 and PNKP, all show exclusively neurological phenotypes with little signs of systemic involvement. Mutations in APTX are associated with ataxia-oculomotor apraxia 1 (AOA1) (OMIM #208920) (Date *et al*., 2001; Moreira *et al*., 2001); a single catalytic mutation in TDP1 is linked to spinocerebellar axonal neuropathy 1 (SCAN1) (OMIM #607250) (Takashima *et al*., 2002; El-Khamisy *et al*., 2005; Interthal *et al*., 2005b); and mutations in PNKP are found in patient with MCSZ syndrome (microcephaly, early-onset, intractable seizures and developmental delay) (OMIM #613402) (Shen *et al*., 2010; Reynolds *et al*., 2012), cerebellar degeneration and polyneuropathy (Poulton *et al*., 2013) and AOA4 (OMIM #616267) (Bras *et al*., 2015).

1.3.2.6 Transcription-coupled base excision repair (TC-BER)

Although the role of TC-NER in repair of bulky lesions in actively transcribed gene is well-characterised (**Section 1.3.2.3**), there is increasing evidence supporting the notion of a transcription-associated sub-pathway of BER (TC-BER). It has been shown that TC-NER factors confer protection against oxidative DNA damage. CSB promotes BER by stimulating the activities of PARP1 (Flohr *et al*., 2003; Thorslund *et al*., 2005) and APE1 (Wong *et al*., 2007); XPC stimulates activity of OGG1 and APE1 (Errico *et al*., 2006; Kassam and Rainbow, 2007; Melis *et al*., 2011; de Melo *et al*., 2016); and XPG promotes binding of NTH1 to thymine glycols for repair by BER (Klungland *et al*., 1999). It is not clear though, if non-bulky lesions such as 8-oxo-G can stall RNA Pol II *per se* (Tornaletti, 2005; Charlet-Berguerand *et al*., 2006; Guo *et al*., 2013). It has been suggested that the sequence complexity and the chromatin structure surrounding the lesion may affect whether TC-NER or BER is utilised for repair (Yu *et al*., 2000;

Allgayer *et al*., 2013). Interestingly, in the mitochondria, CSA and CSB promote repair of 8-oxo-G lesions via the BER, as core components of the NER pathway are not identified in the mitochondria (Dianov *et al*., 1999; Stevnsner *et al*., 2002). Therefore, the neurological and premature aging phenotype of CS patients could be attributed to excessive damage to the mitochondrial genome (Stevnsner *et al*., 2008).

Protein-linked SSBs, such as TOP1-cc, are also known to block the transcription machinery (Bendixen *et al*., 1990; Ljungman and Hanawalt, 1996; Wu and Liu, 1997). Repair by TDP1 is specific to actively transcribed region of the genome, as in TDP1-deficient cells, inhibition of RNAP II elongation by α-amanitin abrogated accumulation of TOP1-cc, while inhibition of replication by aphidicolin showed no such response (El-Khamisy *et al*., 2005; Miao *et al*., 2006). Another BER factor, NEIL2, has also been shown to preferentially interact with active RNAP II and the transcriptional regulator heterogeneous nuclear ribonucleoprotein-U (hnRNP-U) (Banerjee *et al*., 2011).

1.3.2.7 Double-strand break repair (DSBR)

DSBs, although less frequent than base modifications or SSBs, pose serious threat to genome stability, as they can lead to chromosomal rearrangements, deletions, duplications, and activation of cell death mechanisms (Jackson, 2002). DSBs are inevitably generated during DNA replication and cell division. It is therefore not surprising that many factors in DSBR are also involved in cell cycle checkpoints, as mentioned in **Section 1.3.1**.

There two main DSBR pathways – homologous recombination (HR) and non-homologous end-joining (NHEJ). The two pathways are mechanistically distinct and result in different repair outcomes. The pathway choice is dependent on factors such as the cell cycle status, the complexity of the DNA damage, and the chromatin structure surrounding the damage (Symington and Gautier, 2011). 53BP1 (Tumour suppressor p53-binding protein 1) is considered an important mediator in the DDR following DSB, as well as on the repair pathway choice. Following its recruitment to a

DSB site by ubiquitinated H2A and H2AX (Doil *et al*., 2009; Stewart *et al*., 2009), 53BP1 promotes relaxation of heterochromatin to allow the repair machinery to access the break (Noon *et al*., 2010; Goodarzi *et al*., 2011). Furthermore, phosphorylation of 53BP1 by ATM recruits RIF1 (Replication Timing Regulatory Factor 1) to the damage site, which have been shown to inhibit BRCA1-mediated end resection during G1-phase (Bunting *et al*., 2010; Bothmer *et al*., 2011; Chapman *et al*., 2013; Di Virgilio *et al*., 2013; Escribano-Diaz *et al*., 2013; Feng *et al*., 2013; Zimmermann *et al*., 2013). During S/G2 phase, where the chromatin is likely already relaxed, 53BP1 plays a less crucial role in DSBR. BRCA1 displaces 53BP1 from the DSB site (Chapman *et al*., 2012; Kakarougkas *et al*., 2013) and recruits the E3 Ubiquitin ligase UHRF1 (Ubiquitin-like, with PHD and RING finger domains 1) to polyubiquitinates RIF1, promoting its dissociation from 53BP1 (Zhang *et al*., 2016).

1.3.2.8 Non-homologous end-joining (NHEJ)

NHEJ is the DSBR pathway utilised throughout the cell cycle, but predominantly in G1- and G2-phases of the cell cycle, where homologous sister chromatids are not available (Beucher *et al*., 2009).

NHEJ involves tethering of the two ends of the DSB, various degree of end-processing, and ligation of the ends to complete the repair, with or without loss of some nucleotide sequences at the ends (**Fig. 1.5**). It has been estimated that ~ 80 % of DSBs induced by IR are efficiently repaired by NHEJ within 30 minutes (Beucher *et al*., 2009).

In its simplest form, canonical/classical NHEJ (c-NHEJ) is initiated by binding and stabilisation of the DSB ends to the heterodimer Ku70/Ku80, which aligns the ends of the break (Yoo and Dynan, 1999; Walker *et al*., 2001) and recruits and activates the DDR kinase DNA-PK (Gottlieb and Jackson, 1993; Suwa *et al*., 1994; Jin *et al*., 1997; Uematsu *et al*., 2007). DNA-PK binds to the two ends and forms a bridging “synaptic complex” to stabilise the break (DeFazio *et al*., 2002) and prevents initiation of resection by HR factors such as Exo1 (Mimitou and Symington, 2010). DNA-PK also

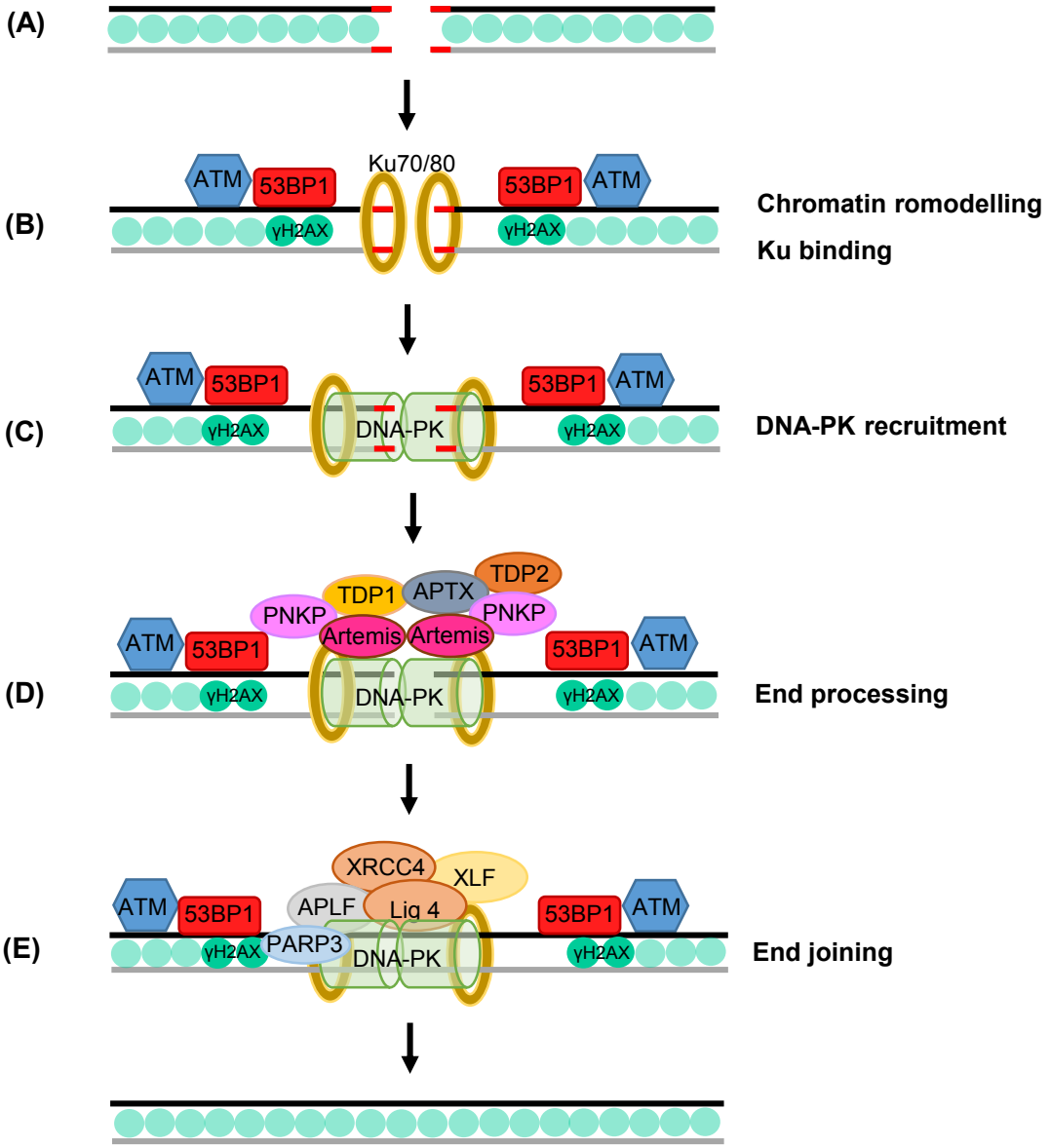

Figure 1.5 The non-homologous end-joining pathway. (A) A double strand break arising outside S-phase elicits **(B)** ATM-mediated phosphorylation of 53BP1 and H2A histones, promoting chromatin relaxation and binding of Ku70/80 to the DSB ends. **(C)** Ku70/80 recruits and activates DNA-PK, which in turn recruits **(D)** end-processing factors Artemis, PNKP, APTX, TDP2 and TDP1 to clean up the ends. **(E)** PARylation of the scaffold protein APLF by PARP3 promotes recruitment of the Lig4/XRCC4/XLF complex to join the break ends. Adapted from Hartlerode & Scully, 2009; Heo *et al.*, 2015; Xu *et al.*, 2012.

promotes assembly of downstream NHEJ repair factors including end-processing enzymes, XRCC4-Ligase 4 (Lig4), and XRCC4-like factor (XLF) (Critchlow *et al*., 1997; Ahnesorg *et al*., 2006; Costantini *et al*., 2007). PARP3 and APLF also promote the retention and activity of XRCC4-Lig4-XLF (Rulten *et al*., 2011; Grundy *et al*., 2013).

In c-NHEJ, where minimal end-processing is required, XRCC4-Lig4 stabilises the break ends (Grawunder *et al*., 1997; Grawunder *et al*., 1998), and Lig4 seals the ends (Schar *et al*., 1997; Teo and Jackson, 1997; Wilson *et al*., 1997; Tomkinson *et al*., 2006). XLF is important in completion of the Lig4 catalytic cycle and recycling Lig4 for further use (Riballo *et al*., 2009).

With more complex DNA ends, like in SSBR, end-processing requires several structural-specific nucleases. Artemis is a well-characterised endonuclease with hairpin processing, 5' exonuclease, and 3'-PG processing activity (Ma *et al*., 2002; Ma *et al*., 2005; Povirk *et al*., 2007; Li *et al*., 2014). Together with ATM, it is required for V(D)J recombination of immunoglobulin genes (Ma *et al*., 2002; Riballo *et al*., 2004). PNKP, the 5' and 3' phosphatase required in BER/SSBR, has also been shown to play a similar role in NHEJ (Ward, 1998; Chappell *et al*., 2002; Bernstein *et al*., 2005; Koch *et al*., 2004; Karimi-Busheri *et al*., 2007; Mani *et al*., 2010; Segal-Raz *et al*., 2011). Similarly, APTX (**Section 1.3.2.5**) has also been implicated in NHEJ (Rass *et al*., 2007). The more recently characterised TOP2-DSB repair factor, TDP2, also functions in the NHEJ pathway (Gómez-Herreros *et al*., 2013). TDP2 cleaves the 5'-phosphotyrosyl bond in TOP2-cc, leaving re-ligatable 5'-OH ends (Cortes Ledesma *et al*., 2009).

There is also an alternative end-joining (A-EJ) pathway that is slower and more error-prone (Kabotyanski *et al*., 1998; DiBiase *et al*., 2000; Wang *et al*., 2003; Iliakis *et al*., 2004; Terzoudi *et al*., 2008). It has been observed in c-NHEJ and HR-deficient cells (Audebert *et al*., 2004; Audebert *et al*., 2006; Geuting *et al*., 2013). The trigger and mechanism of this pathway is less well-understood. It is postulated that PARP1 is the

DSB sensing factor in the absence of Ku70/80 (Wang *et al*., 2006), and the ligation step is carried out by XRCC1-Lig3α or Lig1 (Audebert *et al*., 2004; Wang *et al*., 2005; Liang *et al*., 2008; Simsek *et al*., 2011; Della-Maria *et al*., 2011; Paul *et al*., 2013). Components of the HR pathway such as the MRE11 and CtIP have also been shown to promote A-EJ (Ma *et al*., 2003; Lee and Sang, 2007; Bennardo *et al*., 2008; Deriano *et al*., 2009; Rass *et al*., 2009; Xie *et al*., 2009; Yun and Hiom, 2009; Zhuang *et al*., 2009; Lee-Theilen *et al*., 2010; Zhang and Jasin, 2011), which could explain the characteristic generation of microhomologies (short stretch of homologous sequences) at the junction of repair indicative of end-resection.

Defects in NHEJ core components such as Ku70/80, DNA-PK, Lig4, Artemis and XLF result in with gross genomic instability, immunodeficiency, tumourigenesis, radiosensitivity, and neurodevelopmental defects (O'Driscoll and Jeggo, 2006).

1.3.2.9 Homologous recombination (HR)

The HR pathway depends on using a sister chromatid with homologous sequence as the template for repairing both strands of the damaged DNA, therefore it should only be activated in cycling cells, in the late S- and G2 phases of the cell cycle, for repair of lesions that have already undergone replication. HR has a slower repair kinetic, but is virtually error-free (Kasparek and Humphrey, 2011). **Fig. 1.6** illustrates how SSBs arising during early S-phase can be converted to one-ended DSBs, or two-ended DSBs in late S-phase, and require repair by HR (Caldecott, 2008).

In the HR pathway, the MRN complex (MRE11, RAD50 and NBS1) is the early sensor of DSBs (D'Amours and Jackson, 2002; Tauchi *et al*., 2002). Upon binding it stabilises the DSB ends, MRE11 initiates 5' – 3' resection and displaces Ku from the ends, inhibiting repair by NHEJ (Petrini *et al*., 2001; D'Amours and Jackson, 2002). NBS1 activates ATM through autophosphorylation and monomerisation (Uziel *et al*., 2003; Lee and Paull, 2004; Lee and Paull, 2005). ATM phosphorylates a multitude of substrates involved in the DDR (**Section 1.3.1.1**), including the histone variant H2AX

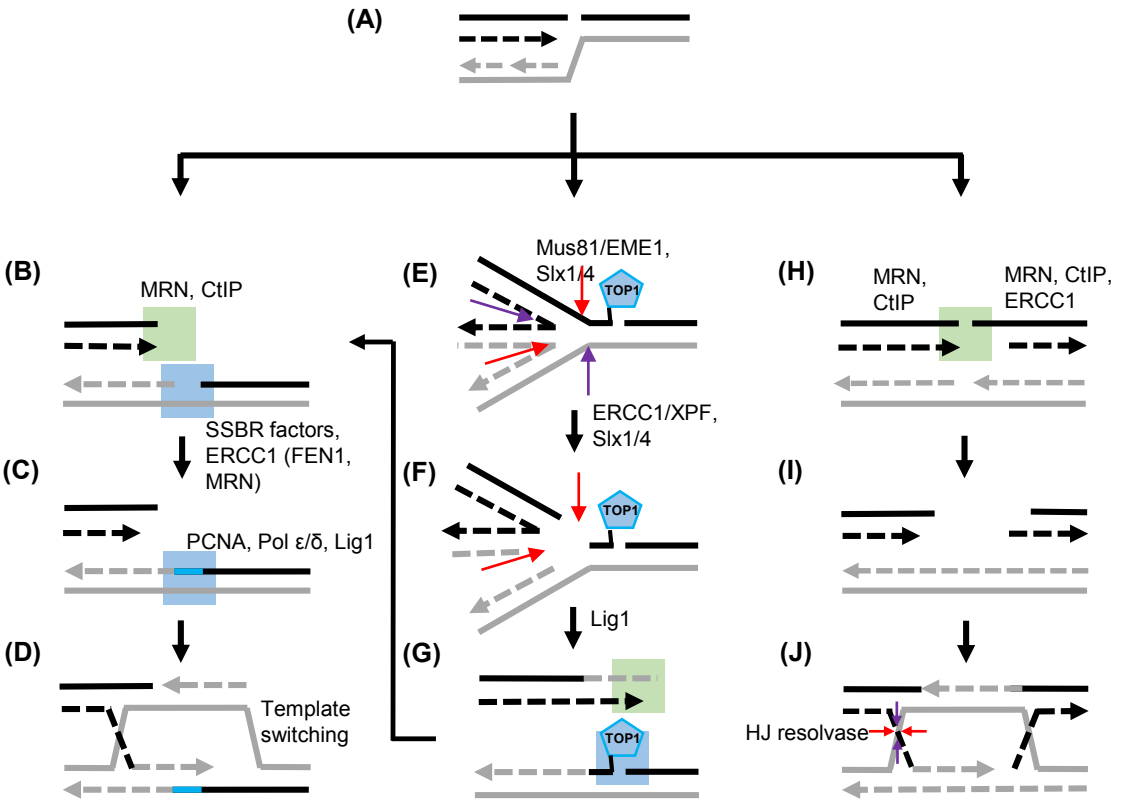

Figure 1.6 Replication-coupled repair of SSBs. (A) Collision of the replication machinery with a SSB results in **(B)** a one-ended DSB formed by the sister chromatid (green box) and a residual SSB (blue box). **(C)** Repair of the DSB is initiated by 3' to 5' excision by CtIP in conjunction with MRN, while the SSB ends are processed by SSBR factors, or structure-specific nucleases such as ERCC1-XPF at 3'-termini, FEN1 at 5'-flapped termini, or the MRN complex at 5'- and possibly 3'-termini. Gap filling is then carried out by the replicative polymerases Pol ε and/or Pol δ and associated factors, and the nick ligated by Lig1. **(D)** Homologous recombination (HR) by RAD51-mediated template switching completes repair of the excised DSB ends. **(E)** In the case of CPT-induced SSB, increased torsional stress promotes reversal of the replication fork by annealing of the daughter strands, essentially formation a double Holliday junction (HJ). **(F)** action of HJ resolvase Mus81/Eme1 (red arrows) and ERCC1/XPF (purple arrows) and subsequent repair by Lig1 results in **(G)** a one-ended DSB (green box) and a TOP1-associated SSB (blue box). Further repair follows steps (B) – (D). **(H)** If the SSB or one-sided DSB is not repaired in a timely manner, a converging replication fork or new origin firing past the SSB result in a two-sided DSB (green box). **(I)** End resection by CtIP and MRN allows further repair by HR. Adapted from Caldecott, 2008; Kim *et al.,* 2013.

on ser139 (γH2AX) (Rogakou *et al*., 1998; Burma *et al*., 2001) and BRCA1 (Cortez *et al*., 1999; Kim *et al*., 1999; Gatei *et al*., 2000a), which initiates the chromatin relaxation process (Hu *et al*., 1999; Bochar *et al*., 2000; Ye *et al*., 2001), and 53BP1, which is crucial in maintaining the ATM signalling through the G2/M checkpoint (You *et al*., 2005; Noon *et al*., 2010; Shibata *et al*., 2010).

The ends are then more extensively resected by nucleases Exo1, DNA2 and BLM (Gravel *et al*., 2008; Liao *et al*., 2008; Nimonkar *et al*., 2008; Zhu *et al*., 2008; Mimitou and Symington, 2009; Cejka *et al*., 2010a; Nimonkar *et al*., 2011; Sturzenegger *et al*., 2014), generating ssDNAs with 3' overhangs, which are rapidly coated by RPA which prevents formation of secondary structures (Sung and Klein, 2006). With the help of BRCA2/PALB2, RAD51 nucleofilament then displaces RPA to promote homology search by strand invasion of the sister chromatid (Sharan *et al*., 1997; Wong *et al*., 1997; Pellegrini *et al*., 2002; San Filippo *et al*., 2006; Sung and Klein, 2006; Carreira *et al*., 2009; Sy *et al*., 2009; Dray *et al*., 2010; Holthausen *et al*., 2010; Jensen *et al*., 2010; Liu *et al*., 2010; Thorslund *et al*., 2010). This results in the formation of the D-loop, within which RAD51 is gradually dissociated by RAD54, allowing access of DNA polymerases for DNA synthesis on the invading strand (Petukhova *et al*., 1998; Petukhova *et al*., 1999; Solinger *et al*., 2002; Li and Heyer, 2009; Wright and Heyer, 2014).

The invading strand then can either be displaced back and anneal with its antiparallel (non-sister chromatid) strand, and the nick sealed by Lig1 (Goetz *et al*., 2005), resulting in non-crossover; or it can be stabilized in the D-loop by ligating to the 3' end of the DSB on the same strand, allowing repair synthesis on the antiparallel strand, forming a double Holliday junction structure (Pâques *et al*., 1999). The structure can then be processed by resolvases such as GEN1, Mus81 and SLX1 into crossover and non-crossover products (Chen *et al*., 2001; Constantinou *et al*., 2002; Andersen *et al*., 2009; Fekairi *et al*., 2009; Munoz *et al*., 2009; Svendsen *et al*., 2009; Wechsler *et al*.,

2011), or converted to a hemi-catenone by BLM then resolved by topoisomerase 3 (TOP3) into non-crossover products (Ira *et al*., 2003; Wu and Hickson, 2003; Cejka *et al*., 2010b; Hickson and Mankouri, 2011). Mutations in key HR components such as BRCA1, BRCA2, RAD51, RAD54, PALB2 and p53 are associated with tumourigenesis. In addition, mutations in BLM helicase that suppresses illegitimate crossovers are associated with developmental delay (OMIM #210900). Defective meiosis-specific recombination (e.g. DMC1) is associated with male infertility (Bannister *et al*., 2007).

1.3.2.10 The Fanconi anaemia (FA) pathway

So-called due to the clinical presentation of patients with genetic mutations in factors involved in this pathway, the FA pathway is important for repair of ICLs during S-phase. It does this by co-ordinating factors of NER, HR and translesion synthesis (TLS) polymerases, although the molecular mechanisms of many of the FA factors are currently unknown.

The FA factors can be divided into: 1) the FA core complex (consisting of FANCA, FANCB, FANCC, FANCE, FANCG, FANCF, FANCL and FANCM); 2) the ID2 complex (FANCD2, FANCI); and the downstream repair proteins (BRCA2/FANCD1, Rad51, PALB2/FANCN, BACH1) (Moldovan and D'Andrea, 2009).

Upon replication fork stalling by an ICL, DDR is triggered when ATR phosphorylates and recruits HR factors including Rad51 and BRCA1 (Taniguchi *et al*., 2002; Pichierri and Rosselli, 2004; Zhu and Dutta, 2006). ATR also recruits the core FA complex to the damage site through FANCM and FAAP24 (Collis *et al*., 2008; Kim *et al*., 2008; Huang *et al*., 2010; Schwab *et al*., 2010; Wang *et al*., 2013). FANCL then mono-ubiquitinates FANCD2-FANCI to stabilise it at the damage site (Seki *et al*., 2007; Alpi *et al*., 2008; Longerich *et al*., 2009). Monoubiquitinated FANCD2/FANCI (ID2 complex) then recruits FAN1 (Fanconi anaemia associated nuclease 1) (Kratz *et al*., 2010; MacKay *et al*., 2010; Smogorzewska *et al*., 2010) and XPF/ERCC1 nucleases to incise the DNA backbone on the leading strand and unhook the ICL (De Silva *et al*.,

2000; Kuraoka *et al*., 2000; Niedernhofer *et al*., 2004). The ubiquitin signalling pathway is also important in the polymerase switching during translesion synthesis (TLS). At stalled replication forks, the replication clamp PCNA is ubiquitinated by Rad18 and Rad6 (Hoege *et al*., 2002; Stelter and Ulrich, 2003; Kannouche *et al*., 2004; Davies *et al*., 2008), to switch its affinity for replicative DNA polymerases to bypass polymerases (Polη, Polκ, Polι, Polξ and Rev1), which are able to use the damaged base as template and allow replication to proceed past the lesion (Waters *et al*., 2009). The unhooked ICL is then excised by the NER machinery (reviewed by Wood, 2011), and finally the DSB formed by Mus81 and the replication runoff is repaired by HR (Hinz, 2010).

Genetic defects in the FA pathway present clinically early in life, with very diverse features including bone marrow failure, acute myeloid leukaemia, head and neck cancers, skin and skeletal abnormalities, microcephaly, and multiple organ abnormalities (Neveling *et al*., 2009). Defective TLS is associated with increased genomic instability, as exemplified by the human disease xeroderma pigmentosum variant (XPV) (Masutani *et al*., 1999; Johnson *et al*., 1999). It can be inferred that a degree of tolerance to some mutagenic lesions is preferable to the consequences of DSBs such as chromosomal rearrangement and translocations.

1.3.3 Apoptosis, senescence and autophagy

When a cell fails to restore genome stability due to the quantity or complexity of the DNA damage sustained, it is still possible to prevent malignant transformation by undergoing apoptosis, senescence or autophagy. The choice between these outcomes depends on many factors, such as the cell cycle status and the severity of the damage, although many factors overlap in all three pathways.

Apoptosis is programmed cell death closely linked to the DDR. The process is intrinsically linked to the release of mitochondrial inner membrane proteases such the cytochrome c and caspases, under the regulation of BCL-2 protein family (Czabotar *et*

al., 2014). In the context of DNA damage and cell cycle checkpoint activation, sustained p53 hyper-accumulation increases expression of pro-apoptotic factors such as BAX, NOXA, PUMA, and FAS receptor (Lane, 1992), which promotes cell death through activation of the caspase cascade (Haupt *et al*., 2003). There is also a p53-independent pathway of initiating apoptosis through CHK1/CHK2-dependent activation of transcription factor E2F1, which promotes expression of factor p73 (another member of the p53 protein family), which activates pro-apoptotic factors such as BAX, PUMA and SCOTIN, as well as its anti-apoptotic isoform like ΔNp73 (Ramadan *et al*., 2005). In addition, DNA damage can also trigger the NF-κB-dependent activation of caspases through the IKK (IκB kinase) complex (Janssens and Tschopp, 2006).

Senescence refers to a permanent arrest in cell cycle progression in normally cycling cells. DNA damage and oxidative stress are well-characterised triggers of cellular senescence (Campisi and d'Adda di Fagagna, 2007; van Heemst *et al*., 2007). Not surprisingly, p53 plays a very similar role in maintaining cell cycle arrest as during the G1/S checkpoint activation, through activation of p21 and inhibition of CDK2 function (**Section 1.3.1.2**). Another pathway involves the retinoblastoma protein (pRB) activation by p16, and subsequent inhibition of E2F-dependent transcription of pro-proliferation factors (Becker and Haferkamp, 2013).

In postmitotic cells such as neurons and cardiomyocytes, where senescence is not feasible, autophagy becomes an important mechanism to systematically remove protein aggregates, dysfunctional organelles, or intracellular microbes through lysosome-mediated degradation (Cuervo, 2004; Klionsky *et al*., 2007). The formation of autophagosomes is regulated by multiple factors such as nutritional deprivation (Lum *et al*., 2005; Bergamini *et al*., 2007; Mörck and Pilon, 2007; Bishop and Guarente, 2007), oxidative stress (Filomeni *et al*., 2015), as well as endothelial reticulum (ER) stress (Ogata *et al*., 2006; Yorimitsu *et al*., 2006; Høyer-Hansen and Jäättelä, 2007). Autophagy usually promotes cellular viability but can lead to

accelerated cell death when apoptosis is inhibited (Shimizu *et al*., 2004; Levine and Yuan, 2005), and conversely, inhibition of autophagy in the presence of nutritional deprivation promotes cell death by apoptosis (Maiuri *et al*., 2007).

1.4 DNA topoisomerases

DNA topoisomerases resolve topological stresses in the DNA double helix as it unwinds during processes such as DNA replication, transcription, DNA recombination, and chromatin remodelling. During these processes, positive or negative supercoils can build up in the still annealed double strands on either side of the separated strands, as the DNA double helix folds back onto itself and becomes entangled, preventing any further DNA unwinding. Therefore, supercoils must be removed as they arise. Topoisomerases are thus indispensable for life and are conserved from prokaryotes to all eukaryotes (Forterre *et al*., 2007).

Topoisomerases modulate DNA topology by transiently breaking the backbone of the DNA, allowing movement of the DNA strand relative to itself or to another DNA strand, resealing the break, and then dissociating from the DNA. They can be broadly classified as type I or type II topoisomerases. The former breaks the backbone on one strand of the DNA, while the latter breaks both strands (Wang, 2002). Type I topoisomerases can further be divided into type IA, which forms covalent linkage to the 5'-phosphate group of the phosphodiester bond of the backbone, and IB, which covalently links to the 3'-phosphate group (Wang, 2002). Type II topoisomerases can similarly be divided into type IIA and IIB. There are six known topoisomerases in humans: TOP1 (type IB), TOP1mt (type IB), TOP2α (type IIA), TOP2β (type IIA), TOP3α (type IA), and TOP3β (type IA) (Wang, 2002) (**Fig. 1.7**).

1.4.1 Catalytic cycle

Upon non-covalent binding around the DNA strand, a topoisomerase utilises a tyrosine residue in the catalytic site to deprotonate the scissile phosphate of the DNA backbone

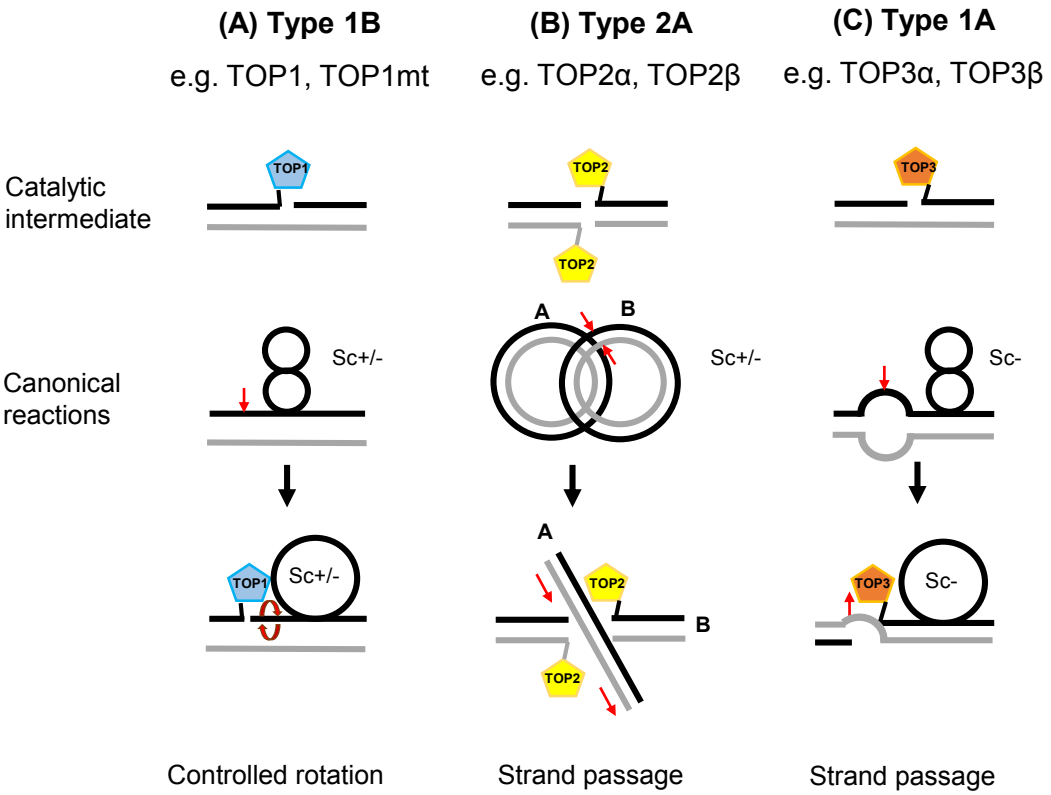

Figure 1.7 Types of vertebrate topoisomerases. Topoisomerases can be classified according to their modes of action. **(A)** A type 1B topoisomerase (TOP1 and TOP1mt in humans) incises one strand of the DNA while being covalently attached to the 3' end of the nick. It can cleave both in front of a polymerase (positively supercoiled "Sc+") or behind a RNA polymerase (negatively supercoiled "Sc-"), and allow controlled rotation of the cleaved strand around its own axis to relieve the supercoiling. **(B)** A type 2A topoisomerase (TOP2α and TOP2β in humans) incises both strands of the DNA simultaneously, while being covalently attached to the 5' ends of the nick. TOP2 enzymes can cleave both positively and negatively supercoiled DNA, but they are especially important in separating sister chromatids post-replication. The strand passage reaction is ATP-dependent. **(C)** A type 1A topoisomerase (TOP3α and TOP3β in humans) incises one strand of the DNA where the two strands are separated by negative supercoiling. It attaches to the 5' end of the nick and passes the intact strand through the broken strand. The process is also ATP dependent. Adapted from Pommier *et al.*, 2016.

(a nucleophilic reaction), breaking the phosphodiester bond of the DNA backbone and creating a covalent phosphotyrosine bond between the topoisomerase and the backbone (Champoux, 2001). The nick on the backbone then allows another DNA strand to pass through (in the case of type IA and type II topoisomerases), or the nicked strand can swivel around the intact strand (type IB) to release the torsional tension (Champoux, 2001). To reseal the nick, the hydroxyl group generated by breaking of the phosphodiester bond deprotonates the phosphotyrosine, thus restoring the phosphodiester bond and releasing the topoisomerase from the DNA backbone (Champoux, 2001).

1.4.2 Cellular functions

As topoisomerases are required wherever topological stress arises in the genome, they can bind supercoiled DNA with low sequence specificity (Spitzner and Muller, 1988; Porter and Champoux, 1989; Capranico *et al*., 1990; Jaxel *et al*., 1991). Type IB and type II topoisomerases preferentially bind supercoiled dsDNAs (Wang, 2002), reflecting their ability to resolve positive and negative supercoils. Type IA topoisomerases, as necessitated by their mechanism of action, require a short stretch of ssDNA for binding (Wang, 1971; Srivenugopal *et al*., 1984; Wilson *et al*., 2000; Wang, 2002). Their supercoiling relaxing property is also less efficient than that of type II topoisomerases (change of one linking number per catalytic cycle instead of two), therefore they were predicted to be inefficient for resolving positive supercoils (Kirkegaard and Wang, 1985; Plank *et al*., 2005).

1.4.2.1 Chromatin remodelling

DNA transactions such as replication, transcription, recombination and damage repair that require modification or displacement of the nucleosomes to allow access for the involved proteins also often require changes in DNA topology. It is therefore not surprising that topoisomerases are required during chromatin remodelling. For example, it has been shown in yeast that the chromatin remodelling activity of the

Switch/Sucrose Non-Fermentable (SWI/SNF) complex is dependent on the activities of TOP1 and TOP2 (Gavin *et al*., 2001). Conversely, TOP1 and TOP2 are targeted to sites of active transcription or replication through interaction with the catalytic subunit of SWI/SNF, SMARCA4 (Dykhuizen *et al*., 2013; Husain *et al*., 2016).

In general, TOP1 is more closely associated with transcription-mediated chromatin remodelling, while TOP2 is more specific for replication-mediated remodelling. For instance, TOP1 has been shown to displace nucleosomes at transcription initiation sites (Khobta *et al*., 2006; Durand-Dubief *et al*., 2011; Baranello *et al*., 2010; Baranello *et al*., 2016); while TOP2α has an established role in postmitotic chromatid decatenation and nucleosome assembly (Hirano and Mitchison, 1993; Dykhuizen *et al*., 2013; Farr *et al*., 2014; Broderick *et al*., 2015; Nielsen *et al*., 2015; Shintomi *et al*., 2015).

1.4.2.2 DNA replication

During DNA replication, as the replication fork progresses, positive supercoils accumulate ahead of the replication bubble. As the replication machinery rotates around the replication fork along the DNA helical axis, the tension in the positive supercoils is redistributed toward the back of the replication machinery and cause the newly synthesised DNA to intertwine (Peter *et al*., 1998). The activities of type IB and type IIA topoisomerases are therefore required: type IB to remove the positive supercoils and type IIA to separate the tangled replicated strands (Brill *et al*., 1987; Kim and Wang, 1989; Strumberg *et al*., 2000).

As two replication forks converge, the short piece of parental strands in between (termed “hemicatenane”) becomes too short for a type IB topoisomerase to bind to. In this case, type IA topoisomerase could resolve the tension in the single-stranded region of the parental strands, converting two replication forks into one (DiGate and Marians, 1988; Nurse *et al*., 2003; Suski and Marians, 2008). Type II topoisomerase

can then resolve the supercoiling in the two double-stranded replicated strands (Lucas *et al*., 2001; Cebrián *et al*., 2015).

Type IB and II topoisomerases have also been implicated in initiation of replication (Rampakakis *et al*., 2010), as they localise to a subset of replication origins (Abdurashidova *et al*., 2007; Falaschi *et al*., 2007; Falaschi, 2009; Rampakakis and Zannis-Hadjopoulos, 2009; Hu *et al*., 2009).

Interestingly, in mammalian cells, TOP2 appears to negatively regulate replication initiation (Gonzalez *et al*., 2011; Gaggioli *et al*., 2013), which could be important for suppression of aberrant replication initiation at sites of RNA:DNA hybrids (R-loops) (Kaguni and Kornberg, 1984).

At completion of DNA replication, the daughter chromosomes must separate to allow proper segregation during mitosis. The centromeres play an important role in the process. Type II topoisomerases have been shown to associate with centromeric proteins like Aurora kinase B and Polo-like kinase 1 (PLK1), supporting its role in unlinking (decatenating) daughter chromosomes at the centromeres during mitosis (Holm *et al*., 1985; Uemura and Yanagida, 1986; Nitiss, 2009; Coelho *et al*., 2008; Baxter *et al*., 2011; Edgerton *et al*., 2016).

1.4.2.3 Transcription

During transcription, it has been observed that positive supercoiling is generated ahead of the transcription machinery; in addition, negative supercoils build up behind it (Liu and Wang, 1987). The formation of negative supercoils has been proposed to be due to the inability of the transcription machinery to rotate around the DNA helical axis, thus the DNA rotates instead (Maaløe, 1966). As transcription of most mRNAs is confined in the nucleolar “transcription factories”, anchorage of the DNA loop to the nuclear membrane and to the ribosomes (in the case of transcription-coupled translation) likely impede the mobility of the DNA and the transcription machinery relative to each other.

Although in transcription, there is no problem of formation of intertwined daughter strands, negatively supercoiled strands have the propensity to hybridise to the elongating nascent RNA strand, forming stable R-loops, especially in long genes with highly repetitive sequences such as rDNAs (Aguilera and García-Muse, 2012).

Both type IB and II topoisomerase have been shown to reduce R-loop formation in rDNA genes (El Hage *et al*., 2010), with TOP1 primarily responsible for removal of negative supercoils and TOP2 more important for resolving positive supercoils (French *et al*., 2011).

It is worth noting that TOP1 has an additional kinase activity unrelated to its DNA-relaxation activity. TOP1 phosphorylates the splicing factor ASF/SF2 to promote RNA maturation (Rossi *et al*., 1996), thereby preventing annealing of the nascent RNA to the ssDNA template (Tuduri *et al*., 2009).

Other than removing supercoils, topoisomerases also play a role in regulating gene expression at promoter and enhancer regions. For example, TOP1 interacts with the TATA-binding protein (TBP) subunit of the transcription activator, TFIID complex, and promotes its binding to TATA box (Kretzschmar *et al*., 1993; Merino *et al*., 1993; Shykind *et al*., 1997). TOP1 also interacts with RNA Pol II paused near transcription initiation sites to promote transcription elongation (Baranello *et al*., 2016). In some but not all cases, the DNA cleaving activity of TOP1 is required, such as at androgen receptor-regulated enhancers (Puc *et al*., 2015). Similarly, TOP2β has been shown to induce DSBs at the sites of several ligand-dependent promoters (Ju *et al*., 2006; Haffner *et al*., 2010; Williamson and Lees-Miller, 2011; Trotter *et al*., 2015), as well as a subset of neuron-specific early response genes (Madabhushi *et al*., 2015).

Pharmacological inhibition of TOP1 and TOP2 showed differing effect on transcription, with TOP1 stalling occurring mainly along elongating transcripts, while TOP2 stalling mainly at promoter regions (Collins *et al*., 2001). The response was also highly variable amongst genes of different lengths and chromosomal and episomal promoters,

suggesting the importance of chromosomal architecture in transcription. More specifically, in human cancer cell lines HCT116, MCF7 and MDA-MB-231, CPT downregulated transcription of long genes that were highly expressed, such as genes involved in RNA degradation, cell cycle, basal transcription factors and ubiquitin-proteasome pathways, while activating transcription of short inactive genes in the oxidative phosphorylation, ribosome and p53 signalling pathways (Solier *et al*., 2013). It was proposed that CPT-induced TOP1-cc downregulate transcription at long genes through arresting RNA Pol II (Ljungman and Hanawalt, 1996; Desai *et al*., 2003); inhibiting RNA splicing (Solier *et al*., 2004; Solier *et al*., 2010); and upregulation of p53-dependent miRNA-142-3p (Solier *et al*., 2013).

1.4.2.4 DNA recombination

DSBR by HR can give rise to double Holliday junctions (dHJs) (**Section 1.3.2.9**). This is resolved by the HJ resolvosome, which consists of the RecQ helicase BLM, RPA-like factors RecQ-mediated genome instability proteins 1 and 2 (RMI1 and RMI2), and TOP3α (Wu *et al*., 2006; Hartung *et al*., 2008; Kaur *et al*., 2015). The helicase activity of BLM forces the two HJs to converge, making the dHJ resemble the structure of two colliding replication forks. TOP3α, stabilised by RMI1 and RMI2, binds the hemicatenane region and gradually decatenates the crossover strands, until they are completely separated and non-crossover products are generated (Wu and Hickson, 2003; Plank *et al*., 2006).

On the other hand, during meiosis, DSBs are generated by the TOP4-like protein SPO11, which promotes recombination by recruiting the MRN complex, RAD51, CtIP, and DMC1-like factors (Baudat *et al*., 2000; Neale *et al*., 2005; Li and Ma, 2006; Keeney, 2008; Hartsuiker *et al*., 2009), thus promoting genetic diversity in the daughter cells.

1.4.2.5 Mitochondrial DNA replication and transcription

In the mitochondria, mtDNA replication and transcription also require the action of topoisomerases. TOP1mt, TOP2α, TOP2β, and TOP3α have all been found in the mitochondria (Zhang *et al*., 2001; Wang, 2002; Zhang *et al*., 2004a; Plank *et al*., 2005), although their mechanisms of action are less well-characterised.

1.4.3 Cellular response to TOP1-cc

Given the DNA-nicking property of the topoisomerases, the potential of introducing genomic instability increases if their catalytic cycle fails to complete, resulting in polymerase-blocking protein-DNA adducts. It has been shown that TOP1 can become trapped on the DNA backbone if it incises near endogenous DNA lesions such as base modifications, AP sites, nicks and mis-incorporated RNA (Pommier *et al*., 2003), which lack the 5' hydroxyl group required for the re-ligation step. Trapped TOP1 (TOP1-cc) *per se* do not elicit DDR associated with DNA breaks, which is masked by the bulk of the protein. **Fig. 1.2** illustrates that during DNA replication, collision with the replication machinery or excessive build-up of positive supercoiling in front inhibits progression of the replication fork, causing cytotoxic DSBs (Sordet *et al*., 2009). During transcription, stalling by TOP1-cc promotes formation of stable RNA/DNA hybrids (R-loops) that inhibit replication fork progression and associated ssDNA's that are prone to spontaneous degradation or mutagenesis (Aguilera, 2002; Li and Manley, 2006; Aguilera and García-Muse, 2012).

The most well-characterised repair pathway of TOP1-cc to date, as mentioned in **Section 1.3.2.5**, involves the PARP1-TDP1-PNKP-XRCC1-Lig3α branch of SSBR (Pommier *et al*., 2006; Ashour *et al*., 2015). APE1 has also been shown to process 3'-phosphotyrosyl ends (Harrigan *et al*., 2007). PARP1 is known to accumulate in actively transcribing sites (Kraus and Lis, 2003; Krishnakumar *et al*., 2008) and also physically interacts with TOP1 (Bauer *et al*., 2000). It has been shown that trapped TOP1 is rapidly ubiquinated and proteasomally degraded (Lin *et al*., 2008; Lin *et al*., 2009),

together with the stalled RNAPII if present (Ratner *et al*., 1998); and that degraded TOP1-DNA adduct is the preferred substrate of TDP1 (Desai *et al*., 2003; Lin *et al*., 2009). Degradation of TOP1 has been shown to be dependent the E3 Ub ligases Cullin 3 (Cul3) (Zhang *et al*., 2004b) and Cullin 4B (Cul4B) (Kerzendorfer *et al*., 2010).

It is interesting that trapped TOP1 is also modified by SUMOylation (Mao *et al*., 2000; Horie *et al*., 2002), but the intended effect is not yet defined. It has been proposed to play a role in translocating TOP1-cc from the nucleolus to the nucleoplasm (Mo *et al*., 2002; Rallabhandi *et al*., 2002; Christensen *et al*., 2004), inhibiting ubiquitination of TOP1 (Horie *et al*., 2002), or signalling recruitment of more free TOP1 (Horie *et al*., 2002), or TDP1 (Hudson *et al*., 2012) to the damage sites.

Given that most the genome is transcriptionally silent, it is likely that transcription-independent pathways to repair TOP1-cc exist. Furthermore, in replicating cells, excessive accumulation of TOP1-cc would saturate the SSBR machinery, leading to collision of TOP1-cc with replication forks and formation of DSBs (Pouliot *et al*., 2001). Indeed, it has been demonstrated in yeast and mammalian cells that both HR and NHEJ pathways confer resistance against CPT in the absence of Tdp1 (Pommier *et al*., 2003). Mre11/Rad50/Sae2 and Mus81/Mms4 (Mus81/EME1 in humans), together with Slx1/Slx4 can resect several nucleotides 5’ of the TOP1-cc end, leaving a 3’-hydroxyl end for gap repair (Deng *et al*., 2005; Hamilton and Maizels, 2010; Sacho and Maizels, 2011; Regairaz *et al*., 2011). As these endonucleases do not require access to the phosphotyrosine bond like TDP1, degradation of TOP1 might not a prerequisite for this mode of repair.

The NER pathway is also implicated in the repair of TOP1-cc. CSB defective patient cells show sensitivity to CPT, and in yeast the 3’ endonuclease Rad1/Rad10 (XPF/ERCC1 in humans) possess activity against single-stranded 3’-phosphotyrosyl moieties similar to TDP1 (Vance and Wilson, 2002; Zhang and Jasin, 2011; Takahata

et al., 2015). Multiple NER factors such as RPA, pol δ, FEN1 and Lig1 catalyse the downstream repair *in vitro* (Takahata *et al*., 2015), suggesting repair during S-phase.

Notably, since lower eukaryotes lack several key SSBR factors such as PARP1, XRCC1 and Lig3α (Kelley *et al*., 2003), it is likely that the SSBR pathway of TOP1-cc repair evolved later to manage the larger genome size and/or the higher transcriptional activity in specialised postmitotic tissues such as neurons. More recently, experiments in yeast and *in vitro* human cell extracts also suggest a role of TDP1 in the NHEJ pathway (Bahmed *et al*., 2010; Heo *et al*., 2015), likely of functional significance in G2 or postmitotic cells.

1.4.4 Clinical relevance of TOP1 poisons

Given the multiple pathways available to repair TOP1-cc, it is unlikely that TOP1-cc arising endogenous DNA lesions would elicit a dramatic DDR response such as checkpoint arrest or apoptosis, except in the case of cells under unusually high oxidative or replicative stresses. This differential DDR response between fast- and slow-growing cells forms the basis of several new classes of anti-cancer therapeutics. For example, PARP1 inhibitors are highly selective against fast-growing tumours, especially those defective in DSBR (Helleday, 2011). By compromising SSBR, more SSBs are converted to DSBs in fast-replicating cells, and if DSBR is defective, can undergo cell cycle arrest (**Section 1.3.1**) and apoptosis (**Section 1.3.3**).

Topoisomerase poisons, unlike most enzymatic inhibitors, rely on the catalytic activity to form cleavage complexes, which then trigger DDR and apoptosis (Liu *et al*., 2000). Camptothecin was the original TOP1 poison discovered in the Chinese plant *Camptotheca Accumulata* (Wall and Wani, 1995). It had been used as an anti-cancer drug long before its mechanism of action was understood. Structural work by the Pommier group and others have later shown that it stabilises TOP1 on the DNA backbone nick by forming hydrogen bonds with the TOP1 catalytic residues and the -1 T and +1 G bases surrounding the nick (Staker *et al*., 2002; Staker *et al*., 2005;

Ioanoviciu *et al*., 2005; Marchand *et al*., 2006). Therefore, CPT is specific to TOP1 both in a sequence- and structural manner.

However, the effects of TOP1 inhibitors on DNA transcription and replication also target haematopoietic stem cells and postmitotic cells, leading to immunosuppression, cardiotoxicity and neurotoxicity over time (Moertel *et al*., 1972; Muggia *et al*., 1972). Due to its potent cytotoxicity, CPT is no longer used in the clinical setting. Currently, CPT analogues such as topotecan (TPT) and irinotecan (CPT-11) are FDA-approved for use in advanced colorectal, ovarian, cervical, and small-cell lung cancers (Pommier, 2006). CPT and non-CPT analogues currently in clinical trials are summarized in **Table 1.1** (Xu and Her, 2015).

Besides the unwanted cytotoxicity, the main challenges to develop next-generation TOP1 inhibitors lie with improving compound stability and overcoming development of resistance (Beretta *et al*., 2013). As over time, even a single point mutation in TOP1 can potentially confer resistance. The rationale of combination therapy is that, by simultaneously generating TOP1-cc and inhibiting TOP1-cc repair, synthetic lethality can be achieved at lower or non-cytotoxic doses. For example, combination of a PARP1 (Delaney *et al*., 2000; Thomas *et al*., 2007; Zander *et al*., 2010; Kummar *et al*., 2011; Patel *et al*., 2012; Samol *et al*., 2012; LoRusso *et al*., 2016) or TDP1 inhibitor and TOP1 poison would inhibit TOP1-cc repair by SSBR; while combination with ATM, ATR, CHK2 or TDP2 inhibitors would hinder repair by DSBR (Shao *et al*., 1997; Tse and Schwartz, 2004; Flatten *et al*., 2005; Pommier *et al*., 2005; Elsayed *et al*., 2016). Alternatively, TOP1 poisons can be used as a neo-adjuvant drug to sensitize localized solid tumours such as glioblastomas to radiotherapy (Vredenburgh *et al*., 2009).

Name	Trial phase	Indications
Belotecan (CKD-602)	Approved (South Korea)	Advanced metastatic cancer, SCLC
Diflomotecan (BN80915)	Phase II (Ipsen)	Advanced solid tumors
Gimatecan (ST-1481, LBQ707)	Phase I/II (Sigma-Tau, Novartis)	SCLC, Ovarian
Lurtotecan (Liposomal OSI-211, NX 211)	Phase II (Astellas, NCLC)	
Exatecan mesylate (DX-8951f)	Phase II/III (Daiichi)	Sarcoma, Pancreatic, Gastric, Liver
Indenoisoquinolines (LMP400, LMP776)	Phase I	

Table 1.1: *Topoisomerase 1 inhibitors in clinical trials and their indications*

(Adapted from Hu & Her, 2015. *Biomolecules,* 5**,** 1652-70)

1.5 TDP1

TDP1 is one of the more recently discovered member of the SSBR pathway. Its activity to resolve TOP1-cc is conserved from yeast to human (Yang *et al*., 1996; Pouliot *et al*., 1999; Interthal *et al*., 2001; El-Khamisy *et al*., 2005), highlighting its evolutionary importance. This activity has also been implicated in resistance against anti-cancer TOP1 and TOP2 poisons (Barthelmes *et al*., 2004; Nivens *et al*., 2004; Liu *et al*., 2007; Meisenberg *et al*., 2014b), and therefore has been under investigation as a candidate for combination therapy with topoisomerase poisons.

1.5.1 Structure and substrates

Human TDP1 is a 68.5 kDa (608 amino acids) enzyme that belongs to the phospholipase D (PLD) superfamily and contains two distinct HKD motifs ($HXK(X)_4D(X)_6GSXN$) essential for its catalytic activity (Interthal *et al*., 2001). The N-terminus domain (first 150 amino acids in human TDP1) is poorly conserved and only present in higher eukaryotes (Davies *et al*., 2002). The crystal structure of the C-terminus domain of human TDP1 reveals two symmetrical α-β-α domains each consisting of seven beta sheets and two alpha helices, and a central catalytic site (Davies *et al*., 2002). Perpendicular to the boundary between the two domains, a narrow, positively-charged cleft of 8 Å runs through one side of the active site, while a widening cone-shaped cleft of up to 20 Å of mixed charge runs through the other side (Davies *et al*., 2002). This conformation allows binding of ssDNA in the narrow cleft and a TOP1 peptide moiety in the cone-shaped cleft (Davies *et al*., 2002; Debéthune *et al*., 2002; Davies *et al*., 2004; Interthal and Champoux, 2011).

Further structural and mutational studies revealed that TDP1 resolves TOP1-cc in a two-step reaction, firstly nucleophilic attack of the scissile phosphate by the H263 residue and protonation of the tyrosyl residue by the H493 residue cleave the TOP1 peptide from the DNA backbone, while forming a covalent phosphohistidine bond between TDP1 H263 and the 3’ phosphate end of the DNA backbone; the second step

involves activation of a water molecule by H493, which catalyses hydrolysis of the phosphohistidine bond and release of TDP1 (Interthal *et al*., 2001; Davies *et al*., 2003). Mutation of H493 therefore has a dominant negative effect, leading to formation of covalent TDP1-DNA intermediates similar to TOP1 (Interthal *et al*., 2005a; Hirano *et al*., 2007). Resolution of these TDP1-DNA intermediates has been proposed to be carried out by TDP1 itself (Interthal *et al*., 2005a), as TDP1 has been shown to process the 3'- phosphoamide bond in the TDP1-DNA intermediate *in vitro* (Interthal *et al*., 2005a); and that heterozygous carriers of H493R mutation do not develop SCAN1 (Takashima *et al*., 2002).

TDP1 has also been shown to process a variety of physiologically relevant 3' termini, such as 3'-phosphoglycolate from oxidative damage and 3'-dRP from monofunctional alkylating agents (Inamdar *et al*., 2002; Interthal *et al*., 2005a; Zhou *et al*., 2009).

Besides its 3' phosphodiesterase activity, TDP1 also has limited 3' exonuclease activity, which removes one nucleoside from DNA or RNA with 3'-hydroxyl ends (Interthal *et al*., 2005a; Dexheimer *et al*., 2010). This activity has been linked to repair of lesions induced in the nucleus and mitochondria by chain-terminating anti-cancer and anti-viral nucleoside analogues (Huang *et al*., 2013; Tada *et al*., 2015).

1.5.2 Cellular functions

TDP1 is ubiquitously expressed in most human and mouse tissues, both in the nuclear and mitochondrial compartments (Hirano *et al*., 2007; Das *et al*., 2010; Fam *et al*., 2013a).

Cell lines established from SCAN1 patients, *Tdp1*$^{-/-}$ mice, and *TDP1*$^{-/-}$ DT40 cells all show hypersensitivity to CPT (El-Khamisy *et al*., 2005; Interthal *et al*., 2005b; Miao *et al*., 2006; Hirano *et al*., 2007; Katyal *et al*., 2007; Das *et al*., 2009; El-Khamisy *et al*., 2009; Hawkins *et al*., 2009; Murai *et al*., 2012), while overexpression of TDP1 increases resistance to CPT (Barthelmes *et al*., 2004; Nivens *et al*., 2004), confirming the role of TDP1 in repair of TOP1-cc in higher eukaryotes. Physical interaction of

TDP1 with XRCC1/Lig3α of the BER/SSBR pathway in mammalian cell lines (Plo *et al*., 2003; El-Khamisy *et al*., 2005) supports the prediction based on the crystal structure that TDP1 participates in the repair of single-stranded TOP1-linked DNA breaks in higher eukaryotes.

However, accumulation of DSBs with 3'-PG ends was also detected in SCAN1 patient-derived LCLs and *Tdp1*$^{-/-}$ MEFs (Zhou *et al*., 2005; Hawkins *et al*., 2009). Moreover, *Tdp1*$^{-/-}$ MEFs and DT40 cells are sensitive to 3'-PG DSB-inducing drug bleomycin (Hirano *et al*., 2007; Murai *et al*., 2012), while SCAN1 LCLs and TDP1-deficient HeLa cells are sensitive to calicheamicin (Zhou *et al*., 2009). Taken together, these data indicate that TDP1 also participates in the repair of 3'-PG DSBs in the cellular context. Binding of TDP1 to DSB ends has been proposed to be achieved through binding to a short 3' overhang of the DSB (Zhou *et al*., 2009), a conformational change of the active site *in vivo*, or a 90° rotation of the dsDNA relative to the narrow cleft of TDP1, so that only 3 bases at a time are in contact with the narrow cleft (Raymond *et al*., 2005).

The role of TDP1 on repair of TOP2-cc linked DSBs is less clear. *TDP1*$^{-/-}$ DT40 cells showed sensitivity to the TOP2 poison etoposide (Murai *et al*., 2012), while this was not observed in SCAN1 cells (Miao *et al*., 2006) or *Tdp1*$^{-/-}$ MEFs (Hirano *et al*., 2007). *In vitro* biochemical assays showed no TDP1 processing of 5' phosphotyrosyl substrate (Cortes Ledesma *et al*., 2009), while in yeast TDP1 has been shown to process a more physiologically relevant substrate with TOP2 peptide-linked 5' phosphotyrosyl terminus (Barthelmes *et al*., 2004; Nitiss *et al*., 2006; Borda *et al*., 2015). These inconsistent observations could be due to cell line- or species-specific modifications of TDP1 activity *in vivo*; and highlight the importance of identifying intracellular modifiers of TDP1 activity that may contribute to the disease phenotype of SCAN1, or when designing inhibitors against TDP1.

There are accumulating evidence supporting that the N-terminus domain of TDP1 regulates TDP1 function in the cellular context, through post-translational modifications and protein-protein interactions, which are discussed in detail in **chapters 3 and 4**.

1.5.3 Spinocerebellar axonal neuropathy 1 (SCAN1)

To date, three individuals with confirmed SCAN1 diagnosis have been described (OMIM #607250). They were all from a large consanguineous family and were homozygous for the TDP1 H493R mutation (Takashima *et al*., 2002). The presenting symptom was ataxic gait of adolescent onset. Clinical evaluation showed distal muscle weakness, areflexia, and disturbed proprioception. Cognition was normal in all three individuals. MRI scan showed cerebellar atrophy in individuals 1 and 2; and nerve conduction studies showed demyelination of the sural nerve in individual 3. All three individuals had mild hypoalbuminaemia and hyperlipidaemia. Mutational screens for Spinocereberllar ataxia (SCA) 1, 2, 3, 6, 7 and Friedreich ataxia (FRDA) were all normal for individual 1, and screens for metabolic disorders were negative in individual 2 (OMIM #607250) (Takashima *et al*., 2002). Taken together, the clinical phenotype from these three individuals resembles that of Ataxia Oculomotor Apraxia 1 (AOA1) (OMIM #208920), except for a later age of onset.

The lack of signs of genomic instability and immunodeficiency, and the overlap with AOA1 phenotype, suggest that the pathology of TDP1 H493R mutation is likely due to defective SSBR in postmitotic neurons. Lymphoblastoid cell lines from the three SCAN1-affected individuals were defective in repair of replication-independent chromosomal SSBs induced by CPT and H_2O_2 (El-Khamisy *et al*., 2005); as were cerebellar neurons and primary astrocytes from *Tdp1*$^{-/-}$ mice (Katyal *et al*., 2007). However, *Tdp1*$^{-/-}$ mice do not develop ataxia (Katyal *et al*., 2007). It has therefore been proposed that the pathogenic lesions in SCAN1 are a combination of TOP1-cc, TDP1-DNA intermediates (Interthal *et al*., 2005a; Hirano *et al*., 2007; Hawkins *et al*., 2009), and 3'-PG SSBs from endogenous ROS (Zhou *et al*., 2005), that together form a

vicious cycle to generate SSBs that eventually inhibit transcription and lead to cellular dysfunction (Caldecott, 2008).

Since cerebellar ataxia is a frequent symptom of mitochondrial DNA diseases (Lax *et al*., 2012), it has also been suggested that TDP1 and APTX may play a more important role in protecting the mitochondrial genome than the nuclear genome (Kazak *et al*., 2012; Sykora *et al*., 2012). As mitochondrial TOP1 has been implicated in maintaining mtDNA integrity (discussed in **Section 6.1.2**), if TDP1 plays a significant role in repair of TOP1mt-cc and oxidative mtDNA damages (Das *et al*., 2010), these could be the additional pathogenic lesions in SCAN1. This hypothesis was investigated and described in detail in **chapters 5** and **6**.

1.5.4 Tumorigenesis and targeted therapy

TDP1 has also been an emerging player in the field of cancer research, primarily because of its broad-spectrum of substrates that imply the potential to modulate sensitivity of vertebrate cells to TOP1, TOP2 poisons (Barthelmes *et al*., 2004; Nivens *et al*., 2004; Interthal *et al*., 2005b; El-Khamisy *et al*., 2005; Miao *et al*., 2006; Katyal *et al*., 2007; Murai *et al*., 2012), as well as alkylating agents (Alagoz *et al*., 2013), radiotherapy (El-Khamisy and Caldecott, 2007), and chain-terminating nucleoside analogues (Huang *et al*., 2013; Tada *et al*., 2015). However, precisely because of its broad-spectrum activity, finding a target that specifically inhibits TDP1 activity has proven challenging.

Chemical compounds known to inhibit TDP1 in vitro include vanadate and tungstate, which were used to co-crystalise with TDP1 (Davies *et al*., 2002), however they are broad-spectrum inhibitors of phosphatases (Makinen, 1985; Stankiewicz and Gresser, 1988). Antibiotics such as aminoglycosides (neomycin B, paromomycin and lividomycin) and bacterial ribosome inhibitors (thiostrepton, clindamycin and puromycin) showed weak inhibition of TDP1 *in vitro* (Liao *et al*., 2006), and they are also broad-spectrum inhibitors of PLD enzymes (Huang *et al*., 1999). Furamidine

(DB75, NSC 305831), an anti-parasitic drug (Thuita *et al*., 2012), showed higher potency than the aminoglycosides and ribosome inhibitors, and likely acted through forming a ternary structure with ssDNA and TDP1, similar to CPT (Pommier, 2006; Antony *et al*., 2007). Interestingly, co-administration of furamidine and irinotecan augmented the effect of irinotecan on ameliorating nephritis in mouse model of systemic lupus erythematous (SLE), possibly through inhibition of DNA relaxation and subsequent binding by anti-dsDNA antibodies (Frese-Schaper *et al*., 2014; Keil *et al*., 2015), indicating potential non-oncologic application for a TDP1 inhibitor. Two phosphotyrosine mimetics, methyl-3,4-dephostatin and NSC88915, identified through high-throughput screens (Dexheimer *et al*., 2009; Marchand *et al*., 2009), provided insights on the molecular basis for TDP1 active site inhibition. Lastly, using high-throughput DT40 whole cell lysate assay to validate activity in the cellular context, two new compounds, NCGC00183974 and JLT048, were identified to selectively interact with TDP1 over TDP2 (Marchand *et al*., 2014). However, neither compounds induced cell killing by CPT in cultured cells, suggesting either inefficient uptake by cells, unknown cellular mechanisms that inactivate the compounds, or a cell line-specific compensatory upregulation in TDP1 activity level.

It was therefore becoming clear that finding effective TDP1 inhibitors in terms of cytotoxicity also relies on understanding the downstream compensatory response that determines the ultimate cell fate. One of these responses appears to be regulation of TDP1 expression and function, as illustrated by several recent studies. Expression and enzymatic activity of TDP1 was found to be higher in over 50 % of a panel of 34 treatment-naïve primary non-small cell lung carcinomas (NSCLC) compared to adjacent non-cancerous tissues from the same individuals (Liu *et al*., 2007); this was supported by another study using nanosensors to measure TDP1 activity *in situ*, whereby the activity was increased in 24 NSCLC tissues compared to adjacent non-cancerous tissues (Jakobsen *et al*., 2015). These findings suggest regulation of TDP1

function is intrinsic to tumourigenesis in NSCLC. In addition, there appeared to be a reciprocal downregulation of XPF overexpression in tumours overexpressing TDP1 (Liu *et al*., 2007), suggesting crosstalk between the parallel repair pathways of TOP1-cc repair. Another study showed that TDP1 mRNA levels were increased in a panel of 147 treatment-naïve primary rhabdomyosarcomas compared to normal skeletal tissues, and the protein levels of TDP1 as well as PARP1 were increased in 5 of the studied rhabdomyosarcoma cell lines compared to control cell lines (Fam *et al*., 2013b). Concomitant silencing of TDP1 and pharmacologic inhibition of PARP1 by rucaparib sensitised rhabdomyosarcoma cells to the DNA-damaging and cell-killing effect of CPT more than in control cells, suggesting an intrinsic DNA repair defect in these rhabdomyosarcoma cell lines that was compensated by TDP1 and PARP1 (Fam *et al*., 2013b). On the other hand, downregulation of TDP1 expression was found in six out of nine of lung cancer tissues from the NCI-60 panel, two of which showed undetectable TDP1 mRNA level and enzymatic activity, as well as increased DSBs after CPT treatment (Gao *et al*., 2014).

The studies described so far found heterogeneity in response to CPT in tissues with altered TDP1 expression levels. However, two small-scale studies suggest the ratio of TDP1:TOP1 may be a useful predictor of cellular response to CPT in colorectal cancers (Meisenberg *et al*., 2014a) and small cell lung cancers (Meisenberg *et al*., 2014b).

1.6 General aims and objectives

At the start of this project, the catalytic mode of action of TDP1 was well-established; its role in repair of TOP1-associated DSBs in yeast has been demonstrated; its association with components of the SSBR machinery was discovered in mammals; and a strong association of TDP1 catalytic mutation with the SCAN1 disorder was

established. However, little was known about how its function is regulated in the cellular context.

The interaction between XRCC1/Lig3α and TDP1 through its N-terminus domain (NTD) (El-Khamisy *et al*., 2005) was intriguing. It raised questions of the function of the NTD that evolved in higher eukaryotes. Perhaps in higher organisms, the larger genomic size and longer cellular lifespan would require a more efficient and regulated SSBR machinery, including TDP1. Does the addition of the NTD affect the catalytic activity in anyway? Does it change the tertiary structure or the stability of the protein? Does it promote recruitment of TDP1 to sites of chromosomal breaks? Does it mediate interaction of TDP1 with other enzymes that participate in repair of TOP1-cc? All these questions are highly relevant to the process of developing effective TDP1 inhibitors as discussed in **Section 1.5.4**.

On the other hand, a major question of the specific vulnerability of cerebellar neuronal cells in SCAN1 patients remains. As the cerebellum is a metabolically active organ, with high ATP demand and high levels of ROS as by-products, I hypothesised that TDP1 may play a protective role against DNA damage in tissues with high levels of endogenous ROS. Specifically, I investigated whether cells with high endogenous ROS accumulate more chromosomal breaks in the absence of TDP1; whether TDP1 was involved in the repair and/or production of endogenous ROS; and whether these chromosomal damages impact on mitochondrial functions and cellular viability.

In short, the original contribution of this thesis is to provide insight into the cellular function of human TDP1, by characterising NTD-mediated post-translational modifications of the protein, and its role in the mitochondria.

CHAPTER 2

Materials and Methods

2.1 General chemicals and equipment

General laboratory chemicals were obtained from Sigma Aldrich or Fisher Scientific unless otherwise specified. Restriction endonucleases were obtained from New England Biolabs or Roche Diagnostic. DNA and RNA oligonucleotides were synthesised by Eurofins MWG Operon (Ebersberg, Germany) or Integrated DNA Technologies (Leuven, Belgium). Cell culture media and nutritional supplements were obtained from Gibco® Invitrogen or Sigma Aldrich. Foetal bovine sera of South American origin were sourced by Sigma Aldrich (F6524) or PAN-Biotech (Aidenbach, Germany). Tetracycline tested FBS of South American origin was from Labtech (FB1001T/500). Cell culture plastic-ware was manufactured by Nunc™ or Corning.

2.2 Molecular biology techniques

2.2.1 DNA plasmids

Sources of all plasmid DNA constructs used in this thesis are indicated in **Tables 2.1, 2.2, and 2.3** respectively.

For yeast two-hybrid experiments, bait protein cDNA sequences were encoded in the pGBKT7 vector (Clontech, 630443), which contains the GAL4 DNA-binding domain (amino acids 1 – 147) and a c-Myc epitope tag upstream of the multiple cloning site (MCS). Constitutive expression of the fusion protein in yeast is under the control of the *ADH1* promoter. The vector also contains a *TRP1* nutritional marker and kanamycin resistance gene for selection in yeast and *E. coli*, respectively.

The cDNA sequences of prey proteins were encoded in the pACT2 AD vector (Clontech, 638822), which contains the GAL4-activation domain (amino acids 768 – 881) and a HA epitope tag upstream of the MCS. Constitutive expression of the fusion protein in yeast is under the control of the *ADH1* promoter. The vector also contains a

Plasmid DNA construct	Source/Reference
pGBKT7	Clontech
pGBKT7-TDP1	Prof. Sherif El-Khamisy
pGBKT7-TDP1$^{1-150}$	Prof. Sherif El-Khamisy
pGBKT7-TDP1$^{151-608}$	Prof. Sherif El-Khamisy
pGBKT7-TDP1^{S81A}	This thesis
pGBKT7-TDP1$^{S81A\ 1-150}$	This thesis
pGBKT7-TDP1$^{S81A\ 151-608}$	This thesis
pGBKT7-TDP1^{S81E}	This thesis
pGBKT7-TDP1^{K111R}	This thesis
pACT2	Clontech
pACT2-APTX	Prof. Keith Caldecott
pACT2.6-ERCC1	Dr John Rouse (Muñoz *et al.*, 2009)
pACT2-Ku80	Prof. Keith Caldecott
pACT2-Lig3α	Prof. Keith Caldecott (Caldecott *et al.*, 1996)
pACT2-SLX1	Dr John Rouse (Muñoz *et al.*, 2009)
pACT2-UBE2I	This thesis
pACT2-XPF	Dr John Rouse (Muñoz *et al.*, 2009)
pACT2-XRCC1	Prof. Keith Caldecott
pACT2-XRCC4	Prof. Keith Caldecott

Table 2.1: *Yeast two-hybrid constructs*
Plasmid DNA constructs used in this thesis for yeast two-hybrid analysis and their sources.

.

Plasmid DNA construct	Source/Reference
pCI-puro-Myc	Prof. Keith Caldecott
pCI-puro-Myc-TDP1	This thesis
pCI-puro-Myc-TDP1^{S81A}	This thesis
pCI-puro-Myc-TDP1^{S81E}	This thesis
ΔT-Myc-DEST	Dr Helfrid Hocheggar
ΔT-Myc-DEST -UBE2I	This thesis
pMX-PIE-TopBP1-ER	Dr Oskar Fernandez-Capetillo (Toledo *et al.*, 2008)
pMX-PIE-TDP1	This thesis
pMX-PIE-TDP1^{S81A}	This thesis
pMX-PIE-TDP1^{K111R}	Dr Jessica Hudson (Hudson *et al.*, 2012)
pMX-PIE-SOD1	This thesis
pMX-PIE-SOD1^{G93A}	This thesis
pMC-EGFPP-N-TDP1	Dr Morten Christensen
pMC-EGFPP-N-TDP1^{K111R}	Mr Chris Rookyard (Hudson *et al.*, 2012)
pEGFP-C1-SUMO1	Prof. Alan Lehmann
pMSP-shUBE2I	Open Biosystems/Dharmacon (clone V2HS_171771)
pcDNA6.2-GW-EmGFP	Thermo Fisher (cat. No. K4936-00)
pcDNA6.2-GW-EmGFP-miTDP1	This thesis
pcDNA5-FRT-His	Prof. Stuart Wilson
pcDNA5-FRT-miScr	Prof. Stuart Wilson
pcDNA5-FRT-miTDP1	This thesis
pcDNA5-FRT-TDP1^{TR}-miScr	This thesis
pcDNA5-FRT-TDP1^{TR}-miTDP1	This thesis
pcDNA5-FRT-SOD1-mi TDP1	This thesis
pcDNA5-FRT-SOD1^{G93A}-miScr	This thesis
pcDNA5-FRT-SOD1^{G93A}-miTDP1	This thesis
pcDNA5-FRT-TOP1mt-miScr	This thesis
pcDNA5-FRT- TOP1mt-miTDP1	This thesis
pcDNA5-FRT-TOP1mt^{T554A,N558H}-miScr	This thesis
pcDNA5-FRT-TOP1mt^{T554A,N558H}-miTDP1	This thesis

Table 2.2: *Mammalian expression constructs*
Plasmid DNA constructs used in this thesis for expression of the indicated cDNA in mammalian cells and their sources.

Plasmid DNA construct	Source/Reference
pET28b-SOD1	Dr Majid Hafezparasat
pET28b-SOD1^{G93A}	Dr Majid Hafezparasat
pcDNA5-FRT-TOP1mt	Dr Martin Meagher

Table 2.3: *Miscellaneous constructs used as cDNA templates*
Plasmid DNA constructs used in this thesis for subcloning the indicated cDNA into mammalian expression constructs and their sources.

LEU1 nutritional marker and ampicillin resistance gene for selection in yeast and *E. coli*, respectively.

For protein expression in mammalian cells, the vectors pCI-puro-Myc (Promega, E1731), pMC-EGFP-P-N (Barthelmes *et al*., 2004), pMX-PIE and pcDNA5-FRT were used. The pCI-puro-Myc vector contains a c-Myc epitope tag upstream of the MCS, which is useful for co-immunoprecipitation (Co-IP) experiments by Myc pull-down. The constitutional expression of the fusion protein is driven by the CMV promoter/enhancer sequence. The vector also contains a puromycin resistance gene under the SV40 promoter regulation for selection in mammalian cells; and an ampicillin resistance gene for propagation in *E. coli* cells.

The pMC-EGFP-P-N vector, derived from the plasmid pMC-2PS-delta HindIII-P (Mielke *et al*., 2000), contains the EGFP fluorophore epitope tag downstream of the MCS, which allows expression of C-terminally-tagged fusion proteins, useful for fluorescence microscopy and FACS experiments. The constitutional expression is driven by the CMV promoter/MPSV (myeloproliferative sarcoma virus) enhancer sequence. The vector allows expression of the puromycin resistance gene with the fusion protein as a bicistronic transcript linked by an Internal Ribosomal Entry Site (IRES) element. The vector also has an ampicillin resistance gene for propagation in *E. coli.*

For difficult to transfect mammalian cells, the pMX-PIE (pMX-puromycin-IRES-EGFP) vector was utilised for gene transfer by retroviral transduction of the virus packaging cells. The retrovirus vector was derived from the pMX vector (Kitamura *et al*., 2003), and contains an EGFP epitope tag downstream of the MCS linked by an IRES element, and puromycin and ampicillin selection markers. The transcript unit is flanked by the retroviral (Moloney Murine Leukaemia virus, or MMLV) long terminal repeats (LTRs) on the 5’ and 3’ ends. The LTRs encodes eukaryote-like promoter/enhancer sequences for transcription of the gene of interest after integration into the genome of

the virus packaging cell line, which also contains the viral *env* gene that encodes envelop protein required for assembly of complete viral particles.

The pcDNA5-FRT vector was used to encode cDNAs of proteins that require inducible expression, due to cytotoxicity from constitutional overexpression. The vector contains a CMV/2x TetO2 promoter/enhancer sequence upstream of the MCS, and a Flp Recombinase Target (FRT) site upstream of a hygromycin resistance gene, which is activated upon Flp recombinase-mediated integration into the host genome.

For microRNA-mediated gene silencing in mammalian cells, the expression vector pcDNA6.2-GW/EmGFP-miR (Life Technologies, K4939-00) was used. It allows polycistronic transcription of the EmGFP tag and up to three miRNA sequences under the control of the CMV promoter. It has blasticidin and spectinomycin resistance markers for selection in mammalian and bacterial cells, respectively.

2.2.2 Propagation of plasmid DNA

Chemically competent DH5α *E. coli* cells were slowly thawed on ice. 1 µg of plasmid DNA was incubated with 50 µL of cells on ice for 30 minutes. Cells were heat-shocked in 42°C water bath for 45 seconds, and cooled on ice for 2 minutes. 500 µL of LB was added to the cells, and the culture was incubated at 37°C for 1 hour at 225 rpm shaking. Transformants were selected on LB agar plates with 50 µg/mL selection antibiotic (ampicillin, kanamycin, or spectinomycin) at 37°C overnight. Single colonies were inoculated in 5 mL (for minipreps) or 100 mL (for midipreps) LB media with 50 µg/mL of appropriate selection antibiotic, and culture was incubated at 37°C overnight shaking at 225 rpm. Plasmids were extracted using the Qiagen DNA extraction kits (QIAprep® Spin Miniprep Kit and QIAprep® Plasmid Midiprep Kit) following the manufacturer's instructions.

2.2.3 Quantification of DNA/RNA concentration

Plasmid DNA concentration was determined using the NanoDrop ND-Spectrophotometer (software version V) at a wavelength of 230 nm. A ratio of 260/280 absorbance between 1.8 – 2.0 indicates the preparation is free from contaminants that strongly absorbs at 280 nm.

2.2.4 DNA agarose gel electrophoresis

Electrophoresis grade agarose was dissolved in 1 x TBE buffer (89 mM Tris, 89 mM boric acid, 2 mM EDTA pH 8.0) to make 1 % w/v agarose gels. 2 µg/mL ethidium bromide was added to the gel mixture and the gel was poured and set in a gel tray. DNA samples were loaded to the gel in 1 x loading buffer (0.04 % w/v bromophenol blue, 2.5 % w/v Ficoll). 1 kb plus DNA ladder (Invitrogen, 10787018) was loaded as marker. The sample was subjected to electrophoresis at 100 V for 40 minutes. DNA was visualised by UV transillumination.

2.2.5 DNA sequencing

Plasmid DNA was sequenced by Sanger-sequencing (GATC Biotech) using plasmid-specific primers.

2.2.6 TOPO-TA Cloning

FastStart High Fidelity PCR System (Roche Applied Science, 03553426001) was used to generate PCR fragment for subsequent TOPO-TA Cloning. In a 25 µL reaction, 10 ng of template DNA, 200 µM dNTPs, 200 µM of each oligonucleotide primers, 1 U of Taq DNA polymerase, 1.8 mM $MgCl_2$, and 1 µL of DMSO were added in 1 x reaction buffer. Thermocycling was performed on a Techne TC-3000 x thermocycler (Bibby Scientific) as follows: initial denaturation at 95°C for 2 minutes; 35 cycles of 95°C for 30 seconds, (T_m of primers -5°C) annealing for 30 seconds, 72°C extension for 45 seconds plus 1 minute per additional kb plasmid length; with final extension at 72°C for 7 minutes.

Freshly amplified PCR product was analysed by agarose gel electrophoresis for specificity of the amplicon. Further purification was performed if necessary using the Qiaquick Gel Extraction Kit (Qiagen). The TOPO-TA Cloning Kit (Invitrogen) was used to ligate the PCR product with the pCR2.1-TOPO vector using the following reaction: 1 µL of salt solution, 1 µL of vector, 4 µL of PCR product. The ligation reaction was incubated at room temperature for 15 minutes, then added to 50 µL of the chemically competent TOP10 cells supplied with the kit. The cells were kept on ice for 10 minutes, then heat-shocked in 42°C water bath for 45 seconds, and cooled on ice for 2 minutes. 500 µL of LB was added to the cells, and the culture was incubated at 37°C shaking at 225 rpm for 1 hour. The transformants were selected on LB agar plates containing 50 µg/mL ampicillin and 40 mM x-gal at 37°C overnight. Single white colonies were picked to inoculate 5 mL LB media with 50 µg/mL ampicillin overnight at 37°C shaking at 225 rpm. Plasmid DNA was extracted with the QIAprep® Spin Miniprep Kit following manufacturer's instructions. Purified minipreps were then digested with appropriate restriction endonucleases and analysed by agarose gel electrophoresis to confirm correct size and orientation of the inserts. Plasmid DNA with the correct size and orientation of inserts were then analysed by PCR sequencing to confirm no extra mutations were introduced to the insert during initial PCR amplification.

2.2.7 Restriction endonuclease digestion

DNA of the appropriate concentration (0.5 – 5 µg) was incubated with 1 – 2 U of appropriate restriction enzyme for 2 hours at 37°C. Complete digestion of the DNA was determined by comparison to an undigested control sample by agarose gel electrophoresis. If appropriate, DNA fragments were purified using Qiagen QIAquick® Gel Extraction Kit and the DNA concentration was quantified as described above.

2.2.8 DNA ligation

DNA ligation reactions were set up according to Sambrook and Russell protocol

(Sambrook and W Russell, 2001) at vector to insert molar ratio of $\geq$ 1:3. Reactions were incubated with 1 U of T4 DNA ligase overnight at 16°C in a total volume of 10 µL. 5 µL of the ligation reaction was transformed into chemically competent DH5α cells as described above in **Section 2.2.6**. Plasmid DNA was extracted according to manufacturer's instructions for the QIAprep® Miniprep Kit (Qiagen, 27104). The presence of the insert and correct orientation was confirmed by digestion of the plasmid by restriction digest and analysis by agarose gel electrophoresis.

2.2.9 Site-directed mutagenesis

The KOD Hot Start DNA polymerase (Merck Millipore, 71086) was used to for PCR-based site-directed mutagenesis. Primers used are listed in **Table 2.4**. In a 50 µL reaction, 75 ng template DNA, 15 µM forward and reverse primers, 5 µL dNTPs (2 mM of each nucleoside), 2 µL $MgSO_4$ (25 mM), 1 µL PCR-grade DMSO and 1 µL KOD polymerase were added to 1 x reaction buffer. Thermocycling was performed using a Techne TC-3000X thermocycler with these conditions: initial denaturation at 95°C for 5 minutes; 18 cycles of 95°C for 1 minute, (T_m of primers -5°C) annealing for 1 minute, 68°C extension for 1 minute/kb template DNA; and final extension at 68°C for 10 minutes. 5 µL of the amplified PCR reaction was analysed by agarose gel electrophoresis to assess specificity of the amplicon. 20 U of *Dpn1* (NEB, R0176) was added to the rest of the PCR reaction to digest away methylated parental strand of the template by incubation at 37°C for 1 hour. 5 µL of the digested PCR reaction was then used to transform 100 µL of chemically competent DH5α cells as described in **Section 2.2.6**. Single colonies were picked to inoculate 5 mL of LB with 50 µg/mL appropriate selection antibiotic, cultures were grown for 16 hours at 37°C shaking at 225 rpm. Plasmid DNA was extracted using the QIAprep® Spin Miniprep Kit following manufacturer's instructions. Restriction endonucleases digestion followed by agarose gel electrophoresis was used to identify clones with correct insert size and orientation. These clones were sequenced by GATC Biotech (Konstanz, Germany), to confirm

Primer name	Sequence
TDP1^{S81A} (F)	GGCAGAAAAGCGGTGCCCAGGAGGACCTCGGC
TDP1^{S81A} (R)	GGCGAGGTCCTCCTGGGCACCGCTTTTCTGCC
TDP1^{S81E} (F)	GGCAGAAAAGCGGTGAGCAGGAGGACCTCGGC
TDP1^{S81E} (R)	GGCGAGGTCCTCCTGCTCACCGCTTTTCTG CC
TDP1^{K111R} (F)	GCTGAGAAAGTGGTGATCAGAAAGGAGAAAGACATCT CT
TDP1^{K111R} (R)	AGAGATGTCTTTCTCCTTTCTGATCACCACTTTCTCAG C
TDP1^{TR} miRNA #1 (F)	GAGGTTCACGATATCAAGCAGCGCGAAAGTGAGGAAG AAAAG
TDP1^{TR} miRNA #1 (R)	CTTTCGTCGCTGCTTGATATCGTGAACCTCCTCCCATA ATC
TDP1^{TR} miRNA #2 (F)	CTTCTGCCTCTCAAGTAGCGACGATGAGCTGCAACCA G
TDP1^{TR} miRNA #2 (R)	CTCATCGTCGCTACTTGAGAGGCAGAAGCCGAGGTCC TC
TOP1mt^{T456A,N460H} (F)	GCCCTGGGCGCGTCCAAGCTCCACTACCTGG
TOP1mt^{T456A,N460H} (R)	CCTGGGGTCCAGGTAGTGGAGCTTGGACGCGCCCAG GGC

Table 2.4: *Site-directed mutagenesis PCR primers*
Primers were designed according to the QuikChange XL Site-Directed Mutagenesis Kit from Stratagene to incorporate a single amino acid change at the protein level. For targeting-resistant cDNA, silent mutations were introduced using primers designed according to Zheng *et al*., 2004 *Nucl. Acid Res.* 32(14): e115. Nucleotide changes are indicated in red.

presence of the desired mutation.

2.2.10 Phenol: chloroform DNA extraction

To extract DNA from samples containing proteins, an equal volume of phenol:chloroform:isoamyl alcohol solution (VWR, A0944.0100) was added to the DNA solution. The mixture was vortexed briefly, then centrifuged at 13000 rpm for 5 minute. The top layer was carefully transferred to a clean tube, and mixed with equal volume of chloroform:IAA, vortexed briefly, then centrifuged at 13000 rpm for 2 minutes. The top layer is again transferred to a clean tube, then mixed with 2 x volume of 100 % ethanol containing 0.3 M sodium acetate and 20 µg glycogen. The DNA was precipitated by incubating at -80°C for 45 minutes and centrifugation at 13000 rpm for 30 minutes. The supernatant was carefully transferred to a clean tube, and the DNA pellet was washed twice with 70 % ethanol. The pellet was then air-dried until transparent, and resuspended in 50 µL distilled water. If after DNA quantification, the concentration was lower than expected, the saved supernatant was centrifuged again and the DNA pellet processed as described above.

2.3 Yeast two-hybrid assay

2.3.1 Yeast media

YPD medium: 20 g/L peptone, 10 g/L yeast extract, 20 g/L yeast granulated agar (for plates), 2 % glucose

Yeast minimum medium with Histidine (His+ YMM): 80 mg/L adenine, 40 mg/L histidine, 20 g/mL yeast granulated agar (for plates), 2 % glucose, 6.7 g/L yeast nitrogen base

Yeast minimum medium without Histidine (His- YMM): 80 mg/L adenine, 2 % glucose, 6.7 g/L yeast nitrogen base with ammonium sulphate, 25 mM 3-amino-1,2,4-triazole, 20 g/mL yeast granulated agar (for plates).

2.3.2 Yeast strain maintenance and storage

Wildtype *S. cerevisiae* strain Y190 (Clontech) was grown at 30°C on YPD agar plate, and re-streaked on fresh plate every third day or when cells turned pink. Transformed Y190 was selected and maintained on YMM plates. For long-term storage, untransformed Y190 cells were stored in YPD medium with 25 % glycerol at -80°C. Transformed cells were stored in YMM with 25 % glycerol at -80°C.

tdp1Δ/rad1Δ S. cerevisiae strain (YW812) was generated by Thomas Wilson (Vance and Wilson, 2002) and provided by Keith Caldecott.

2.3.3 Small-scale lithium acetate yeast co-transformation

2.3.3.1 Stock solutions

10 x TE buffer: 100 mM Tris HCl, 10 mM EDTA, pH 7.5. Autoclave to sterilise.

10 x Lithium acetate (LiAc): 1 M lithium acetate, pH 7.5 with dilute acetic acid. Autoclave to sterilise

50 % PEG: 50 % w/v PEG (MW 3350) in sterile distilled H_2O. Dissolve by warming to 50°C

Salmon sperm DNA: 10 mg/mL salmon sperm DNA (Sigma, D1626), sonicated 2 x 30 seconds

2.3.3.2 Preparation of competent Y190 cells

20 mL YPD medium was inoculated with a few colonies of healthy Y190 cells. Cells were grown at 30°C overnight at 200 rpm. Overnight culture was diluted in YPD medium to an OD_{600} of ~ 0.2_{AU} and incubated at 30°C at 200 rpm until OD_{600} reached $0.6 – 0.8_{AU}$ (at least two divisions). Culture was centrifuged at 2500 rpm for 5 minutes, then the pellet washed with 1 x TE buffer, followed by washing with 1 mL 100 mM LiAc. Cells were resuspended with 400 µL 100 mM LiAc, 50 µL of cell suspension were transferred to a 1.5 mL Eppendorf tube, briefly centrifuged to remove the LiAc, and

kept on ice until ready to use.

2.3.3.3 Lithium acetate transformation

Salmon sperm DNA was denatured by boiling at 90°C for 10 minutes, then cooled on ice for 10 minutes. The following were added to the cell pellet in this order: 240 µL 50 % PEG, 36 µL 1 M LiAc, 10 µL salmon sperm DNA, 1 – 5 µg plasmid DNA, and sterile H_2O to make up to 360 uL final volume. The transformation reaction was vortexed vigorously for 1 minute, then incubated at 30°C for 30 minutes. The cells were heat-shocked in 42°C water bath for 20 minutes (strain specific), then centrifuged at 6000 rpm for 15 seconds. The cells were gently resuspended in 1 mL sterile H_2O, and 200 µL of the suspension was plated on His+ YMM selection plate. Transformants were selected by growing at 30°C for 72 hours. 10 – 20 colonies were transferred to 100 µL 1 x TE, and 50 µL each were plated on fresh His+ and His- YMM selection plates, then incubated for 2 – 3 days at 30°C until enough healthy cells were gown for β-galactosidase lift assay.

2.3.4 β-galactosidase lift assay

Stock solutions

Z buffer: 62.5 mM Na_2HPO_4,40 mM NaH_2PO_4, 10 mM KCl, 1 mM $MgSO_4$

X-gal: 40 mg/mL in dimethylformamide

Cells from His+ YMM selection plate were transferred to a 3 mm Whatman filter paper by gentle pressure applied with a roller. The filter paper was then snap frozen with liquid nitrogen for 10 seconds and thawed completely at room temperature. This was repeated three times to permeabilise the yeast cell wall. The filter paper was place with cells side up on top of a clean 3 mm Whatman filter paper pre-soaked in x-gal/Z-buffer solution (83.5 µL X-gal, 10 mL Z Buffer, 27 µL β-mercaptoethanol) at 30°C for up to 8 hours until blue colour development.

2.3.5 Histidine prototrophy

Following lithium acetate transformation, Y190 cells were grown on YMM plates lacking histidine for 72 hours at 30°C. Successfully transformed clones would co-express histidine thus allowing for growth on His- YMM plates.

2.3.6 Quantitative β-galactosidase assay

2.3.6.1 Preparation of yeast culture

For each yeast strain 1 – 2 mm of cells from a single colony was picked to inoculate 5 mL His+ YMM (for transformed strain) or YPD medium (for untransformed strain), and incubated at 30°C at 250 rpm shaking for 16 hours. Overnight culture was diluted in 50 mL YPD medium, and incubated at 30°C at 250 rpm shaking until OD_{600} reached $0.5 – 0.8_{AU}$ (at least two doubling cycles). 10 mL of the culture was pelleted for the assay.

2.3.6.2 Liquid culture assay

Cell pellets were washed and resuspended in 300 µL buffer 1 (100 mM Hepes, 155 mM NaCl, 4.5 mL L-aspartate, 1 % w/v BSA, 0.05 % v/v Tween 20, pH 7.3). 10 µL cell suspension was diluted in 990 µL buffer 1 and OD_{600} was measured with a spectrophotometer. 100 µL of cell suspension was snap frozen in liquid nitrogen for 30 seconds, and thawed in 37°C water bath for 30 seconds. Three freeze-thaw cycles were required to permeabilise the cell wall. The cells were then mixed with 700 µL of 2.23 M CPRG in buffer 1. When reaction mixture turned from yellow to red, 500 µL of 3 mM $ZnCl_2$ was added to stop the reaction. Cells were spun down and the OD_{578} of the supernatant was measured. β-galactosidase units were calculated as:

$$1000 \times OD_{578} / (t \times V \times OD_{600})$$

where t = stop time – start time (in minutes), V = 0.1 x concentration factor

1 unit of β-galactosidase is defined as the amount which hydrolyses 1 µmol of CPRG to chlorophenol red and D-galactose per minute per cell.

2.3.7 Yeast protein extraction

Yeast culture prepared as for quantitative β-galactosidase assay was pelleted and washed twice with distilled H_2O. Cells were then lysed in 100 µL SDS lysis buffer (8 M urea, 5 % w/v SDS, 40 mM Tris-HCl pH 6.8, 0.1 mM EDTA pH 8.0, 0.4 mg/mL bromophenol blue, 1 % v/v β-mercaptoethanol, 1 % v/v yeast protease inhibitors cocktail) per 7.5 OD_{600} units of cells, at 70°C for 10 minutes. To completely disrupt the cell wall, 100 µL of acid-washed glass beads was added to the lysate, followed by vigorous vortexing for 1 minute, centrifugation at 14000 rpm for 5 minutes, and boiling the supernatant at 90°C for 5 minutes.

2.3.8 Yeast two-hybrid library screen

2.3.8.1 Test transformation

Maxiprep of the pACT2 human cDNA library was serially diluted to 10^{-4}, 10^{-5}, 10^{-6} and 10^{-7} on ice. 20 µL of freshly thawed DH10β cells were diluted with 30 µL of sterile H_2O. 1 µL of DNA was added and gently mixed, and the cells were then transferred to a 1 mm electroporation cuvette. The cells were electroporated at 200 Ω, 25 µF, 2.0 kV, and immediately transferred to 1 mL SOC medium and recovered for 1 hour at 37°C shaking at 225 rpm. 100 µL of the culture was plated on LB plates containing 100 µg/mL ampicillin and grown at 37°C overnight. Transformation efficiency was calculated and the concentration of DNA dilution that gave at least 10^7 clones per µg DNA was used for subsequent large-scale library transformation.

2.3.8.2 Large-scale library transformation of DH10β

Stock solutions

2 x LB: 100 g peptone, 50 g yeast extract, 50 g NaCl. Bring to 5 L with sterile H_2O

2 x LB agarose: 1.8 g SeaPrep agarose (Lonza, 50302), 450 mL 2 x LB. Make 10 bottles of 500 mL. Stir to dissolve and autoclave.

2 x LB glycerol: 43.75 mL 2 x LB, 6.25 mL 100 % glycerol. Autoclave.

His+ Trp- YMM: 50 mg/L adenine, 50 mg/L histidine, 150 mg/L leucine, 125 mg/L lysine, 50 mg/L methionine, 50 mg/L uracil, 2 % glucose, 6.7 g/L yeast nitrogen base with ammonium sulphate, yeast granulated agar (for plates)

Bottles of 2 x LB agarose were warmed to 37°C and supplemented with 100 µg/mL ampicillin. 200 µL of DH10β cells were diluted with 300 µL of sterile H_2O, and transformed with 10 x the optimal amount of library DNA that gave 10^7 transformants as determined by small-scale test transformation. 1/10 of the transformation was added to each bottle of 2 x LB agarose, and stirred for 2 minutes. Bottles were then cooled in ice bath for 1 hour, then incubated at 30°C for 2 days. Thereafter, transformants were collected by stirring the agarose for 2 minutes, then centrifuging 100 mL of the culture at 6000 rpm for 20 minutes at room temperature. The pellet was resuspended in 50 mL sterile 2 x LB glycerol, cooled on ice for 1 hour, then stored at -80°C for long-term. The remainder of the 900 mL culture was similarly centrifuged to recover the cell pellet, then washed with distilled H_2O at 4500 rpm for 10 minutes. Plasmid DNA was extracted using the Qiagen Endotoxin-free Maxiprep kit following the manufacturer's instructions.

2.3.8.3 Optimisation of library transformation

Y190 cells were first transformed with the bait plasmid pGBKT7-TDP1 or pGBKT7-TDP1^{S81E} using the small-scale lithium acetate based method as outlined in **Section 2.3.3.3**. Single clones of stable transformants were propagated on His+ Trp- YMM plate, or stored in 25 % glycerol at -80°C for long-term. These clones were then transformed with the human cDNA library in pACT2 (pACT2-cDNA library) as described in **Section 2.3.3.3**. 10-fold serial dilutions of the transformation reaction were plated on His+ YMM plates at 30°C for 3 days. Transformation efficiency was determined by:

Cfu/µg = (No. of clones x final cell volume) / (volume plated x dilution factor x µg DNA)

2.3.8.4 Library transformation

Once the optimal concentration of library DNA that gave 10^7 transformants or higher per µg DNA was identified, the large-scale transformation was performed. A few colonies of Y190 stably transformed with pGBKT7-TDP1 or pGBKT7-TDP1^{S81E} were used to inoculate 20 mL of His+ Trp- YMM and grown at 30°C at 200 rpm overnight. After measuring the OD_{600} of the overnight culture, the culture was diluted approximately 1:6 to give an OD_{600} of 0.2 and a volume of ~ 120 mL. The culture was then incubated at 30°C shaking at 200 rpm for approximately 4 hours until the OD_{600} reached 0.6. The cells were pelleted at 4500 rpm for 8 minutes, washed once with sterile water, then washed with 3 mL of 100 mM LiAc, and resuspended in a final volume of 1.2 mL of 100 mM LiAc. The library transformation was then performed as for the small-scale lithium acetate transformation in 21 simultaneous repeats, including one transformation using the empty pACT2 vector as negative control for histidine prototrophy. After heat-shock the cells were washed and pelleted, and the entire transformation reaction was plated on His- YMM plate and grown at 30°C for 5 – 7 days. Single colonies that formed were picked and re-streaked on a His+ YMM and a His- YMM plate each and grown for 3 days at 30°C. A few colonies from each His- YMM plate were picked and used to inoculate 2 mL of His- YMM culture overnight at 30°C shaking at 200 rpm. From the overnight culture, 0.7 mL was frozen down in 25 % glycerol for long-term storage, the remaining was used for plasmid extraction and analysis.

2.3.8.5 Plasmid extraction and analysis

Approximately 1.3 mL of the freshly grown cells in His- YMM culture was pelleted and resuspended in 250 µL of Buffer P1 of the Qiagen Miniprep kit. 250 µL of acid-washed glass beads were added to the cell suspension, and the mixture vortexed vigorously for

1 minute to disrupt the cell wall, then briefly centrifuged. The supernatant was then used for plasmid extraction using the Qiagen Miniprep kit following the manufacturer's instructions, and the plasmid eluted with 25 µL EB buffer. The plasmid DNA was then used to transform the electrocompetent *E. Coli* strain DH10β. 5 µL of DNA was mixed with 50 µL of DH10β cells and transferred to a 1 mm electroporation cuvette on ice, the electroporation was performed at 2 kV, 200 Ω, 25 µF, and the cells were immediately transferred to a 1.5 mL Eppendorf tube containing 1 mL SOC medium and recovered at 37°C at 225 rpm for 1 hour. The entire transformation mixture was plated on LB agar plate containing 50 µg/mL ampicillin and incubated at 37°C overnight. One single colony was then picked from each plate to inoculate 5 mL LB medium containing 50 µg/mL ampicillin and grown at 37°C overnight. The overnight culture was used to extract the pACT library plasmid DNA using the Qiagen Miniprep kit according to the manufacturer's instructions. The purified plasmid DNA was then sequenced by GATC Biotech. The DNA sequence was identified using the Genome Browser Human BLAT database (Feb. 2009 version) hosted by the University of California Santa Cruz (http://genome.ucsc.edu/cgi-bin/hgBlat?command=start).

2.4 Yeast clonogenic survival assay

Wildtype (Y190) or *tdp1*Δ *rad1*Δ (YW812) *S. cerevisiae* cells were transformed with pGKT7 plasmids encoding myc-TDP1, myc-TDP1^{S81A} or Myc (empty vector) as described in **Section 2.3.3.3**. The transformants were selected on His+ Trp- YMM plates at 30°C for 72 hours. A single colony was picked from each plate and resuspended in 200 µL sterile water and serially diluted at 10-fold up to 10^{-4} dilutions. 10 µL from each dilution was plated on His+ Trp- YMM with or without 20 µM of CPT. Cells were left at 30°C for 72 hours to form macroscopic colonies.

2.5 Mammalian cell culture

2.5.1 Maintenance of cell lines

The human cell lines A549, HEK293, MRC5 were grown as monolayers in α-MEM media supplemented with 10 % FCS, 100U Penicillin, 100 µg Streptomycin, and 2 mM L-glutamine. Cells were maintained in humidified 5 % CO_2 incubators set at 37°C for no more than 20 passages.

Primary mouse embryonic fibroblasts were grown as monolayers in D-MEM media containing 4500 mg/L D-glucose, sodium bicarbonate, and pyruvate supplemented with 15 % FCS, 100 U Penicillin, 100 µg Streptomycin, 2 mM L-glutamine and 1 x non-essential amino acid solution. Cells were maintained in humidified 2 % O_2, 5 % CO_2 incubators set at 37°C for no more than 7 passages. Mouse embryonic fibroblasts grown for more than 13 passages were considered immortalised, and were maintained in growth media lacking non-essential amino acids, and at normal atmospheric O_2 level.

Chicken DT40 B-lymphocytes were grown in suspension at no more than 10^6 cells/mL in RPMI medium supplemented with 10 % FCS, 1 % chicken serum (Sigma, 16110-082), 100 U Penicillin, 100 µg Streptomycin, 2 mM L-glutamine and 25 µM β-mercaptoethanol. Cells were maintained in humidified 5 % CO_2 incubators set at 39°C for no more than 40 passages.

Human lymphoblastoid cells (AG87 and JRL1) were grown in suspension at a density of 5×10^5 cells/mL. Cells were maintained in RPMI1640 media supplemented with 10 % FCS Good US origin (PAN Biotech, P40-38500), 100 U Penicillin, 100 µg Streptomycin, and 2 mM L-glutamine.

Flp-In T-Rex 293 cells (Thermo Fisher, R780-07) were grown in monolayer and maintained in DMEM supplemented with 10 % Tetracycline-free FCS (Biosera, FB1001T/500), Pen/Strep, L-glutamine, 100 µg/mL zeocin (InvivoGen, ant-zn-1) and

10 µg/mL blasticidin (InvivoGen, ant-bl-1).

For long-term storage cells were suspended in 1 mL aliquots of 90 % FBS with 10 % DMSO, slowly cooled to -80°C overnight and transferred to liquid nitrogen storage. To revive cells, the frozen aliquot was quickly thawed in 37°C water bath and resuspended in warmed media. Cells were centrifuged at 1500 rpm for 5 minutes to remove residual DMSO, and grown in fresh media for 2 – 3 passages before experimental use.

2.5.2 DNA-mediated gene transfer

2.5.2.1 Calcium phosphate co-precipitation

Plasmid DNA for transfection was prepared using Qiagen Plasmid Midiprep Kit following manufacturer's instructions. HEK293 cells in logarithmic phase of growth were seeded at a density of 5×10^6 cells per 10 cm dish and left to adhere at 37°C overnight. Fresh media was added to the cells one hour prior to transfection. 0.5 mL of DNA/$CaCl_2$ mix (10 µg of plasmid DNA, 245 mM $CaCl_2$) was added drop-wise to 0.5 mL of 2 x Hepes Buffered Saline (275 mM NaCl, 1.5 mM Na_2HPO_4, 55 mM Hepes) and mixed by continuous bubbling using a Pasteur pipette. The transfection mixture was then added drop-wise over cells. Cells were incubated at 37°C overnight, then washed twice with PBS, and left to recover in fresh media for another 24 hours before harvesting.

2.5.2.2 Liposome-based transfection reagent

Plasmid DNA for transfection was prepared using Qiagen® Plasmid Midiprep Kit. A549 or Flp-In T-Rex 293 cells in logarithmic phase of growth were seeded at a density of 2×10^5 cells per 3.5 cm dish and left to adhere at 37°C overnight. Fresh media was added to the cells one hour prior to the transfection. 3 µL Genejuice transfection reagent (Novagen, 70967-3) per µg plasmid DNA was added drop-wise to 100 µL serum free OptiMEM culture medium, mixed briefly and incubated for 5 minutes at

room temperature. 1 – 2 µg of each plasmid DNA was added drop-wise to the Genejuice®/medium, mixed by pipetting and incubated for 10 – 15 minutes at room temperature. 100 µL of Genejuice®/DNA mix was added drop-wise to the cells and incubated for 24 hours at 37°C.

2.5.2.3 Retroviral transduction

The retroviral packaging cell line Phoenix (gift from Dr Conchita Vens) were transfected with pMXPIE-TDP1, pMXPIE-TDP1^{K111R}, pMXPIE-hSOD1, pMXPIE-hSOD1^{G93A} or pMX-PIE (empty vector) using GeneJuice Transfection Reagent as described by manufacturer. Transfection efficiency was estimated by GFP co-expression using fluorescence microscopy. If the estimated transfection efficiency was above 80 %, the supernatant containing recombinant protein-expressing retrovirus particles was collected and filter-sterilised. 10 µg/mL polybrene was added to improve viral adherence to target cell surface. The supernatant was then added to a 6 cm dish containing 2 x 10^5 adherent immortalised *Tdp1*$^{-/-}$ MEFs and incubated at 37°C overnight. The supernatant was removed and replaced with fresh growth media and left for another 24 hours before harvesting.

2.5.3 Gene-targeted silencing

The sequences of RNAi-mediated gene silencing are listed in **Table 2.5**. Approximately 3 x 10^5 MRC5 cells in log phase growth were suspended in 5 mL normal growth media in 6 cm dish immediately before transfection. 80 µL of serum-free medium Opti-MEM was mixed with 5 µL of Metafectene Pro Transfection Reagent (Cambio, T040-2.0). In a separate tube, 80 µL of Opti-MEM was mixed with 80 µM of siRNA. The siRNA mixture was added to the Metafectene mixture, and incubated at room temperature for 20 minutes. The Metafectene/siRNA mixture was then added drop-wise on top of the cells, and incubated at 37°C for 24 hours. A second transfection was then repeated, and cells were harvested after further 24-hour

Target	Sequence
Scrambled siRNA	UUCUUCGAACGUGUCACG
Human TOP1 siRNA* (NM_003286.2)	#1 GAAAAUGGCUUCUCUAGUC #2 GAUUUCCGAUUGAAUGAUU #3 GCACAUCAAUCUACACCCA #4 CGAAGAAGGUAGUAGAGUC
Human TDP1 siRNA* (NM_001008744.1)	#1 GGAGUUAAGCCAAAGUAUA #2 UCAGUUACUUGAUGGCUUA #3 GACCAUAUCUAGUAGUGAU #4 CUAGACAGUUUCAAAGUGA
Scrambled shRNA*	TGCTGTTGACAGTGAGCG**ATCTCGCTTGGGCGAGAGT** **AAG**TAGTGAAGCCACAGATGTACTTACTCTCGCCCAA GCGAGAGTGCCTACTGCCTCGGA
Human UBE2I shRNA* (NM_194260.2)	TGCTGTTGACAGTGAGCG**AGCCTACACGATTTACTGC** **CAA**TAGTGAAGCCACAGATGTATTGGCAGTAAATCGT GTAGGCCTGCCTACTGCCTCGGA
TDP1 miRNA (NM_001008744.1)	#1 TGCTGATCACTACTAGATATGGTCCAGTTTTG GCCACTGACTGAC**TGGACCATCTAGTAGTGAT** #2 TGCTGATCACTGCTGGACAGACACCAGTTTT GGCCACTGACTGAC**TGGTGTCTCCAGCAGTGAT**

Table 2.5: *RNAi sequences*
* indicate purchases from Dharmacon. TDP1 miRNA designed using Thermo Fisher BLOCK-iT™ RNAi Designer (https://rnaidesigner.lifetechnologies.com/rnaiexpress/design.do) and synthesized by Integrated DNA Technologies, Belgium)

incubation.

MRC5 cells in log phase growth were seeded at 8 x 10^4 in 3 cm petri dishes, 16 – 24 hours before transfection. Transfection of the plasmid encoding shRNA against UBE2I was done using Genejuice transfection reagent. After 48 hours cells were transferred to T75 flasks and stably integrated clones were selected with 0.5 µg/mL puromycin for 7 days.

2.5.4 Selection and maintenance of stable cell lines

MEFs transduced with hTDP1, hTDP1^{K111R}, hSOD1 and hSOD1^{G93A} were selected with 1 µg/mL puromycin for 3 days. Pooled populations of stable clones were analysed for GFP expression by fluorescence microscopy, and TDP1 or SOD1 expressions by Western blotting using antibodies against TDP1 or SOD1 antibody, respectively (**Tables 2.6A, 2.7A**).

Stable Flp-In T-Rex 293 cell lines expressing miRNA sequences were selected with 100 µg/mL hygromycin B (Invivogen, ant-hg-1) for 3 weeks until formation of macroscopic colonies. Single colonies were picked and expanded for 2 more weeks. The cells were then harvested and the whole cell lysates analysed for protein expression by Western blotting using antibodies listed in **Tables 2.6A** and **2.7A**.

2.6 Analyses of cellular protein extracts

2.6.1 Preparation of whole cell protein extracts

Approximately 5 x 10^5 cells were harvested, washed with PBS twice, resuspended in 50 µL of lysis buffer (20 mM Tris-HCl pH 7.5, 10 mM EDTA pH 8.0, 100 mM NaCl, 1 % Triton X-100, 1 x protease inhibitor cocktail (Roche, 4693159001), 1 x phosphatase inhibitor cocktail (Roche, 4906837001), 25 U.ml^{-1} benzonase (Merck, 71205) and incubated on ice for 30 minutes. Cell lysates were cleared by centrifugation at 13000 rpm at 4°C for 15 minutes. The concentration of soluble proteins was quantified

by the Bradford assay (Bio-Rad, 500-0001). For long-term storage the cell lysates were kept at -80°C.

2.6.2 Protein co-immunoprecipitation

Human HEK293 cells were seeded at 2 x 10^6 cells per 10 cm petri dish 24 hours before transfection. Cells were transfected with plasmids coding for Myc-tagged proteins of interest using calcium phosphate-based method and harvested after 48 hours. For cross-linking experiments, cells were fixed with 1 % paraformaldehyde for 10 minutes, washed once with PBS, washed with 100 mM glycine, then washed again with PBS. 200 µL lysis buffer (20 mM Hepes pH 7.4, 40 mM NaCl, 2 mM $MgCl_2$, 0.5 % NP40, 1 x protease inhibitor cocktail, 1 x phosphatase inhibitor, 20 mM *N*-ethyl maleimide, and 25 $U.ml^{-1}$ benzonase) was used to lyse 10 cm dish of cells on ice for 30 minutes. The lysate was centrifuged at 13000 rpm for 10 minutes at 4°C to isolate the soluble fraction, 30 µL of which was removed and resuspended in 30 µL of 2 x SDS lysis buffer and boiled at 90°C for 15 minutes, the sample was used as input control on a SDS-PAGE gel later. For the rest of the lysate, the NaCl concentration was adjusted to 140 mM, and 2 µL of anti-Myc antibody was added. The lysate was incubated with the antibody for 1 hour at 4°C, then in 30 µL proteinase G beads for 1 hour at 4°C. The beads were centrifuged at 1500 rpm, and washed at least three times with wash buffer (20 mM Hepes pH 7.4, 140 mM NaCl). The beads were resuspended in 50 µL 2 x SDS-PAGE lysis buffer (**Section 2.6.3**), boiled at 90°C for 15 minutes, then briefly centrifuged. 10 µL of the supernatant was loaded on SDS-PAGE gel along with the 3 µL of the input sample.

2.6.3 SDS-polyacrylamide gel electrophoresis (SDS-PAGE)

For protein fractionation by SDS-PAGE, polyacrylamide gels were made using the Sambrook and Russell method (Sambrook and W Russell, 2001) and cast in a 1 mm XCell SureLock Mini-Cell cassette (Fisher Scientific, VXNC2010). 50 – 100 µg of

soluble proteins from each cell lysate sample were mixed with SDS-PAGE lysis buffer (final concentration 50 mM Tris pH 8.0, 2 % w/v SDS, 10 % v/v glycerol, 0.1 % w/v bromophenol blue, 200 mM DTT). Samples were denatured at 90°C for 5 minutes, briefly centrifuged, then loaded onto a polyacrylamide gel. The Precision Plus Protein Dual Colour Standards (Bio-Rad, 1610374) was used as protein marker for proteins between 10 – 250 kDa. Electrophoresis was performed in the XCell SureLock Mini-Cell system using 1 x SDS running buffer (25 mM Tris, pH 8.3, 192 mM glycine, 0.1 % SDS) at 150 V for 1.5 – 2 hours.

The fractionated protein samples were either visualised by Coomassie brilliant blue staining (Bio-Rad, 161-0435) for 30 minutes, followed by de-staining in 30 % methanol, 10 % acetic acid; or processed for Western blotting by transferring to a 0.45 µm nitrocellulose membrane (Bio-Rad, 170-4271) at 25 V for 1.5 hour in transfer buffer (25 mM Tris, pH 8.3, 192 mM glycine, 20 % methanol) using the XCell SureLock Mini-Cell system.

2.6.4 Western blotting

Nitrocellulose membrane with transferred proteins was blocked with blocking buffer (5 % milk, 0.1 % Tween-20 diluted in PBS) for 1 hour at room temperature. The primary antibody was diluted in blocking buffer according to **Table 2.6A**. The membrane was incubated in the primary antibody overnight at 4°C, then washed three times for 5 minutes with PBS containing 0.1 % Tween-20. The HRP-conjugated secondary antibodies (**Table 2.7A**) were diluted 1:4000 in blocking buffer. The membrane was incubated in the secondary antibody for 1 hour at room temperature, then washed three times for 5 minutes with PBS containing 0.1 % Tween-20. The membrane was then incubated in the Clarity Western ECL blotting substrate (Bio-Rad, 1705060) for 5 minutes at room temperature and visualised using the ChemiDoc MP gel docking system (Bio-Rad, 1708280).

A

Antibody	Host species	Source (cat. no.)	Concentration
β-actin	Mouse	Sigma (A5316)	1:2000
Gal4-AD	Rabbit	Millipore (ABE476)	1:2000
GFP	Rabbit	Abcam (ab290)	1:2000
Ligase 3	Mouse	Abcam (ab587)	1:2000
Myc	Mouse	Cell Signalling (2276)	1:2000
Human OXPHOS cocktail	Mouse	Abcam (ab110411)	1:500
SOD1	Rabbit	Santa Cruz (sc-11407)	1:1000
TDP1	Rabbit	Abcam (ab4166)	1:2000
TOP1	Mouse	Santa Cruz (sc-32736)	1:1000
TOP1mt	Rabbit	Abcam (ab135423)	1:250
β-Tubulin	Mouse	Abcam (ab7792)	1:2000
UBE2I	Rabbit	Abcam (ab21193)	1:2000
VDAC1	Rabbit	Abcam (ab15895)	1 µg/ml
p-XRCC1 (S485, T488)	Rabbit	Bethyl Laboratories (A300-231A)	1:2000

B

Antibody	Host species	Source (cat. no.)	Concentration
53BP1	Rabbit	Bethyl Laboratories (A300-271A)	1:1000
p-H2AX (Ser139)	Mouse	Millipore (05-636)	1:800

Table 2.6: *Primary antibodies*
Source, type and working concentration for primary antibodies used for (A) immunoblotting and (B) immunofluorescence.

A

Antibody	Host species	Source (cat. no.)	Concentration
Mouse IgG (H + L)-HRP Conjugate	Goat	Bio-Rad (170-6516)	1:4000
Rabbit IgG (H + L)-HRP Conjugate	Goat	Bio-Rad (170-6522)	1:4000

B

Antibody	Host species	Source (cat. no.)	Concentration
Goat Anti-Mouse IgG (H+L)-Alexa Fluor 488	Goat	Molecular Probes (A28175)	1:800
Rabbit IgG-Alexa Fluor 555	Goat	Molecular Probes (A27039)	1:800

Table 2.7: *Secondary antibodies*
Source, type and working concentration for secondary antibodies used for (A) immunoblotting and (B) immunofluorescence.

2.6.5 TDP1 activity assay using the Gyrasol system

WCE proteins prepared as described in **Section 2.6.1** was diluted to 1 µg/µL in 1 x assay buffer (50 mM Tris pH 8.0, 5 mM $MgCl_2$, 80 mM KCl, 0.05 % TritonX-100) supplemented with 1 mM DTT. 13-mer DNA oligonucleotide substrate with 5'-FITC label and 3'-phosphotyrosine (5'-FITC-GATCTAAAAGACT(pY)-3') (Midland Certified Reagent, TX, USA) was diluted to 30 nM in 1 x assay buffer. 2 µg of WCE proteins was incubated with 10 nM substrate in 1 x assay buffer in a 15 µL reaction volume in a 384-well black flat-bottomed immunoassay plate for 10 minutes at 25°C. 30 µL of enhancer buffer (Gyrasol Technologies, KS, USA) and 2 µL sensor buffer (Gyrasol Technologies, KS, USA) were mixed together and added to each well to quench the reaction. FITC fluorescence was immediately measured using a BMG Labtech Pherastar plate reader at excitation and emission wavelengths of 490 nm and 520 nm, respectively (Walker *et al.*,2014).

2.6.6 TDP1 activity assay using C5.5-conjugated oligonucleotide substrate

Reactions were performed in 10 µL reaction volumes containing assay buffer (25 mM HEPES, pH 8.0, 130 mM KCl, 1 mM DTT), WCE (50 – 100 ng) and 50 nM Cy5.5 labelled substrate oligomer containing a 3 ′ -phosphotyrosyl group, (5 ′ -(Cy5.5)-GATCTAAAAGACT(pY)-3 ′) (Midland Certified Reagent Company Texas, USA).Reactions were carried out at 37°C for 1 hr and stopped by addition of 10 µL loading buffer (44 % deionized formamide, 2.25 mM Tris-borate, 0.05 mM EDTA, 0.01 % xylene cyanol, 1 % bromophenol blue). Samples were then heated at 90°C for 10 minutes prior to separation on a 20 % Urea SequaGel (Fisher, EC-833-1) by gel electrophoresis at 150 V for 1 hr. Reaction products were visualised by gel imaging using the Bio-Rad ChemiDoc MP imaging system at 635 nm and bands quantified using Image Studio Lite v5.2 (LI-COR).

Primer name	Sequence
Human ND1 (F)	CCCTAAAACCCGCCACATCT
Human ND1 (R)	GAGCGATGGTGAGAGCTAAGGT
Human B2M (F)	CCAGCAGAGAATGGAAAGTCAA
Human B2M (R)	TCTCTCTCCATTCTTCAGTAAGTCAACT
Human TOP1mt* 15873 (F)	TACTCAAATGGGCCTGTCCT
Human TOP1mt* 15873 (R)	AAAGACTTTTTCTCTGATTTGTCC
Mouse CO1 (F)	TGCTAGCCGCAGGCATTAC
Mouse CO1 (R)	GGGTGCCCAAAGAATCAGAAC
Mouse NDUFV1 F1	CTTCCCCACTGGCCTCAAG
Mouse NDUFV1 R1	CCAAAACCCAGTGATCCAGC

Table 2.8: *qPCR primers*
qPCR primers used for amplifying gDNA of the target genes and their sequences from 5’ to 3’.

2.6.7 Protein stability assay

Human TDP1, TDP1^{S81A} and TDP1^{S81E} were cloned into mammalian expression vector pCI-puro-Myc, and transfected into human A549 cell line using Genejuice transfection reagent. Expression levels were confirmed at two days by Western blotting. Transfected cells were treated with 30 μM CPT for 2 hours at 37°C, washed and left to recover in normal growth media for up to 24 hours in the presence or absence of cycloheximide, an inhibitor of protein synthesis. Samples were taken at 6- and 24-hour intervals to assess TDP1 expression levels by Western blotting.

2.7 DNA damage repair assays

2.7.1 Clonogenic survival assay

Sod1$^{+/+}$ and *SOD1*$^{G93A+/-}$ primary MEFs were seeded at 2000 – 10000 cells per 9 cm petri dish and incubated overnight in normal growth media. Similarly, immortalised *Tdp1*$^{-/-}$ MEFs complemented with wildtype hSOD1, hSOD1^{G93A} or empty vector were seeded at 1000 – 5000 cells; MRC5 cells were seeded at 500 – 3000. Cells were then treated with CPT (1 hour at 37°C), x-ray (250 kV at 12 mA), or H_2O_2 (10 minutes on ice), at the indicated doses. Cells treated with CPT or H_2O_2 were washed twice in PBS, and grown in normal growth media for 7 days. Cells were then fixed with 80 % ethanol for 15 minutes and stained with 1 % methylene blue. Percentage of colony survival was normalised to mock-treated sample. The average $\pm$1 standard errors of the mean (S.E.M.) were calculated from 3 independent experiments.

2.7.2 Cell viability assay using CellTiter-Blue reagent

Flp-In T-Rex 293 cells were induced with 1 μg/mL doxycycline for 24 hours, then seeded at densities of 2000 – 20000 cells/100 μL, and treated with the indicated concentrations of CPT or TBH in the absence of doxycline for 48 hours. Cell viability was measured using the CellTiter-Blue Viability Assay kit (Promega, G8080). 20 μL of the CellTiter-Blue reagent was mixed with the cells and incubated at 37°C for 1 hour.

Fluorescence intensity was measured at Ex584/Em590-10 nm using a FLUOstar Omega microplate reader (BMG Labtech). Viability of untreated cells was set to 1 and error bars represent standard error from 3 independent biological repeats.

2.7.3 Alkaline single cell gel electrophoresis (comet assay)

Immortalised *Tdp1*$^{+/+}$ and *Tdp1*$^{-/-}$ MEFs (~ 3 x 10^5 cells/sample) were suspended in normal growth media (for IR treatment) or cold PBS (for H_2O_2 treatment) and subjected 20 Gy (caseum 137, Cammael 1000) or 10 µM H_2O_2 on ice, then incubated in normal growth media at 37°C for the indicated repair time. Repair was stopped by placing cells on ice and replacing media with cold PBS. ~ 5,000 cells were mixed with equal volumes of PBS and 1.2 % type VII agarose (Sigma, A0701) at 42°C, and plated on frosted microscope slides pre-coated with 0.6 % agarose and chilled until set. Cells were then incubated in lysis buffer (2.5 M NaCl, 10 mM Tris-HCl, 100 mM EDTA pH 8, 1 % Triton X-100, 1 % DMSO, pH 10) at 4°C for 1 hour, and washed twice with cold distilled water. Slides were equilibrated in alkaline electrophoresis buffer (50 mM NaOH, 1 mM EDTA, 1 % DMSO) for 45 minutes, then subjected to electrophoresis at 12 V (100 mA) for 25 minutes. Quantification of DNA breaks were performed using Comet Assay IV software, counting 100 cells per sample.

2.7.4 Modified alkaline single gel electrophoresis for TOP1-cc detection

For modified alkaline comet assay that detects protein-linked DNA breaks, 0.8 mg/mL proteinase K was added to the cells straight after CPT or H_2O_2 treatment, cells were then mixed with equal volumes of PBS and 1.2 % type VII agarose and plated on frosted microscope slides pre-coated with 0.6 % agarose. Lysis was performed in the presence of 0.4 mg/mL proteinase K at 37°C for 3 hours. Slides were then processed as described in the previous section.

2.7.5 γH2AX and 53BP1 immunofluorescence assay

Tdp1$^{-/-}$ MEFs complemented with hTDP1, hTDP1^{K111R}, or empty vector were plated on 13 mm round coverslips in 30mm dish format and incubated overnight. Cells were then treated with 2 Gy γ-irradiation or 1 μM CPT (1 hour at 37°C), and repaired for the indicated periods. Cells were washed three times with PBS and fixed with 3 % paraformaldehyde for 10 minutes. Cold 0.2 % Triton was added for 2 minutes to permeate cell membrane, cells were then washed 3 time with PBS, and incubated in 2 % BSA for 30 minutes. Cells were probed with primary antibodies listed in **Table 2.6B** for 30 minutes at room temperature, washed 3 times with PBS, then stained with fluorophore-conjugated secondary antibodies listed in **Table 2.7B** for 30 minutes and washed 3 times with PBS. The coverslips were transferred to 26 x 76 mm microscope slides and fixed with VectorShield mounting medium H-1000 (Vector). Cells were visualised on a Nikon E400 microscope and γ-H2AX foci (red channel) were counted in 50 GFP-positive cells (complemented with pMXPIE-TDP1, pMXPIE-TDP1^{K111R} or pMX-PIE alone).

2.7.6 UV laser tracking using confocal microscopy

MRC5 cells (control and UBE2I knockdown) growing in log phase were plated at 1 x 10^5 cells per 3 cm dish and transfected with either pMC-EGFPP-TDP1 or pMC-EGFPP-TDP1^{K111R} using GeneJuice transfection reagent (Novagen). After 24 hours, transfection efficiency was assessed by FACS analysis of GFP-positive cells. At least 3 x 10^5 cells were fixed with cold 70 % ethanol at 4°C for at least 4 hours, washed once with PBS, then resuspended in 0.5 mL PBS and transferred to a BD Falcon 35 μm cell strainer in 12 x 75 mm polystyrene tube and analysed on a FACS Canto machine (BD Biosciences). Mean EGFP intensities of 10^4 cells were recorded for each cell line.

A parallel transfection was performed on cells similarly plated on 3 cm glass-bottomed

dishes (MatTek) for confocal microscopy. At 24 hours post-transfection, cells were stained with 10 µg/mL Hoechst 33285 (Sigma) for 30 minutes at 37°C. Cells were then visualised under a Zeiss Axiovert confocal microscope with 40x/1.2-W objective. GFP-positive cells were irradiated with 351 nm UVA (4.36 J/m^2) on an area of 0.1 µm width "track" and images were taken at 5-second intervals for 95 seconds. Quantification of track fluorescence intensity was performed using LSM 520 Meta software.

2.8 Mitochondrial morphological and functional assays

2.8.1 Qualitative analysis of mitochondrial network morphology by high resolution fluorescence microscopy

2 x 10^5 MEFs were seeded on glass coverslips (0.08 – 0.13 mm) in 6-well dishes and treated with or without 10 µM tert-Butyl hydroperoxide (TBH) for 24 hours at 37°C. Cells were stained with 250 nM of Mitotracker Deep Red FM (Life Technologies, M22426) for 30 minutes, then fixed with 3 % paraformaldehyde for 10 minutes. Cell membranes were permeabilised with cold 0.2 % Triton-X100 for 2 minutes, washed three times with PBS, then stained with 1:10000 DAPI. Coverslips were then mounted on microscope slides with VectorShield Mounting medium (Vector Laboratories, H-1000). Single-cell images were taken with Core DeltaVision at 60 x magnification, 640 x 640 resolution, with excitation filters for DAPI or Cy5, with Z-stacking. 3D images were deconvoluted using the OMERO software.

2.8.2 Quantitative analysis of mitochondrial membrane potential by FACS

3 x 10^5 MEFs were seeded in 6-well dishes for 24 hours at 37°C. Cells were stained with 250 nM Mitotracker Red CMXRos (Life Technologies, M22425) and Mitotracker Green FM (Life Technologies, M7514) for 30 minutes, then harvested and washed twice with PBS and analysed on a BD FACSCanto machine (BD Bioscience) using the PE and FITC channels. Mean fluorescence intensity from 10^4 events were recorded.

2.8.3 Quantitative analysis of mitochondrial superoxide production by FACS

3 x 10^5 MEFs were seeded in 6-well dishes for 24 hours at 37°C. Cells were treated with 1 μM rotenone or DMSO (mock) for 10 minutes at 37˚C, then stained with 250nM MitoSOX Red (Life Technologies, M36008) for 30 minutes at 37˚C, then harvested and washed twice with PBS and analysed on a BD FACSCanto machine (BD Bioscience) using the PE channels. Mean fluorescence intensity from 10^4 events were recorded.

2.8.4 Mitochondrial bioenergetics profiling by Seahorse Bioanalyzer

10^6 Flp-In T-Rex 293 cells were induced by 1 μg/mL doxycycline for 24 hours, then seeded at 6 x 10^4 cells per well in a XF24 cell microplate (Seahorse Bioscience, 100777-004) pre-coated with Cell-Tak cell adhesive (Corning, 354240) in 575 μL XF assay media (Seahorse Bioscience, 101022-100) supplemented with 4.5 mg/mL glucose, 2 mM L-glutamine and 1 x sodium pyruvate. Cells were incubated at 37°C with atmospheric CO_2 for 1 hour. A XF24 flux plate pre-hydrated in calibrant (Seahorse Bioscience, 100840-000) was loaded with 75 μL of 10 μM oligomycin, 82.5 μL of 3 μM FCCP, and 91.6 μL of 5 μM rotenone (final concentrations of 1 μM, 0.3 μM and 1 μM, respectively) diluted in the supplemented XF assay medium. Three basal readings were taken over 3 minutes each after 3 minutes of mixing and 2 minutes waiting. The same protocol was repeated after addition of each drug. Cells were then washed with PBS once, and incubated in normal growth medium containing 25 μg/mL Hoechst 33342 at 37°C for 30 minutes. The images were captured with an IN Cell Analyzer 6000 cell imaging system (GE Healthcare), and the nuclei number in each well was quantified using the IN Cell Developer software (GE Healthcare).

2.9 Mitochondrial DNA metabolism

2.9.1 Mitochondrial DNA copy number quantification by qPCR

3×10^5 MEFs were treated with or without 240 µM H_2O_2 for 1 hour on ice, washed twice with PBS, then left to recover in normal medium for 24 hours. Cells were then harvested and the genomic and mitochondrial DNA extracted using the Qiagen DNAeasy Blood and Tissue Kit (Qiagen, 69504). The DNA concentrations were measured using the QuantiFluor dsDNA system (Promega, E2670) and a FLUOstar Omega microplate reader (BMG Labtech) at EX485/EM520. The DNA templates were diluted to 10 ng, then serial dilutions of 10^{-1} – 10^{-5} were used to establish the standard curve for the mtDNA amplification reaction; and serial dilutions of 10^{-1} – 10^{-3} were used to establish the standard curve for the nDNA amplification reaction. For the qPCR reaction, 1 µL of DNA and 15 µM of each primer (**Table 2.8**) were diluted in 2 x LightCycler 480 SYBR-Green I mastermix (Roche, 04707516001) and TE buffer in a 20 µL reaction volume, and amplified using the following cycling conditions: initial 95°C for 2 minutes, then 40 cycles of 95°C for 10 second and 60°C for 20 seconds, with signal acquisition at end of each cycle using a Roche LightCycler 480 qPCR machine. Mitochondrial copy number was calculated by $2 \times 2^{(\Delta CT)}$ whereby ΔC_T = NDUFV1 average C_T – CO1 average C_T.

2.9.2 Mitochondrial transcript abundance by RT-qPCR

Total RNA from 5×10^6 Flp-In cells was extracted using Qiagen RNAeasy Plus kit (Qiagen, 74134) as per manufacturer's instructions, which included removal of genomic DNA from the samples, followed by reverse transcription of 5 µg total RNA using the Tetro cDNA synthesis kit (Bioline, BIO-65042). PCR primers used are listed in **Table 2.9**. Removal of genomic mtDNA contamination was confirmed by standard PCR amplification of non-reverse transcribed sample and analysis by DNA gel electrophoresis. Quantitative PCR was set up using 1:10 dilution of cDNA samples and 6 µM of primers in a 1 x SensiMix SYBR Hi-ROX master mix (Bioline, QT605-05) in a

Primer name	Sequence
Human CO1 (F)	GGAGCAGGAACAGGTTGAACAG
Human CO1 (R)	GTTGTGATGAAATTGATGGC
Human CO2 (F)	CCCTTACCATCAAATCAATTGGCC
Human CO2 (R)	ATTGTCAACGTCAAGGAGTCGC
Human ND1 (F)	CTACTACAACCCTTCGCTGAC
Human ND1 (R)	GGATTGAGTAAACGGCTAGGC
Human CYTB (F)	CTGATCCTCCAAATCACCACAG
Human CYTB (R)	GCGCCATTGGCGTGAAGGTA
Human RNR1 (F)	TAGAGGAGCCTGTTCTGTAATCGAT
Human RNR1 (R)	CGACCCTTAAGTTTCATAAGGGCTA
Human GAPDH (F)	ACATCGCTCAGACACCATG
Human GAPDH (R)	TGTAGTTGAGGTCAATGAAGGG

Table 2.9: *RT-qPCR primers*
qPCR primers used for amplifying reverse-transcribed mRNA of the target genes and their sequences from 5' to 3'.

Rotor-Gene 6000 qPCR machine (Corbett Research). The thermocycling conditions are: 95°C for 10 minutes, followed by 40 cycles of 95°C for 15 seconds, 50°C for 15 seconds, and 72°C for 30 seconds.

2.9.3 Quantification of TOP1mt-cc by caesium chloride fractionation

2 x 10^7 Flp-In cells were induced with 1 µg/mL doxycycline for 48 hours and harvested. Mitochondria were isolated using the mitochondria isolation kit for cultured cells (Thermo Scientific, 89874) following manufacturer's instructions. The mitochondria pellet was lysed in 1.1 mL lysis buffer (8 M guanidine hydrochloride, 30 mM Tris-HCl pH 7.5, 10 mM EDTA, 1 % sarkosyl, pH adjusted to 7.5) for 15 minutes at 65°C. 1 mL of mitochondrial lysate was gently layered on top of a 4-step caesium chloride gradient (densities of 1.45 g/ml, 1.5 g/ml, 1.72 g/ml, 1.82 g/mL of 1 mL each) in a 5 mL polyallomer centrifuge tube (Beckman, 326819), and centrifuged at 30000 rpm in a swinging rotor in a Beckman Ultima LE-80K ultracentrifuge for 24 hours at 25°C without brake. From the remaining 100 µL of mitochondrial lysate, 10 µL was mixed with 90 µL of 1 x TE buffer containing 0.5 µg/mL RNAse A and incubated at 37°C overnight. The lysate was briefly centrifuged at maximum speed, then 50 µL of the supernatant was mixed with 50 µL of 1 x TE buffer containing 1:200 dilution of PicoGreen (Invitrogen, P7581). In parallel, 50 µL of 1 x TE (as blank control) and 50 µL of λ DNA diluted to 25 – 500 ng in 1 x TE buffer (as standards) were prepared. DNA concentration was quantified using a FLUOstar Omega microplate reader (BMG) at EX485-12/EM520 spectra. To collect the CsCl fractionated lysates, the centrifuge tube was pierced near the bottom with a 19G syringe needle at 45° (bevel facing upwards), the needle was connected to a peristaltic pump via silicone tubing. Ten fractions of 0.5 mL were collected per cell line. To visualise TOP1mt-cc, the fractions were slot-blotted onto a 0.45 µm nitrocellulose membrane (GE Healthcare, 106000002) pre-wetted in PBS, using equal amounts of DNA across cell lines (equivalent to the amount in 200 µL of the cell line with the lowest DNA concentration). The membrane was air-dried, then

blocked in 5 % milk/TBS for 30 minutes on a shaker. The GFP antibodies (Abcam, ab290) were diluted 1:2000, then added to the membrane, which was left shaking at 4°C overnight. The membrane was then further processed as described in **Section 2.6.4**. Quantification was performed using Image Studio Lite (LI-COR).

2.9.4 Chromatin immunoprecipitation and quantification of TOP1mt-cc

1.5 x 10^7 Flp-In T-Rex 293 cells were induced by 1 µg/mL doxycycline for 48 hours then scraped and lysed in 0.6 mL ChIP lysis buffer (50 mM HEPES-KOH pH 7.5, 140 mM NaCl, 1 mM EDTA pH 8, 1 % Triton X-100, 0.1 % sodium deoxycholate, 0.1 % SDS, 1 x protease inhibitors cocktail) on ice for 30 minutes. The chromatin was sonicated for 30 cycles at 30 seconds on 30 seconds off at high speed setting, then the supernatant collected. A 50 µL aliquot was taken and the remaining chromatin snap-frozen and stored at -80°C. The 50 µL aliquot was treated with 1 µg RNAse A at 37°C for 30 minutes, then 25 µg of Proteinase K at 45°C for 30 minutes. The DNA was extracted using phenol-chloroform and precipitated by ethanol (**Section 2.2.10**), and run on a 1.5 % TBE-agarose gel to confirm that the size of the sheared chromatin ranged from 200 – 500 bp. The frozen chromatin was then thawed and 45 µL (10 % of total chromatin) was set aside as input. The remainder was diluted 4-fold with RIPA buffer (50 mM Tris-HCl pH 8, 150 mM NaCl, 2 mM EDTA pH 8, 1 % NP-40, 0.5 % sodium deoxycholate, 0.1 % SDS, 1 x protease inhibitors cocktail). 20 µL/sample of GFP-conjugated magnetic agarose beads (Chromotek, gtma-10) were washed with 2 x bead volume of RIPA buffer twice, then blocked in 5 mg/mL BSA/RIPA buffer at 4°C for 1 hour. The GFP beads were then mixed with the diluted chromatin overnight at 4°C. The beads were then washed in a thermomixer at 25°C for 5 minutes in low salt wash buffer (0.1 % SDS, 1 % Triton X-100, 2 mM EDTA, 20 mM Tris-HCl pH8, 150 mM NaCl) twice, then for 5 minutes in high salt wash buffer (0.1 % SDS, 1 % Triton X-100, 2 mM EDTA, 20 mM Tris-HCl pH 8, 500 mM NaCl) twice, for 5 minutes in lithium chloride buffer (0.25 M LiCl, 1 % NP-40, 1 % sodium deoxycholate, 1 mM EDTA,

10 mM Tris-HCl pH 8) once, and finally for 5 minutes in 1 x TE buffer (10 mM Tris pH 9, 1 mM EDTA) twice. The immunoprecipitated complex was then eluted from the beads in 150 µL of elution buffer (1 % SDS, 100 mM $NaHCO_3$). The eluent, together with the input samples, were treated with RNAse A at 37°C for 30 minutes then Proteinase K at 45°C for 30 minutes. The DNA was then purified using phenol chloroform extraction and ethanol precipitation. The pellet was resuspended in 30 µL distilled water.

For qPCR, the input and ChIP samples were diluted 1:10, then 5 µL was mixed with 2.8 µL of 5 µM forward and reverse primers (**Table 2.8**) and 10 µL of 2 x SensiMix SYBR Hi-ROX mastermix (Bioline, QT605-05). The mastermix was aliquoted into 20 µL reaction volumes in duplicates using a robotics workstation (Corbett Robotics, CAS 1200). The PCR reactions were carried out in a Rotor-Gene 6000 qPCR machine (Corbett Research) with thermocycling conditions as follows: 95°C for 10 minutes, then 40 cycles of 90°C for 15 seconds, 50°C for 15 seconds, and 72°C for 30 seconds, with signal acquisition at end of each cycle. Mitochondrial copy number was calculated by $2 \times 2^{(\Delta CT)}$ whereby ΔC_T = B2M average C_T – ND1 average C_T. Enrichment of the TOP1mt-bound region was expressed as percentage to the input sample, and was calculated as: $10 \times 2^{(\text{adjusted Input CT} - \text{IP CT})}$, whereby adjusted Input C_T = Input C_T – 3.32. The percentage input was then normalised against the mtDNA copy number.

2.10 Mitochondrial protein analysis

Mitochondrial pellets from Flp-In T-Rex 293 cells were isolated as described in **Section 2.9.4**. and resuspended in 50 µl homogenisation buffer (0.6 M mannitol, 10 mM Tris-HCl pH 7.4, 1 mM EGTA, 1 mM PMSF, 0.1 % BSA), then quantified using Bradford assay (Bio-Rad, 500-0001). To remove nuclear and cytoplasmic contaminants, 20 ng RNAse-free proteinase K was added per 5 µg of mitochondria for 30 minutes on ice. The reaction was stopped by adding 100 µM PMSF before centrifugation at 12000 g for 10 minutes. The mitochondrial pellets were washed with

Primer name	Sequence
Human ND1 (F)	CCCTAAAACCCGCCACATCT
Human ND1 (R)	GAGCGATGGTGAGAGCTAAGGT
Human B2M (F)	CCAGCAGAGAATGGAAAGTCAA
Human B2M (R)	TCTCTCTCCATTCTTCAGTAAGTCAACT
Human TOP1mt* 15873 (F)	TACTCAAATGGGCCTGTCCT
Human TOP1mt* 15873 (R)	AAAGACTTTTTCTCTGATTTGTCC
Mouse CO1 (F)	TGCTAGCCGCAGGCATTAC
Mouse CO1 (R)	GGGTGCCCAAAGAATCAGAAC
Mouse NDUFV1 F1	CTTCCCCACTGGCCTCAAG
Mouse NDUFV1 R1	CCAAAACCCAGTGATCCAGC

Table 2.8: *qPCR primers*
qPCR primers used for amplifying gDNA of the target genes and their sequences from 5' to 3'.

500 µL homogenisation buffer with 100 mM PMSF and centrifuged as previous. The pellets were then lysed as described in **Section 2.6.1** and quantified with Bradford assay. 5 µg of mitochondrial lysate was fractionated using SDS-PAGE (**Section 2.6.3**) and immunoblotted (**Section 2.6.4**) to assess levels of protein expression.

2.11 Transgenic mice genotyping

Tdp1$^{-/-}$ mice were generated as described previously (Katyal *et al*., 2007). *Tdp1*$^{+/-}$ mice were mated with SOD1^{G93A} mice (Gurney *et al*., 1994) to generate *Tdp1*$^{+/-}$ SOD1^{G93A} males, which were backcrossed with *Tdp1*$^{+/+}$, *Tdp1*$^{+/-}$ or *Tdp1*$^{-/-}$ females. Genotyping of adult mice was confirmed using tail biopsies, which were lysed in 100 µL of 25 mM NaOH at 95°C for 2 hours, then neutralised in 400 µL of 10 mM Tris-HCl pH 8. 5 µL of lysates were used as templates in PCR reactions as described previously (Katyal *et al*., 2007). Genotyping for SOD1^{G93A} was performed using primers Fwd: CATCAGCCCTAATCCATCTGA and Rev: CGCGACTAACAATCAAAGTGA. All animals were housed and maintained in accordance with the institutional animal care and ethical committee at the University of Sussex.

2.12 Statistical analysis

For the survival assays, the mean and standard errors were calculated from at least three biological repeat experiments consisting of three technical replicates at each treatment condition. The *p* values of samples from each time point or concentration were analysed by two-tailed Student t-test. For the alkaline comet assays, the mean and standard errors were calculated from at least three biological repeat experiments consisting of tail moment scores from 50 cells. For H_2O_2 comet assay, the mean comet tail moments of all samples were normalized to the mock-treated wildtype sample. The *p* values of samples from each time point or concentration analysed by two-tailed Student t-test unless otherwise specified. For RT-qPCR experiments, relative quantification of the C_T values of all samples were extrapolated from the standard

curve, and normalized against GAPDH values. The normalized values were then expressed as fold change relative to the control miScr cell line. The mean values and standard errors were calculated from three biological repeat experiments. The *p* values were calculated using two-tailed Student t-tests. For Seahorse analysis, the OCRs under basal and stressed conditions were normalized against cell numbers derived from Hoechst 33342 staining. The mean OCRs and standard errors were calculated from three biological repeat experiments consisting of three technical replicates. The *p* values were calculated using two-tailed Student t-tests.

CHAPTER 3

TDP1 serine 81 mediated interaction with DNA Lig3α promotes TDP1 protein stability and DNA repair

3.1 Introduction

Although catalytic mutation of TDP1 is clearly associated with defective SSBR at a cellular level and cerebellar degeneration at an organism level (Takashima *et al*., 2002; Katyal *et al*., 2007), little was known about the mechanisms that regulate TDP1 function at a molecular level. As with many DNA repair proteins that form stable complexes during the multi-step process, TDP1 has been shown to associate with XRCC1 to increase the efficiency of SSBR (Plo *et al*., 2003). Previous work from our lab has shown that TDP1 directly interacts with another component of the SSBR machinery, DNA ligase 3α (Lig3α), using the yeast two-hybrid system. Specifically, Lig3α binds to the N-terminus domain of TDP1 (El-Khamisy *et al*., 2005). This domain is only present in higher eukaryotes, with very low sequence homology amongst them (Chiang *et al*., 2010). This late addition and rapid evolution of the N-terminus domain suggest a non-essential but advantageous role in the function of the protein. For this reason, the N-terminus domain is highly relevant to the hypothesis of my thesis, i.e. in higher organisms, suboptimal control of the function of TDP1 *in vivo* may contribute to the neurodegeneration phenotype of SCAN1 patients.

Post-translational modifications by small molecule modifiers fine-tune enzymatic activities, protein-protein interactions, subcellular localisation, solubility and degradation. Phosphorylation, the addition of a phosphate group to an amino acid by covalent bonding, is mediated by protein kinases. The kinases ATM, ATR and DNA-PK play a crucial role in orchestrating the complex DNA damage response (**Section 1.3.1.1**), and the lists for their biological substrates are constantly expanding. A proteomic screen of potential substrates of ATM and ATR identified TDP1, and mapped the putative phosphorylation sites to S81, S365, and S563 (Zhou *et al*., 2005; Mu *et al*., 2007). S81 is of particular interest since it is the only site in the N-terminus domain identified in this study. S81 is conserved amongst several higher organisms

(Chiang *et al*., 2010). I was therefore intrigued by the possibility that the interaction between TDP1 and Lig3α may be regulated by phosphorylation of S81 by ATM or ATR in response to DNA damage. If so, this would be the first indication of the regulatory role of the N-terminus domain, which would support the hypothesis that regulation of TDP1 activity is important for TDP1 function in higher organisms.

This may have practical implications, as TDP1 inhibitors are currently being developed as novel anti-cancer drugs (Huang *et al*., 2011). Understanding TDP1 activity in the broader context of DNA repair could help identify potential factors that can contribute to understanding how resistance to TDP1 inhibitors can develop in cancer cells, as well as how neuronal cells repair DNA damage.

In this chapter, I will present evidence for the requirement of S81 phosphorylation in the interaction between TDP1 and Lig3α. I will also assess its functional importance in the cellular context. I will look at how S81 phosphorylation and interaction with Lig3α impacts on TDP1 protein metabolism, catalytic activity, and DNA repair efficiency.

3.2 Methods

3.2.1 Identifying novel protein-protein interactions using yeast two-hybrid assay

First described in 1989 (Fields and Song, 1989), the yeast two-hybrid assay is a well-established method for studying protein-protein interactions in a cellular system. It utilises the fact that many transcription factors in higher eukaryotes are modular, i.e. the different domains can be expressed separately and transcription can be activated when the different domains are brought near each other at the promoter site. In *Saccharomyces cerevisiae*, the transcription factor Gal4 contains a DNA binding domain (BD), and an activation domain (AD). When Gal4-BD is fused to a bait protein and Gal4-AD is fused to a prey protein, if the two proteins of interest interact, the proximity of the two Gal4 domains at its target promoter site would activate transcription of two reporter genes, *his3* and *lacZ* in the Y190 host strain. Activation of

his3 confers histidine prototrophy, which allows growth in histidine depleted medium; while activation of *lacZ* produces β-galactosidase, which metabolises a synthetic galactose substrate (x-gal) and produces a blue by-product.

The procedure of a standard two-hybrid assay involves transforming the host strain with two plasmids, one of which encodes the bait protein fused to Gal4-BD; the other plasmid encodes the prey protein fused to Gal4-AD. The vectors also contain nutritional selection markers to allow selection of clones that stably express the fusion proteins, and a nuclear localisation signal to ensure transcription of the reporter gene. The readouts were performed 72 hours after transformation using histidine prototrophy or β-galactosidase assay.

The advantages of using the yeast two-hybrid system over standard biochemical assays include:

- It utilises an easily manipulated model cellular system with many conserved cellular processes in higher eukaryotes;
- The post-translational processing of proteins is more sophisticated than in prokaryotes;
- It requires only small amount of plasmid DNA, which is easier to prepare than purified proteins;
- The readouts are fast and can be quantitative;
- It allows mapping of the interaction site by testing interaction with truncated or point-mutated forms of the protein of interest.

However, the main caveat in the yeast two-hybrid assay is false positive results. These can be due to technical or biological reasons:

- When proteins are overexpressed, the interaction can be forced (non-specific and not physiological);

- Targeting of proteins tagged with the transcription factor domains to the nucleus can potentially induce non-specific transcription of the reporter genes without physical interaction of the bait and prey proteins (“auto-activation”);
- Overexpression or targeting the proteins of interest to the nucleus may be cytotoxic and inhibits transcription or cell growth;
- Truncated proteins may interact differently than full-length proteins due to conformational changes;
- The interaction between two proteins may be indirect via a third protein or DNA;
- Yeast lacks certain post-translational modifications such as glycosylation, disulphide bonds and certain phosphorylations, which may inhibit interactions in the host species;
- In library screens using a cDNA library, interactions may be biased towards high expressing genes specific to the cell type from which the library is prepared; and each subsequent round of propagation of the cDNA library in bacteria may increase bias towards high expressers in bacteria.

  (Van Criekinge and Beyaert, 1999; Brückner *et al*., 2009).

Measures that I have taken in this thesis to address the possibility of false negative results include:

- For “auto-activation”, include a negative control where Gal4-BD-tagged bait protein and untagged Gal4-AD are overexpressed; use two reporter genes *his3* and *lacZ*;
- Use immunoblotting to confirm levels of over-expressed proteins;
- Use phosphomimetic and phosphomutant versions of the target phosphorylation site;
- Use protein co-immunoprecipitation to validate the interaction in the mammalian system.

3.2.2 Single Cell Gel Electrophoresis (SCGE)/Comet Assay

The comet assay is widely-used for measuring DNA damage in single cells. Originally developed by Östling & Johansson (Ostling and Johanson, 1984) and modified by Singh *et al*. (Singh *et al*., 1988), it was based on the concept of combining DNA electrophoresis with fluorescence microscopy. The procedure entails first "encapsulating" single cells in agarose, then disrupting cellular protein and RNA contents by a detergent and high salt solution. The remaining DNA is then dissociated from the chromatin and nuclear membrane and fills up the entire encapsulated space of the cell, forming a "nucleoid". When the nucleoid is subjected to electrophoresis, damaged DNA ends migrate out of the nucleoid due to loss of supercoiling, forming the appearance of a comet under the microscope when stained with a fluorescent dye that binds dsDNA (Olive and Banáth, 2006). The intensity and length of the comet tail (containing loops of relaxed DNA) relative to the comet head (supercoiled undamaged DNA) can be expressed as the tail moment (Olive *et al*., 1990), which can be calculated for each individual cell.

The main advantages of the comet assay are:

- Simple and inexpensive to set up;
- Can be used on a wide range of nucleated cells;
- Can measure SSBs, DSBs, abasic sites, and protein-linked breaks, and interstrand cross-linked breaks, and the repair kinetics thereof;
- Can detect apoptotic cells (distinct appearance from viable cell with large number of DNA breaks);
- Can detect heterogeneity in response to genotoxins, especially useful in screening of potential drug-resistant clones of cancer cell lines;
- Has high sensitivity especially for SSBs (as low as 50 breaks per cell);
- Does not require a large cell number (as low as a few thousands);
- Does not require radiolabelling as in alkaline elution assay

Disadvantages of the method include:

- Only suitable for fresh live cells
- Requires single cell suspension, therefore not suitable for tissues not easily dissociated without inadvertent damage to the DNA content (can be circumvented in certain tissue types by culturing overnight to allow recovery);
- When working with genetically-modified cell lines, a homogenous expressing population is required expressing and non-expressing cells are weighted equally in the scoring process;
- Does not quantify sizes of DNA fragments;
- The unmodified protocol does not allow distinction between different types of DNA lesions, e.g. H_2O_2 which generates many different types of lesions;
- For drugs requiring long period of treatment (e.g. cisplatin), or breaks rapidly repaired during treatment (e.g. H_2O_2 and CPT), the readout is a mixture of damage induction and repair at steady-state;
- The amount of DNA damage does not necessarily correlate with the cell fate or viability

(Olive and Banáth, 2006)

To conclude, the comet assay is a useful technique in our lab to monitor DNA repair kinetics in cell lines and to screen for DNA damage repair defect of a new cell line (usually from patients, transgenic mice, or genetically-modified human or mouse cell lines). Examples of genotoxins used in this thesis and the predominant lesion they produce are listed in **Table 3.1**.

To assess the cell fate after DNA damage, I used clonogenic survival assay to measure the ability of cells to recover from geneotoxic stress and proliferate to form colonies.

Genotoxins	**Types of DNA breaks**
Hydrogen peroxide (H_2O_2)	SSBs, AP-sites, complex DSBs at high dose, protein-DNA breaks (PDBs)
tert-butyl hydroperoxide (TBH)	SSBs, AP-sites, complex DSBs at high dose
Gamma-ray	SSBs, DSBs (~ 40:1 SSBs:DSBs)
Camptothecin (CPT)	TOP1-cc

Table 3.1 Genotoxins and the types of associated DNA damage.

3.2.3 Clonogenic Survival Assay (Colony Formation Assay)

In the presence of genotoxic stress, immortalised/cancer cell lines can respond by complete recovery, partial recovery, or death. Complete recovery is indicated by retention of reproductive integrity, i.e. the ability to divide indefinitely and form macroscopic colonies. Partial recovery is indicated by retention of viability (to produce proteins and synthesise DNA) for a few cell divisions but not indefinitely (Franken *et al*., 2006). Cell death can occur by apoptosis, autophagy, or necrosis (**Section 1.3.3**). It is noteworthy that loss of specific pathway (e.g. apoptosis) does not usually result in reversion to reproductive integrity, instead an alternative pathway of cell death is often activated (e.g. necrosis).

The clonogenic survival assay was developed as early as 1956 by Puck and Marcus (Puck and Marcus, 1956) to measure the radiosensitivity of HeLa cells. Since then, it has been used to generate most of the radiotherapy and chemotherapy response data on known mammalian cell lines.

The clonogenic survival assay entails plating a known number of single cells in a number of petri dishes corresponding to each treatment condition (usually increasing drug concentrations), then incubating the cells in optimal growth medium until they are fully adhered (but not undergone cell divisions yet), then treating with the genotoxin for a defined period. Cells are left to recover in optimal growth medium to form macroscopic colonies. The plating efficiency of each dish is calculated in percentage as the number of colonies counted divided by the number of cells plated. The surviving fraction is calculated in percentage as the plating efficiency of treated samples to untreated sample. The surviving fraction of each drug concentration can be plotted as a dose-response to obtain a “survival curve”, whereby the IC_{50} of the drug can be deduced.

The clonogenic survival assay is highly sensitive in detecting cellular response to genotoxic drugs. However, it is labour-intensive and time-consuming, making it unsuitable for high-throughput screening.

3.3 Results

3.3.1 The N-terminus domain of TDP1 interacts with Lig3α

To determine the mechanism of interaction between TDP1 and Lig3α using the yeast two-hybrid system, it was important to first confirm the interaction between the N-terminus of TDP1 and Lig3α as previously published (El-Khamisy *et al*., 2005). **Fig. 3.1** shows that the N-terminus domain ($TDP1^{1-150}$) but not the C-terminus domain ($TDP1^{151-608}$) interacted with Lig3α, as detected by both histidine prototrophy and β-galactosidase assays. The interaction was specific, as confirmed by the lack of auto-activation of either Gal4BD-$TDP1^{1-150}$ or the Gal4AD-Lig3α (**Fig. 3.1A**). Immunoblotting of whole cell lysates confirmed all proteins of interest were expressed (**Fig. 3.1B**).

3.3.2 TDP1 S81 mediates interaction with Lig3α

I then generated constructs encoding $TDP1^{S81A}$ (phosphomutant), or $TDP1^{S81E}$ (phosphomimetic with a negatively charged –COOH group). In **Fig. 3.2A**, again using the yeast two-hybrid assay, interaction between TDP1 and Lig3α was shown to be abrogated in the S81A mutant but not in the S81E mutant, indicating that it was likely the phosphorylation status, rather than structural modification, that mediated the loss of interaction. To ascertain whether the apparent mild activation of the *his3* gene in $TDP1^{S81A}$ was significant, quantitative β-gal assay using CPRG as substrate was performed. **Fig. 3.2B,C** show that $TDP1^{S81A}$ interaction with Lig3α was close to background level, i.e. when no TDP1 was expressed.

I then looked at this interaction event in the mammalian cell system using the human alveolar adenocarcinoma cell line A549, suitable for transient over-expression of proteins. Cells were transfected with either Myc-TDP1 or Myc-$TDP1^{S81A}$, and the

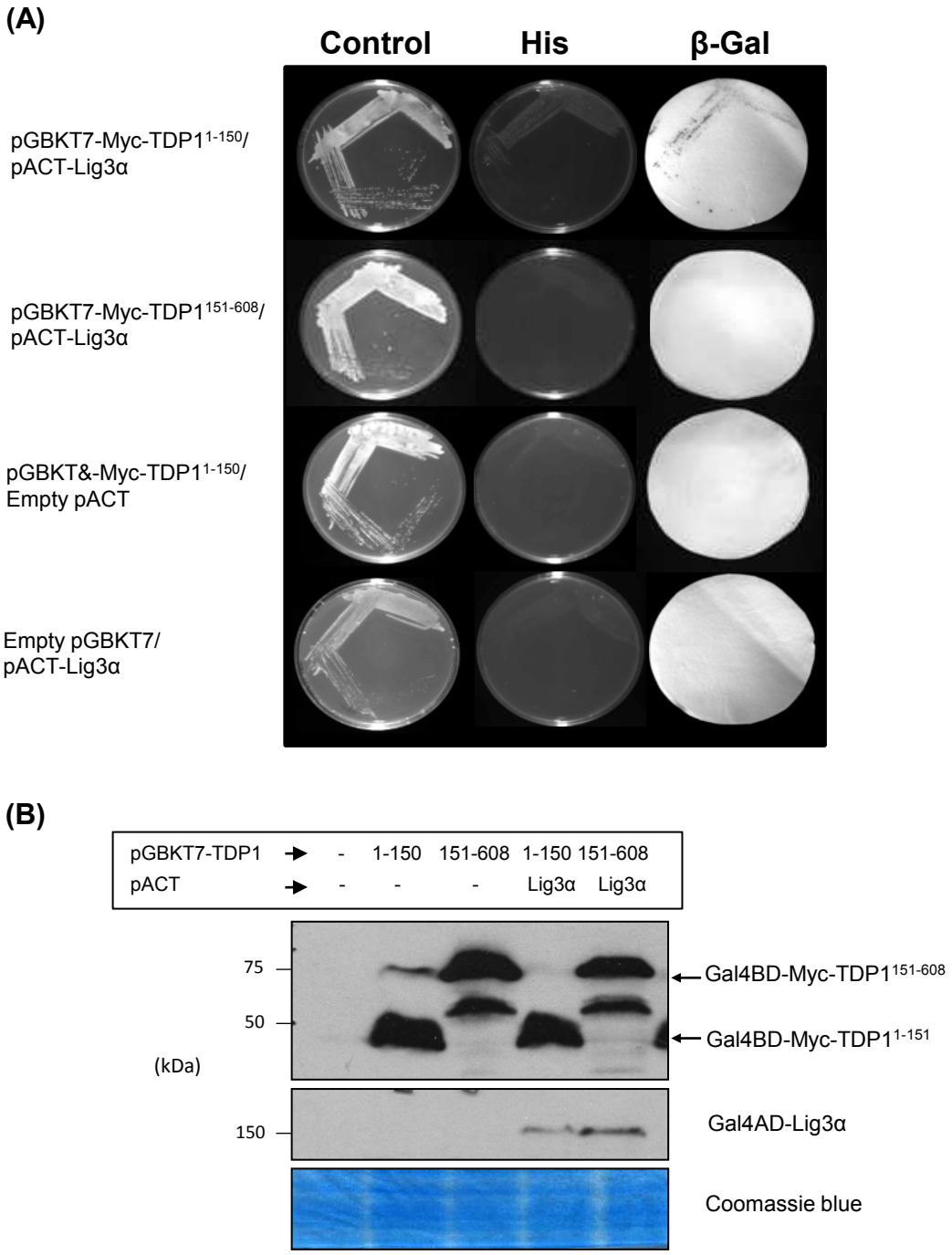

Figure 3.1 The N-terminus domain of TDP1 interacts with Lig3α. (A) Y190 cells co-transformed with the indicated pGBKT7 and pACT constructs were plated onto selective media containing either histidine ("Control") or lacking histidine and containing 3-aminotriazole ("His") to test for the activation of the *his3* reporter gene. The activation of the *β-gal* reporter gene was detected using the filter lifts from control plates ("β-Gal"). **(B)** WCEs (10 µL of 0.075 OD_{600}/µL) from (A) were fractionated with SDS-PAGE and immunoblotted using antibodies against Myc and Gal4AD. WCE from untransformed cells was included as negative control (far left lane). A duplicate gel was stained with Coomassie blue as loading control.

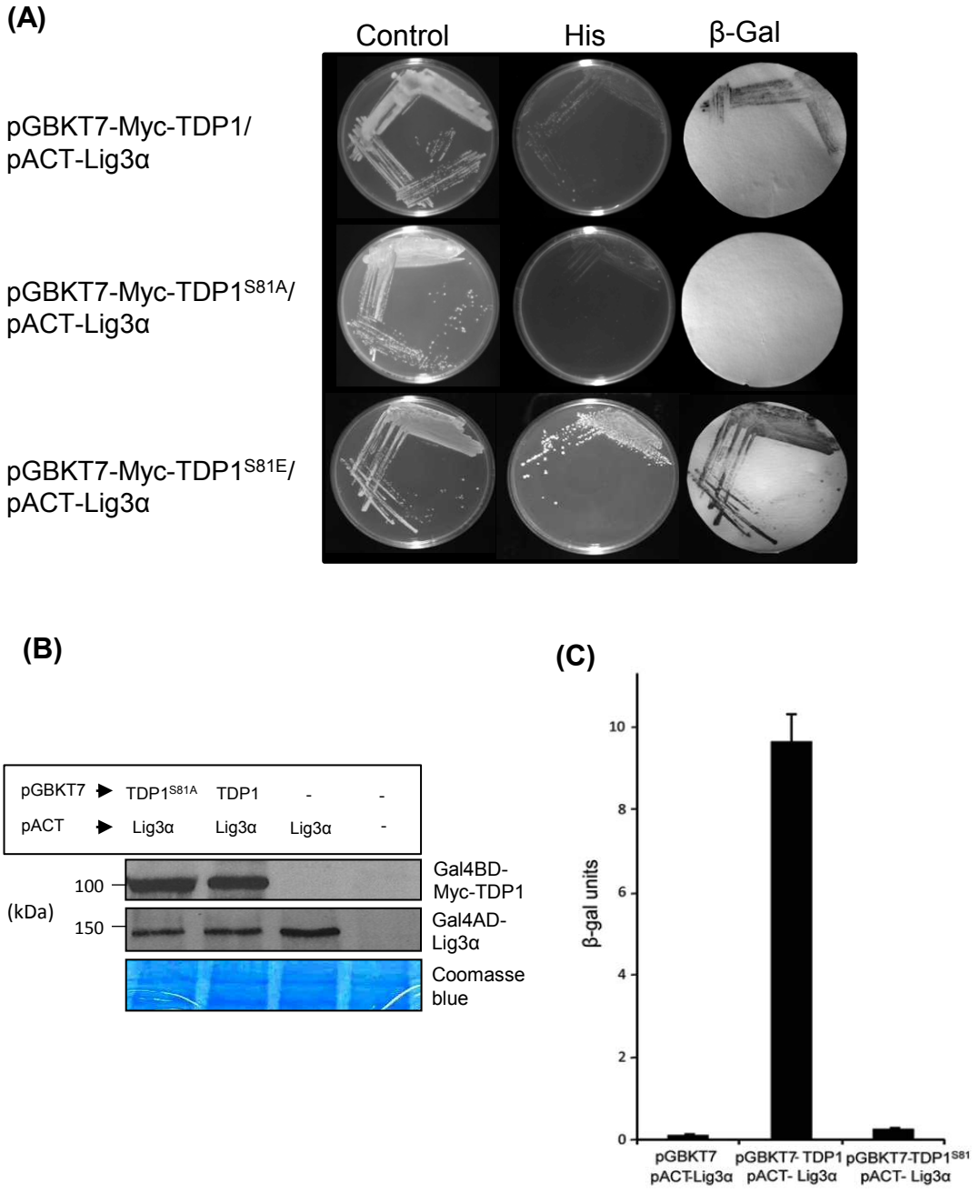

Figure 3.2 TDP1 S81 is required for interaction with Lig3α in yeast two-hybrid system. **(A)** Yeast Y190 co-transformed with pACT-Lig3α and pGBKT7-TDP1, pGBKT7-TDP1^{S81A} or pGBKT7-TDP1^{S81E} were plated onto selective media containing either histidine ("Control") or lacking histidine and containing 3-aminotriazole ("His") to test for the activation of the *his3* reporter gene. The activation of the *β-gal* reporter gene was detected using the filter lifts from control plates ("β-Gal"). **(B)** WCEs (10 µL of 0.075 OD_{600}/µL) were fractionated with SDS-PAGE and immunoblotted using antibodies against Myc and Gal4AD. WCE from untransformed cells was included as negative control (far right lane). A duplicate gel was stained with Coomassie blue as loading control.

interacting proteins purified using Myc immunoprecipitation. The interaction of TDP1^{S81A} with endogenous Lig3α was greatly diminished but not completely abolished (**Fig. 3.3**). This interaction is again TDP1-specific as no Lig3α pull-down was detectable in cells transfected with Myc alone.

3.3.3 Interaction between TDP1 and Lig3α is independent of exogenous genotoxic stress

That the interaction between TDP1 and Lig3α depends on conservation of a putative ATM/ATR consensus site suggests that this interaction may be regulated by DNA damage. To test this, I co-expressed TDP1 and Lig3α in the yeast two-hybrid system, and quantified the interaction after treatment with CPT or IR using CPRG-based quantitative β-gal assay. However, there was no change in the amount of β-gal metabolised at the doses known to induce detectable levels of DNA damage (Redon *et al*., 2003), suggesting the interaction was constitutive (**Fig. 3.4**). This result should be interpreted in the context of the yeast two-hybrid system, whereby the other regulatory mechanisms of the interaction in humans such as XRCC1 and PNK are not conserved in yeast (Kelley *et al*., 2003).

3.3.4 TDP1 S81-mediated interaction with Lig3α promotes TDP1 stability

Incidentally, while I observed that the TDP1$^{1-150}$ truncated protein interacted with Lig3α in the yeast two-hybrid system, I was unable to express the S81A version of TDP1$^{1-150}$ (data not shown), despite correct cDNA sequence and reading frame in the plasmid. To test the possibility that the S81-mediated interaction of TDP1 with Lig3α stabilises TDP1 and prolongs its half-life, I overexpressed Myc-TDP1 or Myc-TDP1^{S81A} in A549 cells, challenged the cells with CPT, then inhibited protein synthesis with cyclohexamide (CHX) for up to 24 hours. Immunoblotting of Myc-TDP1 showed minimal degradation of the wildtype Myc-TDP1 during this period, while the level of Myc-TDP1^{S81A} was visibly lower reduced within 24 hours (**Fig. 3.5A**). Alternatively, inhibiting TDP1 phosphorylation by caffeine, an inhibitor of ATM, ATR and DNA-PK

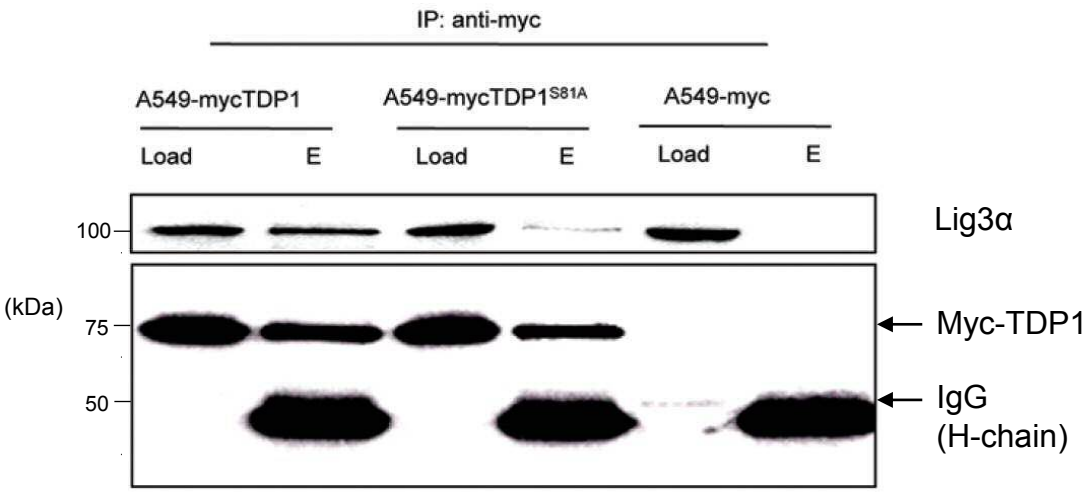

Figure 3.3 TDP1 S81 promotes interaction with Lig3α in human A549 cells. A549 cells were transiently transfected with pCI plasmids encoding Myc-TDP1, Myc-TDP1^{S81A}, or untagged Myc. 100 µg WCEs were immunoprecipitated with antibodies against Myc. Levels of Lig3α, Myc-TDP1 and Myc-TDP1^{S81A} present in WCEs ("Load") and in immunoprecipitated samples ("E") were determined by immunoblotting with antibodies against Lig3α or Myc.

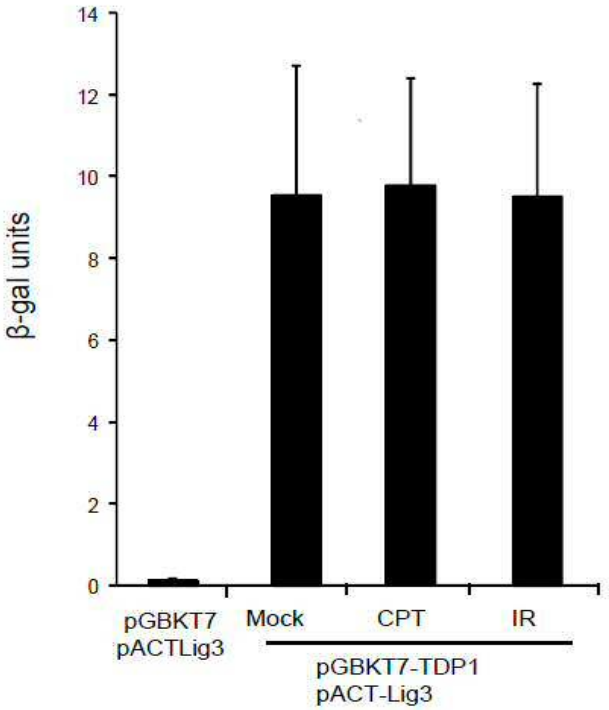

Figure 3.4 Interaction of TDP1 with Lig3α is constitutive in the yeast two-hybrid system. Y190 cells were transformed with the indicated plasmids and selected on yeast minimal medium lacking histidine and containing 3-aminotriazole for 72 hours. Transformants were then grown in complete culture medium for two doubling cycles, followed by treatment with 30 μM CPT for 6 hours or 200 Gy ionising radiation, then harvested. The WCEs were incubated in CPRG until the medium turned from yellow to red colour and the reaction was stopped with 3 mM $ZnCl_2$. The OD_{578} of the supernatant was measured. β-galacosidase units was calculated as 1000 x OD_{578} (t x V xOD_{600}), where t = stop time – start time (in minutes), V = 0.1 x concentration factor. 1 unit of β-galacosidase is defined as the amount which hydrolyses 1 μmol of CPRG to chlorophenol red and D-galactose per minute per cell. 1 unit of β-galactosidase equals the amount of enzyme required to hydrolyse CPRG per minute.

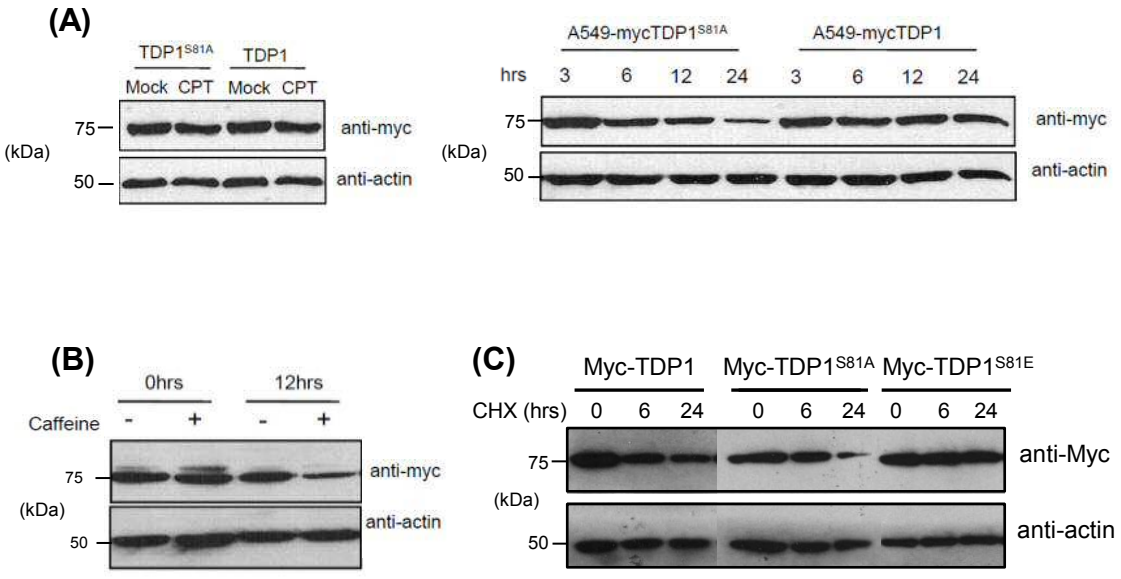

Figure 3.5 TDP1 S81 promotes protein stability (A) A549 cells transfected with the indicated pCI-Myc constructs were treated with DMSO ("Mock") or 35 μM CPT for 2 hours at 37˚C (left), then incubated in CPT-free medium with 10 μg/ml cycloheximide ("CHX") for the indicated time periods (right). **(B)** A549 cells transfected with pCI-Myc-TDP1 were treated with or without 2 mM caffeine for 30 minutes, followed by 35 μM CPT treatment for 2 hours at 37˚C, then incubated in CPT-free medium containing 10 μg/ml cycloheximide ("CHX") and caffeine for 12 hours at 37˚C. Cells were harvested for immunoblotting using antibodies against Myc or β-actin as loading control. **(C)** A549 cells transfected with pCI-Myc-TDP1, pCI-Myc-TDP1^{S81A}, or pCI-Myc-TDP1^{S81E} were similarly treated as described in (A) and WCEs were immunoblotted using antibodies against Myc and β-actin. as loading control. Data collected with help from Prof. Sherif El-Khamisy.

activities (Blasina *et al*., 1999; Hall-Jackson *et al*., 1999; Sarkaria *et al*., 1999; Zhou *et al*., 2000), reduced the stability of wildtype Myc-TDP1 after 12 hours of CHX incubation (**Fig. 3.5B**). To exclude the effect of caffeine as being non-specific, the half-life of the phosphomimetic mutant Myc-TDP1^{S81E} was assessed by CHX and appeared even longer than that of Myc-TDP1 (**Fig. 3.5C**).

Phosphorylation of S81 could promote TDP1 protein stability by inducing a conformational change that inhibits proteasomal targeting, or due to complex formation with Lig3α. This was tested in HeLa cells stably depleted of Lig3α, which were transfected with pCI-Myc-TDP1, treated with CPT, and left to incubate in CHX as described before. In cells depleted of Lig3α, Myc-TDP1 degraded faster than Lig3α-expressing cells (a decrease of 47 % compared to ~ 26 % after 6 hours), which was further exacerbated by treatment with CPT (a decrease of ~ 91 % compared to ~ 67 % after 6 hours) (**Fig. 3.6**). Taken together, these data suggest that TDP1 S81 promotes formation of a stable complex with Lig3α via its N-terminus domain both constitutively as well as in response to CPT treatment, thereby protecting it from degradation.

3.3.5 The catalytic activity of TDP1 is independent of S81

Next we examined whether maintaining protein stability in response to CPT damage was required for enzymatic activity of TDP1. My lab colleague Jean Carroll performed an *in vitro* enzymatic assay using 10 x His-TDP1 and 10 x His-TDP1^{S81A} purified from *E. coli*, and a substrate of 43-mer duplex oligonucleotide containing a nick with a 3'-phosphotyrosyl group (3'-PY) (**Fig. 3.7A**). In the absence Lig3α, the efficiency of 10 x His-TDP1 and 10 x His-TDP1^{S81A} to process the 3'-PY to 3'-hydroxyl group (3'-OH) was similar (**Fig. 3.7B)**. To confirm this in cells, I complemented a CPT-hypersensitive strain of *S. cerevisiae* (*tdp1Δ/rad10Δ*) (Vance and Wilson, 2002) with human TDP1 or TDP1^{S81A}, and observed similar levels of protection against CPT conferred by TDP1^{S81A} as wildtype TDP1 (**Fig. 3.8**). Since *S. cerevisiae* lacks known

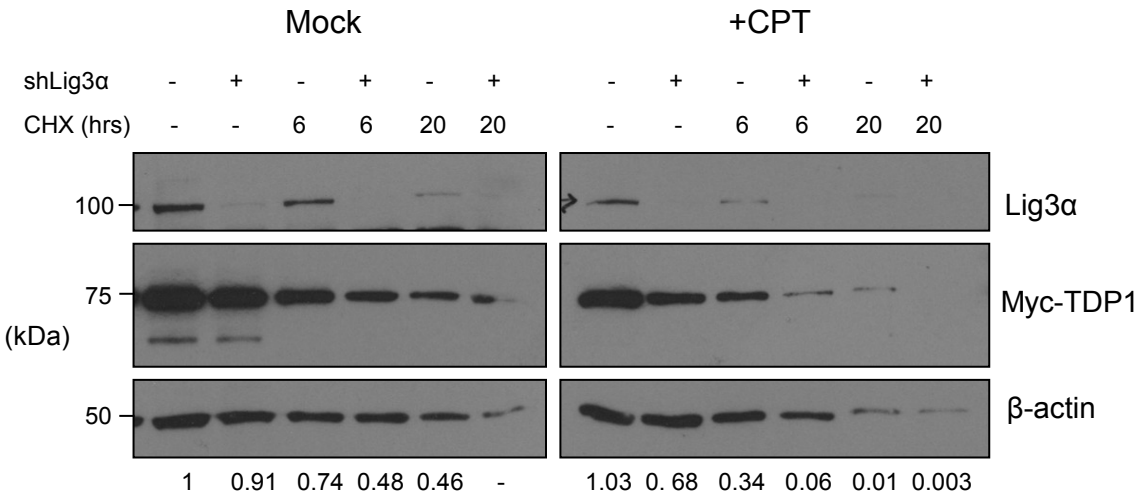

Figure 3.6 Lig3α promotes stability of Myc-TDP1. HeLa cells depleted of Lig3α by shRNA were treated with DMSO ("Mock") or 35 μM CPT for 2 hours at 37˚C, then incubated in CPT-free medium with 1 μg/ml cycloheximide ("CHX") for the indicated time periods. Cells were harvested and the WCEs were immunoblotted with antibodies against Lig3α, Myc or β-actin as loading control. The level of Myc-TDP1 in each sample was quantified and normalised against the β-actin level using ImageJ. The numbers at the bottom row indicate the fraction of Myc-TDP1 of the treated samples relative to the untreated sample (far left lane). Where not shown, quantification was not accurate due to low levels of Myc-TDP1 or β-actin.

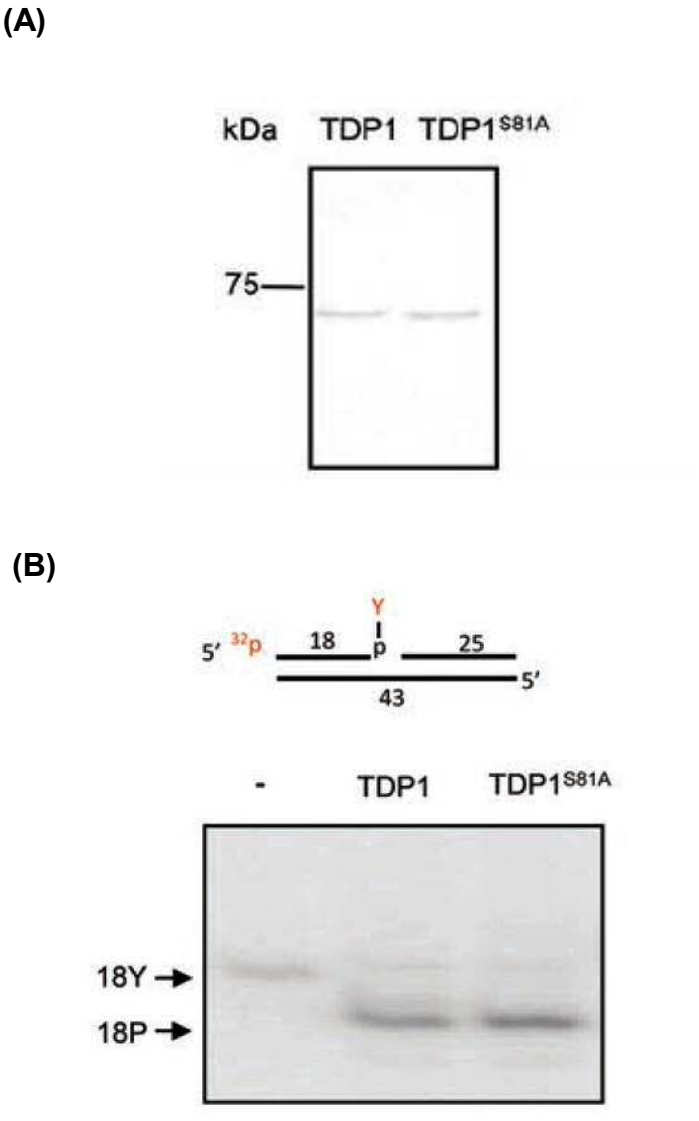

Figure 3.7 TDP1 S81 is not required for enzymatic activity *in vitro*. (A) Histidine-tagged TDP1 and TDP1^{S81A} were purified from BL21 *E. coli* and 300 ng of each was analysed by SDS-PAGE and stained with Coomassie blue. **(C)** 32P-radiolabelled 43-mer duplex (50 nM) containing a nick with a tyrosine (Y) linked to the 3'-terminus of the labelled 18-mer was incubated in the absence or presence of the 30 nM of the indicated purified recombinant proteins for 1 hr at 37°C. Repair products were analysed by denaturing PAGE and phosphorimaging. Positions of the 32P-radiolabelled substrate (18-Y) and product (18-P) are indicated in red. Data collected by Dr Jean Carroll.

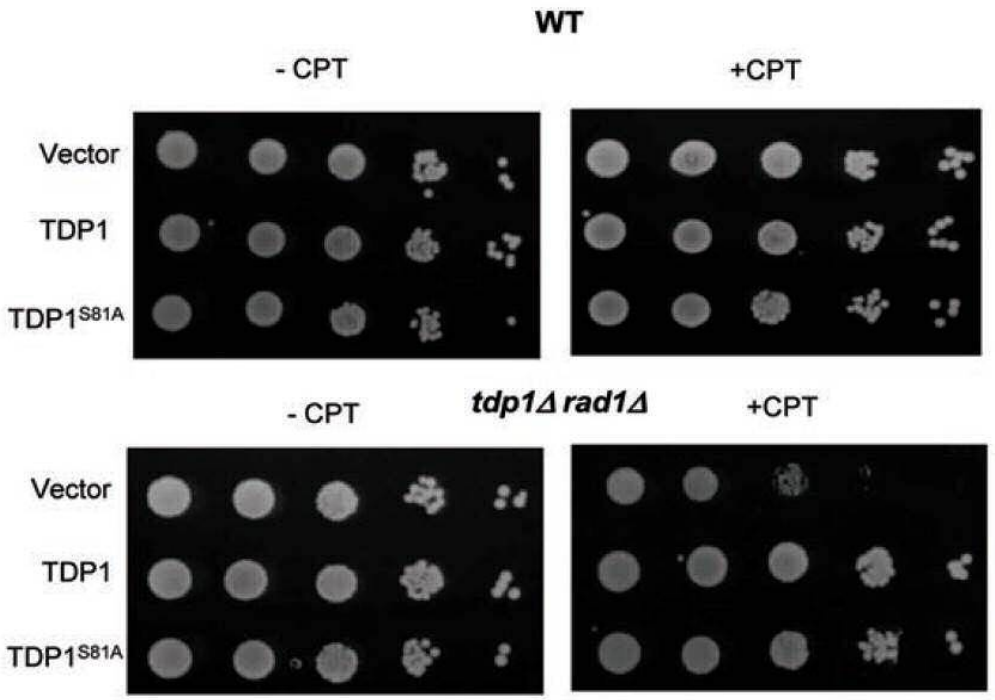

Figure 3.8 Interaction with Lig3α is not required for TDP1 activity *in vivo.* Serial dilutions of wild-type (top) and *tdp1Δ/rad1Δ* (bottom) yeast cells transformed with empty pGBKT7, pGBKT7-TDP1 or pGBKT7-TDP1^{S81A} and plated in 10-fold dilutions onto leucine-lacking media with or without 20 μM CPT, and left to form macroscopic colonies at 30°C for 72 hours.

homologues of Lig3α, XRCC1 and PNK, the rescue was most likely due to the catalytic activity of TDP1^{S81A} and not dependent on interaction with Lig3α.

3.3.6 The rapid phase repair of TOP1-cc by TDP1 is independent of S81

As both the *in vitro* and yeast data relied on expression of the human TDP1 protein in non-native hosts, they may not reflect the situation in human cells. To address this, repair of TOP1-cc was assessed in the SCAN1 patient lymphoblastoid cells complemented with recombinant His-TDP1 or His-TDP1^{S81A} and treated with CPT for 1 hour. Immunoblotting of whole cell lysates at start of CPT treatment showed equal levels of the recombinant proteins (**Fig. 3.9A**). Cells complemented with recombinant TDP1^{S81A} were able to repair TOP1-cc as efficiently as cells complemented with recombinant TDP1, although not to the same extent as wildtype cells (**Fig. 3.9B**). This could be due the dominant negative effect of the TDP1^{H493R} mutation in SCAN1 cells, which gets trapped on the DNA break itself, forming persistent covalent DNA complexes (Interthal *et al*., 2005a). In *Tdp1*$^{-/-}$ MEFs complemented with recombinant hTDP1 or hTDP1^{S81A} (**Fig. 3.10A**), the efficiency of SSBR was comparable between the two groups (**Fig. 3.10B**). Therefore, TDP1 S81 does not seem to be required for rapid phase of repair of repair of SSBs induced by CPT.

3.3.7 TDP1 S81 promotes cellular survival following genotoxic stress

The alkaline comet assay assessed the repair kinetics of primarily SSBs within an hour after damage. However, since TDP1 has also been implicated in the repair of replication-associated TOP DSBs (**Section 1.5.1**), the effect of TDP1^{S81A} on replicating cells was assessed indirectly by measuring clonogenic survival after CPT treatment. *Tdp1*$^{-/-}$ MEFs complemented with recombinant TDP1 or TDP1^{S81A} were challenged with bolus doses of CPT for one hour to induce TOP1-cc, then left to recover in drug-free medium up to 7 – 10 days. Only cells which retained replicative potential were able to form macroscopic colonies. **Fig. 3.11** shows that complementation with recombinant TDP1 rescued the survival of CPT-treated *Tdp1*$^{-/-}$ MEFs while mock (BSA)

(A)

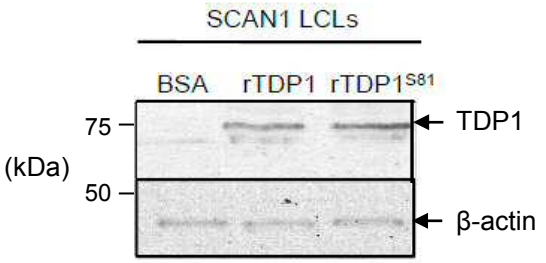

(B)

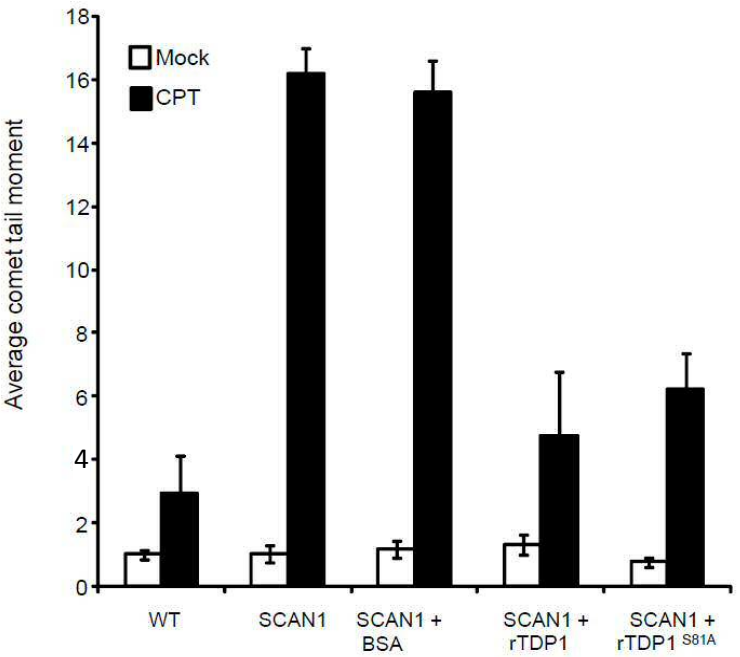

Figure 3.9 TDP1 81 is not required for rapid-phase single-strand break repair in human lymphoblastoid cells. **(A)** SCAN1 lymphoblastoid cells ("LCLs") were electroporated with 200 µg BSA, 10xHis-TDP1, or 10xHis-TDP1^{S81A} and left to recover at 37˚C for 2 hrs. Cells were harvested and WCEs were immunoblotted with antibodies against TDP1 and β-actin as loading control. Arrow points at 10xHis-TDP1. **(B)** LCLs were incubated with 14 µM CPT for 1 hr and DNA strand breakage was quantified immediately by alkaline comet assay. Data are the mean of 3 independent experiements (100 cells per experiment) and error bars indicate ±1 S.E.M. Data collected with help of Prof. Sherif El-Khamisy.

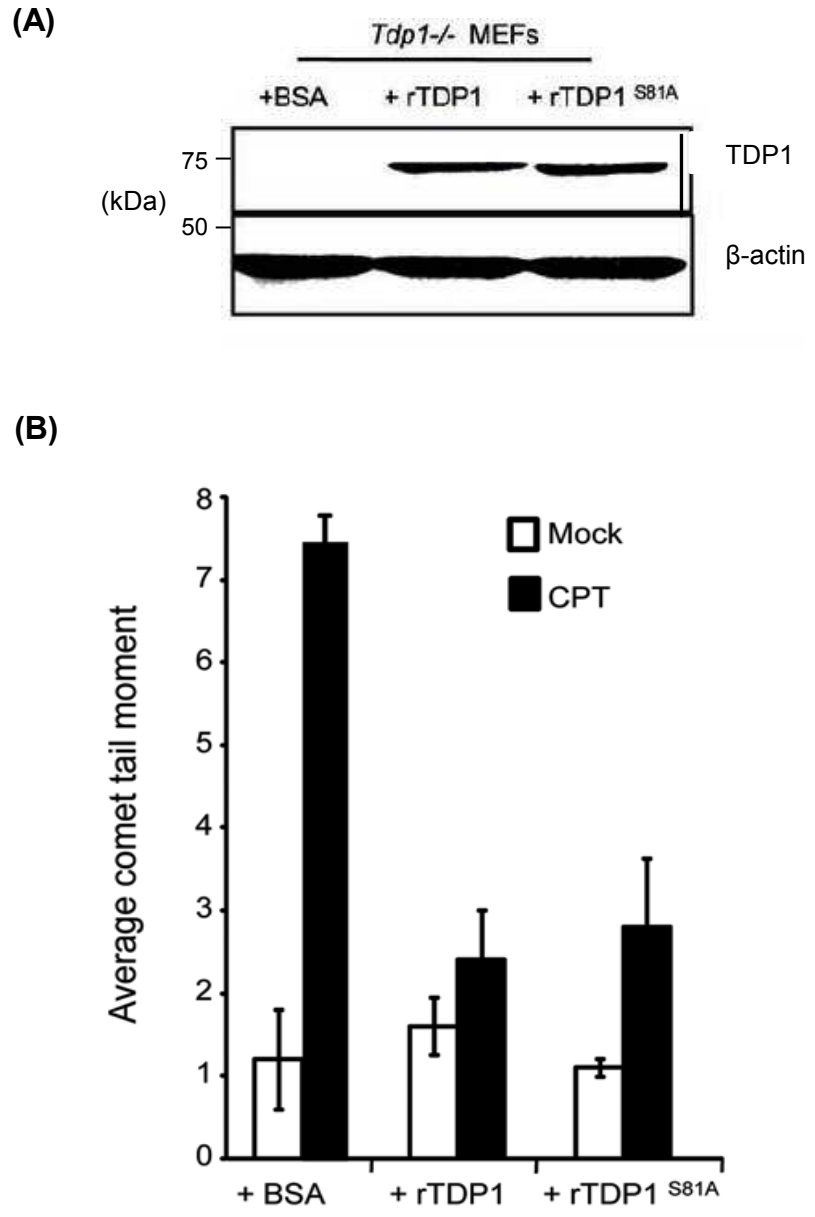

Figure 3.10 TDP1 S81 is not required for rapid-phase single-strand break repair in MEFs. (A) *Tdp1*$^{-/-}$ MEFs were electroporated with 200 µg BSA, recombinant TDP1, or recombinant TDP1^{S81A} and left to recover at 37˚C for 2 hrs. Cells were harvested and WCEs were immunoblotted with antibodies against TDP1 and β-actin as loading control. **(B)** Electroporated cells were treated with 14 µM CPT or DMSO ("Mock") for 1 hr at 37°C. DNA strand breakage was quantified by alkaline comet assay. Data are the mean of 3 independent experiments (100 cells per experiment) and error bars indicate $\pm$1 S.E.M. Data collected with help of Prof. Sherif El-Khamisy.

(A)

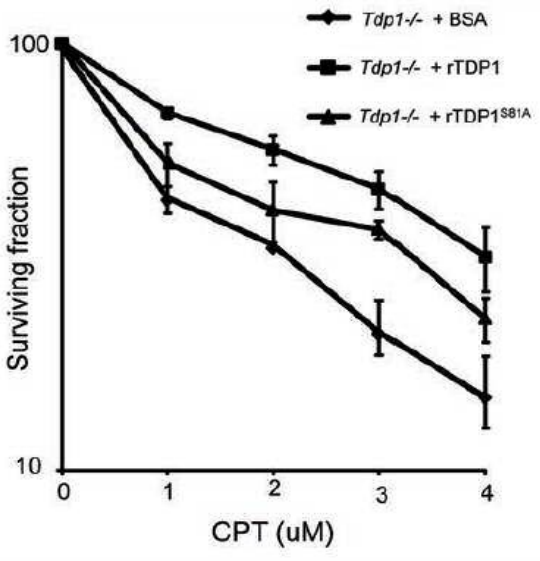

(B)

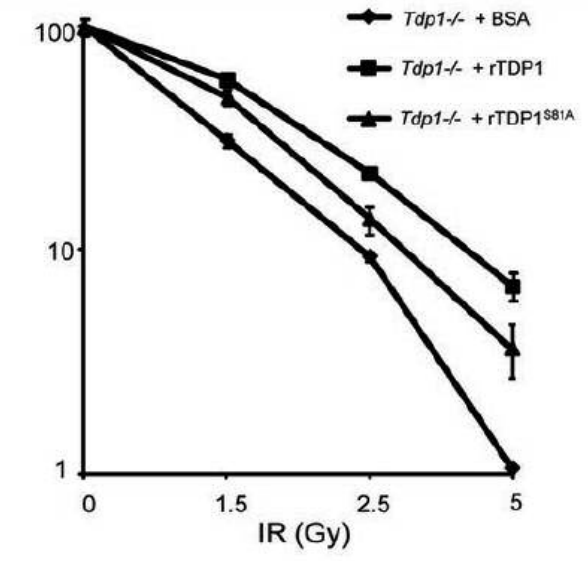

Figure 3.11 TDP1 S81 promotes survival after genotoxic stress in MEFs. *Tdp1*$^{-/-}$ MEFs were electroporated with 200 µg BSA, recombinant TDP1, or recombinant TDP1^{S81A} and left to recover at 37˚C for 2 hrs, Cells were plated in 10 cm dishes and treated with the indicated doses of CPT for 1 hr at 37°C **(A)**, or irradiated with the indicated doses of ionizing radiation (IR) **(B)**. Cells were then left to recover in normal growth medium for 7 – 10 days to allow formation of macroscopic colonies. Surviving fraction was calculated by dividing the number of colonies on treated plates by the number on untreated plates. Data are the mean of 3 independent experiments for each drug and error bars represent ±1 S.E.M. Where not visible, error bars are smaller than the symbols. Data collected with help of Prof. Sherif El-Khamisy.

complemented cells did not. TDP1^{S81A} complementation conferred an intermediate level of resistance, suggesting a defect in repair of TOP-associated DSBs by TDP1^{S81A}.

3.4 Discussion

In this chapter, I have present data confirming that, in the yeast two-hybrid system, human TDP1 directly interacts with Lig3α (**Fig. 3.1, 3.2**), but not XRCC1 or APTX, nor the other candidate proteins of the NER and DSBR pathways tested. I also confirmed the previous finding that TDP1 N-terminus is the binding site for Lig3α (**Fig. 3.1**).

I have then shown that this interaction requires the serine 81 residue both in the yeast two-hybrid system (**Fig. 3.2**) and the mammalian cell system (**Fig. 3.3**) in the absence of exogenous DNA damage. Adding exogenous damage by CPT or IR did not alter the speed or intensity of the interaction in the yeast two-hybrid system (**Fig. 3.4**).

The apparent constitutive nature of interaction between TDP1 and Lig3α needs to be interpreted with caution. As mentioned, protein-protein interactions in a non-native host species may lack physiological regulatory elements. Furthermore, as the quantitative β-gal assay readout can take up to 12 hours, after induction of exogenous DNA damages transcription may be stalled globally, and dampen any effect of increased interaction due to lower protein expression level. A protein co-immunoprecipitation experiment using mammalian cells was performed to address these issues, and will be presented in chapter 4 (**Fig. 4.5**). The result indicates that CPT damage did not alter the quantity of complex formation between TDP1 and Lig3α, suggesting that this interaction is mainly regulated by endogenous sources of damage, the most likely being TOP1-cc in the proximity of abasic sites, oxidised bases, or the transcription or replication machinery (Pommier *et al*., 2003).

Concurrent with my project, a study by Yves Pommier's group also showed that in mammalian cells, TDP1 S81 is phosphorylated in response to CPT and IR (Das *et al*., 2009). This phosphorylation event is dependent on ATM and DNA-PK, and that

phospho-TDP1 co-localises with phospho-ATM, γH2AX and XRCC1 at sites of CPT-induced DSBs. Phosphorylated TDP1 is also retained at sites of DNA damage for up to hours, suggesting a stable complex formation with XRCC1 (Das *et al*., 2009). These findings are consistent with my result, as XRCC1 and Lig3α form a stable heterodimer in the nucleus (Caldecott *et al*., 1994; Caldecott *et al*., 1995).

More recently, the Pommier group also showed a physical interaction between TDP1 and PARP1, a crucial factor in BER/SSBR. PARP1 binds TDP1$^{151\text{-}168}$ (Das *et al*., 2014). PARylation of TDP1 by PARP1 promotes its protein stability, interaction with XRCC1, and recruitment to sites of DNA damage induced by UVA, CPT, (Das *et al*., 2014) and monofunctional alkylating agents (Murai *et al*., 2012; Alagoz *et al*., 2013; Lebedeva *et al*., 2015). Interestingly, inhibition of PARP1 activity seemed to promote accumulation of phospho-S81 TDP1, suggesting a negative feedback mechanism of TDP1 PARylation on S81 phosphorylation.

The fortuitous finding that human TDP1$^{1\text{-}150\ S81A}$ did not express in yeast pointed me to the possibility that S81 may play a role in stabilising the protein. While it is common for truncated proteins to be unstable, the large size of the Gal4BD tag could have stabilised the truncated TDP1$^{1\text{-}150}$. In addition, as Lig3α was absent in yeast (Kelley *et al*., 2003), the stabilising effect was not due to Lig3α. It was therefore important to examined this in human cells. I used cycloheximide to determine the half-lives of Myc-TDP1 and Myc-TDP1^{S81A} in A549 cells (**Fig. 3.5**), as well as HeLa cells depleted of Lig3α (**Fig. 3.6**). The results indicate that in human cells, S81 promotes TDP1 stability by forming a complex with Lig3α. Although it is possible that the N-terminal Myc-tag could alter the protein structure at the N-terminus domain, this was unlikely to be the case, as the finding was reproduced by another group, whereby Flag-TDP1 and Flag-TDP1^{S81A} were used (Das *et al*., 2009). To conclusively test this, tertiary structural analysis would need to be performed, but that would fall outside the time frame of this thesis. However, characterising the binding sites of TDP1 and Lig3α could be of

therapeutic potential, as more effective small molecule inhibitors of TDP1 are being developed to improve the clinical outcome of TOP-based therapies commonly used in breast, lung and colorectal cancers (Huang *et al*., 2011).

Although the molecular mechanism by which TDP1:Lig3α interaction regulates TDP1 protein turnover in cells has been established, *in vitro* the enzymatic activity seemed independent of this interaction (**Fig. 3.7**). This was not too surprising as the N-terminus domain has been shown to be dispensable for catalytic activity *in vitro* (Interthal *et al*., 2001).

Next the effect of TDP1:Lig3α interaction on DNA repair in the chromosomal context was explored. Again, TDP1 S81 phosphorylation appeared not to play a role in the repair of TOP1-cc, which are expected to be predominantly SSBs in the time frame of the treatment **(Fig. 3.9**, **3.10**). It must be noted that recombinant proteins from *E. coli* were used instead of cDNA transfection, as the efficiency of DNA transfection is low in MEFs, therefore unsuitable for comet assay. The possibility of the recombinant proteins lacking important post-translational modifications could explain the discrepancy between my data and that published by Das *et al*, who found a reduction in SSBR capacity after CPT treatment in MEFs complemented with hTDP1^{S81A}. The MEFs used by this group were transduced with lentiviral particles containing the cDNA of the relevant proteins, and repair in cells complemented with wildtype TDP1 was as efficient as Tdp1 MEFs (Das *et al*., 2009).

With the clonogenic survival assay, although a partial defect was seen in cells expressing recombinant TDP1^{S81A} compared to wildtype TDP1, this again could be due to the shorter half-life of the recombinant TDP1^{S81A} without compensation by increased protein synthesis. As shown by Das *et al*, phosphorylated TDP1 is retained at sites of CPT-induced breaks for hours, even long after the removal TOP1-cc. The shorter half-life of TDP1^{S81A} could account for more unrepaired lesions persisting into S-phase and the subsequent cell killing.

To conclude, TDP1 S81 prolongs the protein half-life, likely by forming a stable complex with Lig3α. This interaction does not promote enzymatic activity *in vitro*, but promotes DNA repair efficiency as measured by clonogenic survival assays.

In the next chapter, I will describe the discovery and characterisation of another element of post-translational modification in the N-terminus domain of TDP1 that regulates its DNA repair efficiency – the Small Ubiquitin-like Modifier (SUMO) pathway.

CHAPTER 4

SUMOylation of TDP1 at K111 accelerates recruitment to DNA damage sites and promotes cellular survival after genotoxic stress

4.1 Introduction

Although I have confirmed that TDP1 S81 is required for its interaction with Lig3α, its significance in SSBR and SCAN1 pathology is still not clear. Lig3α knockout mice are embryonically lethal (Puebla-Osorio *et al*., 2006), but Lig3α is dispensable for nuclear SSBR (Gao *et al*., 2011; Simsek *et al*., 2011), as there is a functional overlap with Lig1. As Lig3α is the only form of DNA ligase in the mitochondria, it is possible that TDP1 S81 is more important for mitochondrial DNA repair than nuclear DNA repair. It is also possible that TDP1 interacts with other DNA ligases in the nucleus such as Lig1 or Lig4. To explore the possibility that S81 may mediate specific interactions with other DNA repair proteins, I used the yeast two-hybrid system again to screen for proteins interacting with the TDP1^{S81E} mutant, which acts as a phosphomimetic and should increase the likelihood of detecting S81 phosphorylation-dependent protein-protein interactions. To this end, a novel interacting partner was discovered, which has a clear role in the SUMOylation pathway. This suggests that TDP1 is post-translationally modified by a second mechanism. This chapter describes the characterisation of N-terminus domain – SUMOylation of lysine 111 (K111) by SUMO1, and the mechanism by which it regulates TDP1 function at a cellular level.

4.1.1 The SUMOylation pathway and TOP1

SUMOylation can regulate the activity of target proteins in terms of transcription, stability, protein-protein interaction, and sub-cellular localisation. Increasing evidence confirms its role in DNA damage response and repair (Dou *et al*., 2011). The SUMOylation pathway, similar to the ubiquitination pathway, is a multi-step process involving: 1) processing of SUMO precursor to mature form; 2) activation of SUMO by SUMO-activating enzyme (E1), consisting of the heterodimer Uba2(Sae2)/Aos1(Sae1); 3) conjugation of SUMO to target protein by SUMO-conjugating enzyme (E2), UBC9, with or without the help of a SUMO ligase (E3) (Dohmen, 2004) (**Fig. 4.1**). SUMO

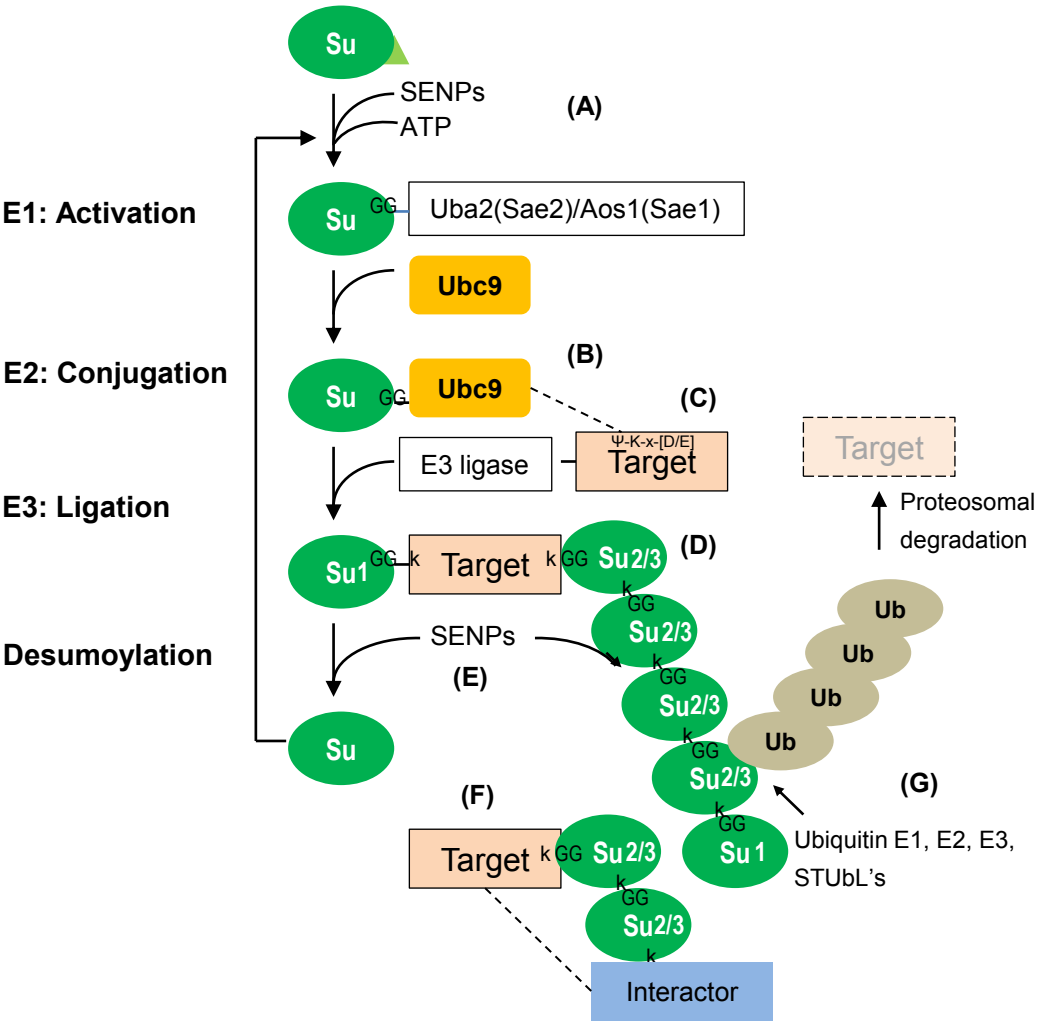

Figure 4.1 The SUMOylation pathway. (A) The SUMO precursor is activated by cleavage of its C-terminal tail by sentrin-specific proteases ("SENPs"), exposing a di-glycine site. The di-glycine site forms a covalent bond with Uba2 of the E1 activating heterodimeric enzyme Uba2/AOS1 in an ATP-dependent reaction. **(B)** Activated SUMO is transferred from Uba2/AOS1 to UBC9 via a transesterification reaction. **(C)** *In vitro*, UBC9 can directly conjugate to the lysine residue in the Ψ-K-x-[D/E] consensus site of the target protein. However *in vivo* it is facilitated by a target-specific E3 ligase, resulting in transfer of SUMO to the target protein. **(D)** SUMO2/3 can form poly-SUMO chains on target proteins while SUMO1 cannot. However SUMO1 can terminate a SUMO2/3 chain. **(E)** De-SUMOylation of target protein occurs through cleavage of SUMO by SENPs. Free activated SUMO can re-enter the pathway and bind another target protein. **(F)** SUMOylation/de-SUMOylation can affect protein-protein interaction by modifying their binding sites. **(G)** Poly-SUMO-chains can be recognised by SUMO-targeted ubiquitin ligases (STUbl's) and be ubiquitinated through the ubiquitination pathway, targeting the protein for proteasomal degradation. Adapted from Dohmen, 2004; Geiss-Friedlander and Melchior, 2007.

conjugation is usually transient, as de-SUMOylation by SUMO/Sentrin-specific proteases (SENPs) is very rapid (Mukhopadhyay and Dasso, 2007; Yeh, 2009). In humans, there are four SUMO paralogues: SUMO-1 to SUMO-4 (Dou *et al*., 2011). SUMO-1 has been shown to interact with TOP1 after CPT damage (Mao *et al*., 2000; Yang *et al*., 2006); and dominant-negative UBC9 mutant is associated with cellular hypersensitivity to CPT (Mo *et al*., 2004; Jacquiau *et al*., 2005). However, TOP1 SUMOylation has also been shown to increase cellular sensitivity to CPT (Horie *et al*., 2002). In addition, although it has been suggested that TOP1 activity is regulated after CPT-induced damage, by translocating TOP1 from the nucleolus to the nucleus (Mo *et al*., 2002), it may not be SUMO-dependent (Christensen *et al*., 2004). The conflicting data possibly reflect the underlying complexity of the mechanisms through which SUMOylation regulates TOP1 activity and DNA damage response. It has been shown that in yeast, SUMO-targeted ubiquitin ligase (STUbl), SUMO-mimetic Rad60, and E3 ligase Nse2 function as TDP1 independent pathway in repairing TOP1 linked breaks (Heideker *et al*., 2011). The identification of a novel interaction between TDP1 and a component of the SUMOylation pathway suggest SUMOylation may have a role in TDP1-mediated DNA repair. Understanding how and why TDP1 is SUMOylated would provide important information on this regulatory system.

4.2 Results

4.2.1 Yeast two-hybrid library screen of TDP1^{S81E} interacting proteins

For the library screen for TDP1 S81 phosphorylation dependent interacting proteins, I used sequential transformation of first the bait plasmid, pGBKT7-TDP1^{S81E}, then the prey, human cDNA library-encoding pACT constructs, in order to improve transformation efficiency of the cDNA library. Y190 cells were transformed with pGBKT7-TDP1^{S81E} and selected in yeast minimal media without leucine. Four individual clones were picked, and the expression of Gal4-BD-TDP1^{S81E} was confirmed by Western blotting (data not shown). A large-scale transformation of the TDP1^{S81E}-

expressing clone with 14 µg of cDNA library was performed, with transformation efficiency of ~ 4 x 10^4 colonies per µg DNA. 56 clones were confirmed by for histidine prototrophy, of which 35 encoded known genes. Fourteen of the 35 clones encoded full-length UBE2I, the human homologue of the SUMO E2 conjugating enzyme UBC9. Two clones encoded SETDB1, which has been recently been identified as a chromatin compacter at sites of DSBs required for efficient homologous recombination (Alagoz *et al*., 2015). Other hits of some interest were KPNA2, MYCBP2, PIAS4, NPM1, and MCART1, which could mediate TDP1 sub-cellular translocation or ubiquitination. However, these clones were either in the wrong orientation or lacked the start codon therefore could not be expressed. To rule out any technical errors during Sanger sequencing, these clones were re-streaked and interaction with $TDP1^{S81E}$ were re-tested by yeast two-hybrid. However, none of the interactions could be reproduced (data not shown).

4.2.2 S81 phosphomimetic mediates TDP1 interaction with UBE2I

The interaction of $TDP1^{S81E}$ with two clones of UBE2I (clone 5 and clone 6) was confirmed by yeast two-hybrid assays (**Fig. 4.2)**. This interaction was mediated by phosphorylation of S81, as wildtype TDP1 was able to interact with UBE2I, while $TDP1^{S81A}$ largely abrogated the interaction, as confirmed by CPRG-based quantitative yeast two-hybrid assay (**Fig. 4.3**). These interactions were specific, as expression of neither pGBKT7-$TDP1^{S81E}$ nor pACT-UBE2I alone auto-transactivated the β-gal or His prototrophic reactions (**Fig. 4.2A, Right panel**) and the expression levels of TDP1, $TDP1^{S81E}$ and $TDP1^{S81A}$ were comparable (**Fig. 4.2B**).

To validate this interaction in mammalian cells, I transfected HEK293 cells with pCI-Myc-TDP1 and immunoprecipitated the whole cell lysates using Myc antibodies. As the step of UBE2I binding to TDP1 to transfer SUMO is likely to be transient, cellular proteins were crosslinked with 1% paraformaldehyde before cell lysis, to increase the chance of detecting this interaction. **Fig. 4.4A** shows that endogenous UBE2I co-

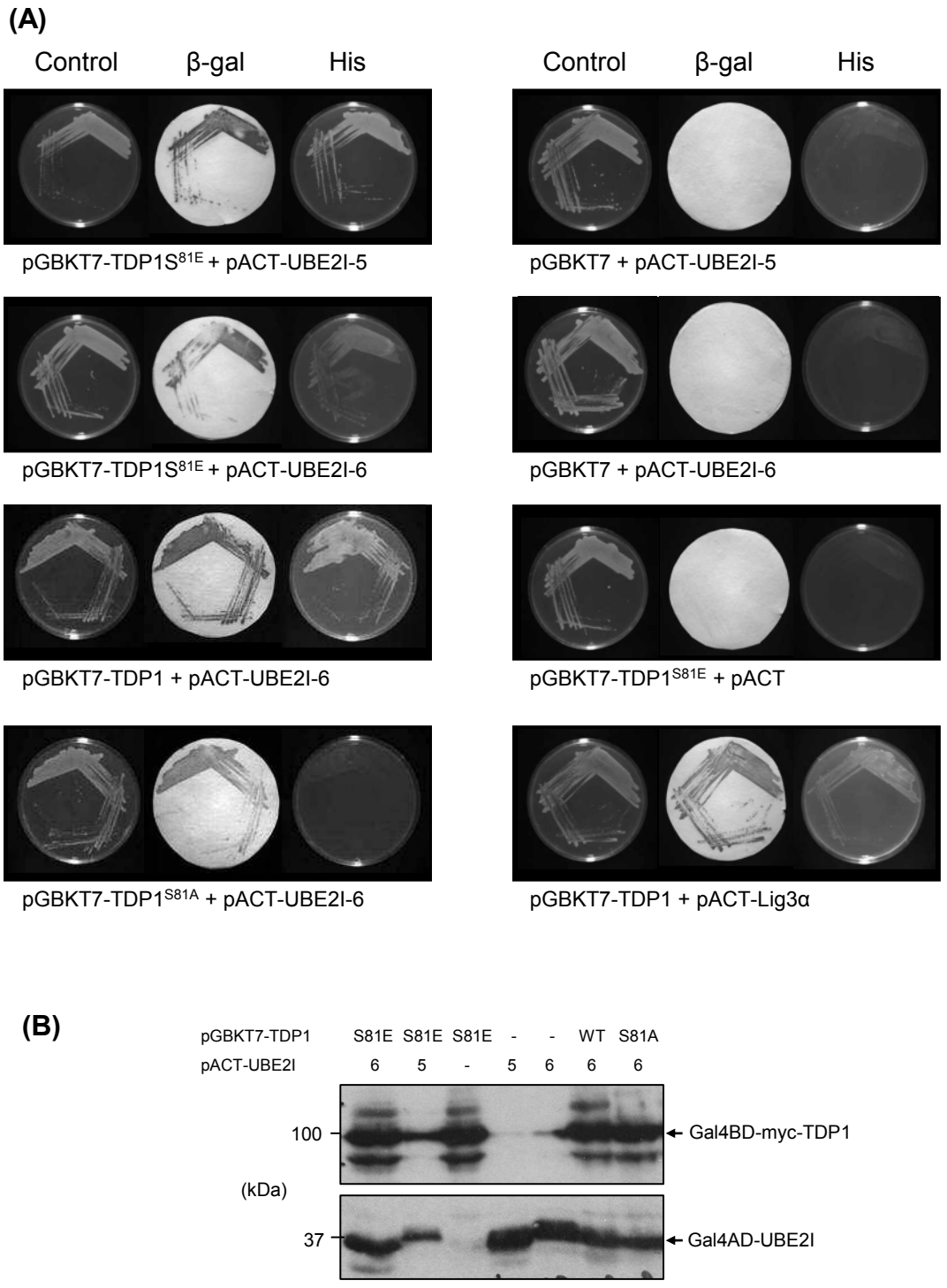

Figure 4.2 Validation of TDP1^{S81E} interaction with UBE2I in yeast two-hybrid. (A) Y190 cells were co-transformed with the indicated pGBKT7 and pACT constructs. Transformants were selected on selective medium containing histidine ("Control") or lacking histidine and containing 3-aminotriazole ("His") to test for the activation of the *his3* reporter gene. The activation of the *β-gal* reporter gene was detected using the filter lifts from control plates ("β-Gal"). **(B)** WCEs (10 µL of 0.075 OD_{600}/µL) were fractionated with SDS-PAGE and immunoblotted using antibodies against Myc and Gal4AD. A duplicate gel was stained with Coomassie blue as loading control.

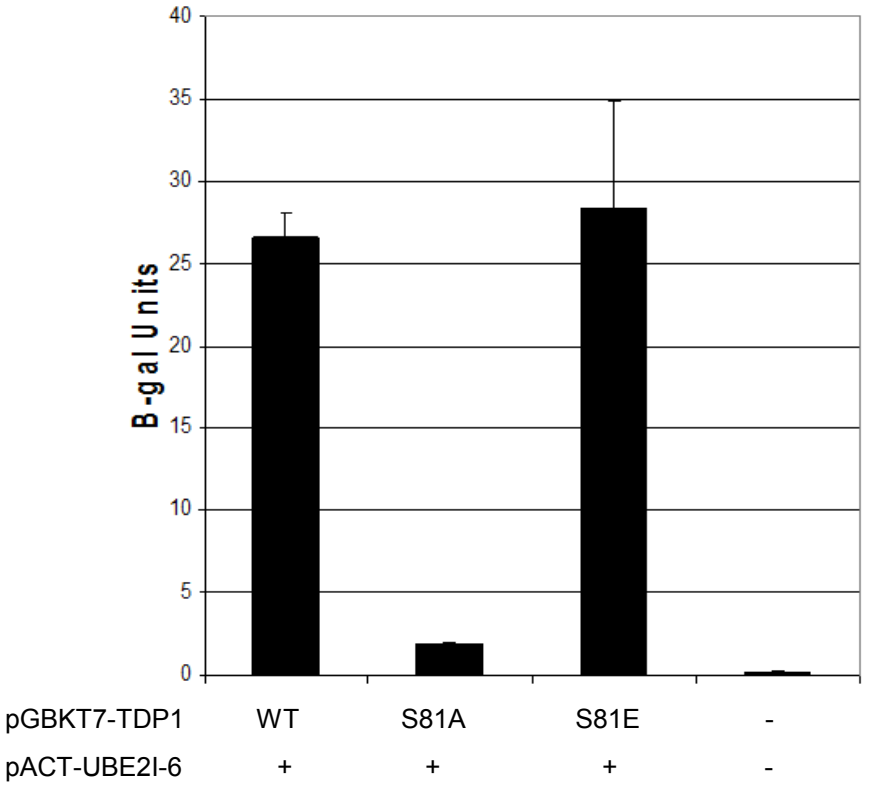

Figure 4.3 Quantification of TDP1 interaction with UBE2I in yeast two-hybrid. Y190 cells were transformed with pACT-UBE2I or pACT and the indicated pGBKT7 constructs and selected on yeast minimal medium lacking histidine and containing 3-aminotriazole. Transformants were then grown in complete culture medium for two doubling cycles and harvested. The WCEs were incubated in CPRG until the medium turned from yellow to red colour and the reaction was stopped with 3 mM $ZnCl_2$. The OD_{578} of the supernatant was measured. β-galactosidase units was calculated as 1000 x OD_{578} (t x V xOD_{600}), where t = stop time – start time (in minutes), V = 0.1 x concentration factor. 1 unit of β-galactosidase is defined as the amount which hydrolyses 1 µmol of CPRG to chlorophenol red and D-galactose per minute per cell. 1 unit of β-galactosidase equals the amount of enzyme required to hydrolyse CPRG per minute. Data are the mean of 3 independent experiments and error bars represent ±1 S.E.M.

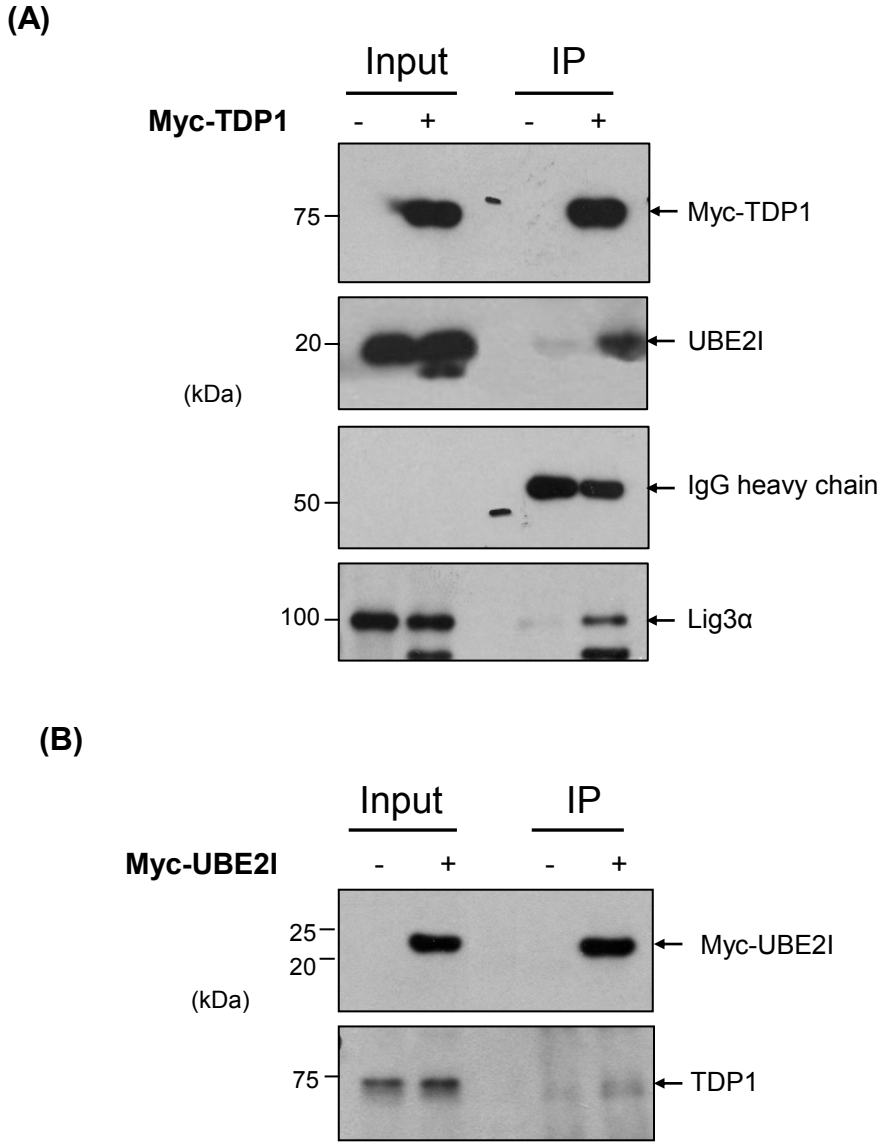

Figure 4.4 TDP1 interacts with UBE2I in HEK293 cells. (A) HEK293 cells were transfected with pCI-Myc-TDP1 (+) or empty pCI-Myc vector (-). 48 hours post-transfection, cells were fixed with 1 % paraformaldehyde for 10 minutes to crosslink proteins, washed with 100 mM glycine, then lysed. WCEs were immunoprecipitated using Myc antibodies. Levels of Myc-TDP1, UBE2I and Lig3α in the WCEs ("Input") and in the immunoprecipitates ("IP") were determined by immunoblotting with antibodies against Myc, UBE2I and Lig3α. Lig3α served as positive IP control. Levels of IgG heavy chain served as loading control. **(B)** HEK293 cells were transfected with ΔT-Myc-DEST-UBE2I or empty ΔT-Myc-DEST vector, and WCEs were immunoprecipitated with Myc antibodies. Levels of Myc-UBE2I and TDP1 in the input and IP samples were determined by immunoblotting with antibodies against Myc and TDP1.

immunoprecipitated with Myc-TDP1 but not untagged Myc. Lig3α blotting was used as positive control and detected no non-specific binding, possibly due to paraformaldehyde fixing. Reciprocal IP showed that endogenous TDP1 co-immunoprecipitated with Myc-UBE2I (**Fig. 4.4B**).

4.2.3 TDP1 is covalently modified by SUMO1

My colleague Dr Jessica Hudson tested SUMO-modification of TDP1 by SUMO1, SUMO2 and SUMO3 in the mammalian system, and confirmed that TDP1 is SUMOylated by all three paralogues, but predominantly by SUMO1 (Hudson *et al*., 2012).

To detect covalent binding of SUMO1 with TDP1 in mammalian cells, I overexpressed Myc-TDP1 and GFP-SUMO1 in HEK293 cells. GFP-SUMO1 appeared to co-immunoprecipitate with Myc-TDP1 (**Fig. 4.5**). Although there were non-specific pull-down of GFP-SUMO1 in cells overexpressing untagged Myc, the interaction was stronger in cells co-transfected with Myc-TDP1 and GFP-SUMO1. In this experiment, the effect of CPT treatment on TDP1/SUMO1 interaction was unclear, as SUMO1 pull-down was increased in the absence of TDP1. Interestingly, Lig3α pull-down appeared to be increased in the presence of GFP-SUMO1, although this was not CPT-dependent.

Taken together, my results indicate that TDP1 is SUMOylated by SUMO1, and this modification may promote TDP1 interaction with Lig3α.

4.2.4 SUMOylation of TDP1 at K111 is not required for interaction with Lig3α

In silico prediction indicated that there are five putative SUMO modification sites on TDP1, two in the N-terminus domain and three in the C-terminus domain (**Fig. 4.6**). Sequence alignment shows that K111 is conserved amongst vertebrates. My lab colleague Dr Jessica Hudson confirmed that K111 is the main SUMOylation site in mammalian cells (Hudson *et al*., 2012). Since K111 is in the N-terminus domain of TDP1, we postulated that it may regulate the function of TDP1.

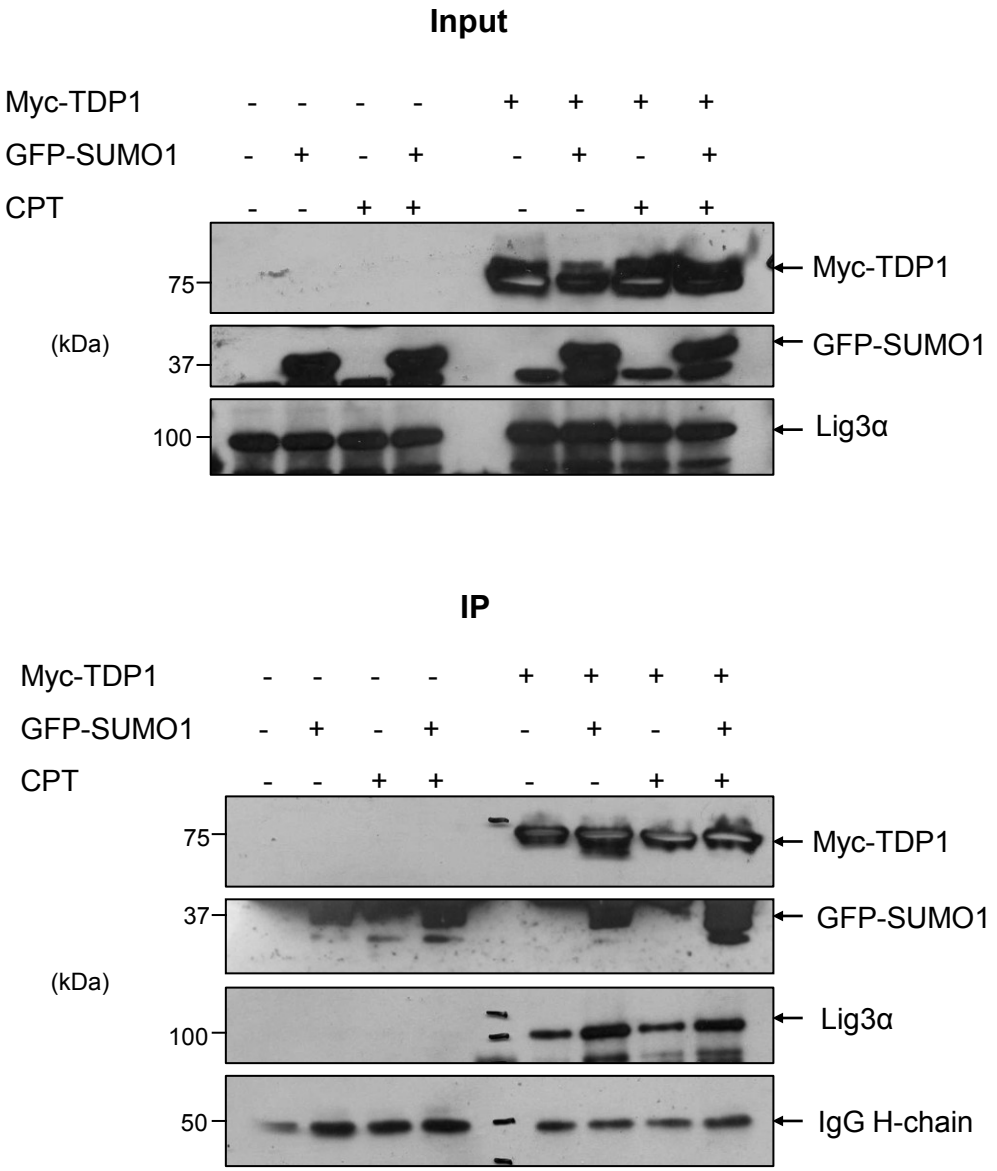

Figure 4.5 TDP1 interacts with SUMO1 in HEK293 cells. HEK293 cells were co-transfected with pCI-Myc-TDP1 ("+") or empty pCI-Myc vector ("-") and pEGFP-C3-SUMO1 ("+") or empty pEGFP-C3 vector ("-"). 48 hours post-transfection the cells were treated with 30 μM CPT ("+") or DMSO ("-") for 30 minutes at 37˚C, washed with PBS, then lysed. WCEs were immunoprecipitated with Myc antibodies. Levels of Myc-TDP1, GFP-SUMO1 and Lig3α present in total cell extracts ("Input") and the immunoprecipitates ("IP") were determined by immunoblotting with antibodies against Myc, GFP and Lig3α. Lig3α served as positive control for Myc-TDP1 IP. Levels of IgG heavy chain served as loading control in the IP samples.

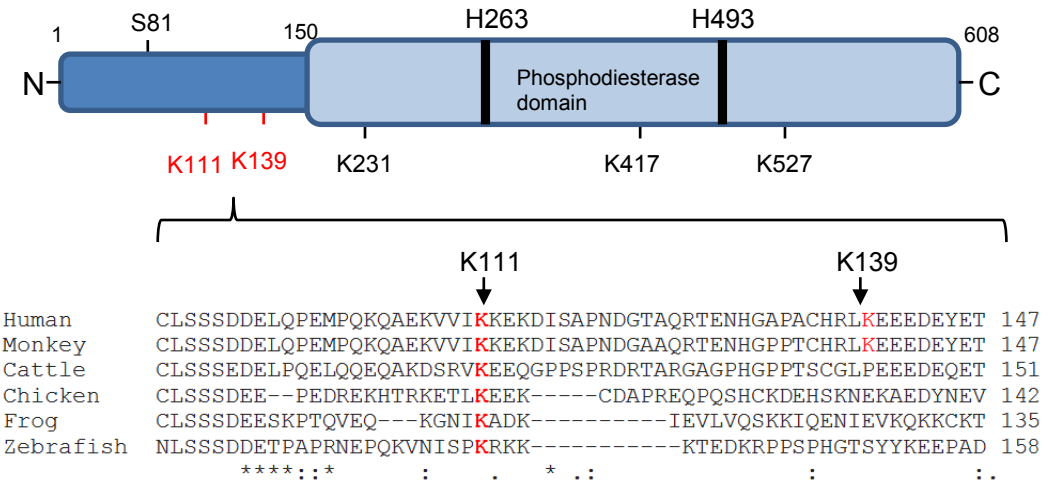

Figure 4.6 TDP1 K111 is conserved in higher eukaryotes. The SUMOsp 2.0 online database was used to predict potential sites for SUMO modification. K111 and K139 were predicted based on the consensus sequence Ψ-K-X-E, while prediction of K231, K417 and K527 was based on non-consensus sites. Multiple sequence alignment of TDP1 using ClustalW indicates that K111 is conserved in humans (*Homo sapiens*; NP_001008744), cattle (*Bos taurus*; NP_001180084; XP_874680), monkey (*Pongo abelii*; XP_002825063), chicken (*Gallus gallus*; XP_421313), frog (*Xenopus tropicalis*; NP_001039242), and zebrafish (*Danio rerio*; XP_700174).

It has been shown that SUMOylation can modulate protein-protein interactions and subcellular localisation of target proteins (Bergink and Jentsch, 2009). This could indirectly regulate TDP1 activity, for example, by promoting its interaction with components of the SSBR or DSBR machinery, and recruiting it to sites of DNA damage.

I first tested whether K111 SUMOylation influenced TDP1 interaction with Lig3α by yeast two-hybrid. Mutation of K111 to arginine (K111R) did not affect TDP1 interaction with Lig3α (**Fig. 4.7**). My lab colleague also confirmed in HEK293 cells that K111R mutation did not abrogate co-immunoprecipitation of Lig3α with TDP1 (Hudson *et al*., 2012).

Another lab member also showed that TDP1^{K111R} mutation did not cause structure conformational changes, nor impact on enzymatic activity *in vitro* (Hudson *et al*., 2012).

4.2.5 TDP1 K111 SUMOylation promotes cell survival after CPT damage

I then tested the importance of TDP1 SUMOylation on DNA repair in mammalian cells. *Tdp1*$^{-/-}$ MEFs complemented with wildtype hTDP1, TDP1^{K111R} or empty vector were treated with CPT or γ-radiation, and the cellular repair response was assessed by clonogenic survival assay. TDP1^{K111R}-complemented cells showed a mild CPT survival defect compared to wildtype TDP1-complemented cells (**Fig. 4.8A, *p < 0*.05; Student's t-test**), but no defect was observed for IR damage repair. The difference in CPT survival was not due to differences in protein expression levels (**Fig. 4.8B**) or cell cycle arrest after CPT, as assessed by FACS (**Fig. 4.9**). These results suggest that TDP1 SUMOylation promotes repair of CPT-induced damage throughout the cell cycle.

4.2.6 TDP1 K111 SUMOylation promotes repair of chromosomal strand breaks induced by CPT and IR

To confirm a direct effect of TDP1 SUMOylation on DNA damage repair, we measured CPT-induced chromosomal strand breaks by the alkaline comet assay. *Tdp1*$^{-/-}$ MEFs complemented with human TDP1^{K111R} accumulated ~ 3 fold more breaks compared to

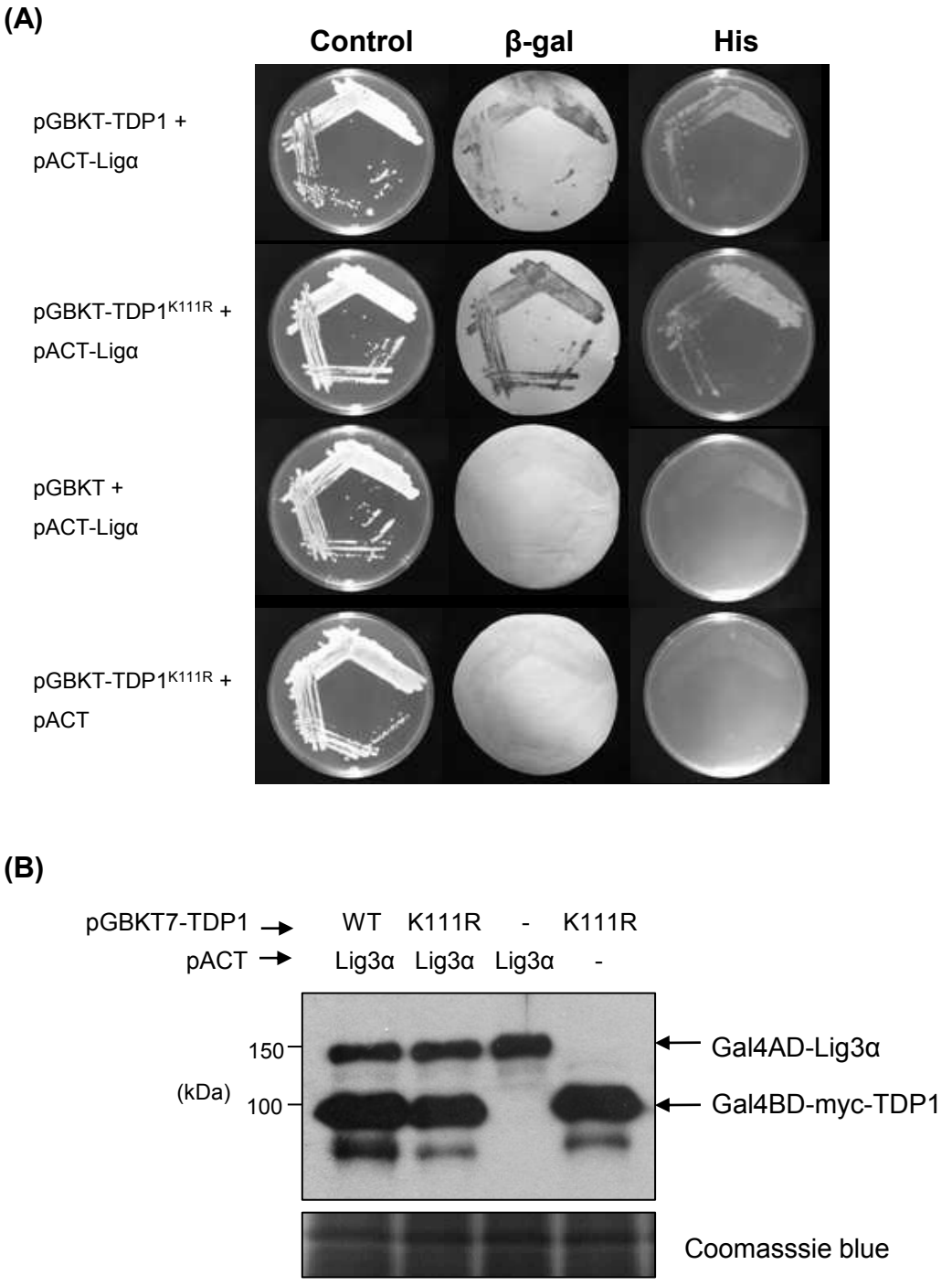

Figure 4.7 TDP1 K111 SUMOylation is not required for interaction with Lig3α. **(A)** Y190 cells co-transformed with the indicated pGBKT7 and pACT constructs were plated onto selective media either containing histidine ("Control") or lacking histidine and containining 3-aminotriazole ("His") to test for the activation of the *his3* reporter gene. Activation of the *β-Gal* reporter gene was determined using filter lifts from control plates ("β-Gal"). **(B)** WCEs (10 µL of 0.075 OD_{600}/µL) from (A) were fractionated with SDS-PAGE and immunoblotted using antibodies against Myc and Gal4AD. A duplicate gel was stained with Coomassie blue as loading control.

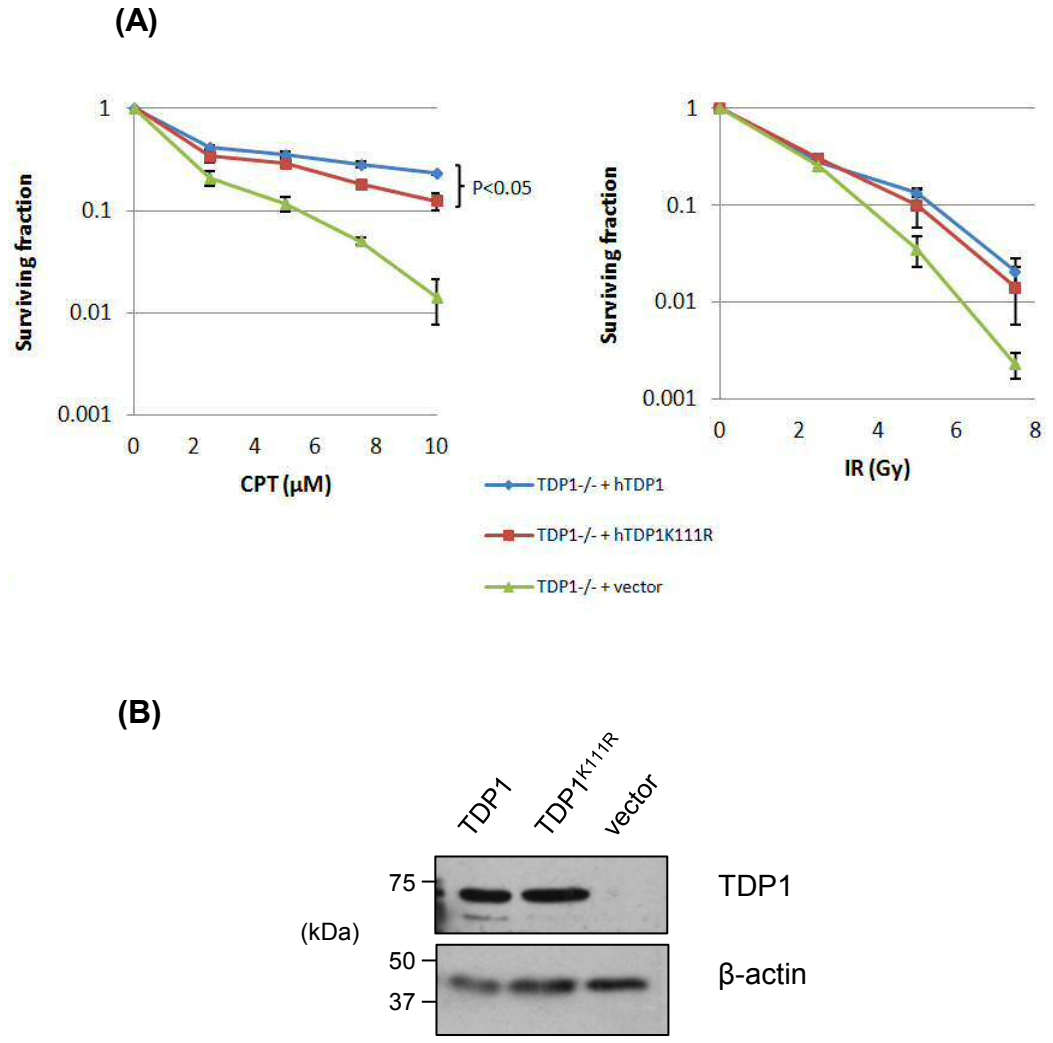

Figure 4.8 TDP K111 SUMOylation promotes cellular survival after CPT damage. (A) *Tdp1*$^{-/-}$ MEFs complemented with hTDP or hTDP1^{K111R} by retroviral transduction were plated on 10 cm dishes and incubated at 37˚C overnight. Cells were then treated with the indicated doses of CPT for 1 hour at 37˚C (left), or x-ray at 12 mA / 250V on ice (right), then left to recover in drug-free medium for 7 – 10 days until macroscopic colonies formed. Surviving fraction was calculated by dividing the number of colonies on treated plates by the number on mock treated plates. Data are the mean of 4 independent experiments and error bars represent ±1 S.E.M. *p* values were derived using two-tailed Student's t-test. **(B)** Expression levels of hTDP1 and hTDP1^{K111R} in *Tdp1*$^{-/-}$ MEF WCEs from experiments in (A) were assessed by immunoblotting with antibodies against TDP1 and β-actin.

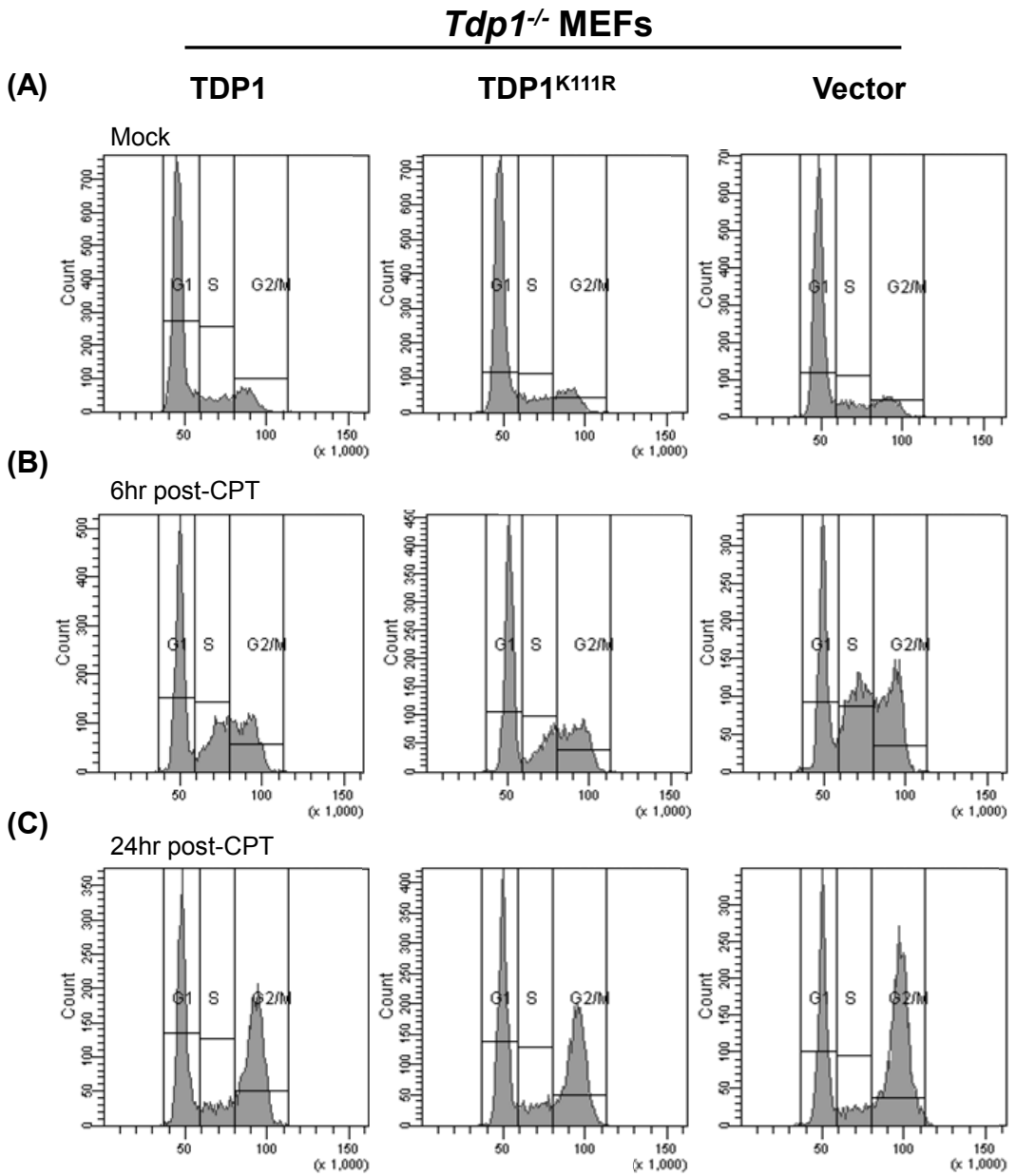

Figure 4.9 TDP1 K111 SUMOylation does not affect cell proliferation. *Tdp1*$^{-/-}$ MEFs complemented with hTDP1, hTDP1^{K111R}, or empty vector were treated with **(A)** DMSO ("Mock"), or **(B)** 20 μM CPT for 1 hour at 37˚C, then recovered in drug-free medium for 6 to **(C)** 24 hours. Cells were fixed with 70 % ethanol and stained with 50 μg/ml propidium iodide. DNA content was analysed by FACS using the 585/42 spectrum filter.

cells complemented with wildtype TDP1 (**Fig. 4.10A**, ***p < 0*.05; Student's t-test**). The difference was due to K111 SUMOylation, as overexpression of SUMO1 in wildtype TDP1-complemented HEK293 cells reduced the number of CPT-induced breaks (**Fig. 4.10B, *p < 0*.01; Student's t-test**), which was not seen with the hTDP1^{K111R}-complemented cells. With IR damage, *Tdp1*$^{-/-}$ MEFs complemented with TDP1^{K111R} accumulated ~ 25 % more breaks than wildtype TDP1-complemented cells (**Fig. 4.10C, *p < 0*.05; Student's t-test**), and showed a delay in the repair kinetics comparable to that of *Tdp1*$^{-/-}$ cells. These results indicate that SUMOylation at K111 promotes DNA repair efficiency of TDP1.

4.2.7 TDP1 SUMOylation does not affect repair of DSBs induced by IR and CPT

Unrepaired CPT and IR induced single-stranded DNA breaks can be converted into cytotoxic double-stranded breaks during DNA replication, which are then repaired by homologous combination (HR). I used immunofluorescence quantification of the DSB marker γ-H2AX to assess DSBR after CPT or IR treatments. After one hour of recovery following CPT treatment, *Tdp1*$^{-/-}$ cells showed a clear delay in the repair of DSBs, while cells complemented with wildtype TDP1 or hTDP1^{K111R} exhibited similar rates of repair (**Fig. 4.11A**). This is in agreement with the cell cycle analysis in **Fig. 4.9B&C** showing no difference in the S- and G2/M arrested populations between cells complemented with hTDP1^{K111R} or wildtype hTDP1. After 2 Gy IR damage, there was no difference in the number of γ-H2AX foci in all three cell lines, indicating that at this IR dosage, TDP1 was dispensable for DSBR (**Fig. 4.11B**). These results suggest the survival defect in TDP1^{K111R}-complemented MEFs treated with CPT was not due to attenuated DSBR or cell cycle checkpoint response.

4.2.8 TDP1 SUMOylation accelerates its recruitment to DNA damage sites

A lab member then showed that TDP1^{K111R} mutation did not affect the nuclear and nucleolar localization of TDP1 after CPT damage (Hudson *et al*., 2012). I then examined the kinetics of EGFP-TDP1 or EGFP-TDP1^{K111R} accumulation at sites of

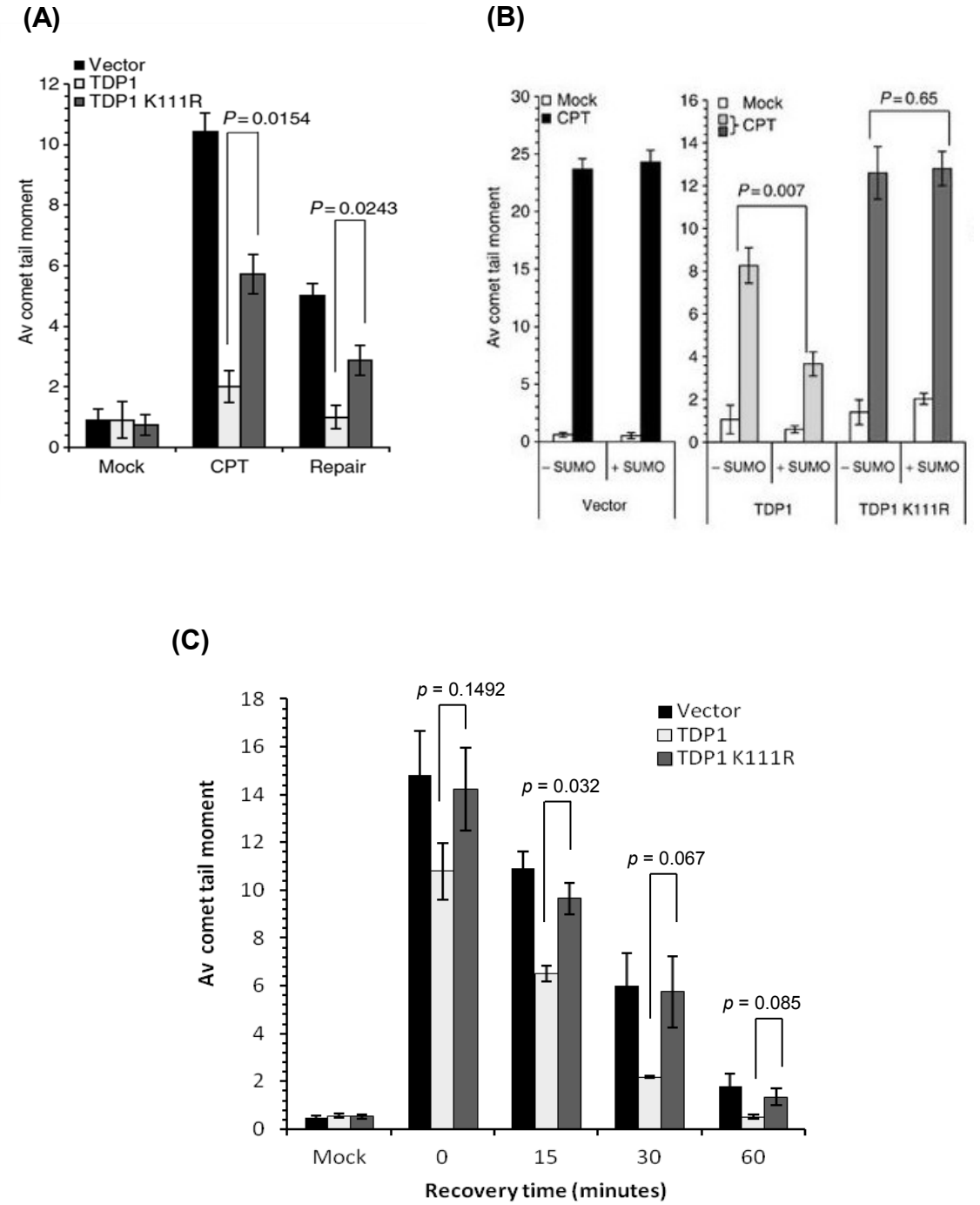

Figure 4.10 TDP1 K111 SUMOylation promotes early-phase repair of SSBs induced by CPT and ionising radiation. *Tdp1*$^{-/-}$ MEFs complemented with hTDP1, hTDP1^{K111R}, or empty vector were treated with **(A)** 20 μM CPT for 1 hour at 37˚C, then incubated in drug-free medium at 37˚C for the indicated periods. DNA strand breakage was quantified by alkaline comet assay. **(B)** HEK293 cells transfected with pCI-Myc-TDP1 or pCI-Myc-TDP1^{K111R} and an empty GFP "−SUMO1" or GFP1-SUMO1 "+SUMO1" vector were treated as described in (A) and analysed by alkaline comet assay. **(C)** MEFs from (A) were treated with 20 Gy γ-ray then left to recover at 37˚C for the indicated periods. DNA strand breakage was quantified by alkaline comet assay. The average of DNA strand breaks was from 3 independent experiments (100 cells per experiment) and error bars represent ±1 S.E.M. *p* values were derived using two-tailed Student's t-test.

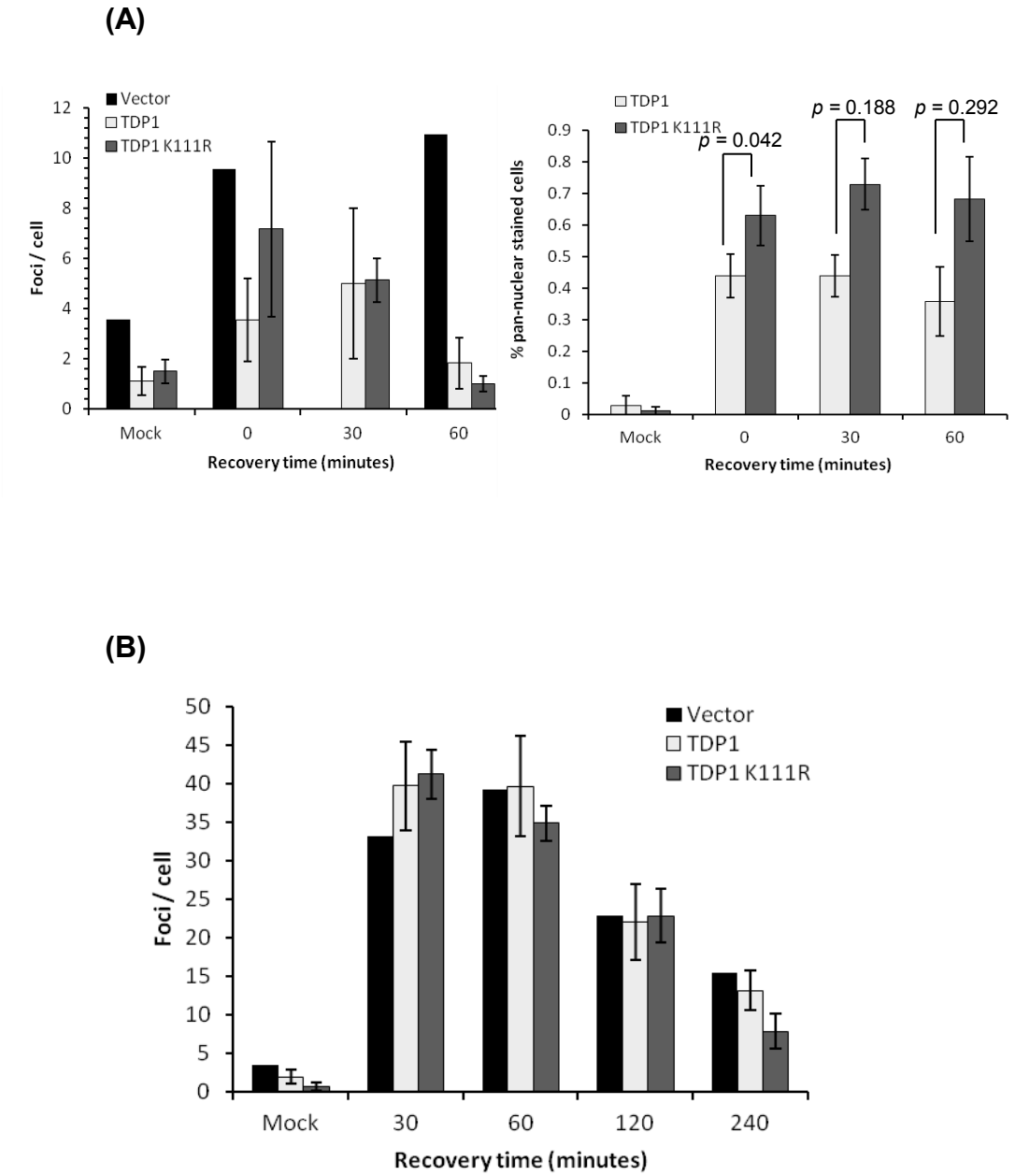

Figure 4.11 TDP1 K111 is not required for repair of double-stranded DNA breaks induced by IR and CPT. (A) *Tdp1*$^{-/-}$ MEFs complemented with hTDP1, hTDP1^{K111R}, or empty vector were treated with 1 μM CPT for 1 hour at 37˚C**,** then incubated in drug-free medium for the indicated periods. Cells were then fixed and immunostained with γH2AX antibodies and DAPI (left). Percentage of cells with more than 80 foci per cell or pan-nuclear staining, indicating S- and G2-phase cells (right). **(C)** *Tdp1*$^{-/-}$ MEFs as in (A) were subjected to 2 Gy γ-ray and left to repair for the indicated periods. Cells were then fixed and immunostained with γH2AX antibodies and DAPI. Data are the mean of 3 independent experiments (50 cells per experiment) and error bars represent ±1 S.E.M. *p* values were derived using two-tailed Student's t-test.

nuclear DNA damage induced by UVA irradiation in live cells. UVA produces a spectrum of DNA lesions that can trap TOP1, as well as 3'-phosphoglycolate and 3'-dRP ends that can be repaired by TDP1 (discussed in **Section 1.5.1**). I used laser microirradiation to induce UVA damage in MRC5 cells overexpressing EGFP-TDP1 or EGFP-TDP1^{K111R} (**Fig. 4.12A, top panel**), and measured the EGFP fluorescence intensity within the laser track before and after damage (**Fig. 4.12B**) as an indicator of recruitment of EGFP-TDP1 or EGFP-TDP1^{K111R} to the sites of DNA damage. The background florescence immediately before irradiation was comparable between EGFP-TDP1- and EGFP-TDP1^{K111R}-complemented cells (**Fig. 4.12A, bottom panel**). After irradiation, EGFP-TDP1^{K111R} accumulated significantly slower than EGFP-TDP1 at the laser tracks during the 90 seconds. Whereas EGFP-TDP1 level peaked within 15 seconds after irradiation, EGFP-TDP1^{K111R} level failed to reach saturation even at 90 seconds (**Fig. 4.12C**). Notably, depletion of the obligate SUMO E2 conjugating enzyme, UBE2I, (**Fig. 4.13A**) in MRC5 cells expressing GFP-TDP1 (**Fig. 4.13B**) attenuated the recruitment of EGFP-TDP1 to the laser track, while having no further impact on recruitment of EGFP-TDP1^{K111R} (**Fig. 4.13C**), suggesting the slower recruitment of GFP-TDP1^{K111R} to DNA damage sites was due to loss of SUMOylation.

4.3 Discussion

TDP1 plays a role in repairing endogenous TOP1-associated DNA breaks (TOP1-cc), and its deficiency leads to neurodegeneration and cerebellar ataxia in humans. Although it is generally accepted that TDP1 functions within the context of the SSBR machinery, how TDP1 is recruited to and activated at the sites TOP1-cc was unclear. This is a physiologically relevant question, as repair of TOP1 breaks have been shown to require high concentrations of TDP1 *in vitro* (Raymond *et al*., 2005). The findings presented in this chapter answer this question by showing a second molecular mechanism through which the N-terminus domain of TDP1 regulates its function, specifically, by increasing its concentration at sites of nuclear DNA damage.

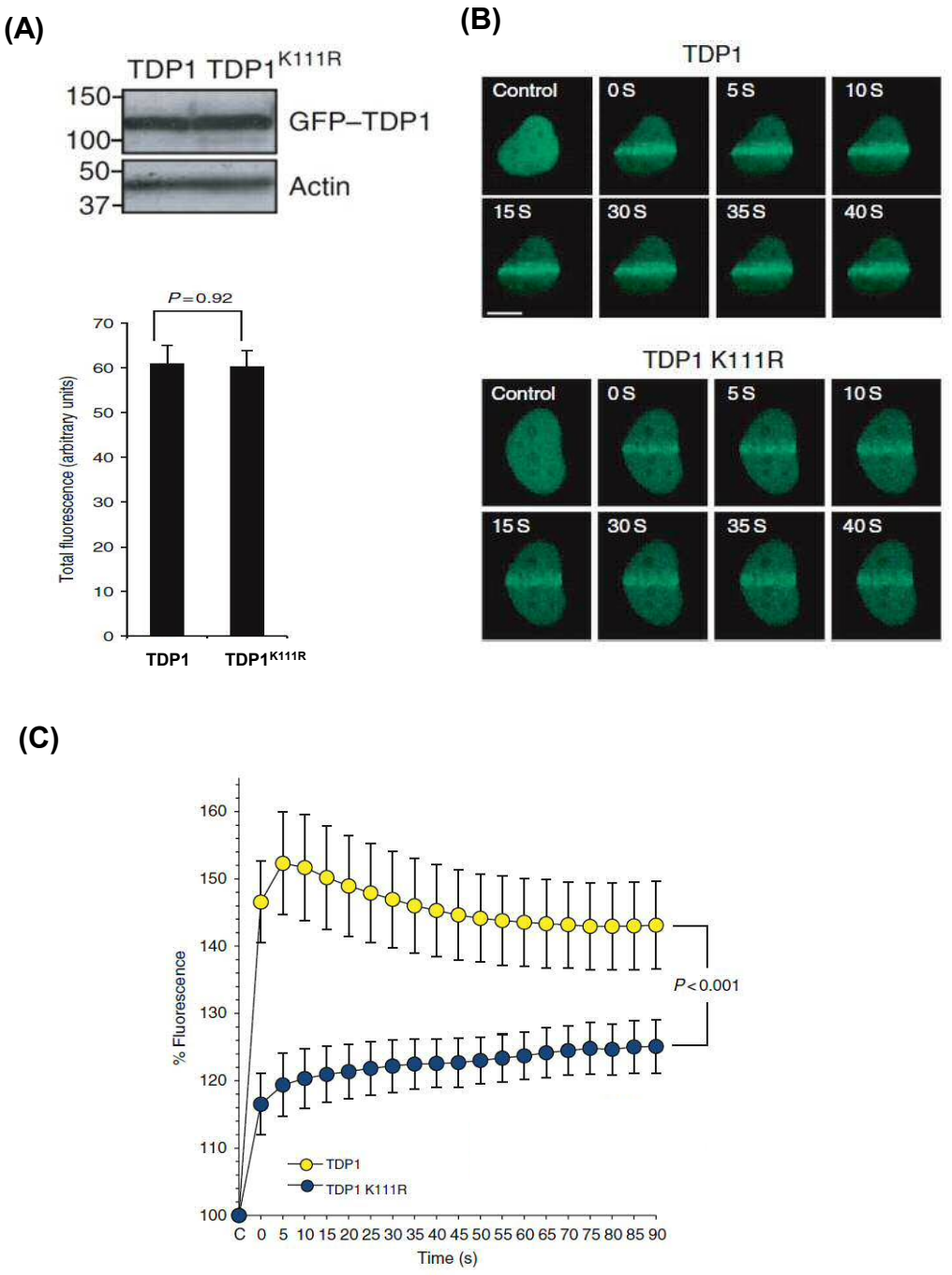

Figure 4.12 TDP1 K111 SUMOylation promotes its accumulation at sites of DNA damage. (A) Human MRC5 cells were transfected with pMC-EGFP-TDP1 or pMCEGFP–TDP1^{K111R} and the expression levels of EGFP-TDP1 and EGFP-TDP1^{K111R} were compared by immunoblotting WCEs with antibodies against TDP1 and β-actin (top) and FACS using the EX493/EM525 spectrum (bottom). **(B)** MRC5 cells from (A) were plated onto glass-bottomed dishes and transfected with pMC-EGFP-TDP1 or pMC-EGFP–TDP1^{K111R}. Cells expressing similar levels of GFP signal were locally irradiated with UV-A laser (351 nm), and images were taken with a Zeiss ConfoCor 2/LSM510 confocal microscope every 5 seconds up to 90 seconds. **(B)** EGFP–TDP1 accumulation at the sites of damage was quantified by LSM 520 Meta software for the indicated time periods, where "C" represents undamaged control. Data are the average of ~ 60 cells measured from 6 independent experiments, and error bars indicate ±1 S.E.M. *p* values were derived using two-tailed Student's t-test. Figures taken from Hudson *et al.,* 2012.

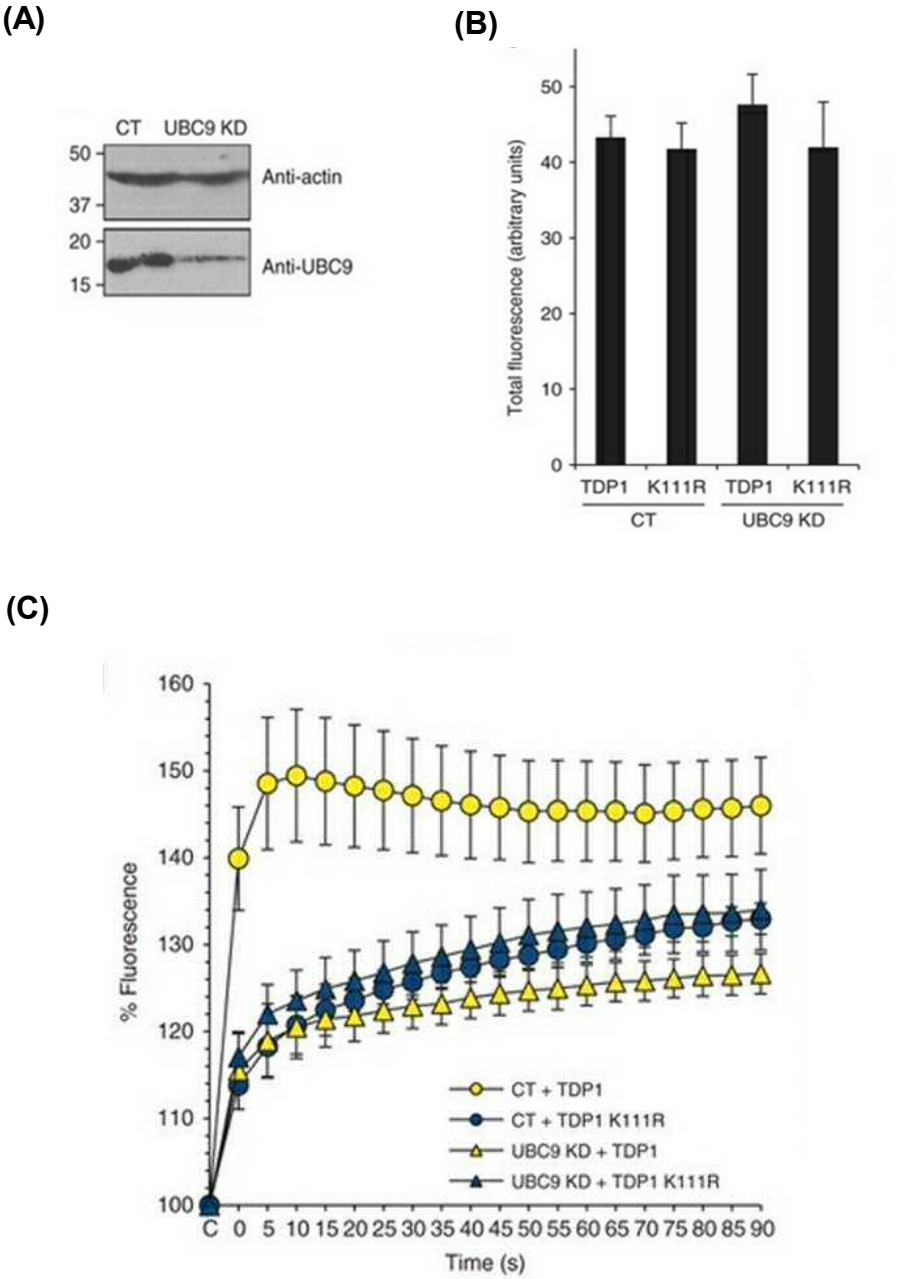

Figure 4.13 UBC9 promotes TDP1 accumulation at sites of DNA damage. (A) MRC5 cells were stably depleted of UBC9 by shRNA transfection and selected with 1 μg/ml puromycin for 2 weeks. Expression levels of UBC9 in knocked-down ("UBC9 KD") and control ("CT") cells were compared by immunoblotting WCEs with antibodies against UBC9 and β-actin. (**B)** MRC5 cells with or without UBC9 knock-down as described in (A) were transfected with pMC-EGFP-TDP1 or pMC-EGFP-TDP1 and the mean EGFP intensity was measured by FACS using the EX493/EM525 spectrum. **(C)** EGFP–TDP1 accumulation at the sites of damage was quantified by LSM 520 Meta software for the indicated time periods, where "C" represents undamaged control. Data are the average of ~ 60 cells measured from 6 independent experiments, and error bars indicate ±1 S.E.M. Figures taken from Hudson *et al.,* 2012.

The interaction of TDP1 with UBE2I, the human homologue of the obligate SUMO E2 conjugating enzyme Ubc9, implies modification of TDP1 by SUMOylation. SUMOylation is an important post-translational modification that regulates protein activity in terms of transcription, stability, protein-protein interaction, and sub-cellular localisation. Increasing evidence confirms its role in DNA damage response and repair (Dou *et al*., 2011).

My results showed that TDP1 interacts with UBE2I/UBC9 in yeast two-hybrid assay and co-immunoprecipitation in HEK293 cells (**Fig. 4.2 – 4.4**). In the yeast two-hybrid assays, interaction of TDP1 with UBE2I was dependent on S81. In human cells, my lab colleague has showed that overexpression of $TDP1^{S81A}$ in HEK293 reduced the *in vitro* SUMOylation of TDP1, while overexpression of $TDP1^{S81E}$ also reduced it, but to a lesser extent than the phosphomutant (Wells, 2014). This could suggest that a dynamic phosphorylation/de-phosphorylation switch is required for maintaining SUMOylation of TDP1. Interestingly, he also identified a casein kinase 2 phosphorylation site at S91/S92 that may negatively regulate SUMOylation. The crosstalk between post-translational modification mechanisms implies a high level of regulation of TDP1 activity in higher organisms.

In HEK293 cells overexpressing Myc-TDP1 and GFP-SUMO1, interaction between TDP1 and SUMO1 appeared to be increased after treatment with CPT (**Fig. 4.5**). However, it appeared to be somewhat non-specific, as SUMO1 pull-down was also increased after CPT treatment in cells not overexpressing Myc-TDP1. Dr Jessica Hudson then showed that there was no detectable increase in SUMO1-conjugated TDP1 after CPT treatment (Hudson *et al*., 2012), suggesting that the interaction is constitutive and likely has a housekeeping function against DNA damage arising from endogenous sources. This is in contrast to the SUMO2/3 modification triggered by damage as seen in COS-7 cells (Saitoh and Hinchey, 2000). However, the preference between SUMO1 or SUMO2/3 modification in response to exogenous damage appears

to be cell line-specific, as SUMO1 modification seems to be the predominant response to exogenous stress in HeLa cells (Vertegaal *et al*., 2006; Impens *et al*., 2014). In HEK293 cells, modifications of protein extracts from PML bodies by both SUMO1 and SUMO3 have been shown to be increased by after arsenic trioxide damage (Galisson *et al*., 2011).

Interestingly, overexpression of SUMO1 increases TDP1 interaction with Lig3α (**Fig. 4.5**). However, SUMOylation of TDP1 at K111 is not required for this interaction in the yeast two-hybrid assay (**Fig. 4.7**), and in HEK293 co-immunoprecipitation experiments (Hudson *et al*., 2012). It is possible that in this case SUMOylation occurs on Lig3α, or another protein such as XRCC1 that can stabilise TDP1/Lig3α interaction (Gocke *et al*., 2005; Bruderer *et al*., 2011; Weber *et al*., 2014).

TDP1 K111 SUMOylation promotes cellular survival following CPT (**Fig. 4.8**), and repair of CPT and IR induced DNA strand breaks (**Fig. 4.10**). The molecular basis of these effects does not appear to be mediated by altered catalytic activity, protein structure and stability, subcellular translocation, interaction with DNA ligase 3α (Hudson *et al*., 2012), involvement in DSBR (**Fig. 4.11**) (El-Khamisy and Caldecott, 2007; Katyal *et al*., 2007) or cell cycle checkpoint signalling (**Fig. 4.9**).

I did observe a significant reduction in the rate of recruitment of TDP1^{K111R} to UVA-induced DNA damage sites (**Fig. 4.12**). This effect was SUMOylation-specific, as depletion of the obligate E2 conjugating enzyme UBE2I/UBC9 decreased the rate of recruitment of TDP1 but not TDP1^{K111R} (**Fig. 4.13**). Although I could only use cells transiently overexpressing EGFP-TDP1 and EGFP-TDP1^{K111R} (due to constitutive TDP1 overexpression being poorly tolerated by mammalian cells), I tried to account for the intrinsic inter-clonal variations by examining only cells expressing similar levels of GFP-TDP1 or GFP-TDP1^{K111R} before UVA irradiation (**Fig. 4.12A, 4.13B**).

Using the transcription inhibitor 5,6-dichlorobenzimidazole 1-b-d-ribofuranoside (DRB), my colleague Mr Chris Rookyard also showed that recruitment of both TDP1 and

TDP1^{K111R} was partially inhibited (Hudson *et al*., 2012). This suggests that: 1) a portion of the UVA-induced DNA damage sites were transcription-mediated SSBs, or 2) a subgroup of TDP1 (independent of the SUMOylation status) is recruited to the damage sites that are being actively transcribed. Given the short duration of the irradiation and recruitment time-course of the laser microirradiation experiment, the latter explanation seems more plausible, although this does not automatically exclude the former explanation. Either way, the implication that TDP1 accumulates at transcriptionally active sites points to its functional significance in postmitotic, highly-transcribing neurons, in which endogenous SSBs are the most abundant chromosomal lesions. Indeed, *Tdp1*$^{-/-}$ mouse neuronal cells complementation with hTDP1^{K111R} could not fully protect against cell killing following CPT treatment compared to cells complemented with wildtype hTDP1 (Hudson *et al*., 2012).

How does SUMOylation promote recruitment of TDP1 at transcription-associated break ends? SUMOylation is widely used to regulate transcription, chromatin remodeling, and DNA damage repair (Garcia-Dominguez, 2013; House *et al*., 2014). One specific mechanism may be through interaction with stalled TOP1, which is SUMOylated after CPT treatment and undergoes proteasomal degradation (Mao *et al*., 2000; Yang *et al*., 2006). This could act as a signal to recruit TDP1 to further process the lesion. Our lab has preliminary data demonstrating interaction between TDP1 and chromatin-bound TOP1 (data not shown).

Further pressing questions include: what is this subgroup of TDP1 that interacts with the transcription machinery? What is its role in repair of transcription-associated SSBs? Does TDP1 associate with products of stalled transcription such as R-loops? Does TDP1 play a role in transcription of the mitochondrial genome?

Clearly, the regulation of TDP1 activity at the cellular level is more complex than we initially anticipated. It also points to new areas of biological processes in which TDP1 is involved. In the next two chapters, I will explore the role of TDP1 in repair of DNA

lesions from endogenous oxidative stress, and the impact it has on mitochondrial functions and cellular viability.

CHAPTER 5

Tdp1 protects against endogenous oxidative stress in mouse embryonic fibroblasts

5.1 Introduction

The second part of my PhD project was to test the hypothesis that TDP1 repairs a broader spectrum of ROS-induced DNA lesions other than TOP1-DNA adducts, which may contribute to cerebellar neurodegeneration.

In postmitotic neurons, oxidative stress induces lesions that can trap TOP1 (Pourquier and Pommier, 2001; Daroui *et al*., 2004; Pommier *et al*., 2003; Katyal *et al*., 2007; Katyal *et al*., 2014), which in turn can impede transcription (Sordet *et al*., 2009; Alagoz *et al*., 2013; Katyal *et al*., 2014), generate DSBs, and activate apoptosis or lead to cellular senescence (Sordet *et al*., 2003; Sordet *et al*., 2009). However, *Tdp1*$^{-/-}$ mice demonstrated only late-onset cerebellar degeneration and no ataxia (Hirano *et al*., 2007; Katyal *et al*., 2007), suggesting that the effect of the unrepaired DNA lesions in the absence of Tdp1 is gradual. This makes the mouse model less useful for studying the role of ROS in SCAN1 *in vivo*, due to the short life-span of the organism.

In vitro studies suggest that TDP1 can repair a broader spectrum of ROS-induced breaks other than TOP1-DNA adducts, such as 3'-phosphoglycolates, 3'-phosphates and abasic sites *in vitro* (Inamdar *et al*., 2002; Interthal *et al*., 2005a; Zhou *et al*., 2005). *Tdp1*$^{-/-}$ astrocytes, MEFs and chicken B-lymphocytes (DT40) showed hypersensitivity to hydrogen peroxide, ionising radiation, and bleomycin which induce broad-spectrum oxidative DNA damage (Hirano *et al*., 2007; Katyal *et al*., 2007; Murai *et al*., 2012). Incidentally, using *Tdp1*$^{-/-}$ MEFs complemented with hTDP1 as a control, I also observed the hypersensitivity to H_2O_2 and IR in *Tdp1*$^{-/-}$ MEFs (**Fig. 5.1**).

However, acute treatment with ROS-inducing agents in cultured cells may not recapitulate the situation induced by endogenous ROS *in vivo*. Our lab has previously generated a mouse model which uncovered the role of another SSBR factor, aprataxin (APTX), against endogenous oxidative stress (Carroll *et al*., 2015). By crossing *Aptx*$^{-/-}$

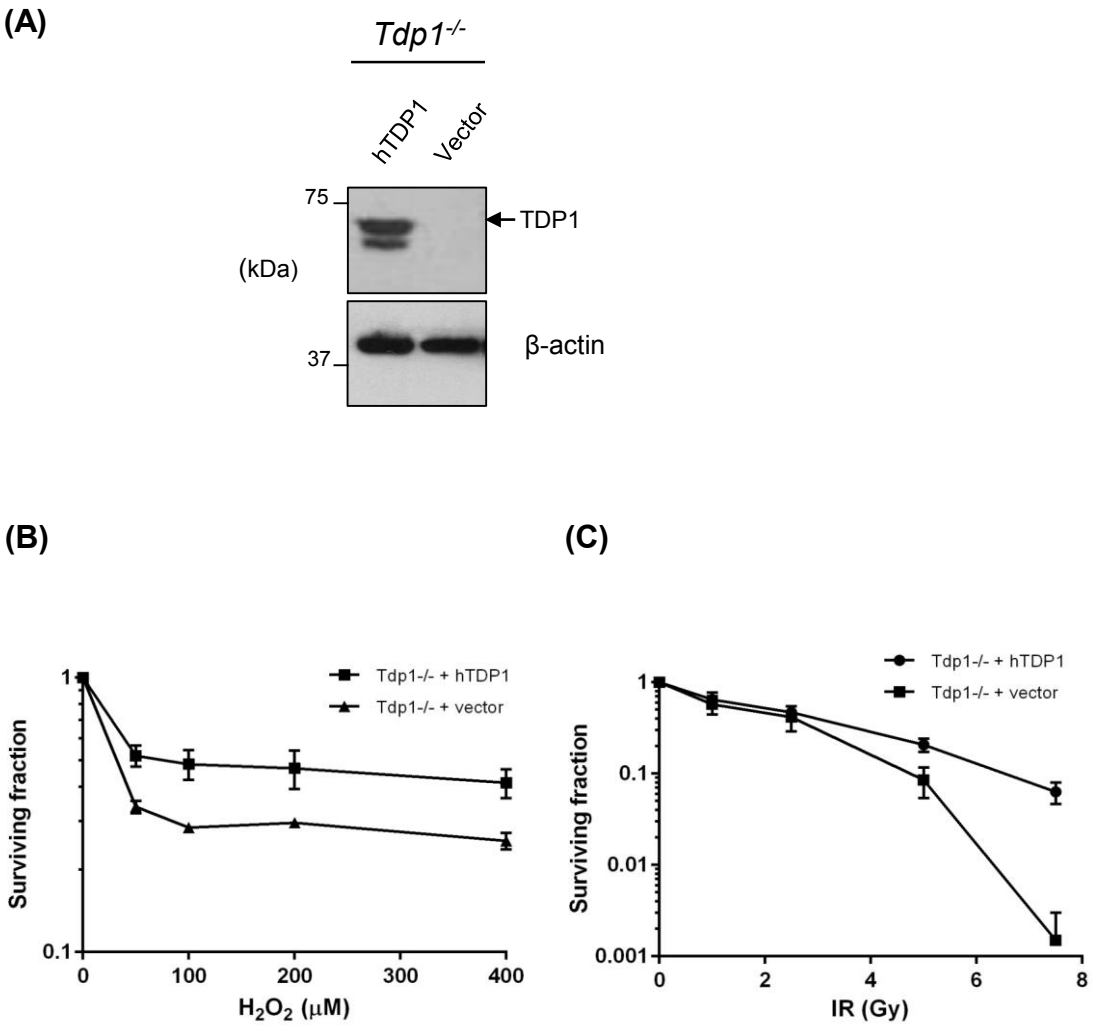

Figure 5.1 *Tdp1*$^{-/-}$ MEFs are sensitive to exogenous ROS. (A) *Tdp1*$^{-/-}$ MEFs were complemented with hTDP1 or empty vector by retroviral transduction and selection in 1 μg/ml puromycin for 2 weeks. WCEs were analysed by immunoblotting using antibodies against human TDP1 and β-actin. Arrow indicate the hTDP1 product. Between 2000 – 6000 MEFs from (A) were plated in 10 cm petri dishes and incubated at 37˚C overnight. Cells were then treated with the indicated doses of H_2O_2 for 10 minutes on ice (**B**), or x-ray at 12 mA / 250V on ice (**C**), then left to recover in normal growth medium for 7 – 10 days until macroscopic colonies formed. Surviving fraction was calculated by dividing the number of colonies on treated plates by the number on untreated plates. Data are the mean of 3 independent experiments and error bars represent ±1 S.E.M.

mice, which exhibited no DNA repair and survival defect against oxidative stress, with mice overexpressing mutated human SOD1 ($SOD1^{G93A}$), which have documented mitochondrial defect and elevated levels of endogenous ROS and ROS-induced DNA lesions (Gurney *et al*., 1994; Robberecht, 2000), it was shown that Aptx indeed repairs endogenous ROS-induced DNA lesions and promotes neuronal viability.

Thus, I used the same approach to generate a mouse model, whereby *Tdp1*$^{-/-}$ mice were crossed with those overexpressing $hSOD1^{G93A}$, to study the role of Tdp1 against endogenous oxidative stress,

5.1.1 Endogenous ROS generation by SOD1^{G93A}

SOD1 is a Cu/Zn superoxide dismutase, ubiquitously expressed in the cytosol, mitochondrial intermembrane space (IMS) (Weisiger and Fridovich, 1973; Okado-Matsumoto and Fridovich, 2001; Sturtz *et al*., 2001), nucleus, and peroxisosomes (Chang *et al*., 1988; Del Maestro and McDonald, 1989; Keller *et al*., 1991; Crapo *et al*., 1992). It acts as a first-line ROS scavenger by converting superoxide to hydrogen peroxide, which is in turn catalysed into water and oxygen by catalase and glutathione peroxidase (Fridovich, 1986).

Mutations of *SOD1* account for ~ 5 % of the motor neuron disease amyotrophic lateral sclerosis (ALS) (Andersen *et al*., 2003; Valentine *et al*., 2005). The pathogenesis of *SOD1*^{G93A} mutation, although rare in ALS patients, has been extensively studied in the transgenic mouse model overexpressing human $SOD1^{G93A}$ (Gurney *et al*., 1994). $hSOD1^{G93A}$-overexpressing mice exhibit higher oxidative stress (Ferrante *et al*., 1997; Andrus *et al*., 1998; Liu *et al*., 1998; Poon *et al*., 2005; Casoni *et al*., 2005) and mitochondrial dysfunctions with reduced ATP production (Jung *et al*., 2002; Browne *et al*., 2006), defective ETC function (Mattiazzi *et al*., 2002; Kirkinezos *et al*., 2005), dysregulation of calcium homeostasis and loss of membrane potential (Damiano *et al*., 2006; Jaiswal and Keller, 2009; Jaiswal *et al*., 2009), and mitochondrial axonal transport (Magrane and Manfredi, 2009; Sotelo-Silveira *et al*., 2009).

The SOD1^{G93A} protein is catalytically active (Cleveland, 1999) but possesses reduced zinc-binding capacity, which destabilizes the structure and promotes aggregate formation (Chattopadhyay *et al*., 2008; Furukawa *et al*., 2008). SOD1^{G93A} aggregates targeted to inclusion bodies are particularly toxic as they can sequester Hsp70 and inhibit proteolysis and overall protein quality control (Matsumoto *et al*., 2005; Matsumoto *et al*., 2006; Wang *et al*., 2009; Weisberg *et al*., 2012). SOD1^{G93A} aggregates in the mitochondria (Vijayvergiya *et al*., 2005; Kawamata and Manfredi, 2008) can sequester the anti-apoptotic protein Bcl-2 and promote motor neuron death (Pasinelli *et al*., 2004; Pedrini *et al*., 2010; Tan *et al*., 2013). SOD1^{G93A} has also been shown to promote apoptosis through the endoplasmic reticulum stress response (Kieran *et al*., 2007; Nishitoh *et al*., 2008). It has also been proposed that the conformational change of SOD1^{G93A} promotes its binding with hydrogen peroxide, converting it to more reactive hydroxyl radicals in the presence of ferric ions through Fenton reaction (Wiedau-Pazos *et al*., 1996). This aberrant peroxidase activity of SOD1^{G93A} has been linked to increased oxidative DNA damage in the mitochondria and nucleus of the spinal cord of SOD1^{G93A} mice (Warita *et al*., 1999; Martin *et al*., 2007) and human SH-SY5Y neuroblastoma cells (Barbosa *et al*., 2010). More recently, it has been shown that SOD1 translocates to the nucleus in response to hydrogen peroxide (but not superoxide) in an ATM-dependent manner, and promotes transcription of anti-oxidant and DNA repair genes (Tsang *et al*., 2014). Whether SOD1^{G93A} translocates to the nucleus as efficiently as wildtype SOD1 is controversial and may depend on the level of overexpression (Sau *et al*., 2011; Barbosa *et al*., 2010; Gertz *et al*., 2012). Taken altogether, there is overwhelming evidence for the increased endogenous ROS production by SOD1^{G93A} overexpression, through multiple mechanisms in the mitochondria and nucleus.

5.2 Results

5.2.1 Generation of hSOD1^{G93A};Tdp1$^{-/-}$ double mutant MEFs

Transgenic *SOD1^{G93A}* male mice (Gurney *et al*., 1994) were crossed with female mice with different Tdp1 backgrounds (Katyal *et al*., 2007), as female *SOD1^{G93A}* mice are infertile. The genotypes of live offspring are listed in **Table 5.1**.

The first observation was that only 2 live births out of the predicted ~ 61 were *SOD1^{G93A};Tdp1$^{-/-}$* double mutants. Secondly, the genotypes of the offspring differed significantly from the predicted Mendelian ratio when the male *SOD1^{G93A}* parents were heterozygous for *Tdp1* deletion (**Table 5.1A**) but not in the case when both copies of *Tdp1* were present (**Table 5.1B**). Specifically, the numbers of *Sod1$^{+/+}$;Tdp1$^{+/-}$* offspring were significantly decreased (6 as opposed to the predicted 54.5). This is unexpected as *Tdp1$^{+/-}$* mice do not have known developmental defects. Conversely, the numbers of *Sod1$^{+/+}$;Tdp1$^{-/-}$* and *hSOD1^{G93A};Tdp1$^{+/-}$* offspring were significantly increased (115 and 96, respectively, compared to the expected 54.5). These anomalies were present at early embryonic state (**Table 5.1C**). Taken together, these findings suggest non-random segregation of the *hSOD1^{G93A}* alleles and *Tdp1* alleles.

The *hSOD1^{G93A}* transgenic mice were generated with multiple copies (~ 10) randomly integrated into the mouse genome (Gurney *et al*., 1994). It may be possible that one copy was inserted close to the *Tdp1* locus. On closer inspection, *SOD1^{G93A}* seemed to co-segregate with the *Tdp1* wildtype allele, making the statistical probability of generating the *SOD1^{G93A};Tdp1$^{-/-}$* offspring very low.

To circumvent this problem, we decided to use a cellular model instead to further investigate the role of Tdp1 in cells with high endogenous ROS levels. To do this, I established *Tdp1$^{-/-}$* MEFs which overexpress either wildtype Sod1 or hSOD1^{G93A}.

5.2.2 Tdp1 modulates levels of SOD1^{G93A}-induced DNA free radicals

To measure the levels of endogenous ROS generated by hSOD1^{G93A}, our collaborator Dr Nick Kassouf used 5,5-Dimethyl-1-Pyrroline-N-Oxide (DMPO) to capture intracellular free radicals induced by UVA photolysis, and analysed the profile by

A

Male parent	$hSOD1^{G93A}; Tdp1^{+/-}$					
Female parent	$Sod1^{+/+}; Tdp1^{-/-}$		$Sod1^{+/+}; Tdp1^{+/-}$		$Sod1^{+/+}; Tdp1^{+/+}$	
Offspring (No. live births)	**Expected**	**Obtained**	**Expected**	**Obtained**	**Expected**	**Obtained**
$Sod1^{+/+}; Tdp1^{+/+}$			6.25	3	2.25	0
$Sod1^{+/+}; Tdp1^{+/-}$	54.5	6	12.5	5	2.25	4
$Sod1^{+/+}; Tdp1^{-/-}$	54.5	115	6.25	14		
$hSOD1^{G93A}; Tdp1^{+/+}$			6.25	14	2.25	5
$hSOD1^{G93A}; Tdp1^{+/-}$	54.5	96	12.5	12	2.25	0
$hSOD1^{G93A}; Tdp1^{-/-}$	54.5	1	6.25	2		
Total	218	218	50	50	9	9

B

Male parent	$hSOD1^{G93A}; Tdp1^{+/+}$					
Female parent	$Sod1^{+/+}; Tdp1^{-/-}$		$Sod1^{+/+}; Tdp1^{+/-}$		$Sod1^{+/+}; Tdp1^{+/+}$	
Offspring (No. live births)	**Expected**	**Obtained**	**Expected**	**Obtained**	**Expected**	**Obtained**
$Sod1^{+/+}; Tdp1^{+/+}$			15.25	9	7	6
$Sod1^{+/+}; Tdp1^{+/-}$	24.5	21	15.25	15		
$Sod1^{+/+}; Tdp1^{-/-}$						
$hSOD1^{G93A}; Tdp1^{+/+}$			15.25	23	7	8
$hSOD1^{G93A}; Tdp1^{+/-}$	24.5	28	15.25	14		
$hSOD1^{G93A}; Tdp1^{-/-}$						
Total	49	49	61	61	14	14

C

Male parent	***hSOD1^{G93A}; Tdp1$^{+/-}$***	
Female parent	***Sod1$^{+/+}$; Tdp1$^{-/-}$***	
Offspring (No. of E12 embryos)	**Expected**	**Obtained**
Sod1$^{+/+}$; Tdp1$^{+/-}$	6.5	0
Sod1$^{+/+}$; Tdp1$^{-/-}$	6.5	14
hSOD1^{G93A}; Tdp1$^{+/-}$	6.5	12
hSOD1^{G93A}; Tdp1$^{-/-}$	6.5	0 (1 underdeveloped embryo)

Table 5.1: *Genotypes of offspring of crossing hSOD1^{G93A} mice with different Tdp1 backgrounds*

Sod1$^{+/+}$ = wild-type *Sod1*; hSOD1$^{G93A+/-}$ = heterozygous for multiple copies of hSOD1^{G93A} transgene; *Tdp1$^{+/+}$* = wild-type *Tdp1*; *Tdp1$^{+/-}$* = heterozygous for *Tdp1* deletion; *Tdp1$^{-/-}$* = homozygous for *Tdp1* deletion.

(A, B): number of offspring surviving past one month postnatal

(C): number of E12 embryos

Highlighted in red where the numbers of offspring obtained differed from predicted.

electron spin resonance (ESR) spectroscopy. He confirmed that the pattern of free radicals captured corresponded to that of purified salmon sperm DNA (Haywood *et al*., 2008; Haywood *et al*., 2011) (**Fig. 5.2A**), suggesting they were of DNA origin. He then showed that *Tdp1*$^{-/-}$ MEFs accumulated ~ 6 fold more carbon adducts than wildtype MEFs (**Fig. 5.2B, *p* < *0*.001; Student's t-test**). Importantly, the level of carbon adducts correlated with SOD1 expression, as overexpression of hSOD1 largely reversed this phenotype (**Fig. 5.2B, *p* < *0*.01; Student's t-test**), while overexpression of SOD1^{G93A} increased the carbon adducts by ~ 12 fold (**Fig. 5.2B, *p* < *0*.01; Student's t-test**). This effect correlated with the level of SOD1^{G93A} expression, as reduction in the ratio of ectopic hSOD1^{G93A} to endogenous SOD1 expression from 1.1 to 0.8 (**Fig. 5.3A**) attenuated the increase in carbon adducts from ~ 12-fold to 8-fold (**Fig. 5.3B**). A further reduction in the ratio of hSOD1^{G93A} to endogenous SOD1 to 0.37 (**Fig. 5.3C**) failed to impact on the level of carbon adducts compared to levels detected in *Tdp1*$^{-/-}$ cells (**Fig. 5.3D**). These data validate the use of ESR in detecting SOD1^{G93A}-induced DNA free radicals in MEFs.

I then examined the correlation between the carbon adducts with TDP1 expression level. For this, we took advantage of a previously established *Tdp1*$^{-/-}$ chicken DT40 cell line, whereby clones of various levels of hTDP1 were stably expressed (Alagoz *et al*., 2014). After confirming the levels of hTDP1 protein (**Fig. 5.4A**) and catalytic activity (**Fig. 5.4B**), we repeated the ESR experiment on these cells. Again the carbon adduct profile was consistent with nucleic acids (**Fig. 5.4C**), and *Tdp1*$^{-/-}$ cells showed ~ 8-fold accumulation of these adducts (**Fig. 5.4D, *p* < *0*.01; Student's t-test**). Complementation with low-expressing level of hTDP1 reduced the carbon adducts by ~ 60 %, and surprisingly, to a lesser extent, by ~ 35 % in the high-expressing TDP1 clone (**Fig. 5.4D**). These data strongly indicate that Tdp1 plays a role in counteracting accumulation of SOD1^{G93A}-induced DNA free radicals in vertebrate cells.

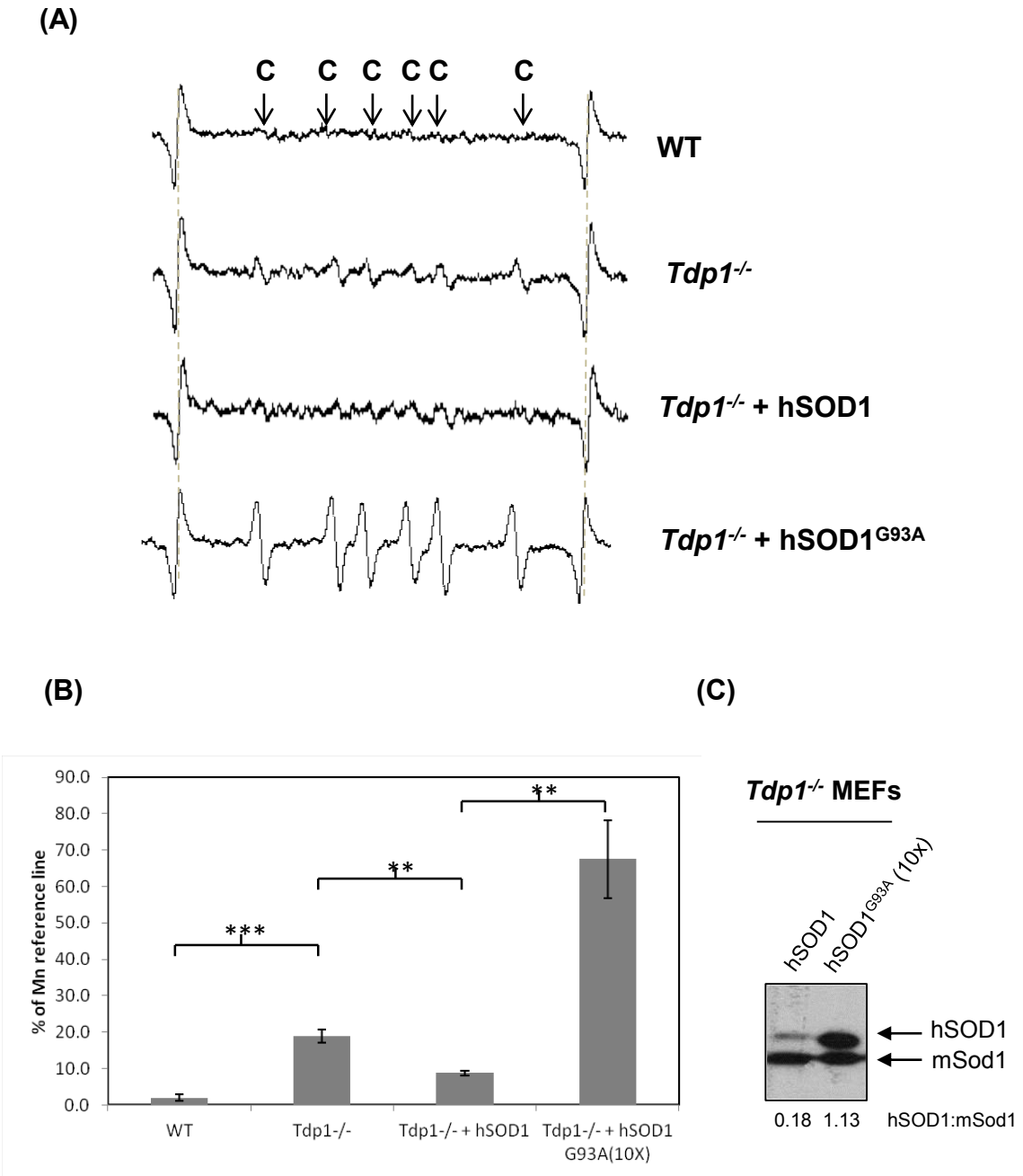

Figure 5.2 Tdp1 prevents accumulation of carbon adducts in DNA molecules induced by ROS in MEFs. (A) Electron spin resonance (ESR) spectra obtained during 30 min UVA-irradiation of WT MEFs or *Tdp1*$^{-/-}$ MEFs complemented with either empty vector, hSOD1 or hSOD1^{G93A}. "C" indicates deflection caused by carbon adducts. **(B)** Bar charts showing the mean integration of all 6 carbon adducts in above spectra noted as a percentage of integrated manganese reference lines. Data are the means of 3 independent experiments and error bars represent $\pm$1 S.E.M. *p* values were derived from two-tailed Student's t-test , whereby ** = $p < 0.01$, *** = $p < 0.001$. **(C)** WCEs (50 µg) for *Tdp1*$^{-/-}$ MEFs complemented with either hSOD1 or hSOD1^{G93A} were fractionated by SDS-PAGE and immunoblotted using antibodies against human and mouse SOD1. Expression levels of hSOD1 and hSOD^{G93A} relative to endogenous mouse Sod1 ("mSod1") were quantified by ImageJ and expressed as fractions in bottom panel. Data collected in collaboration with Dr Nick Kassouf.

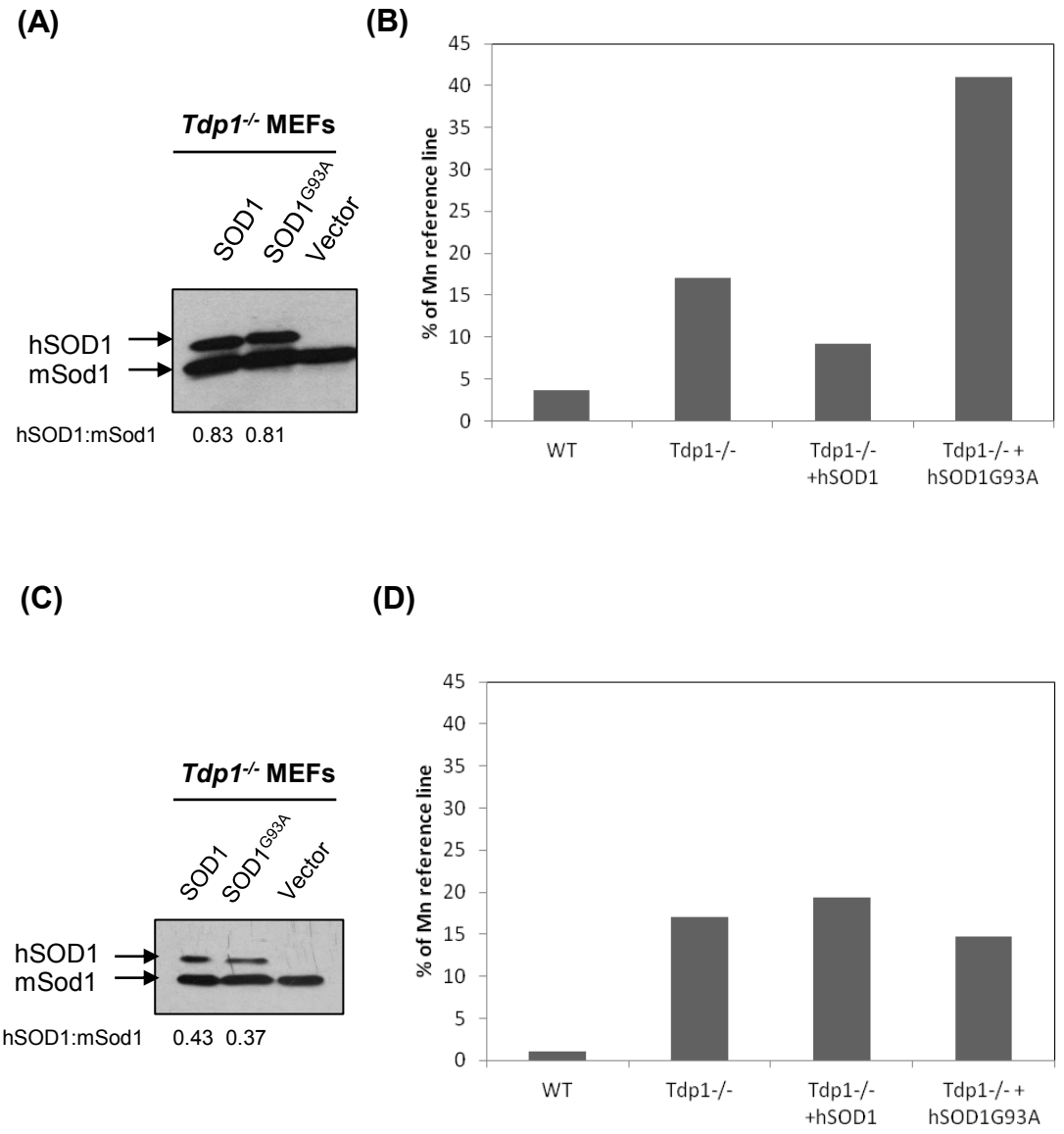

Figure 5.3 Levels of carbon adducts detected by ESR correlate with expression levels of hSOD1 or hSOD1^{G93A}. (A, C) Immunoblotting of *Tdp1*$^{-/-}$ MEF lysates overexpressing hSOD1 or hSOD1^{G93A}. Expression levels of hSOD1 and hSOD^{G93A} relative to endogenous mouse Sod1 ("mSod1") were quantified by ImageJ and expressed as fractions in bottom panel. **(B, D)** Bar chart showing the mean integration of all 6 carbon adducts noted as a percentage of integrated manganese reference lines from ESR data obtained from MEFs in (A). Data collected in collaboration with Dr Nick Kassouf.

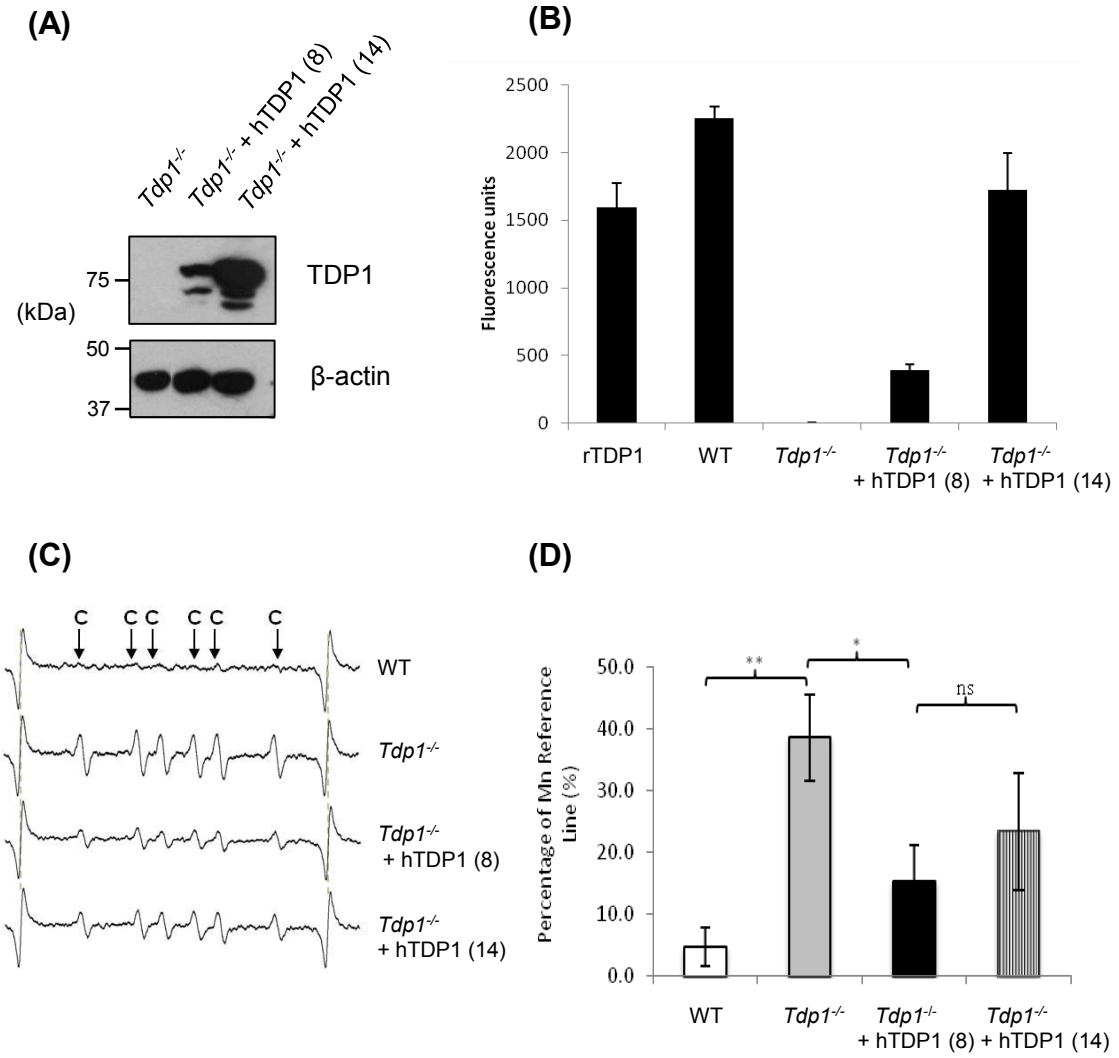

Figure 5.4 TDP1 prevents accumulation of carbon adducts in DNA molecules induced by ROS in chicken DT40 B-lymphocytes. (A) Immunoblotting of two clones of *Tdp1*$^{-/-}$ DT40 cells complemented with human TDP1 (clone 8 and clone 14) using antibodies against human TDP1 and β-actin as loading control. **(B)** Enzymatic activities of DT40 cells from (A) measured *in vitro* using a 13-mer oligonucleotide substrate containing a 3'-phosphotyrosine residue conjugated to a 5'-FITC molecule. WCEs (2 µg) of cells from (A), wildtype DT40 cells ("WT") and 6.25 pM of recombinant human TDP1 ("rTDP1") were incubated with 10 nM of TDP1 substrate for 15 minutes at room temperature. The reaction was stopped and fluorescence intensities from triplicate samples were measured using a BMG Labtech PHERAstar plate reader and analysed by the PHERAstar software. **(C)** Electron spin resonance spectra obtained during 30 min high intensity (80 mW/cm^2) UVA-irradiation of DT40 cells: wildtype ("WT"); Tdp1 knockout ("*Tdp1*$^{-/-}$"); clone 8 with low levels of hTDP1 ("*Tdp1*$^{-/-}$ + hTDP1(8)"); and clone 14 with high levels of hTDP1 ("*Tdp1*$^{-/-}$ + hTDP1(14)"). **(D)** Bar charts showing the mean integration of all 6 carbon adducts shown in (C) noted as a percentage of integrated manganese reference lines. Data are the mean of 3 independent experiments and error bars represent ±1 S.E.M. *p* values were derived from two-tailed Student's t-test , whereby * = $p < 0.05$, ** = $p < 0.01$ and ns = non-significant. Data collected in collaboration with Dr Nick Kassouf.

5.2.3 Tdp1 prevents accumulation of SOD1^{G93A}-induced chromosomal DNA breaks

To determine the consequence of the SOD1^{G93A}-induced DNA free radicals in the chromatin context, I measured chromosomal DNA strand breaks in wildtype and hSOD1^{G93A}-overexpressing MEFs (**Fig. 5.5A**) using the alkaline comet assay after UVA irradiation under the same condition as for the ESR experiment. Immediately after irradiation, there was an increase in DNA strand breaks, with cells overexpressing hSOD1^{G93A} accumulating ~ 50 % more breaks than wildtype cells (**Fig. 5.5B**). This suggests that SOD1^{G93A} overexpression is directly responsible for the generation of chromosomal strand breaks after UVA.

To test whether Tdp1 can repair these breaks, I repeated the experiment using low dose H_2O_2 to induce production of endogenous ROS. H_2O_2 in this case acts as a substrate for SOD1^{G93A}, which converts it to the more reactive hydroxyl and superoxide radicals *in vivo* through the Fenton reaction (Shibata, 2001). After 10 minutes of H_2O_2 treatment, *Tdp1*$^{-/-}$ cells displayed ~ 2-fold more strand breaks than wildtype cells (**Fig. 5.5C, *p* < *0*.001; Student's t-test**), while overexpression of hSOD1^{G93A} in *Tdp1*$^{-/-}$ cells increased the breaks further by ~ 50 % (**Fig. 5.5C, *p* < *0*.05; Student's t-test**). Conversely, overexpression of hSOD1 in *Tdp1*$^{-/-}$ cells suppressed the observed increase in DNA strand breaks to background levels detected in wildtype cells (**Fig. 5.5C**). However, subsequent incubation in H_2O_2-free media led to rapid clearance of SSBs with no detectable difference in repair kinetics (**Fig 5.5D**), suggesting Tdp1 is not essential for repair of SOD1^{G93A}-induced DNA strand breaks. This result is perhaps unsurprising, as Tdp1 is not essential for repair of ROS-induced SSBs, with factors such as glycosylases and APE1 known to play a more prominent role (Demple and Sung, 2005).

However, as recent data from our lab and the McKinnon lab suggest that endogenous ROS (induced by *Atm* deletion in mice) can trap TOP1 near oxidised DNA lesions

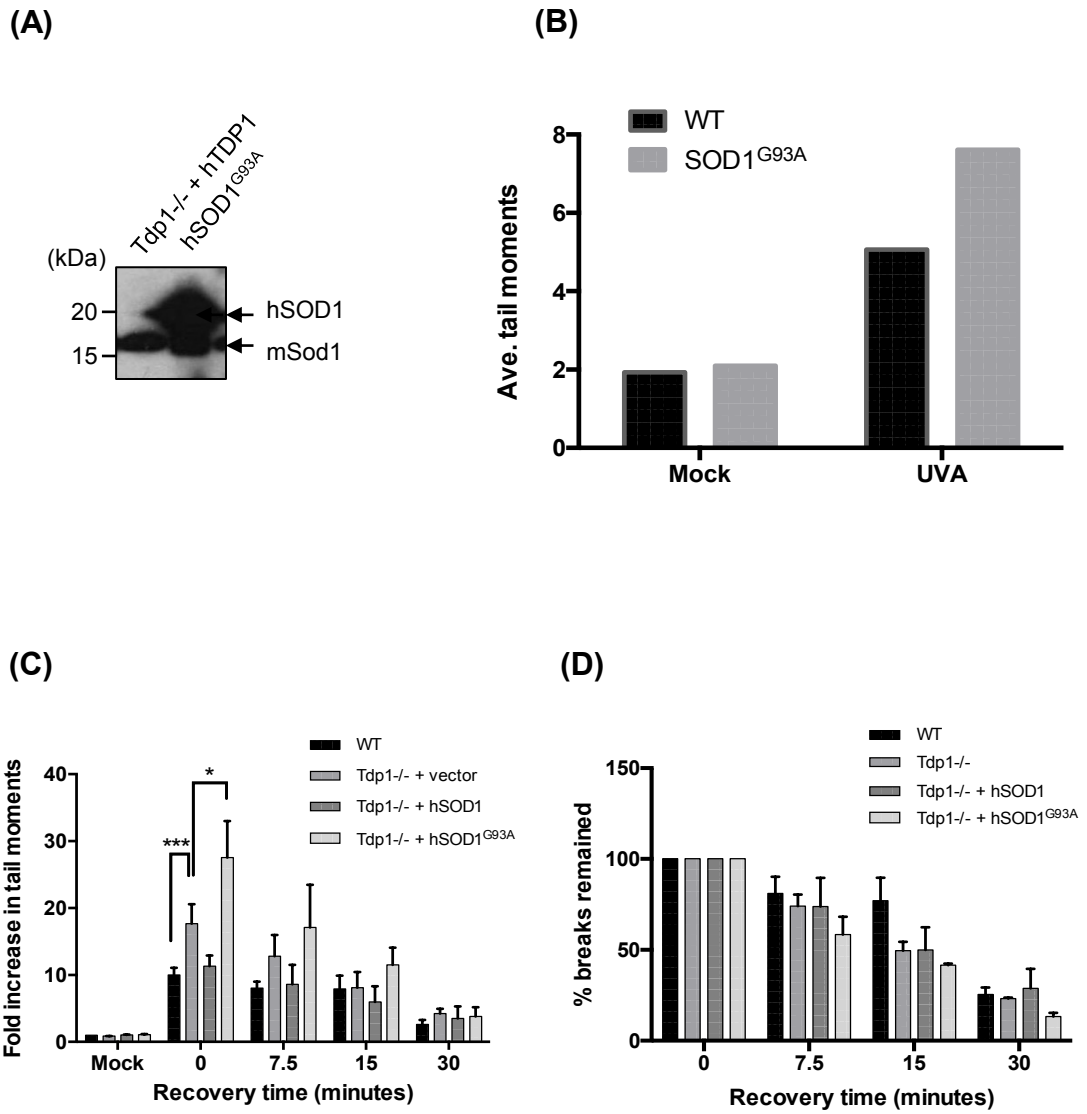

Figure 5.5 *Tdp1*$^{-/-}$ MEFs overexpressing hSOD1^{G93A} accumulate more SSBs induced by H_2O_2. (A) Immunoblotting of WCEs of *Tdp1*$^{-/-}$ MEFs complemented with hTDP1, empty vector, hSOD1^{G93A} and wildtype MEFs overexpressing hSOD1^{G93A} using antibodies against human and mouse SOD1. **(B)** MEFs from (A) were damaged with 1 mW/cm2 UVA irradiation for 30 minutes on ice, and immediately harvested for quantification of SSBs by alkaline comet assay. Average tail moments from 50 cells were quantified using the Comet Assay IV software. **(C)** *Tdp1*$^{-/-}$ MEFs complemented with hTDP1, hSOD1, hSOD1^{G93A} or empty vector were treated with 10 μM of H_2O_2 or PBS ("Mock") for 10 minutes on ice, then left to repair in drug-free medium at 37˚C for the indicated time periods. SSBs induced were measured using the alkaline comet assay. Average tail moments from 50 cells were quantified using the Comet Assay IV software. **(D)** Data from (C) expressed as percentage of remaining breaks. Data are the mean of 3 independent experiments and error bars represent ±1 S.E.M. *p* values were derived from paired two-tailed Student's t-test , whereby * = $p < 0.05$, *** = $p < 0.001$.

(Alagoz *et al*., 2013; Katyal *et al*., 2014), forming TOP1 cleavage complexes (TOP1-cc) that are physiological substrates for TDP1, it was important to assess the levels of ROS-induced TOP1-cc in TDP1-proficient and -deficient cells.

5.2.4 TDP1 promotes repair of TOP1-mediated chromosomal DNA breaks induced by ROS

Due to the bulk of TOP1 peptide, TOP1-cc cannot normally be detected by alkaline comet assay. However, pre-digestion with proteinase K prior to gel electrophoresis can unmask all protein-bound DNA strand breaks. To detect TOP1-specific DNA adducts, I used a stable MRC5 cell lines whereby TDP1 was depleted alone or in combination with TOP1 (**Fig. 5.6A**). I then repeated the alkaline comet assay with proteinase K treatment. As a control experiment, TOP1-cc were induced with CPT treatment. As expected, wildtype and TDP1-depleted cells accumulated comparable levels of TOP1-cc, since TDP1 is known to be involved only in the repair of CPT-induced TOP1-cc. Depletion of TOP1 markedly reduced formation of TOP1-cc both in the presence or absence of TDP1, although the reduction was less in the absence of TDP1 (**Fig. 5.6B**). This difference was unlikely to be due to increased formation of TOP1-cc in TDP1 deficient cells, but rather a higher residual TOP1 level as confirmed by immunoblotting (**Fig. 5.6A**). Similarly, after H_2O_2 treatment, TDP1 deficient cells accumulated similar levels of protein DNA adducts as in wildtype cells, of which ~ 50 % were TOP1-dependent, as shown by their reduction in TOP1 depleted cells (**Fig. 5.6B**). When TDP1 was co-depleted, only ~ 25 % of TOP1-cc were abolished, suggesting more TOP1-cc were formed in the absence of TDP1. However, the TDP1-dependent proportion could be slightly lower, as more TOP1-cc could have been formed because of the higher residual TOP1 levels (**Fig. 5.6A**).

Although the exact proportion of ROS-induced TOP1-cc accumulated in the absence of TDP1 was unclear, the consequences of accumulation of these lesions on cell replicative potential were significant in the absence of TDP1, as revealed by clonogenic

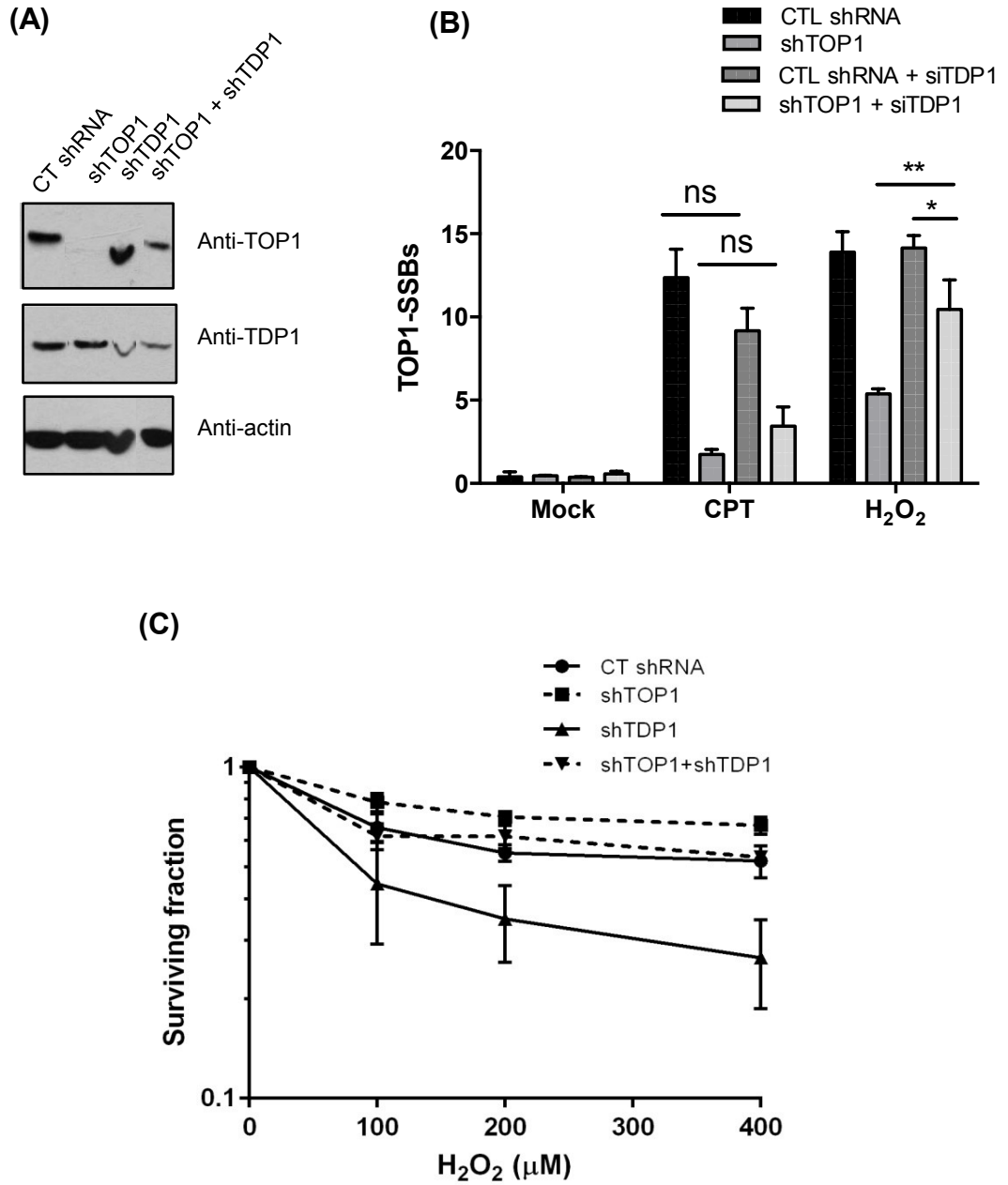

Figure 5.6 H_2O_2 induces TOP1-linked breaks in MRC5 cells. (A) MRC5 cells were stably depleted for TOP1, TDP1, or both, using shRNA's and maintained in 1 μg/ml puromycin selection. Cells transduced with scrambled shRNA ("CT shRNA") acted as control for off-target effects of the shRNA's. WCEs were immunoblotted with antibodies against TOP1, TDP1, and β-actin as loading control. **(B)** Cells from (A) were treated with 50 μM of CPT for 1 hour at 37°C or 10 μM H_2O_2 for 10 minutes on ice, and immediately analysed for DNA breaks using modified alkaline comet assay, which measures both protein-linked breaks and frank breaks. **(C)** Cells from (A) were treated with the indicated doses of H_2O_2 for 10 minutes on ice, and left to recover in drug-free medium for 7 – 10 days to form macroscopic colonies. Data are the mean of 3 independent experiments and error bars represent ±1 S.E.M. *p* values were derived from paired two-tailed Student's t-test , whereby * = $p < 0.05$, ** = $p < 0.01$ and ns = non-significant.

survival assays (**Fig. 5.6C**). Depletion of TOP1 rescued survival after H_2O_2 in TDP1-depleted cells by ~ 3 fold (from ~ 20 % – 60 % at 400 μM H_2O_2), whereas in TDP1-proficient cells there was only a 1.2 fold rescue (from ~ 60 – 70 % at 400 μM H_2O_2).

In summary, these results indicate that in mammalian cells TDP1 prevents initial stage accumulation of chromosomal breaks induced by endogenous ROS. A significant proportion of these breaks is TOP1-mediated and counteracted by TDP1. It is also likely that TDP1 can repair non-TOP1-mediated breaks induced by oxidative stress. The unexpected role in inhibiting formation of oxidative DNA lesions alerted us to the possibility that TDP1 may function at the level of oxidant production, located in the mitochondria.

5.2.5 Tdp1 maintains mtDNA copy number

Although TDP1 has been identified in mammalian mitochondria (Das *et al*., 2010; Fam *et al*., 2013a), its molecular role was not clearly characterised. The mitochondrial DNA also relies on topoisomerases for DNA transactions such as replication and transcription, and vertebrate cells have a mitochondrial specific isoform of TOP1, TOP1mt. One probable function of mitochondrial TDP1 would be to repair mitochondrial TOP1 (TOP1mt)-cleavage complexes, which have been shown to be induced by TOP1 poisons (Zhang and Pommier, 2008; Dalla Rosa *et al*., 2014) and ROS (Medikayala *et al*., 2011). If this were true, TDP1-deficient cells should accumulate more mtDNA breaks than wildtype cells.

To assess mitochondrial genome instability, I quantified mtDNA copy numbers with or without H_2O_2 induction and 24-hour recovery using qPCR (Chan and Chen, 2009). In the unstressed condition, *Tdp1*$^{-/-}$ cells had 50 % fewer mtDNA copies (250 as opposed to 500) compared to wildtype cells; SOD1^{G93A} overexpression was not associated with mtDNA loss; while the overexpression of SOD1^{G93A} in *Tdp1*$^{-/-}$ cells resulted in a further reduction of mtDNA copy number (~ 100) (**Fig. 5.7**). After oxidative stress, mtDNA copy numbers were increased by ~ 2 fold in all cell lines examined. Increase in

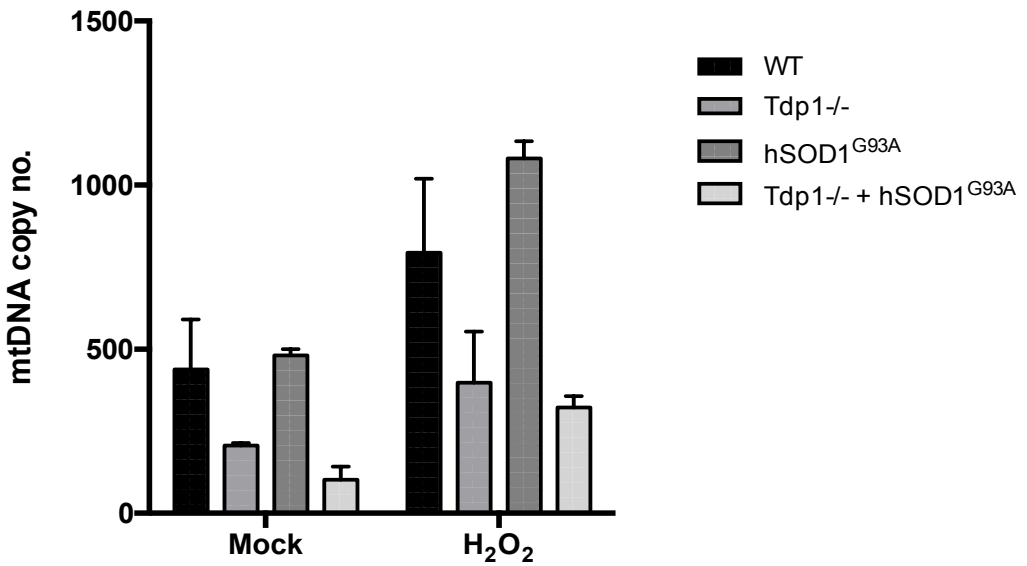

Figure 5.7 *Tdp1*$^{-/-}$ MEFs show attenuated mitochondrial DNA synthesis after oxidative stress. MEFs were treated with 240 μM of H_2O_2 or PBS ("Mock") for 1 hour on ice then left to recover in drug-free medium for 24 hours. Total gDNA was extracted using the Qiagen DNAeasy Blood and Tissue Kit. 1 ng of gDNA was used as mitochondrial DNA template and 10 ng of gDNA was used as nuclear DNA template. The template was mixed with 2x SYBR-Green I PCR mastermix and the PCR reaction was carried out in triplicates. Concentrations of starting templates were derived from C_T values of standard curves for the mtDNA and nDNA reactions. Mitochondrial copy number was calculated by 2 x $2^{(\Delta CT)}$ whereby ΔC_T = B2M average C_T – ND1 average C_T. Data represent the averages of 2 independent experiments and error bars denotes upper and lower ranges.

mitochondrial DNA synthesis is a known compensatory mechanism during mitochondrial stress (Lee *et al*., 2000; Hori *et al*., 2009). The proportional increase in all the cell lines suggests neither Tdp1 nor SOD1^{G93A} are required for mtDNA synthesis after acute oxidative stress. The loss of mtDNA in unstressed *Tdp1*$^{-/-}$ cells that is associated with endogenous (SOD1^{G93A}-mediated), but not exogenous ROS, suggest that there may be a more sustained and global change in mitochondrial function and mass when Tdp1 is inactivated. To test this, I first visualised the gross mitochondrial network morphology with fluorescence microscopy.

5.2.6 Tdp1 inactivation is associated with mitochondrial stress

Using the membrane potential specific probe TMRM, which is specific for depolarised (functional) mitochondria, our collaborator Dr Martin Meagher did not see obvious morphological differences in the mitochondrial network in *Tdp1*$^{-/-}$ MEFs compared to the wildtype. However, treatment with TBH, a stable analogue of H_2O_2, showed a discernible increase in mitochondrial lengths ("mitochondrial fusion") in *Tdp1*$^{-/-}$ cells (**Fig. 5.8**). This suggests that *Tdp1*$^{-/-}$ cells have a lower threshold for oxidative stress, as mitochondrial hyper-fusion is a known compensatory response to counteract mitochondrial stress (Friedman and Nunnari, 2014). Strikingly, the hyper-fusion phenotype changed to that of hyper-fission in *Tdp1*$^{-/-}$ cells when SOD1^{G93A} was overexpressed, whereby the mitochondria were highly fragmented and circularised, indicating a decompensated state of severe mitochondrial stress (**Fig. 5.8**).

To assess the degree of mitochondrial stress quantitatively, I used flow cytometry to measure the fluorescence intensities of membrane potential-specific probe, Mitotracker Red CMXRos, and non-membrane potential-specific probe, Mitotracker Green. The total mitochondrial mass is indicated by the fluorescence intensity of Mitotracker Green, while the membrane potential is expressed as the fluorescence intensity of Mitotracker Red CMXRos normalised to Mitotracker Green. **Fig. 5.9A** shows that in cells overexpressing hSOD1^{G93A}, which are known to have dysfunctional mitochondria

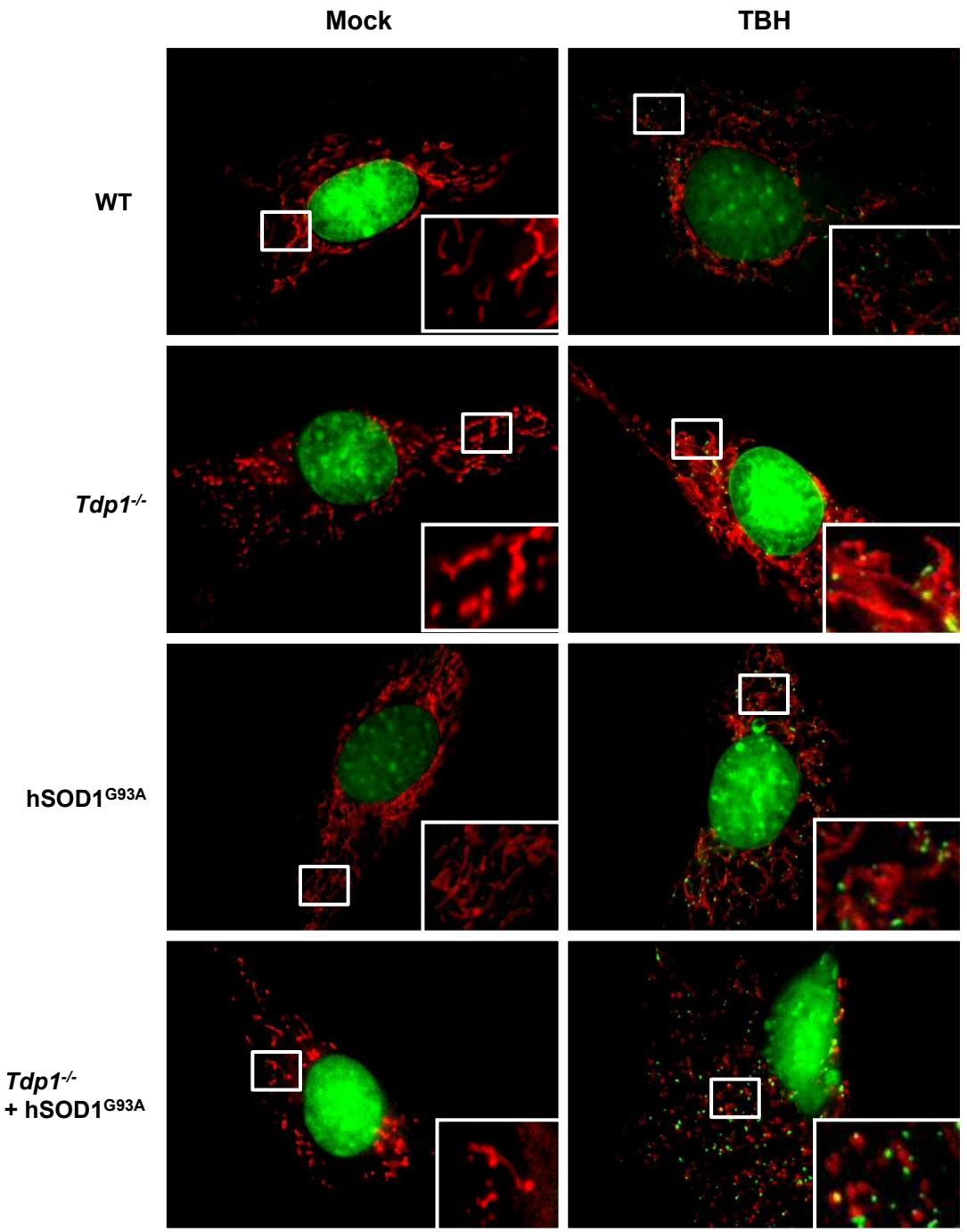

Figure 5.8 Overexpressing hSOD1^{G93A} in *Tdp1*$^{-/-}$ MEFs increases mitochondrial fragmentation. Cells were seeded at 5 x 10^5 in WillCo-dish® Glass Bottom dishes and treated with 10 µM tert-butyl-hydroperoxide ("TBH") at 37°C for 24 hours. Cells were then stained with 3 µl PicoGreen (for dsDNA) for 45 minutes at 37°C and 5 nM tetramethylrhodamine, tethyl ester, perchlorate (TMRM) at 37°C for 10 minutes. Blow-up images in white boxes. Experiment performed by Dr Martin Meagher.

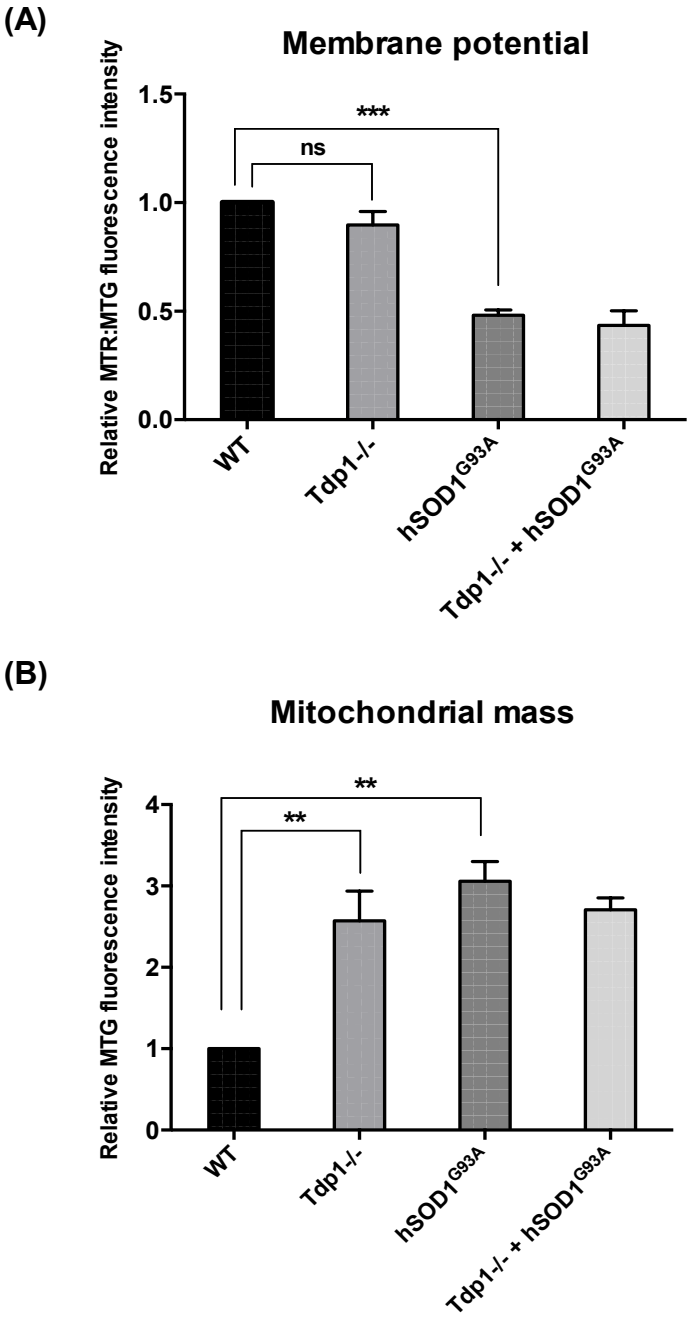

Figure 5.9 *Tdp1*$^{-/-}$ MEFs show increase mitochondrial mass in absence of exogenous stress. (A) Wildtype ("WT"), Tdp1 knockout ("*Tdp1*$^{-/-}$"), wildtype overexpressing hSOD1^{G93A}, (hSOD1^{G93A}) and *Tdp1*$^{-/-}$ overexpressing hSOD1^{G93A} ("*Tdp1*$^{-}$/- + hSOD1^{G93A}") MEFs were incubated in 250 nM Mitotracker Green ("MTG") to stain mitochondria irrespective of membrane potential, for 30 minutes at 37˚C, washed with PBS, then analysed by fluorescence-activated cell sorting using using the EX493/EM525 spectra. **(B)** Mock treated MEFs from (A) were incubated in 250 nM MTG and 250 nM Mitotracker Red (MTR) (to stain for metabolically active mitochondria with negative membrane potential) for 30 minutes at 37˚C, washed with PBS, then analysed by FACS using the EX493/EM525 and EX565/EM670 spectra. Relative MTR:MTG fluorescence intensity denotes the membrane potential normalised to total mitochondrial mass. Data are the means of 3 independent experiments and error bars indicate $\pm$1 S.E.M. *p* values were derived from two-tailed Student's t-test , whereby ns = non-significant, ** = $p < 0.01$, *** = $p < 0.001$, and ns = non-significant.

(discussed in **Section 5.1.1**), the membrane potential decreased by ~ 50 % compared to wildtype cells, even though there was a ~ 3-fold compensatory increase in total mitochondrial mass. This is consistent with an accumulation of dysfunctional mitochondria. Interestingly, while *Tdp1*$^{-/-}$ MEFs had a normal membrane potential comparable to wildtype cells (**Fig. 5.9A**), the mitochondrial mass was also increased by ~ 3 fold (**Fig. 5.9B**). This data, together with the heightened response in mitochondrial morphology dynamics to oxidative stress (**Fig. 5.8**), suggests that the need for *Tdp1*$^{-/-}$ cells to markedly increase mitochondrial biogenesis may be a compensatory response to some underlying mitochondrial dysfunction (Lee *et al*., 2000). To further support this notion, intra-mitochondrial ROS production, specifically, of superoxide, was measured using FACS analysis of MitoSOX Red fluorescence. *Tdp1*$^{-/-}$ MEFs showed ~ 2-fold higher superoxide level relative to wildtype cells, while hSOD1^{G93A}-overexpressing cells showed ~ 4 fold more (**Fig. 5.10A**). The fluorescence signal was specific to mitochondrial superoxide, as treatment with the ETC complex I inhibitor rotenone increased the signal in all three cell lines by ~ 4 fold (**Fig. 5.10B**). The extent of increase was comparable in all the cell lines, suggesting that the mitochondrial defect in *Tdp1*$^{-/-}$ and hSOD1^{G93A}-overexpressing MEFs was not specific to complex I dysfunction.

5.2.7 Tdp1$^{-/-}$ *MEFs are more sensitive to endogenous ROS induced by SOD1*^{G93A}

To assess whether the mitochondrial dysfunction in *Tdp1*$^{-/-}$ negatively impacts cellular resistance against endogenous ROS, I quantified clonogenic survival after H_2O_2 induction, using SOD1 and SOD1^{G93A} overexpression to modulate the levels of endogenous ROS. Overexpression of SOD1^{G93A} sensitized *Tdp1*$^{-/-}$ cells to H_2O_2 while SOD1 overexpression offered some protection (**Fig. 5.11A, $p < 0.05$; Student's t-test**). In contrast, overexpression of SOD1^{G93A} had no impact on cell survival of wildtype cells (**Fig. 5.11B**), suggesting the protective effect against endogenous ROS was Tdp1-specific.

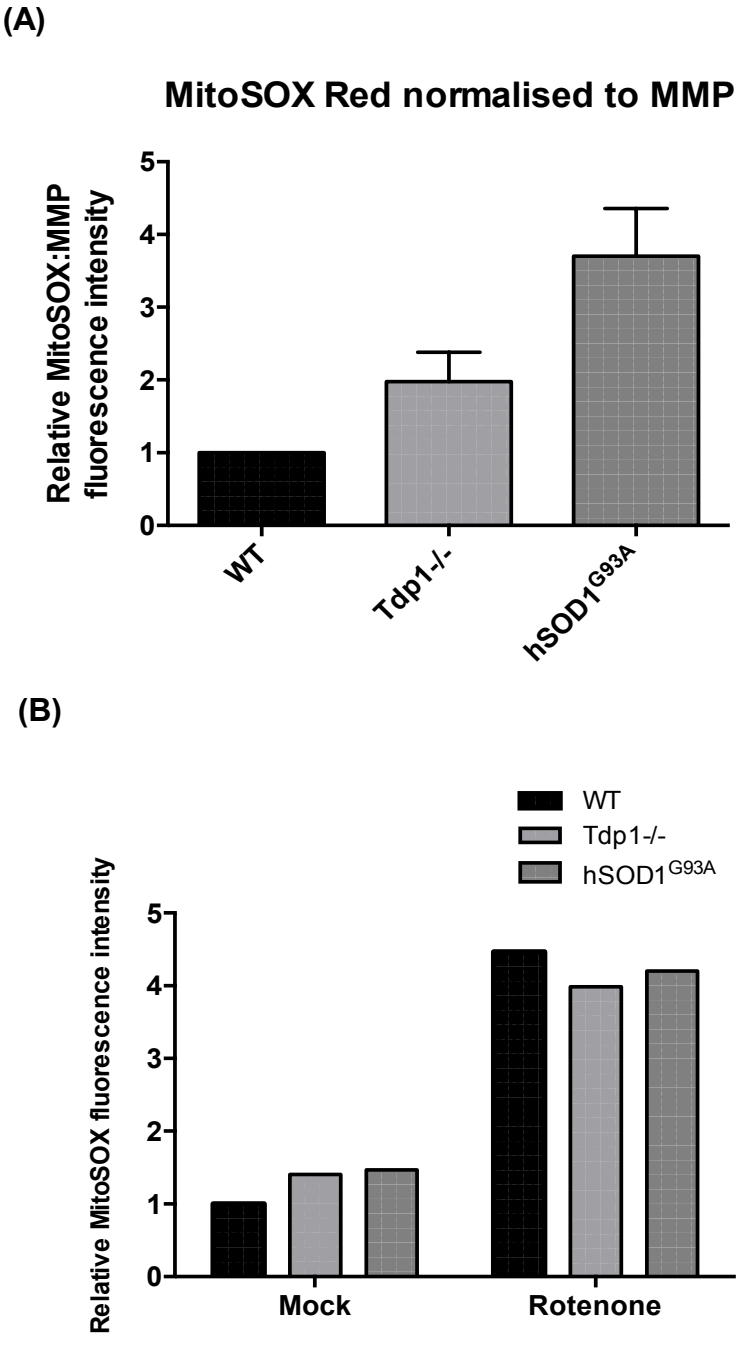

Figure 5.10 *Tdp1*$^{-/-}$ MEFs show increased mitochondrial superoxide not specific to complex I dysfunction. (A) MEFs were incubated in 250 nM MitoSOX Red, for 15 minutes at 37˚C in the dark, washed with PBS, then analysed by FACS using the EX488/EM575 spectra. Data represent the average of 2 independent experiments and error bars indicate the upper and lower ranges. **(B)** MEFs were treated with 1 μM rotenone or DMSO ("Mock") for 10 minutes at 37°C, then stained with 250 nM MitoSOX Red in the dark, for 15 minutes at 37˚C, washed with PBS, and analysed by FACS using the EX488/EM575 spectra.

(A)

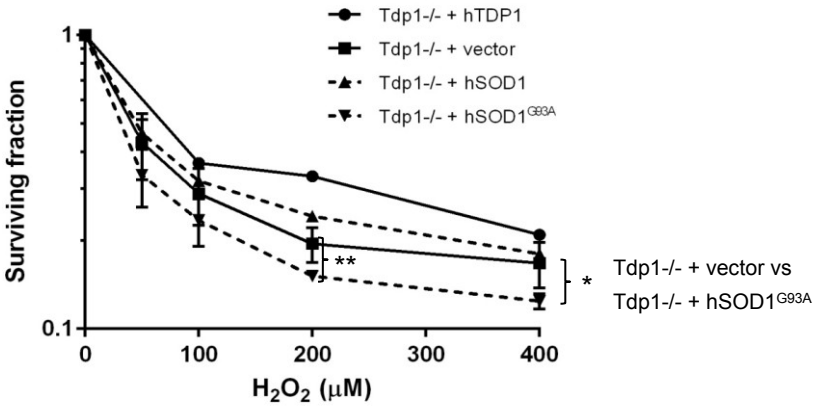

(B)

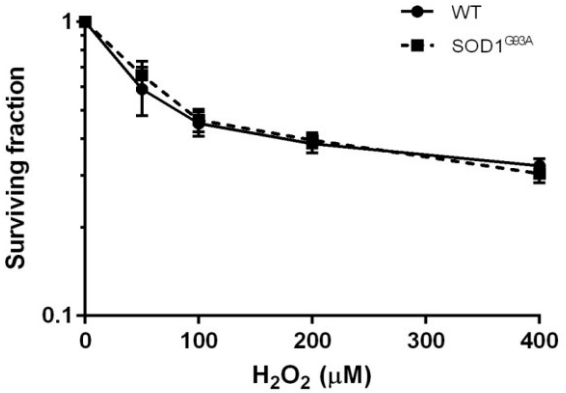

Figure 5.11 Overexpression of hSOD1^{G93A} hypersensitisizes *Tdp1*$^{-/-}$ MEFs to H_2O_2. (**A), (B)** MEFs were plated in 10 cm petri dishes overnight, then treated with the indicated doses of H_2O_2 for 10 minutes on ice. Cells were left to recover in drug-free medium for 7 – 10 days until macroscopic colonies formed. Data are the mean of 3 independent experiments and error bars represent ±1 S.E.M. *p* values were derived from paired two-tailed t-test , whereby * = $p < 0.05$, ** = $p < 0.01$.

5.3 Discussion

Oxidative stress is a major contributing factor in aging and neurodegeneration, and oxidative DNA damage with defective repair is implicated in an increasing number of diseases such as cancer, metabolic disorders, and neuromuscular diseases.

In this chapter, I have shown that the SOD1/SOD1^{G93A}-overexpression system modulates the levels of endogenous ROS in vertebrate cells, and that Tdp1 is protective against oxidative stress in several ways: *Tdp1*$^{-/-}$ MEFs accumulate more endogenous ROS, nuclear oxidative DNA breaks, and reduced cellular replicative potential which are all exacerbated in a high endogenous ROS background.

In the nucleus, there was strong evidence of TDP1 being a broad-spectrum end-processing factor involved in the repair of oxidised DNA ends (discussed in **Section 1.5.1**). However, in the cellular context, my comet data demonstrate that Tdp1 is dispensable for repair of oxidative DNA breaks, but instead is required to prevent formation of these lesions, which include TOP1-cc. This prompted us to think outside the nucleus and look at the source of ROS production itself.

The mitochondria are the major source of ROS production, and they are also intimately involved in cellular proliferation and the apoptotic pathway. Mitochondrial respiratory function is closely regulated by cellular energy demands via its own gene expression regulatory mechanisms. The mitochondrial genome relies on nuclear-encoded repair factors for maintenance, one of which may be TDP1. Although its precise molecular mechanism of action in the mitochondria has not been elucidated, its importance can be inferred from the hallmark ataxic phenotype, a common manifestation of mitochondrial disorders, in TDP1-mutated patients.

I first tested whether Tdp1 plays a role in repair of mtDNA breaks induced by endogenous ROS using long-range qPCR, which would detect polymerase-blocking lesions along the whole length of the mitochondrial genome. Although highly sensitive,

this assay does not distinguish the number of lesions per copy of mtDNA. But rather, it quantifies the number of mtDNA molecules that contain at least one lesion. Although the result from Das *et al.* suggests that *Tdp1*$^{-/-}$ MEFs have a higher proportion of mtDNA molecules containing unrepaired lesions after H_2O_2 damage, the concentration of H_2O_2 used was 10 – 100 fold higher than what I used to induce endogenous ROS. Indeed, using the published condition of H_2O_2 treatment resulted in amplification of non-specific products, likely due to excessive fragmentation of the mitochondrial genome. The second concern of the LR-qPCR assay is the difficulty in assessing the C_T values accurately with a low reaction efficiency due to the size of the amplicons. Thirdly, the DNA intercalating dye SYBR Green I is known to inhibit DNA polymerase progression and confound melting curve analysis (Gudnason *et al*., 2007), making its use unsuitable for qPCR analysis of long amplicons. Due to these reasons, I decided to investigate the question of whether Tdp1 plays a role in overall mitochondrial genome stability by measuring the mtDNA copy numbers.

The observation that Tdp1 promotes mtDNA stability in the unperturbed state could be explained in several ways: 1) that Tdp1 plays a role in mitochondrial biogenesis; 2) that it prevents accumulation of protein-DNA adducts, specifically of TOP1mt-cc that can lead to large-scale loss of mtDNA molecules; or 3) that TDP1 regulates activity of mitochondrial transcription A (TFAM), which has been shown to positively correlate with mtDNA number (Ekstrand *et al*., 2004; Pohjoismäki *et al*., 2006; Lu *et al*., 2013; Mei *et al*., 2015). The first hypothesis conflicts with our Mitotracker data, which showed that *Tdp1*$^{-/-}$ cells exhibited increased mitochondrial mass. The second hypothesis is supported by the 3'-phosphotyrosine-specific activity of TDP1 in the mitochondria (Das *et al*., 2010), as well as the observation that overexpression of a toxic form of TOP1mt that is converted to TOP1mt-cc causes significant loss of mtDNA without loss of mitochondrial mass (Dalla Rosa *et al*., 2014). To confirm this, the use of biochemical assays to show accumulation of TOP1mt-cc in the absence of Tdp1 would be

important. The third hypothesis is partially related to the second hypothesis, as TOP1mt has been shown to physically associate with TFAM, and TOP1mt itself negatively regulates mitochondrial transcription (Sobek *et al*., 2013). The latter two hypotheses will be addressed in the next chapter.

In the long-term, persistent high endogenous ROS level coupled with loss of mtDNA and/or inhibition of mtDNA replication and transcription can affect overall mitochondrial function. This is demonstrated in *Tdp1*$^{-/-}$ cells overexpressing hSOD1^{G93A}, which showed increased proportion of dysmorphic and dysfunctional mitochondria characterised by increased superoxide production (Cassina *et al*., 2008). This dysfunction may have pathophysiological relevance in determining cell survival in tissues with high endogenous ROS load.

In summary, my findings support the hypothesis that Tdp1 plays a protective role in response to oxidative stress, through its role in the repair of nuclear TOP1-cc, as well as its role in maintaining mitochondrial function in a high endogenous ROS background. The exact mechanism of its action in the mitochondria is unclear, but possibly linked to the removal of TOP1mt-cc. This hypothesis was further investigated and will be presented in the next chapter.

CHAPTER 6

Human TDP1 promotes mitochondrial DNA transcription and Redox homeostasis

6.1 Introduction

In the previous chapter, I described the use of the $SOD1^{G93A}$ overexpression system to investigate the effects of high levels of endogenous ROS on *Tdp1*$^{-/-}$ MEFs. My findings so far indicate that Tdp1 promotes cellular resistance against oxidative stress, through its role in maintaining mitochondrial DNA biogenesis and the overall health of the mitochondria.

In this chapter, I will describe the use of a human inducible cell line system to investigate the role of human TDP1 on mitochondrial DNA metabolism, primarily on its functional interaction with mitochondrial TOP1 (TOP1mt).

My primary hypothesis was that TDP1 plays a role in the removal of excess TOP1mt-cc in the presence of high oxidative stress, in a similar manner as in the nucleus, thus promoting restoration of mtDNA integrity, replication and transcription in response to oxidative stress.

6.1.1 Mitochondrial DNA structure and metabolism

The mitochondrial genome is organized in structures on the inner membrane known as nucleoids, each consisting of 2 – 10 copies of double-stranded circular mtDNA molecules that closely associate with regulatory proteins, such as mitochondrial transcription factor A (TFAM) (Spelbrink, 2010).

Each human mtDNA molecule contains intron-less coding sequences for 13 proteins of the electron transfer chain (ETC) subunits, interspersed with 22 tRNA's, and 2 ribosomal RNA (rRNA) subunits, 12S and 16S (**Fig. 6.1**). Seven of the 14 subunits of ETC complex I (NADH dehydrogenase) are encoded by mitochondrial genes *ND1, ND2, ND3, ND4L, ND4, ND5* and *ND6.* The mitochondrial subunit of complex III (cytochrome bc_1) is encoded by *Cyt b*. Complex IV (cytochrome c oxidase) subunits are encoded by *COX1, COX2,* and *COX3* in the mitochondria. Complex V (ATP

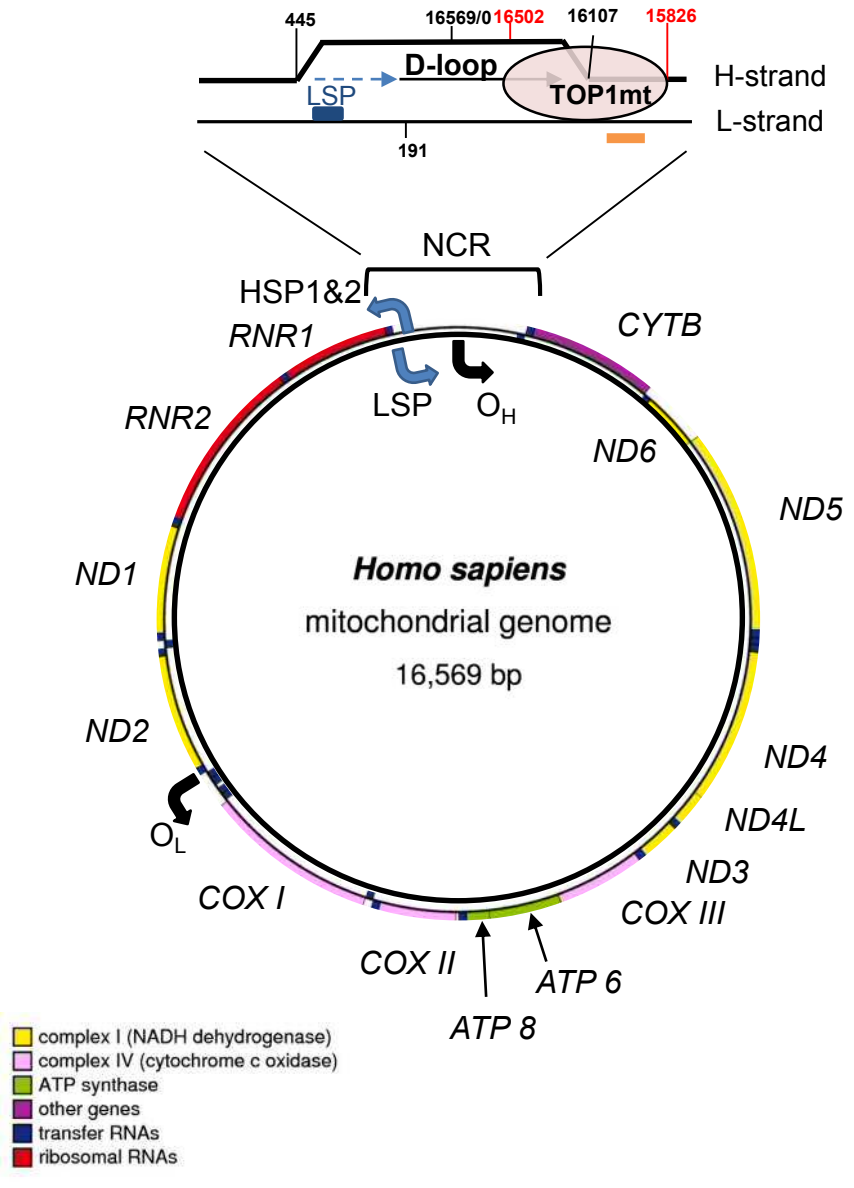

Figure 6.1 Organisation of human mitochondrial genome and TOP1mt binding site. The mtDNA molecule contains a GC-rich heavy strand (H-strand) (outer circle) and light strand (L-strand) (inner circle) encoding 13 genes for the respiratory complexes I, III, IV, V, 12S and 16S rRNA's, and 22 tRNA's. The non-coding region (NCR) contains the L-strand promoter ("LSP"), the two H-strand promoters ("HSP"), and the H-strand replication origin ("O_H"). The D-loop represents a three-strand structure of 908 bp containing a short transcript from LSP as primer for replication of the H-strand leading strand. Orange bar denotes position of TOP1mt* ChIP-qPCR sequence (position 15872-15972) (related to Figure 7.17). Figure drawn with OrganellarGenomeDRAW: http://ogdraw.mpimp-golm.mpg.de/cgi-bin/ogdraw/pl. Annotation adapted from Taanman, 1999; Dalla Rosa *et al.*, 2014.

synthase) subunits are encoded by *ATP6* and *ATP8*. With the exception of *ND6*, all the protein-coding genes are located on the guanine-rich heavy chain.

Transcription of mtDNA initiates at three promoter sites: HSP1, for the transcription of the 2 rRNA's (encoded by *MT-RNR1* and *MT-RNR2*, respectively); HSP2, for transcription of a long polycistronic mRNA of the protein-coding genes and t-RNA's; and LSP, for transcription of a polycistronic mRNA of the *ND6* gene and 8 tRNA's (Falkenberg *et al*., 2007). Nuclear-encoded mitochondrial RNA polymerase (POLRMT) and transcription factors TFAM, transcription factor B1 (TFB1M) and transcription factor B2 (TFB2M) form part of the transcription machinery (Falkenberg *et al*., 2002; McCulloch *et al*., 2002). Termination of transcription, post-transcriptional processing, and intra-mitochondrial translation all require import of nuclear-encoded factors.

Replication of mtDNA is intrinsically coupled to transcription since replication initiation of the heavy chain depends on transcription from the LSP site and the short transcript serves as a primer for DNA synthesis (Chang and Clayton, 1985; Chang *et al*., 1985; Clayton, 1991). Replication of the heavy chain then frequently stalls ~ 650 bp downstream of the origin (O_H), forming a displacement loop (D-loop) (Clayton, 1991). It is believed that D-loop plays a role in regulating the transition from transcription to replication by interacting with nuclear-encoded regulating factors such as TFAM and single-stranded-DNA-binding protein (mtSSB) that determine whether replication re-initiates and continues to completion for the heavy chain strand (Takamatsu *et al*., 2002). Around two-thirds of the way relative to the O_H, replication of the light chain initiates in the opposite direction, apparently utilizing the elongating daughter strand of the heavy chain as the priming sequence. Like transcription, mtDNA replication elongation requires the concerted activities of nuclear-encoded DNA polymerase gamma (Polγ) (Hance *et al*., 2005), mitochondrial helicase TWINKLE (Tyynismaa *et al*., 2004), POLRMT (Wanrooij *et al*., 2008), mitochondrial single-stranded DNA-binding protein (mtSSB) (Korhonen *et al*., 2004), RNAse H1 (Cerritelli *et al*., 2011), DNA Lig3

(Simsek *et al*., 2011) and topoisomerases (Zhang and Pommier, 2008; Sobek and Boege, 2014).

6.1.2 Mitochondrial TOP1 (TOP1mt)

The circular nature of mitochondrial DNA requires topoisomerases for its replication and transcription. In vertebrates, TOP1mt is the only topoisomerase specifically evolved for handling mitochondrial DNA (Rosa *et al*., 2009). Encoded by a nuclear gene duplicated from that of nuclear TOP1, the TOP1mt transcript has a shorter N-terminus domain, which contains the mitochondrial targeting sequence (MTS) instead of nuclear localization sequence (NLS) (Zhang *et al*., 2001). TOP1mt also has a highly similar mode of action of cleavage and religation of ssDNA's as nuclear TOP1 (Zhang *et al*., 2007). However, TOP1mt activity is restricted to mtDNA, and is unable to interact with nuclear DNA (Rosa *et al*., 2009). It appears that TOP1mt is specialised to be most active in an alkaline environment, in the presence of divalent cations (Ca^{2+}, Mg^{2+}), consistent with the conditions of the mitochondrial matrix (Burke and Mi, 1994; Zhang *et al*., 2001).

It has been proposed that TOP1mt plays a role in DNA replication and transcription in the mitochondria, although there is likely functional overlap between TOP1mt and mitochondrially localised TOP2β and TOP3α (Sobek and Boege, 2014). It is therefore intriguing to understand what requirement drove the conservation of the TOP1mt gene in vertebrates. Understanding this may provide novel druggable targets for modulating mitochondrial-mediated apoptosis and DNA repair pathways in cancer therapy.

MEFs derived from *Top1mt*$^{-/-}$ mice display defective OXPHOS, as reflected by increased ROS production and activation of glycolysis; as well as compensatory responses to oxidative stress such as increased mitochondrial fusion, retrograde nuclear signaling, activation of the DNA damage response, and autophagy (Douarre *et al*., 2012). A similar pattern of mitochondrial dysfunction was induced in *Top1mt*$^{-/-}$ mice cardiomyocytes after treatment with doxorubicin, a TOP2 inhibitor used in cancer

therapy (Khiati *et al*., 2014). TOP1mt has also been shown to be necessary for mtDNA replication in mice hepatocyte regeneration after carbon tetrachloride (CCl_4) damage, a potent hepatotoxin that induces excessive lipid peroxidation (Khiati *et al*., 2015).

At the molecular level, TOP1mt binds predominantly at the non-coding region (NCR) which contains the two promoters for the light and heavy strands and the replication origin of the heavy strand (**Fig. 6.1**) (Zhang and Pommier, 2008; Dalla Rosa *et al*., 2014), which supports its involvement in resolving negative supercoils that arise from bidirectional transcription and replication (Zhang *et al*., 2014). TOP1mt also physically interacts with mitochondrial RNA polymerase and transcription factor TFAM, suggesting its localization to active transcription sites (Sobek *et al*., 2013). Surprisingly, in contrast to its nuclear counterpart, TOP1mt appears to inhibit mitochondrial transcription, independent of retrograde nuclear signalling (Sobek *et al*., 2013). Both depletion and overexpression of TOP1mt induced mitochondrial respiratory dysfunction (Douarre *et al*., 2012; Sobek *et al*., 2013).

Taken together, it is plausible that TOP1mt maintains mitochondrial health by adjusting the level of basal topological tension required for optimal transcription and replication. The expression level of TOP1mt is regulated by c-Myc, which also regulates the expression of many nuclear-encoded mitochondrial proteins (Zoppoli *et al*., 2011).

6.1.3 Mitochondrial bioenergetics

Numerous cellular processes that expend energy require ATP, which is produced by phosphorylation of ADP in the mitochondria. In mammalian cells, more than 80% of ATP production is coupled to oxidative phosphorylation (OXPHOS) (Papa *et al*., 2012), a process whereby electrons are transported from NADH to oxygen through a series of reduction/oxidation (Redox) reactions along the electron transport chain (ETC). The ETC is made up of protein complexes I – V located on the inner membrane, coupled with release of protons into the intermembrane space (IMS) (**Fig. 6.2**) (Hatefi, 1985). The potential energy from the proton gradient generated between the IMS and the

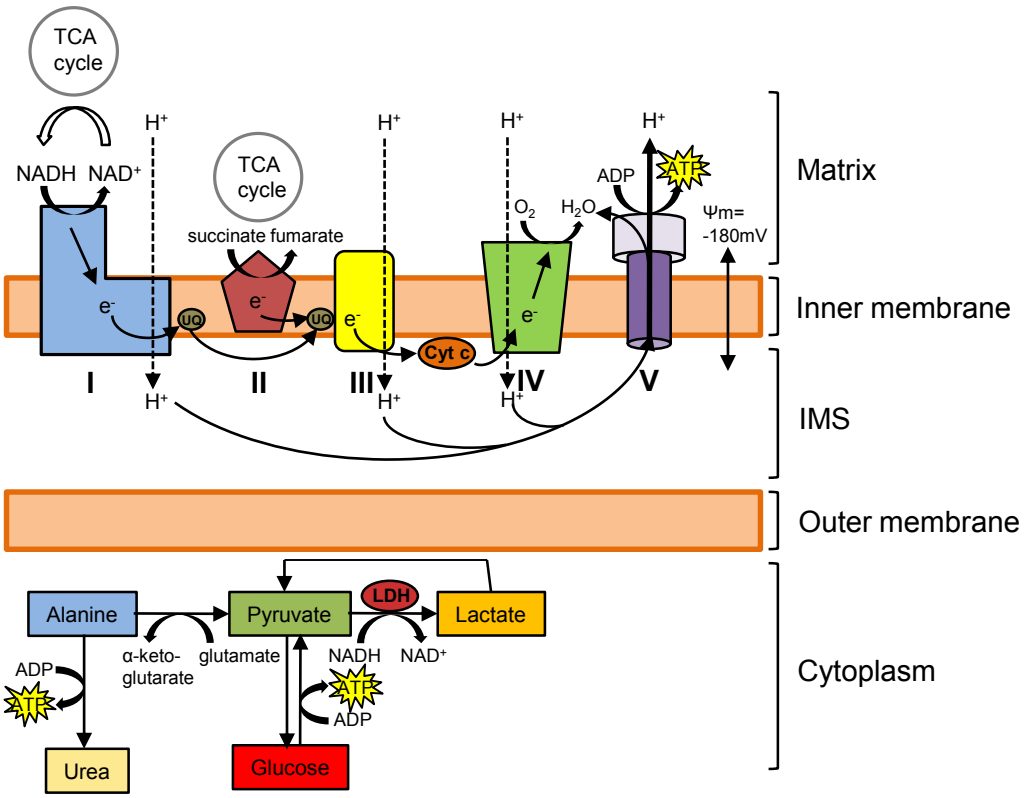

Figure 6.2 Mitochondrial bioenergetic pathways. NADH, generated in the tricarboxylic acid ("TCA") cycle, is oxidised by complex I, producing electrons that are transferred to ubiquinone ("UQ"), coupled with translocation of protons ("H^+") to the Inter-membrane space ("IMS"). Similarly, oxidation of succinate to fumarate as part of the TCA cycle generates electrons that are transferred to UQ and translocation of H^+ to the IMS. In complex III, electrons from reduced UQ are transferred to cytochrome c ("Cyt C"), coupled with H^+ translocation. Complex IV then accepts the electrons from Cyt C to reduce O_2 to H_2O, coupled with more H^+ translocation. Finally the proton gradient, or membrane potential ("ψm") then drives the molecular motor ATP synthase, or complex V, to generate ATP from ADP. In the cytoplasm, anaerobic respiration is carried out by metabolising glucose to pyruvate, generating ATP and lactate as by-products. Deamination of amino acids also produces ATP. Anaerobic respiration is less efficient in ATP production and also promotes lactic acidosis, thus increasing extracellular acidification rate (ECAR). Adapted from Lemarie & Grimm, 2011.

matrix (also known as “membrane potential”) is then used to drive ATP production by phosphorylation of ADP (Lemarie and Grimm, 2011). At resting state, where mitochondrial concentration of ADP is low, OXPHOS efficacy is low, as reflected by the oxygen consumption rate (OCR) (Brand and Nicholls, 2011). While under condition of high ATP demand, the influx of ADP into the mitochondria triggers proton flow through Complex V to generate ATP; the decrease in proton gradient facilitates electron flow through the ETC, thus increasing the OCR (Klingenberg, 2008). Thus, OCR is a measure of both ATP demand and efficacy of the ETC.

To assess the two components independently, inhibitors of the ETC and ATP synthase can be used, as summarized in **Fig. 6.3**. Inhibition of ATP synthase (Complex V) by oligomycin prevents the majority of protons from re-entering the matrix and greatly reduces the efficacy of the ETC (termed “oligomycin-sensitive respiration” or “coupled respiration”). A small proportion of protons re-enter the matrix through uncoupling proteins, a process known as “proton leak” or “uncoupled respiration” (Brand and Nicholls, 2011). Carbonyl cyanide-p-trifluoromethoxyphenylhydrazone (FCCP) acts as an uncoupling agent that temporarily increases the concentration of protons in the matrix independent of Complex V that drives electron flow through the ETC at the maximum rate (Benz and McLaughlin, 1983). The FCCP-induced OCR is a measure of the maximum capacity of the ETC (also termed the “spare respiratory capacity”) utilized in response to a sudden increase in ATP demand. Lastly, inhibition of Complexes I and III by rotenone and antimycin A, respectively, disrupts electron flow through the ETC, greatly reducing the efficiency of OXPHOS and mitochondrial OCR, and increasing leakage of electron to attack oxygen molecules, forming superoxide anions (O_2^-) (Turrens and Boveris, 1980; Sugioka *et al*., 1988).

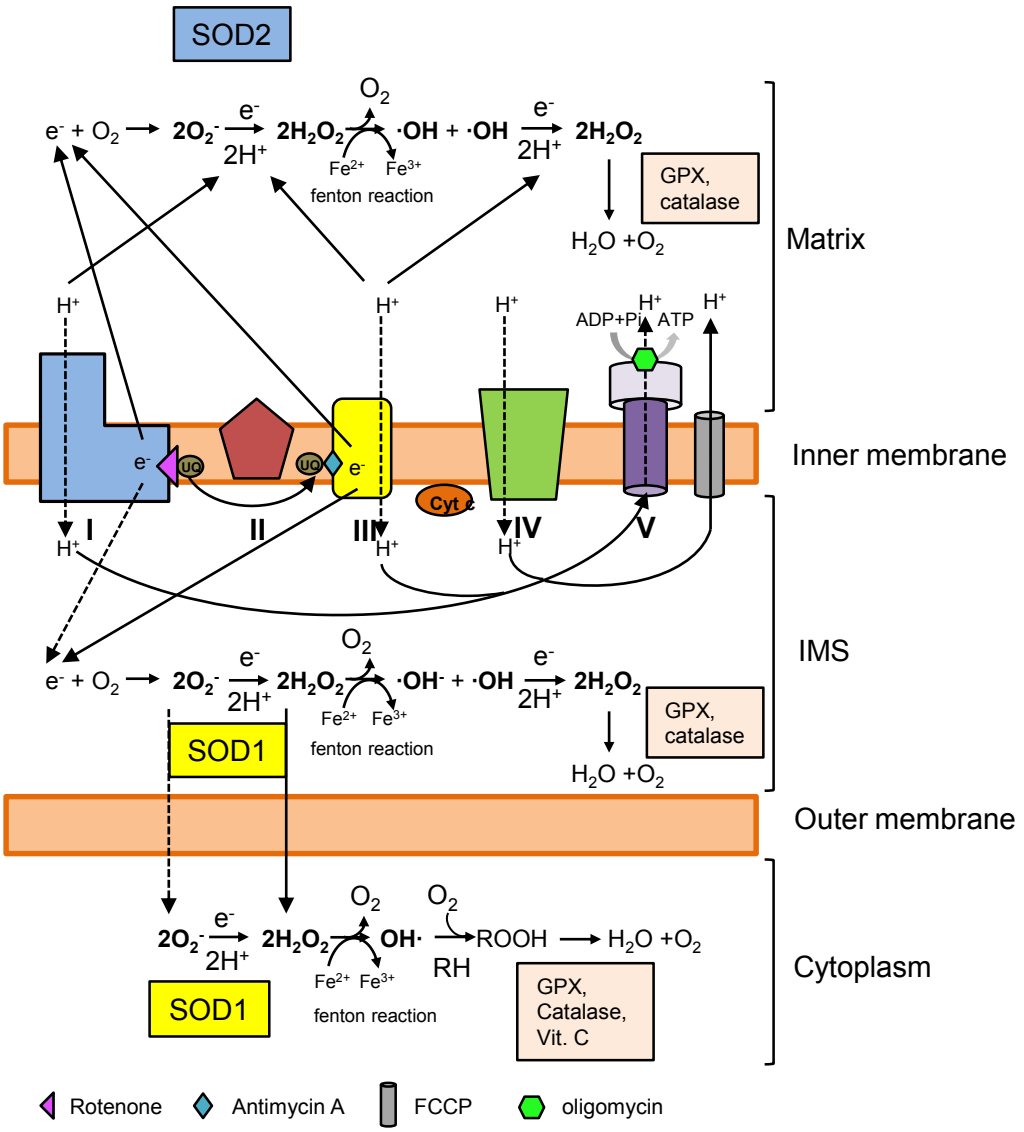

Figure 6.3 ETC dysfunction, ROS generation and detoxification. Rotenone and antimycin A inhibit reduction of UQ by complexes I and III, respectively, thus disrupt the ETC, reduce H^+ translocation and increase superoxide ("O_2^-") formation in the matrix, IMS, and into the cytoplasm. Superoxide dismutases ("SOD2" in the matrix and "SOD1" in the IMS and cytoplasm) transform O_2^- into less reactive hydrogen peroxide ("H_2O_2"), which is further neutralised to H_2O and O_2 by glutathione peroxidase ("GPX") and catalase. In the absence of these ROS scavengers, or in the presence of ferrous cations ("Fe^{2+}"), excess H_2O_2 can diffuse out of the mitochondria or disintegrate into highly reactive hydroxyl radicals ("•OH"), which can react with another •OH molecule to form more H_2O_2, or more commonly, attack lipid polymers ("RH") to form lipid peroxyl radicals ("ROOH"), which rely on GPX, catalase and vitamin C ("Vit. C") for neutralisation. FCCP and oligomycin inhibit ATP production by promoting proton leak, disrupting the proton gradient and thus uncoupling ATP production with OXPHOS, eventually shutting down the ETC. Adapted from Lemarie & Grimm, 2011.

6.2 Method

To investigate whether TDP1 plays a role in the mitochondria in removal of excess TOP1mt-cc in the presence of high oxidative stress, the *Tdp1*$^{-/-}$ MEFs could be used again to overexpress a toxic form of TOP1mt (TOP1mt^{T546A,N550H}), published by the Pommier group (Dalla Rosa *et al*., 2014), with a propensity to forming stable TOP1mt-cc . The N550H mutation enhances the DNA nicking reaction, while the T546A mutation inhibits the re-ligation reaction. There are several advantages of using the toxic TOP1mt (abbreviated as "TOP1mt*" hereafter) over TOP1 poisons such as CPT or topotecan (TPT). Firstly, it is mitochondria specific, without the associated nuclear DNA damage that make CPT and TPT highly cytotoxic. Secondly, uptake across the mitochondrial outer membrane is limited for hydrophobic small molecules. Thirdly, the alkaline environment of the mitochondrial matrix can readily inactivate these drugs.

However, there were several concerns of using the MEFs to study mitochondrial functions:

- The wildtype and *Tdp1*$^{-/-}$ MEFs were not isoclonal, so were the wildtype and *Tdp1*$^{-/-}$ cells overexpressing hSOD1 or hSOD1^{G93A}. Given the high heterogeneity between MEF cell lines, an observed functional phenotype in *Tdp1*$^{-/-}$ MEFs could be due to Tdp1-independent factors;
- To obtain isoclonal MEFs, *Tdp1*$^{-/-}$ cells complemented with hTDP1 was generated. However, expression of hTDP1 was gradually suppressed over one month, indicating perhaps cytotoxicity or survival disadvantage;
- Although immortalised by transformation, MEFs seem to retain sensitivity to atmospheric oxygen and require maintenance in low oxygen incubators, to which our lab lacked access at the time of the project.

The alternative of using an existing TDP1 knockdown MRC5 cell line posed several problems as well:

- TDP1 silencing using siRNA was not consistent and efficient enough for clonogenic survival and comet assays;
- Attempts to generate stable knockdown cell lines using shRNA were unsuccessful due to cytotoxicity.

Additionally, from a biological point of view, it would be interesting to see if the role of TDP1 in the mitochondria is comparable between human and mouse, as there was no strong evidence in the literature at that time. For these reasons, I generated an inducible cell line for TDP1 depletion in human HEK293 cells using the commercially available Flp-In T-Rex 293 cell line from Life Technologies (R780-07), which has the major advantage of allowing simultaneous, inducible silencing of TDP1 and overexpression of exogenous proteins of interest, such as TOP1mt or $SOD1^{G93A}$.

In this chapter I will outline the method I used to establish the cell lines, validate the known functional phenotypes of TDP1 depletion, and characterise the mitochondrial functional phenotype of these cell lines.

6.2.1 The Flp-In T-Rex 293 system

The commercially available Flp-In T-Rex 293 (Flp-In) cell lines are engineered to contain a single Flp recombination target (FRT) site in a transcriptionally active region of the genome. The FRT site allows binding of exogenously expressed Flp recombinase (originally derived from *S. cerevisiae*) and exchange of genetic sequences flanked by the FRT site (O'Gorman *et al*., 1991). The host genomic FRT site has a hygromycin resistance gene downstream which is only activated after successful Flp-mediated recombination event. This allows for selection of clones that have stably integrated the gene of interest between the FRT sites. The rationale behind the use of the exogenous system of genomic recombination is to ensure controlled, specific genome editing, and a homogenous expression from a single copy genomic insert across the whole cell population. In addition, the Flp-In T-Rex system allows for

tetracycline/doxycycline induction of expression of the gene of interest, thus circumventing some of the problems of cytotoxicity associated with constitutive gene expression/deletion. The Flp-In T-Rex cells stably express the tetracycline repressor (TetR), which binds to the two Tet operator 2 ($TetO_2$) sequences within the CMV promoter upstream of the gene of interest in the absence of tetracycline. When tetracycline is present, it interacts with TetR and sequesters it from the $TetO_2$ sites, subsequently inducing transcription of the gene of interest. **Fig. 6.4** summarizes the principle of the system.

For the purpose of my project, the Flp-In T-Rex 293 cells have some technical limitations:

- The parental HEK293 cell line is genetically highly transformed, making the homogenous expression of a single copy gene across the whole cell population presumably less reliable, especially in continually cultured cells;
- They are not strongly adherent cells, making assays that rely on high plating efficiency such as clonogenic survival assays, immunofluorescence, and the Seahorse assay technically more difficult.
- They have a large nuclear:cytoplasmic ratio, making fluorescence microscopic imaging of the mitochondrial network more challenging.

The measures that I have taken to address these problems include:

- Work with single clones instead of mixed population after establishment of a cell line; monitor homogeneity of GFP expression before each experiment.
- For monitoring cell killing after genotoxic stress, measure viability in a cell population after 72 hours of continuous drug treatment by fluorescence readout, instead of formation of single colonies after a bolus dose of treatment. This would circumvent the need for high plating efficiency, although cell viability does not always correlate with colony-forming (replicative) capacity.

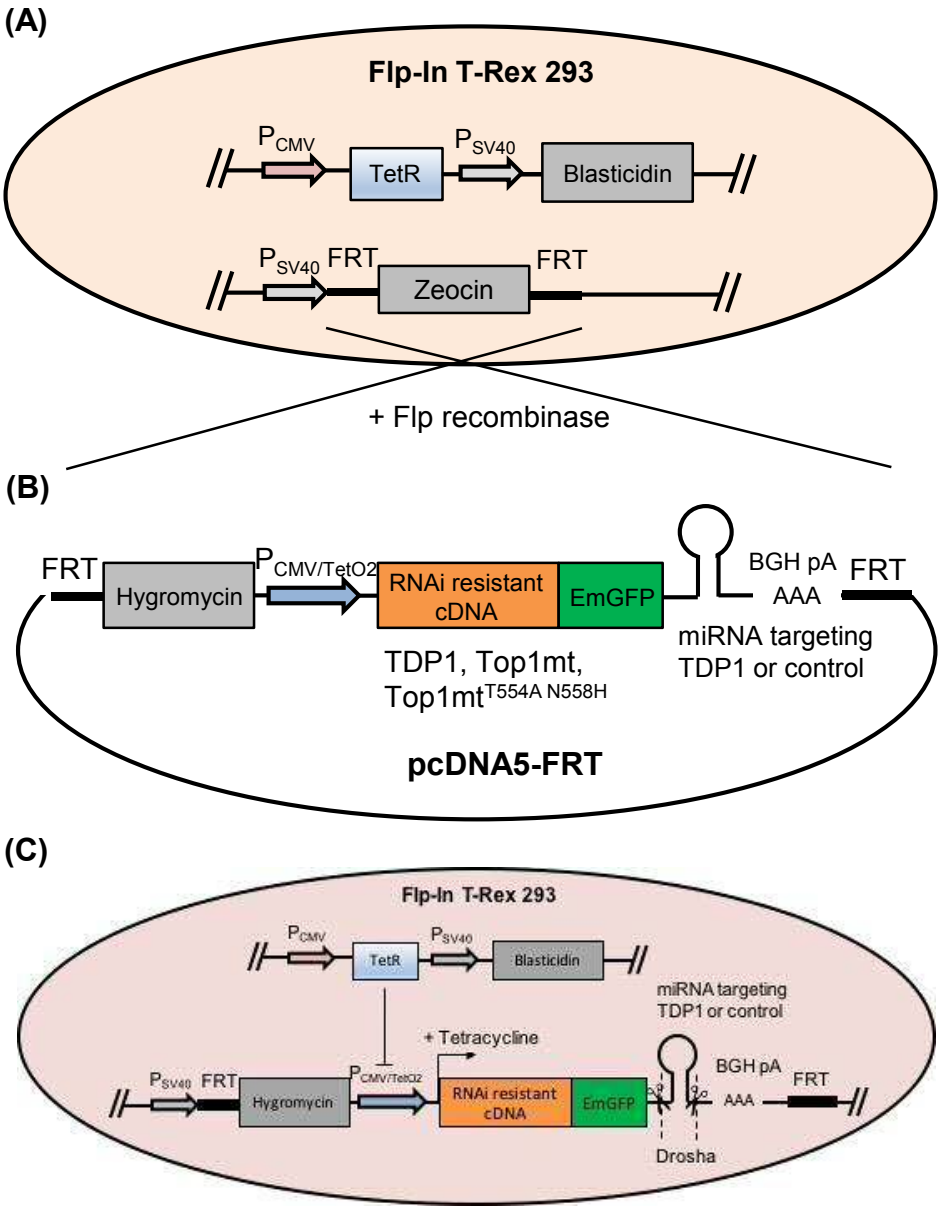

Figure 6.4 Scheme for generating Flp-In T-Rex 293 cells with concomitant RNAi-mediated knockdown of TDP1 and overexpression of various fusion proteins. (A) Host cell with two FRT sequence sites ("FRT"), tetracyline repressor ("TetR"), and blasticidin resistance gene ("Blasticidin") was co-transfected with **(B)** pcDNA5-FRT vector encoding EmGFP-tagged fusion protein ("cDNA") and micro RNA sequence ("miRNA") and pGKFLP vector encoding Flp recombinase. The transformants were selected with 100µg/ml hygromycin for 3 weeks. **(C)** In the absence of tetracycline/doxycyline, the TetR binds the CMV/TetO$_2$ hybrid promoter ("$P_{CMV/TetO2}$") to inhibit downstream transcription. After addition of tetracycline or doxycyline, the repressor is removed and transcription of the cDNA-miRNA sequence is initiated. Upon RNA transcription, excision of the miRNA hairpin by Drosha results in RNAi-mediated knock-down of TDP1, while non-excision results in translation of the recombinant protein.

- For immunofluorescence assays, use of polymer-based coating such as D-poly-lysine on coverslips would reduce loss of cells during washing steps.
- Instead of measuring mitochondrial membrane potential by fluorescence microscopy, use FACS analysis of live cells, and the Seahorse Bioanalyser to measure mitochondrial respiratory functions.
- Use of Cell-Tak, as recommended by Seahorse Bioscience, to adhere cells to the Seahorse Analyser microplate.

6.3 Results

6.3.1 Generation of stable Flp-In T-Rex 293 cell lines

For the purpose of studying the effect of TDP1 deficiency on mitochondrial functions, two miRNA sequences targeting nucleotides 28 – 48 (amino acids 10 – 16) and nucleotides 259 – 279 (amino acids 87 – 93) of the human TDP1 mRNA sequence (NM_001008744.1), were inserted into mammalian expression vector pcDNA6.2-GW-EmGFP, which contains specific flanking sequences to allow processing of the miRNA *in vivo*, as well as an EmGFP tag for monitoring expression. The miRNA-EmGFP fragment was then sub-cloned into the Flp-In system expression vector pcDNA5-FRT, which contains the CMV/TetO_2 promoter, the FRT site for integration into the host genome, and hygromycin resistance gene, to generate the pcDNA5-FRT-miTDP1 plasmid. Similarly, scrambled miRNA sequence was sub-cloned into pcDNA5-FRT to generate pcDNA5-FRT-miScr. For each of these plasmids, full-length cDNA sequences of SOD1^{G93A} (NM_000454), TOP1mt (NM_001258446.1), TOP1mt^{T554A,N558H}, or RNAi-resistant TDP1 (silent mutations at all the amino acids residues) minus the stop codon were sub-cloned 5’ of and in frame with the EmGFP tag. Flp-In T-Rex 293 cells were then transfected with the generated constructs, together with the Flp recombinase-expressing plasmid pPGKFLP, and stable clones were selected with hygromycin for three weeks to generate the following cell lines expressing:

1. Control microRNA (“miScr”)
2. TDP1 microRNA (“miTDP1”)
3. TDP1 microRNA with targeting-resistant TDP1 cDNA complementation (“TDP1 + miTDP1”)
4. Control microRNA with $SOD1^{G93A}$ overexpression (“$SOD1^{G93A}$ + miScr”)
5. TDP1 microRNA with $SOD1^{G93A}$ overexpression (“$SOD1^{G93A}$ + miTDP1”)
6. Control microRNA with TOP1mt overexpression (“TOP1mt + miScr”)
7. TDP1 microRNA with TOP1mt overexpression (“TOP1mt + miTDP1”)
8. Control microRNA with $TOP1mt^{T554A,N558H}$ overexpression (“$TOP1mt^{*}$ + miScr”)
9. TDP1 microRNA with $TOP1mt^{T554A,N558H}$ overexpression (“$TOP1mt^{*}$ + miTDP1”)

The inclusion of target-resistant TDP1 complementation of miTDP1 cell line is an important control, as in a miRNA system, the structure of the synthetic miRNA may mimic an endogenous miRNA, and may cause tissue-specific off-target effects different from siRNA or shRNA transfected cells. Therefore, if a phenotype is observed in miTDP1 cells and is rescued by TDP1 complementation, the phenotype is more likely to be TDP1-specific.

To assess the functional interaction between TDP1 and TOP1mt, instead of depleting TOP1mt, I opted to overexpress either wildtype TOP1mt or the toxic mutant TOP1mt*. The rationale was that assessment of the depletion of endogenous TOP1mt from WCE by immunoblotting depended on a highly sensitive and specific antibody (which was not commercially available at the time of the project), and the residual TOP1mt may be sufficient to compensate like in the case of nuclear TOP1. Interestingly, overexpression of TOP1mt has a known phenotypic defect (Sobek *et al*., 2013), which can be monitored to detect the effect of TDP1. The use of TOP1mt* would give more insight on the molecular mechanism by which TOP1mt negatively regulates mitochondrial transcription, as well as the role of TDP1 on this regulation. Furthermore, the use of an

overexpression system instead of miRNA-mediated knock-down would circumvent the need to establish functional assays to rule out off-target effects of the miRNAs.

To induce miRNA and protein expression, 1 µg/mL doxycycline was added to the growth medium for 24 hours, cells were lysed and protein expression for each sample was analysed by immunoblotting. **Fig. 6.5** shows depletion of endogenous TDP1 specific to doxycycline induction. There was some leaky expression of the targeting-resistant EmGFP-TDP1 in the absence of doxycycline, but more importantly, the control miRNA ("miScr") did not affect the expression level of endogenous TDP1.

6.3.2 Validation of functional phenotype of TDP1 depletion in Flp-In cell lines

Using an *in vitro* TDP1 enzymatic assay, it was confirmed that miTDP1 cell lysates had reduced TDP1 activity, while complementation with the target-resistant EmGFP-TDP1 increased TDP1 activity level (**Fig. 6.6**). miTDP1 cells accumulated ~ 2-fold more CPT-induced chromosomal breaks as measured by alkaline comet assay (**Fig. 6.7, $p < 0.01$; Student's t-test**) and 53BP1 foci formation (**Fig. 6.8, $p < 0.05$; Student's t-test**), and reduced survival after CPT (**Fig. 6.9A**). miTDP1 cells did not show a difference in viability from TDP1 + miTDP1 cells in response to oxidative damage by TBH (**Fig. 6.9B**). Bearing in mind that the doxycycline used to induce TDP1 expression/knockdown could inhibit TDP1 activity (Pommier, 2006), the viability assays were carried out after withdrawal of doxycycline. In both miTDP1 and TDP1 + miTDP1 cells the difference in TDP1 activity levels were maintained up to 72 hours after doxycycline withdrawal (**Fig. 6.9C,D**), suggesting that the lack of TBH sensitivity in miTDP1 cells was not due to loss of TDP1 knockdown.

Nevertheless, as measurement of survival in terms of viability assays do not necessarily correlate with clonogenic assays, and as the nuclear DNA repair assays indicated a TDP1 deficient phenotype, I decided to investigate the role of TDP1 in the mitochondria using the Flp-In T-rex system as planned.

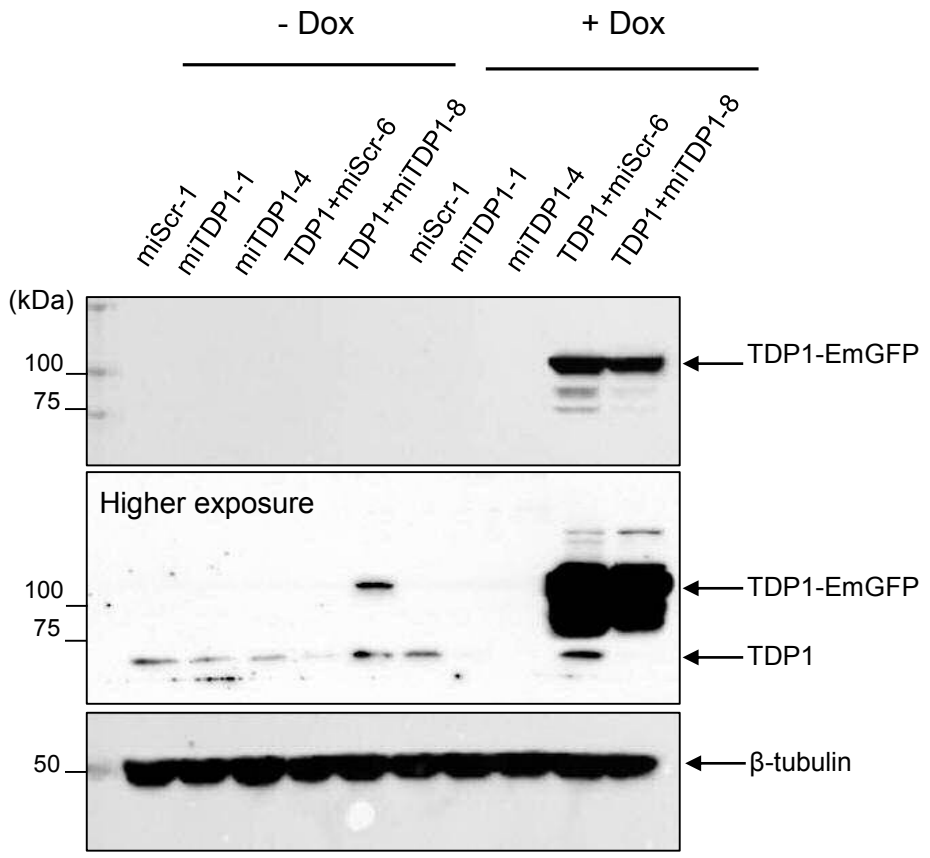

Figure 6.5 Doxycycline induction of TDP1 depletion and complementation in Flp-In T-Rex 293 cells. 5 x 10^5 cells selected in 100 µg/ml hygromycin B and 10 µg/ml blasticidin for 3 weeks were incubated in 1 µg/ml doxycyline for 24 hours, then harvested. 75 µg of WCE was fractionated by SDS-PAGE and immunoblotted using antibodies against human TDP1 and β-tubulin. "miScr" denotes cells expressing scrambled (control) miRNA, "miTDP1" denotes cells expressing TDP1-targeting miRNA, "TDP1 + miScr" denotes cells overexpressing targeting-resistant TDP1 and control miRNA, and "TDP1 + miTDP1" denotes cells overexpressing targeting-resistant TDP1 and TDP1-targeting miRNA. The number at the end of each cell line denotes clone number. "- Dox" indicate no doxycyline treatment, "+ Dox" indicates treatment with doxycyline.

(A)

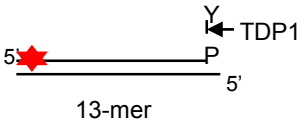

(B)

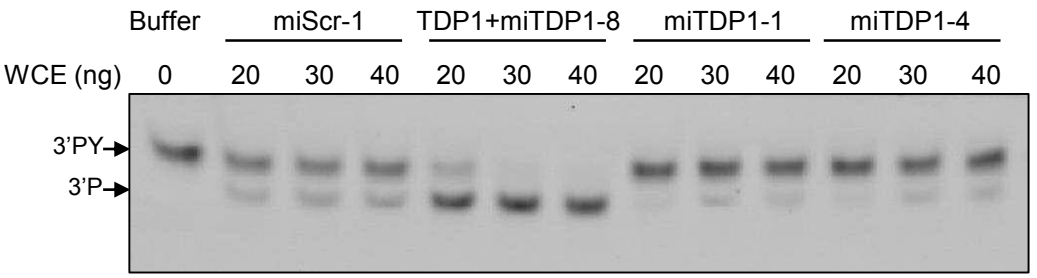

Figure 6.6 *In vitro* TDP1 enzymatic activity of Flp-In T-Rex 293 cell lines. (A) Diagramme of the TDP1-specific substrate consisting of a 13-mer oligonucleotide with tyrosyl residue conjugated to the 3' end and a fluorophore Cy5.5 molecule conjugated at the 5' end, annealed to a 14-mer complementary oligonucleotide. Arrow indicates cleavage of the phosphotyrosine bond by TDP1. **(B)** 5 x 10^5 Flp-In T-Rex 293 cells selected in 100 µg/ml hygromycin B and 10 µg/ml blasticidin for 3 weeks were incubated in 1 µg/ml doxycycline for 24 hours, then harvested and total proteins extracted. The indicated amount of WCE was incubated with 25 nM of TDP1 substrate at 37ºC for 1 hour, then resolved with a 20 % 7.5 M urea SequaGel by electrophoresis. "Buffer" denotes sample with lysis buffer but no WCE. "miScr" denotes cells expressing scrambled (control) miRNA, "miTDP1" denotes cells expressing TDP1-targeting miRNA, and "TDP1 + miTDP1" denotes cells overexpressing targeting-resistant TDP1 and TDP1-targeting miRNA. The number at the end of each cell line denotes clone number.

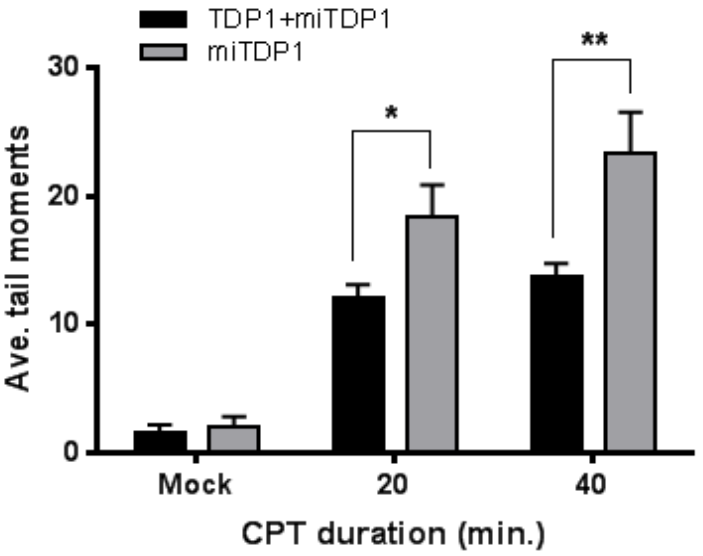

Figure 6.7 Flp-In T-Rex 293 cells with TDP1 knockdown accumulate more CPT-induced chromosomal DNA breaks. 3 x 10^5 Flp-In T-Rex 293 cells were incubated in 1 µg/ml doxycycline for 24 hours, then treated with 50 µM CPT or DMSO ("Mock") for the indicated time periods at 37°C. DNA strand breaks induced were measured using the alkaline comet assay. Average tail moments from 50 cells were quantified using the Comet Assay IV software. Data are the mean of 3 independent experiments and error bars represent ±1 S.E.M. *p* values were derived from one-tailed Student's t-test , whereby * denotes $p < 0.05$ and ** denotes $p < 0.01$.

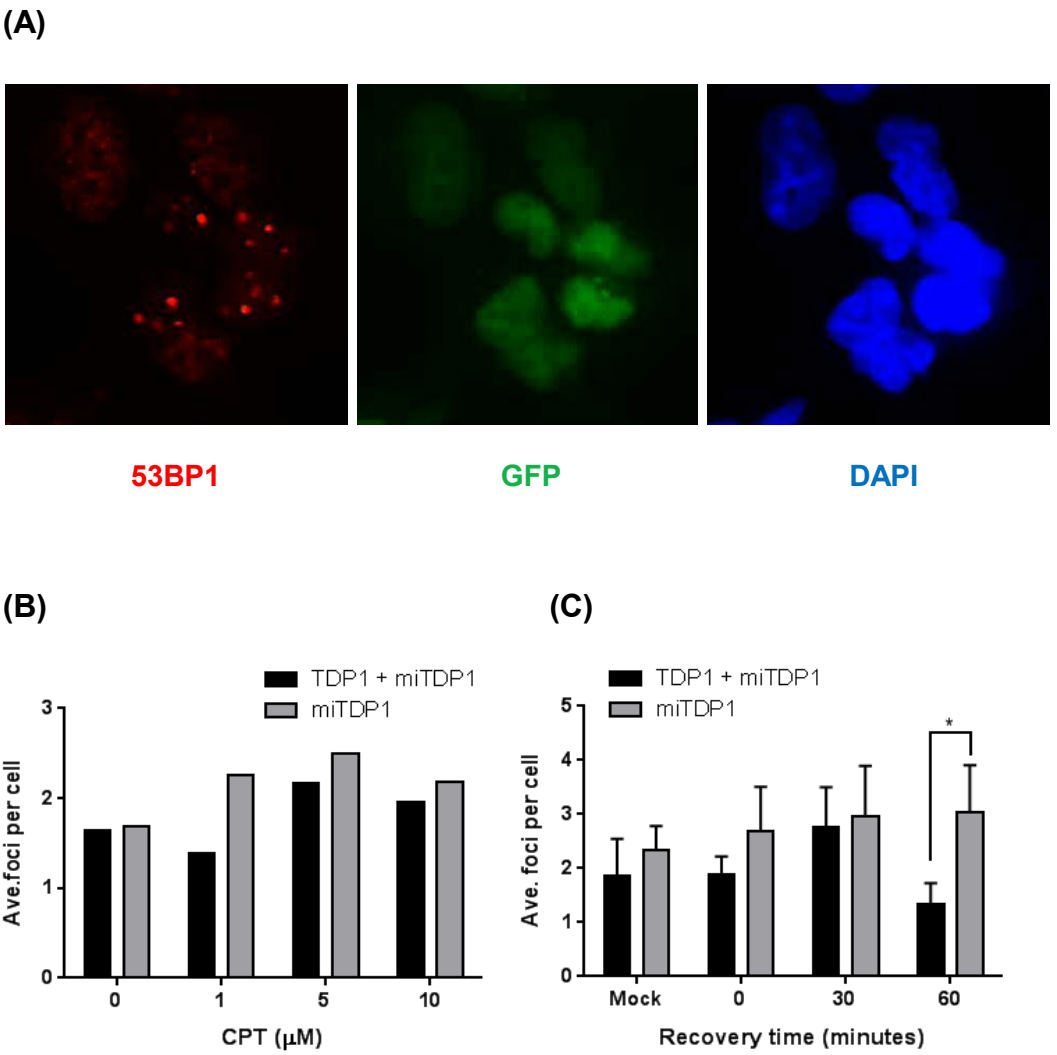

Figure 6.8 Flp-In T-Rex 293 cells with TDP1 knockdown accumulate more CPT-induced DSBs. 5 x 10^4 cells plated on poly-D-lysine-coated coverslips were induced with 1 μg/ml doxycyline for 24 hours, then treated with 1, 5 or 10 μM CPT or DMSO ("Mock") for 1 hour at 37°C, the media was then removed. The cells were washed twice with PBS then incubated in normal growth media for the indicated time periods. Cells were then fixed in 4% PFA for 15 minutes at room temperature, permeated with 0.2 % Triton-X100, then washed with PBS. Cells were then immunostained with antibodies against 53BP1 (red) and GFP (green) for 1 hour at room temperature, and DAPI (blue) for 10 minutes. **(A)** Example of images taken from TDP1+miTDP1-8 cells after CPT. Distinct 53BP1 foci were manually counted. **(B)** Quantification of average 53BP1 foci number per cell from 100 cells. **(C)** Doxycyline-induced cells were treated with 1 μM CPT or DMSO ("Mock") for 1 hour, washed twice with PBS, then recovered in normal growth media for the indicated time periods. Average number of 53BP1 foci per cell from 100 cells were calculated. Data are the mean from 3 independent experiments and error bars denote $\pm$1 S.E.M. *p* values were derived from one-tailed Student's t-test, whereby * denotes $p < 0.05$.

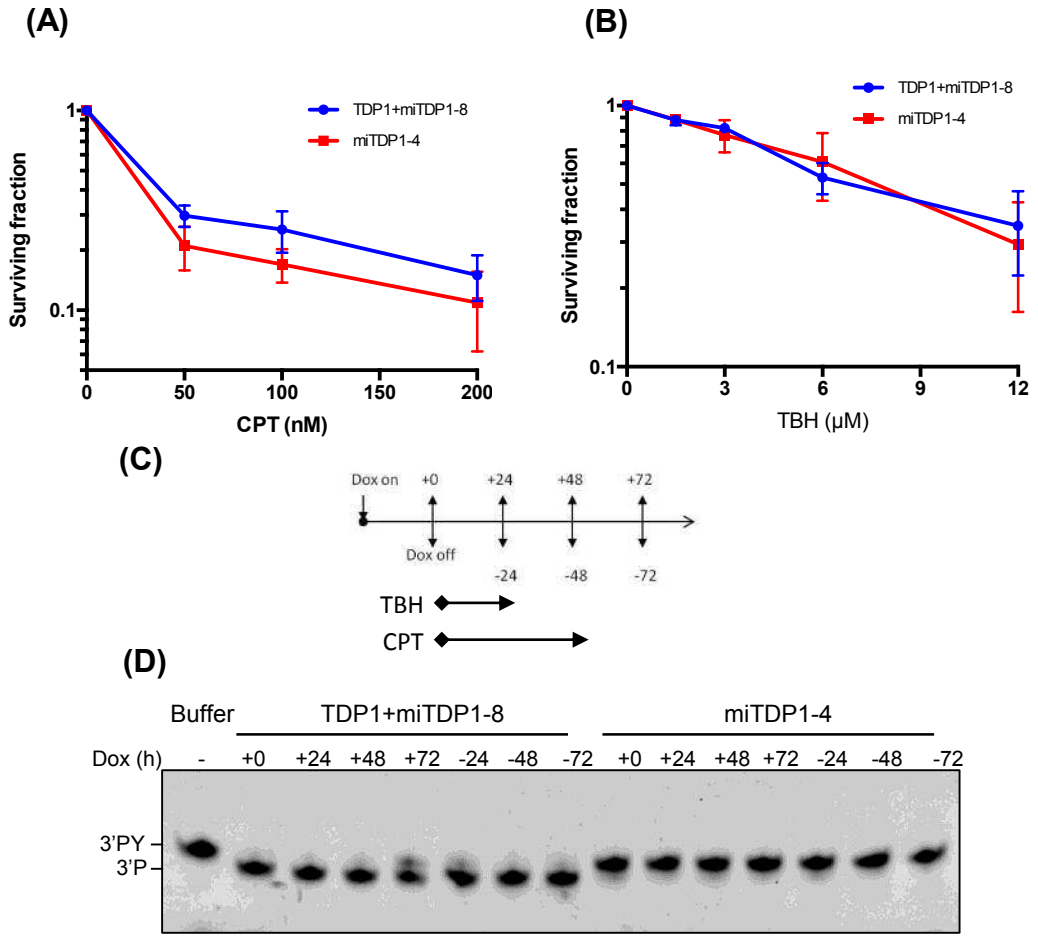

Figure 6.9 TDP1 depletion in Flp-In T-Rex 293 cells reduced viability after CPT but not TBH treatment. **(A, B)** Cells induced with doxycycline were seeded at densities of 2000-20000 cells/100 µl, and treated with the indicated concentrations of CPT or TBH in the absence of doxycycline for 72 hours. 20 µl of CellTiter-Blue reagent was then added to the cells and incubated at 37°C for 1 hour. The fluorescence intensity was measured using a BMG FLUORstar Omega microplate reader with filters of EX544/EM590-10. Data are the mean of 3 independent experiments and error bars represent ±1 S.E.M. **(C)** Scheme of doxycycline induction and CPT or TBH treatment (in hours) Cells were treated with 1 µg/ml doxycycline for 24 hours, followed by treatment with the indicated concentrations of CPT in (A) for 2 hours at 37°C or TBH in (B) for 1 hour at 37°C. Cells were subsequently incubated in media with 1 µg/ml doxycycline for up to 72 hours (+0, +24, +48, +72) or without doxycycline for the indicated hours (-24, -48, -72). **(D)** Cells from (C) were harvested and lysed. 40 ng of WCE was incubated with 25 nM of TDP1 substrate at 37ºC for 1 hour, then resolved with a 20 % 7.5 M urea gel by electrophoresis. "Buffer" denotes sample with lysis buffer but no WCE. "TDP1 + miTDP1" denotes cells overexpressing targeting-resistant TDP1 and TDP1-targeting miRNA, "miTDP1" denotes cells expressing TDP1-targeting miRNA. The number at the end of each cell line denotes clone number.

6.3.3 Overexpression of SOD1^{G93A} in TDP1-depleted cells increased H_2O_2-induced chromosomal breaks

In order to compare the role of TDP1 in the mitochondria between human and mouse, I generated Flp-In cell lines concomitantly depleted of TDP1 and overexpressing SOD1^{G93A} ("SOD1^{G93A} + miTDP1"). However, after 24-hour doxycycline induction, the SOD1^{G93A}-EmGFP signal was only present in < 5 % of the cell population in 4 out of 5 clones screened by FACS, compared to ~ 15 % of the TDP1-proficient cell population overexpressing SOD1^{G93A} (**Fig. 6.10A**). This was not due to reduced level of overall transcription or translation in TDP1-depleted cells, as wildtype SOD1 was expressed in ~ 30 % of TDP1-depleted cells ("SOD1 + miTDP1") (**Fig. 6.10A**). Using immunoblotting, I further confirmed that the expression level of SOD1^{G93A} in TDP1-depleted cells declined between 8 – 16 hours of induction. In contrast, in SOD1 + miTDP1 cells, the overexpression level of SOD1 was unaffected by TDP1 depletion (**Fig. 6.10B**). This could be due to downregulation of SOD1^{G93A} expression to ensure survival of TDP1 deficient cells. Nevertheless, even with low level expression of SOD1^{G93A}, SOD1^{G93A} + miTDP1 cells showed ~ 30 % higher level of chromosomal breaks after 10 minutes of H_2O_2 treatment compared to wildtype, although the subsequent repair of these breaks was independent of TDP1 (**Fig. 6.11, *p* < *0*.05; Student's t-test**). This is consistent with the finding in MEFs as described in **Section 5.2.7**.

6.3.4 Validation of functional phenotypes of TOP1mt and TOP1mt overexpression in Flp-In cell lines*

To further investigate the role of human TDP1 in the mitochondria, and possible functional interaction with TOP1mt, I generated Flp-In cell lines that overexpress TOP1mt-EmGFP in TDP1-proficient or -deficient backgrounds ("TOP1mt + miScr" and "TOP1mt + miTDP1", respectively). In addition, to mimic the increase in TOP1mt-cc due to oxidative stress, I also established cell lines that overexpress the toxic mutant TOP1mt*-EmGFP in the presence or absence of TDP1 knockdown ("TOP1mt + miScr"

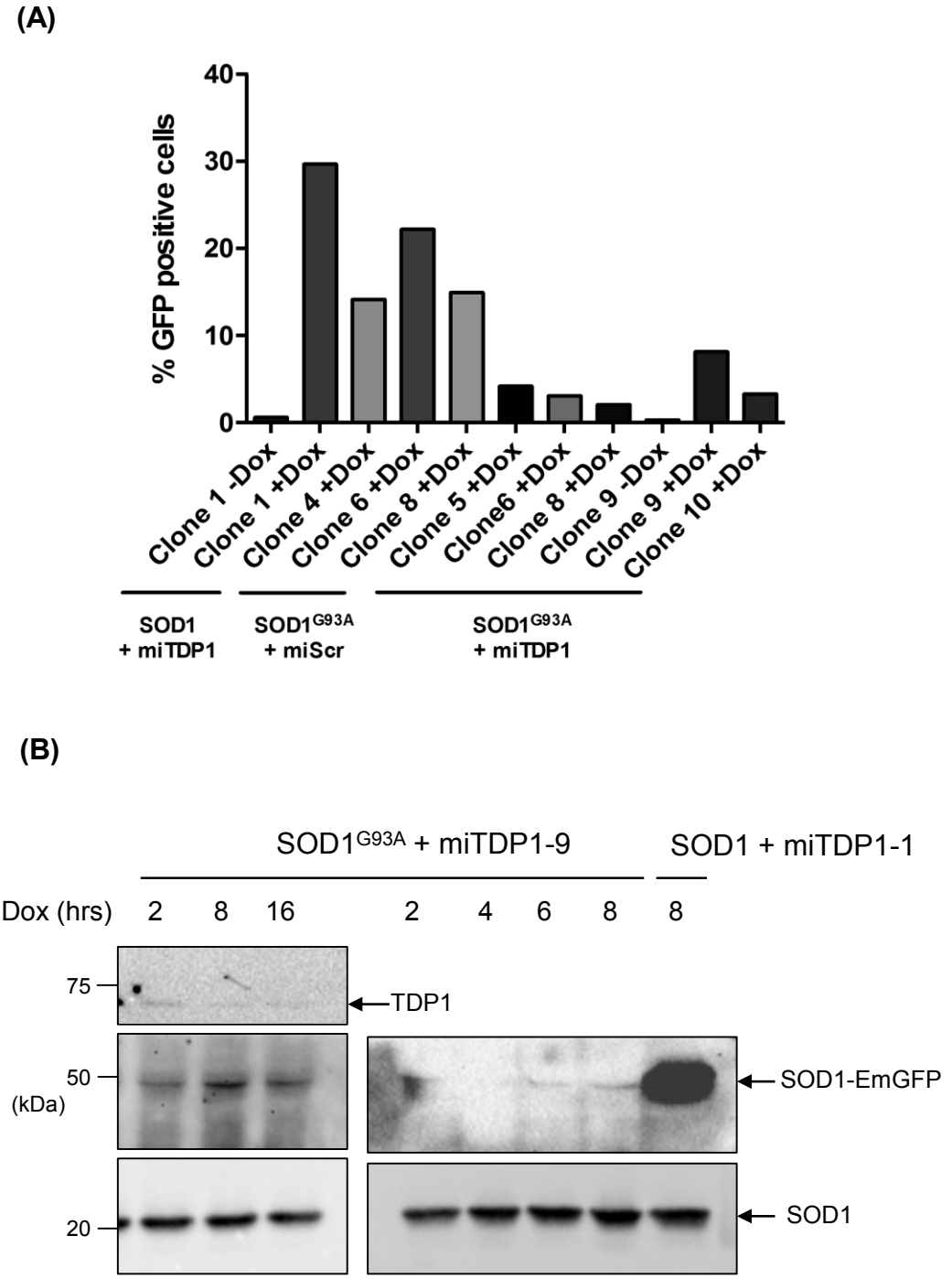

Figure 6.10 SOD1^{G93A} overexpression is attenuated in Flp-In T-Rex 293 cells with TDP1 depletion. 5 x 10^5 cells were incubated in 1 µg/ml doxycycline for 24 hours ("+Dox"), then fixed with 70 % ethanol for 4 hours. Percentage of cells expressing GFP was analysed by FACS. **(B)** 5 x 10^5 cells were incubated in 1 µg/ml doxycycline for the indicated time periods, then harvested. 75 µg of WCE was fractionated by SDS-PAGE and immunoblotted using antibodies against human TDP1 and SOD1. "SOD1 + miTDP1" denotes cells expressing TDP1-targeting miRNA and SOD1. "SOD1^{G93A} + miScr" denotes cells expressing scrambled miRNA and SOD1^{G93A}, while "SOD1^{G93A} + miTDP1" denotes cells expressing TDP1-targeting miRNA and SOD1^{G93A}. The number at the end of each cell line denotes clone number.

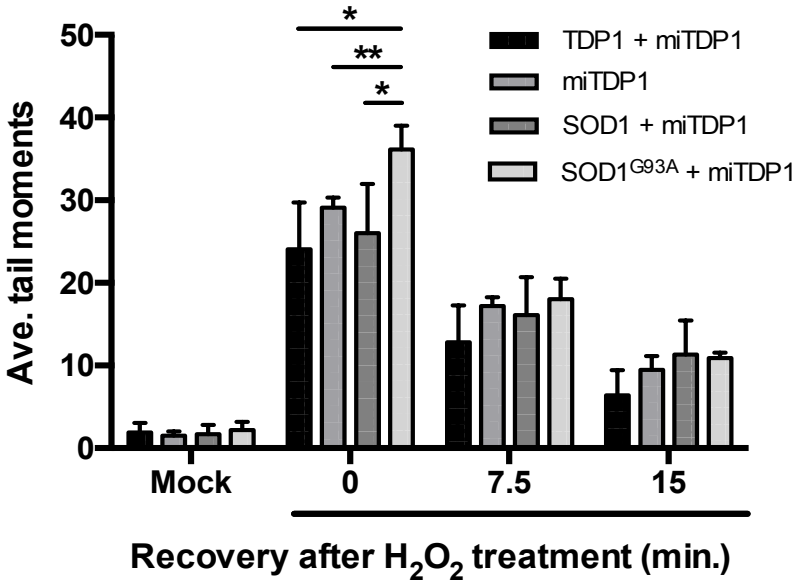

Figure 6.11 Flp-In T-Rex 293 cells expressing SOD1^{G93A} accumulate more SSBs after H_2O_2 treatment. 3 x 10^5 cells from the Flp-In T-Rex 293 stable cell lines were incubated in 1 µg/ml doxycyline for 8 hours, treated with 10 µM H_2O_2 or PBS ("Mock") for 10 minutes on ice, then incubated in drug-free medium for the indicated time periods. SSBs induced were measured using the alkaline comet assay. Average tail moments from 50 cells were quantified using the Comet Assay IV software. Data are the mean of 3 independent experiments and error bars represent ±1 S.E.M. *p* values were derived from two-tailed Student's t-test , whereby * denotes $p < 0.05$ and ** denotes $p < 0.01$.

and “TOP1mt + miTDP1”, respectively). I confirmed the levels of protein expression by immunoblotting (**Fig. 6.12A**), mitochondrial localization of TOP1mt-EmGFP and TOP1mt*-EmGFP (**Fig. 6.12B**), and enzymatic activity of TDP1 in the mitochondria (**Fig. 6.12C**). Interestingly, TDP1 catalytic activity appeared to be upregulated by ~ 20 % in both TOP1mt- and TOP1mt*-overexpressing cells (**Fig. 6.12D**).

As an initial validation of the functional phenotype of TOP1mt overexpression, I designed primers for five peptide-coding transcripts encoded by the mitochondrial genome (**Table 2.9**) and confirmed the specificity of the primers for PCR amplification of a cDNA library prepared from whole cell RNAs (**Fig. 6.13A**). Since the mitochondrial encoded genes are intronless, the primers would also amplify any contaminating mtDNA. With the DNAse treatment, I confirmed that mtDNA was not detectable by PCR in the non-reverse transcribed RNA preparations (**Fig. 6.13B**). I then quantified the levels of the transcripts by RT-qPCR in each cell line. After 24-hour doxycycline induction, TOP1mt overexpression markedly reduced levels of the mitochondrial transcripts by ~ 80 % compared to control cells (**Fig. 7.13C, $p < 0.001$**; **Student’s t-test**), consistent with published data (Sobek *et al*., 2013).

I then validated the phenotype of TOP1mt* overexpression published by Pommier and coworkers (Dalla Rosa *et al*., 2014) by quantifying TOP1mt-cc using caesium chloride (CsCl) fractionation (**Fig. 6.14A**) (Hartsuiker, 2011). Due to the non-specificity of the TOP1mt antibody on immunoblotting of WCE (**Fig. 6.15**) and CsCl fractions (**Fig. 6.14B**), I used purified mitochondrial extracts instead of WCE for CsCl fractionation, and immunoblotted the fractions using anti-GFP antibody, which would detect EmGFP-tagged TOP1mt and TOP1mt*. Non-specific signals were now absent from the free DNA fractions (**Fig. 6.16A,B**). Interestingly, in the absence of exogenous stress or topoisomerase poisons, overexpression of wildtype TOP1mt did not induce more endogenous TOP1mt-cc than in control miScr cells, (**Fig. 6.16A**). Overexpression of TOP1mt*, however, induced ~ 6.5 fold more TOP1mt-cc compared to

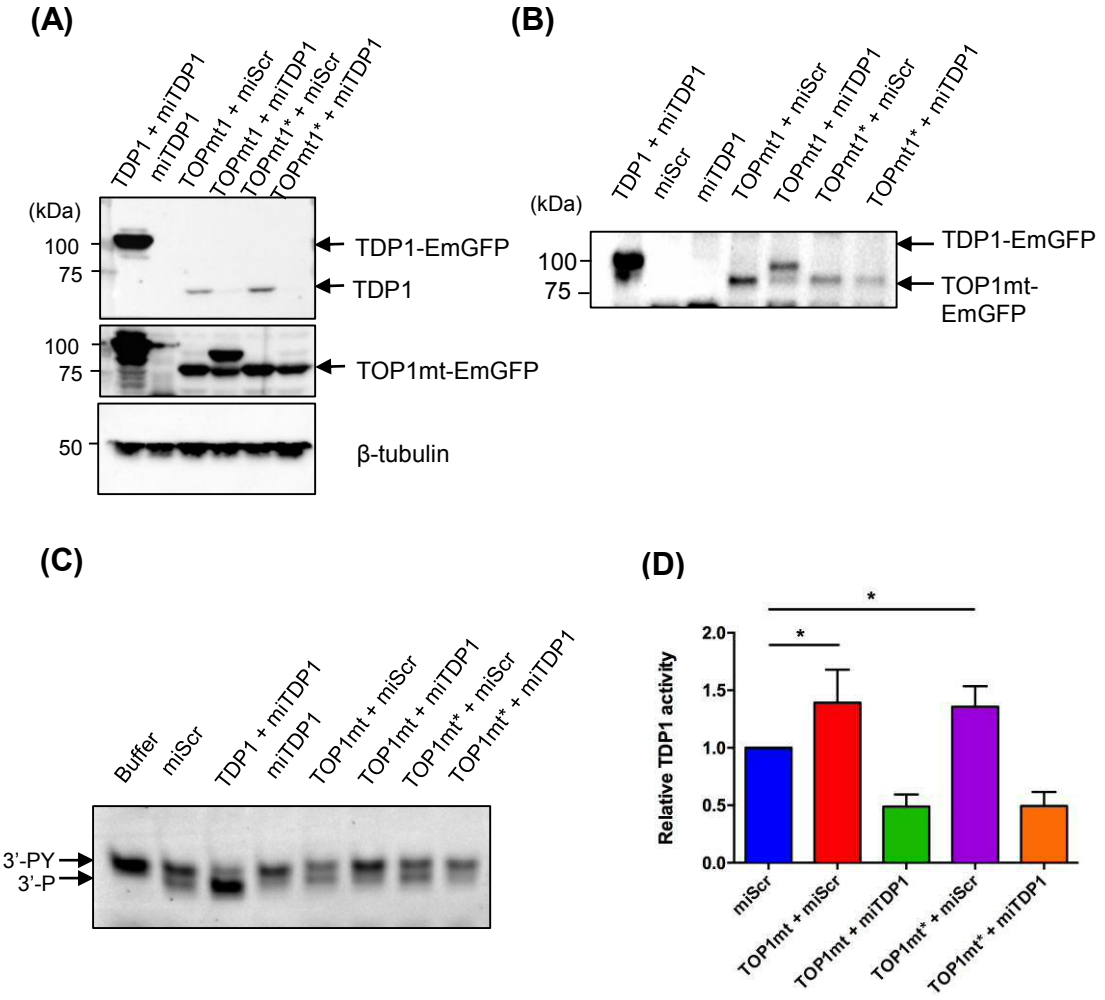

Figure 6.12 Overexpression of TOP1mt or TOP1mt* with concurrent TDP1 depletion in Flp-In T-Rex 293 cells. (A) 10^6 cells were incubated in 1 µg/ml doxycycline for 48 hours, then harvested. 75 µg of WCE was fractionated by SDS-PAGE and immunoblotted with antibodies against TDP1, GFP, and β-tubulin. **(B)** 2 x 10^7 cells were incubated in 1 µg/ml doxycycline for 48 hours, then harvested. Mitochondria were extracted, purified with proteinase K, and lysed. 5 µg total proteins were fractionated by SDS-PAGE and immunoblotted with antibodies against GFP. **(C)** 100 ng of mitochondrial lysate from (B) was mixed with 25 nM of TDP1 substrate at 37ºC for 1 hour, then resolved with a 20 % 7.5 M urea gel by electrophoresis. The substrate and product were detected with the ChemiDoc MP (Bio-Rad) gel imaging system using the Cy5.5 filter. **(D)** Quantification of TDP1 catalytic activity from (C) using Image Studio Lite. TDP1 activity was calculated from the ratio of 3'-P product signal intensity to the total intensity of 3'-P and 3'-PY. Relative TDP1 activity is expressed as TDP1 activity normalised to that of the control miScr cells. "Buffer" denotes sample with lysis buffer but no lysate. "3'-PY" denotes oligonucleotide substrate with 3'-phosphotyrosyl end, "3'-P" denotes oligonucleotide product with 3'-phosphate end, "miScr" denotes cells expressing scrambled miRNA, "TDP1 + miTDP1" denotes cells overexpressing targeting-resistant TDP1-EmGFP and TDP1-targeting miRNA, "miTDP1" denotes cells expressing TDP1-targeting miRNA. "TOP1mt + miScr" denotes cells overexpressing TOP1mt-EmGFP and scrambled miRNA, and "TOP1mt + miTDP1" denotes cells overexpressing TOP1mt and TDP1-targeting miRNA. Data are the mean of 3 independent experiments and error bars represent ±1 S.E.M. *p* values were derived from two-tailed Student's t-test , whereby * denotes $p < 0.05$.

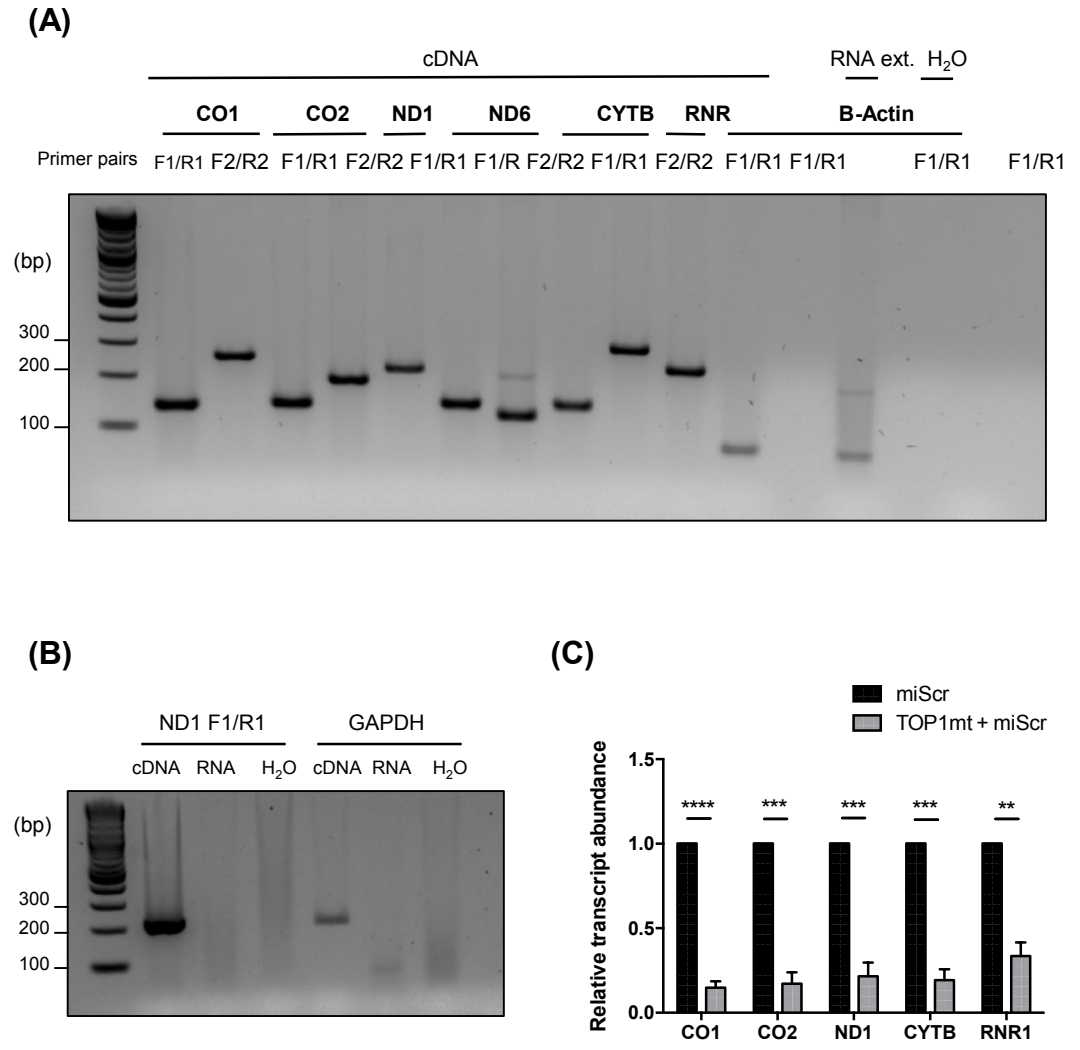

Figure 6.13 Overexpression of TOP1mt reduces abundance of mitochondrial transcripts in Flp-In T-Rex 293 cells. (A) 10^6 cells were incubated in 1 µg/ml doxycyline for 24 hours then harvested. The RNA contents were extracted and 5 µg was reverse-transcribed. PCR was carried out on the cDNA and non-reverse transcribed RNA extract to test the specificity of primers to amplify five of the mitochondrial genes. β-actin was used as positive control and H_2O was used as non-template control (NTC). **(B)** cDNA and non-reverse transcribed RNA extract from (A) was used to test PCR amplification of GAPDH, using ND1 as positive control and H_2O as NTC. **(C)** RT-qPCR quantification of transcript abundance of five mitochondrial genes normalised against GAPDH from cells overexpressing TOP1mt, relative to the abundance of the mitochondrial transcripts miScr control cells. Data are the mean of 3 independent experiments and error bars represent ±1 S.E.M. *p* values were derived from one-tailed Student's t-test. whereby *** denotes $p < 0.001$ and **** denotes $p < 0.0001$.

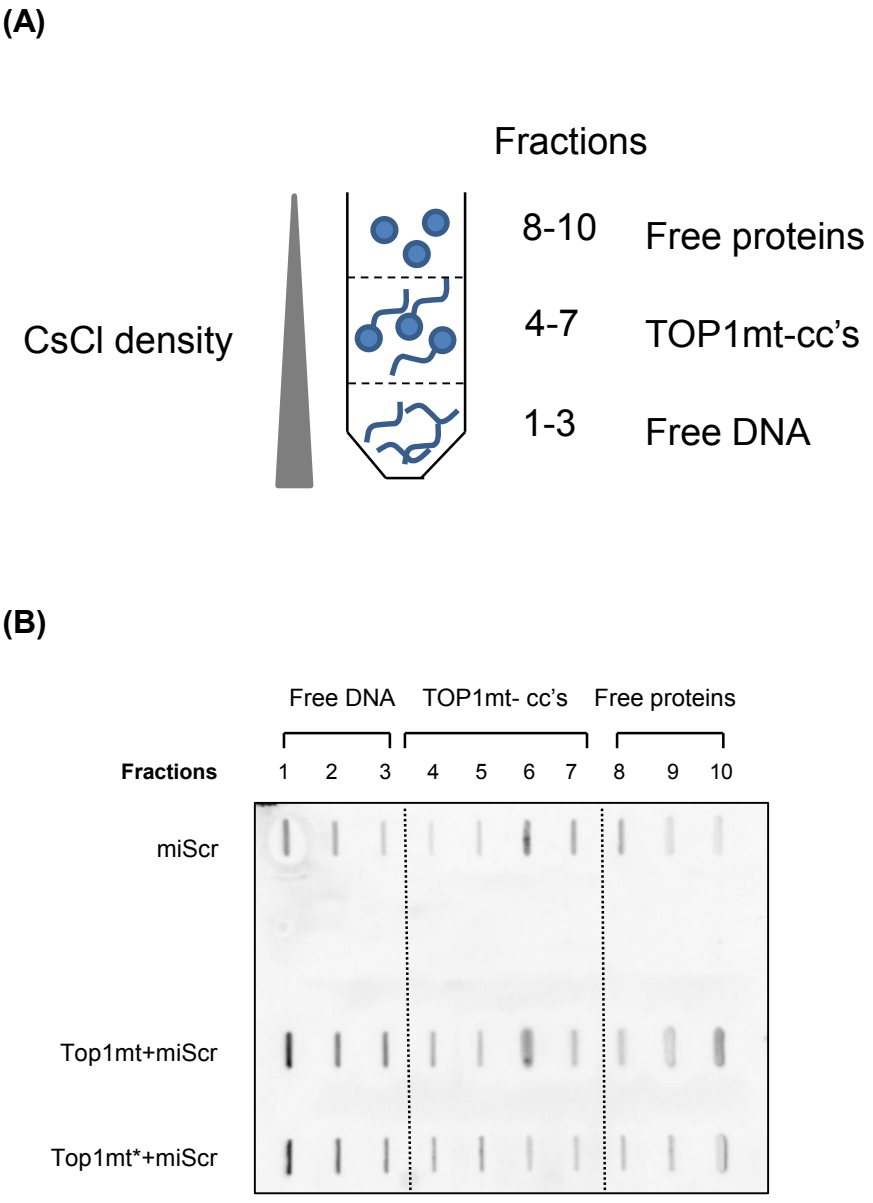

Figure 6.14 Detection of TOP1mt-cc in Flp-In cells by caesium chloride fractionation (A) 2 x 10^6 Flp-In cells were incubated in 1 µg/ml doxycycline for 48 hours, then harvested and lysed. 1 % of the lysate was treated with RNAse A and Proteinase K, then the gDNA concentration was measured by pico-green fluorescence. The remaining lysates were fractionated by caesium chloride ("CsCl") gradient centrifugation for 24 hours. **(B)** 10 equal-volume fractions were collected, starting from the bottom of the tube, and slot-blotted onto nitrocellulose membrane. The volumes loaded were normalised to the gDNA concentration and the equivalent of 7 µg gDNA were loaded in each slot across the cell lines. TOP1mt–cc were detected by immunoblotting with GFP antibodies and visualised by chemiluminescence.

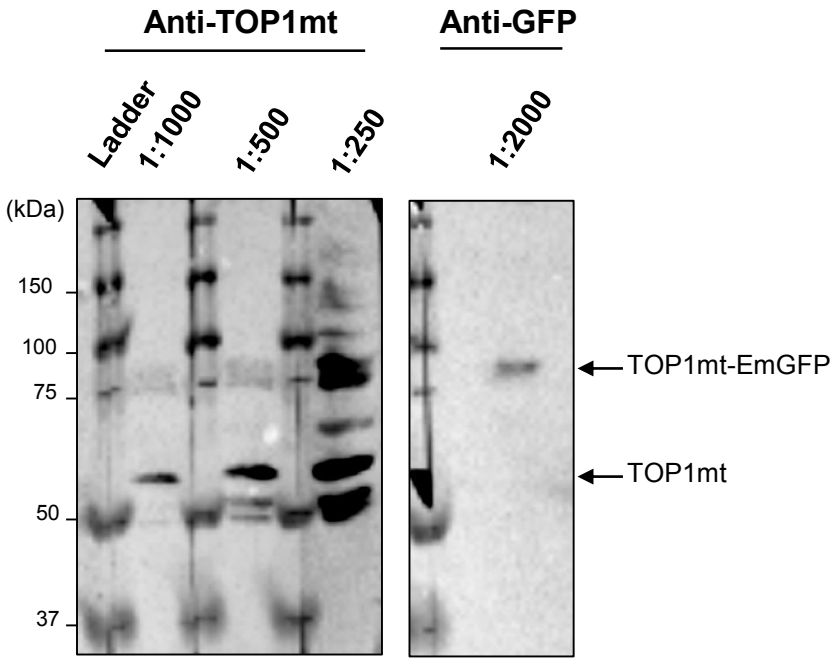

Figure 6.15 Titration of TOP1mt antibodies on WCE of Flp-In T-Rex 293 cells overexpressing TOP1mt-EmGFP. (A) 10^6 cells were incubated in 1 µg/ml doxycycline for 48 hours, then harvested. 75 µg of total proteins from the WCE was fractionated by SDS-PAGE and immunoblotted with antibodies against TOP1mt or GFP at the indicated dilutions and visualised by chemiluminescence.

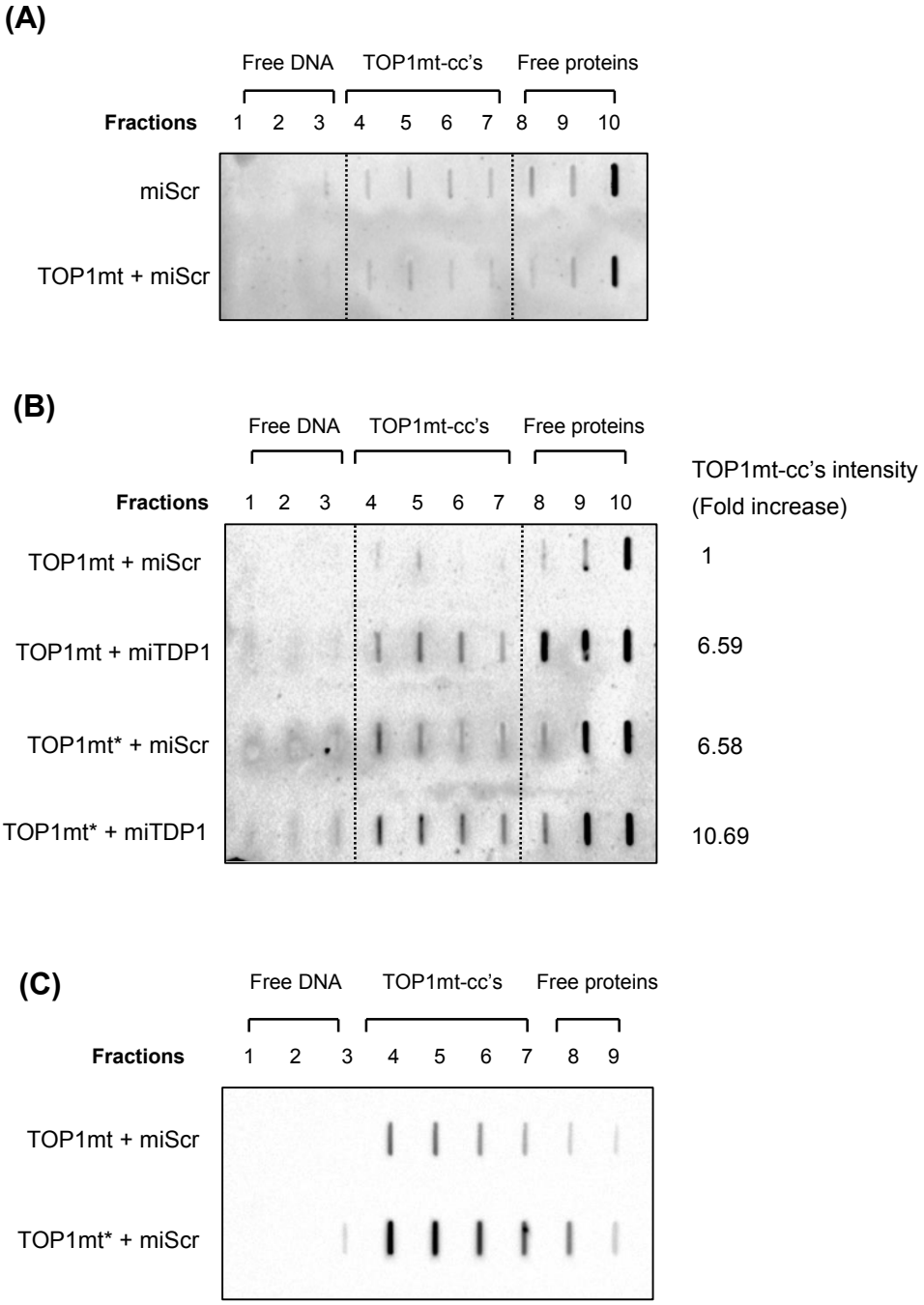

Figure 6.16 TDP1 depletion promotes accumulation of TOP1mt-cc. (A, B) 2 x 10^7 Flp-In cells were incubated in 1 µg/ml doxycyline for 24 hours, then harvested. The mitochondria were extracted then lysed. 1 % of the lysate was treated with RNAse A and Proteinase K, then the gDNA concentration was measured by pico-green fluorescence. The remaining lysates were fractionated by caesium chloride ("CsC")l gradient centrifugation for 24 hours. Ten equal volume fractions were collected, starting from the bottom of the tube, and slot-blotted onto nitrocellulose membrane. The volumes loaded were normalised to the gDNA concentration and the equivalent of 7 µg gDNA were loaded in each slot across the cell lines. TOP1mt–cc were detected by immunoblotting with GFP antibodies and visualised by chemiluminescence. Quantification of total signal intensity of TOP1mt-cc (fractions 4-7) was carried out using Image Studio Lite and normalised to the total intensity from TOP1mt + miScr cells. **(C)** CsCl fractions from B were immunoblotted with antibodies specific to TOP1-DNA complex.

overexpression of wildtype TOP1mt, as detected by antibodies against GFP (**Fig. 6.16B**) as well as TOP1-DNA covalent complexes (**Fig. 6.16C**), confirming the propensity of the toxic mutant to form DNA cleavage complexes.

6.3.5 TDP1 removes TOP1mt-cc in the mitochondria*

Having established the expected functional phenotypes of the Flp-In cell lines overexpressing TOP1mt or TOP1mt*, I then explored the effect of TDP1 depletion in these cell lines. **Figure 6. 16B** shows that depletion of TDP1 increased the level of TOP1mt-cc by 6.6 fold, and a further 1.6 fold in the case of TOP1mt* (i.e. ~ 10.7 fold more than TOP1mt overexpression), suggesting that TDP1 plays a role in removing TOP1mt*-cc's. To further confirm this, I quantified mtDNA covalently linked to TOP1mt* in the presence or absence of TDP1 using qPCR following chromatin immunoprecipitation (ChIP-qPCR) using GFP-Trap® beads. Primers targeting the putative TOP1mt*-EmGFP binding site (position 15873 – 15972) of the mtDNA (**Fig. 6.1, Table 2.8**) (Dalla Rosa *et al*., 2014) were tested for specificity, along with primers for quantifying mtDNA copy number (**Fig. 6.17A, Table 2.8**). The input materials were first analysed for the mtDNA copy numbers, which were comparable amongst the cell lines (**Fig. 6.17B**). I then quantified the amount of TOP1mt*-linked mtDNA by qPCR. The C_T values of the ChIP samples were normalised to that of the corresponding input samples and expressed as percentage input, which was normalised against its relative mtDNA copy numbers. As expected, TOP1mt* overexpressing cells showed > 2-fold more ChIP material specific to the TOP1mt binding site than the negative control cells overexpressing EmGFP alone ("miScr"); and TDP1 depletion further increased the pull-down material by ~ 4 fold (**Fig. 6.17C, $p < 0.05$; Student's t-test**). Thus, TDP1 inhibits accumulation of TOP1mt-cc detectable by qPCR without topotecan treatment.

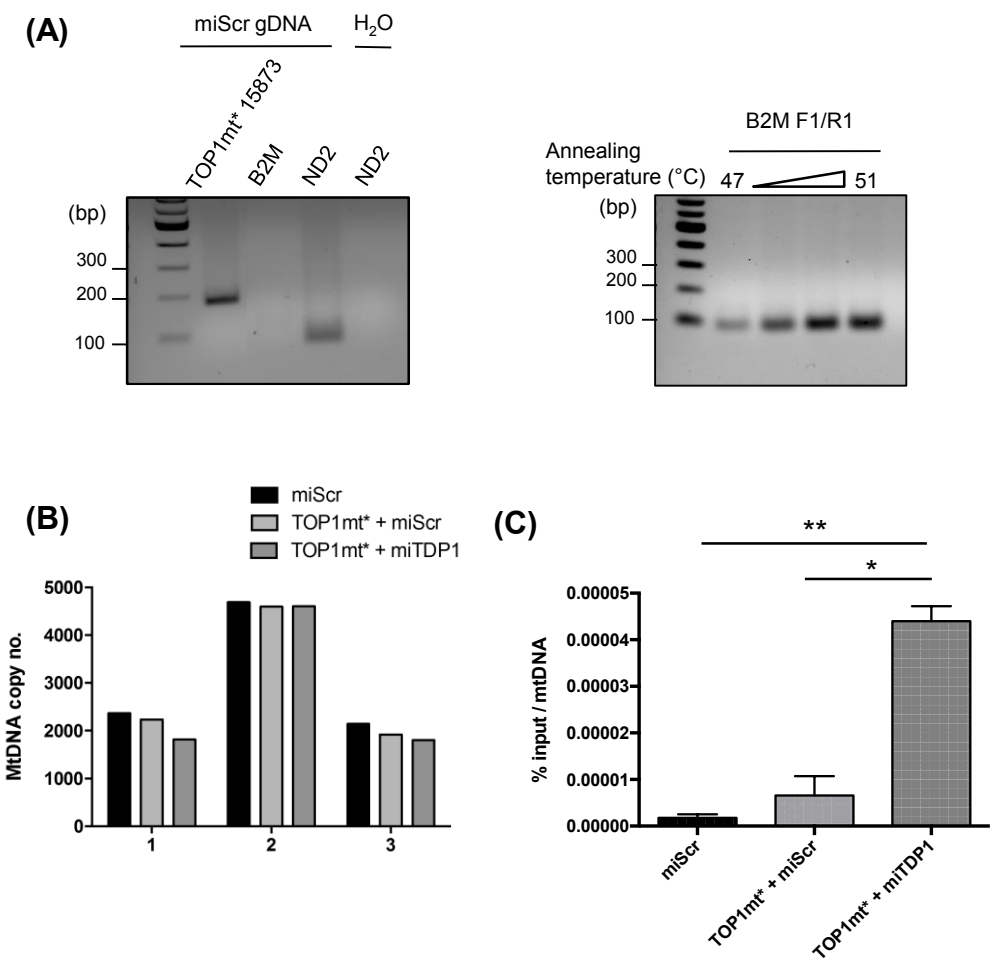

Figure 6.17 TDP1 depletion promotes stalling of TOP1mt* at H-chain replication origin. **(A)** 5 x 10^6 cells were incubated in 1 µg/ml doxycycline for 48 hours, then harvested. The gDNA contents were extracted. *Left panel:* TOP1mt binding site ("15873", denotes region from position 15873 – 15972 of mitochondrial chromosome) was PCR-amplified to test for primer specificity. "B2M" and "ND1" denotes nuclear- and mitochondrial-encoded genomic regions, respectively, used for quantification of mtDNA copy number. *Right panel:* repeat PCR of B2M using a range of annealing temperatures. **(B)** qPCR quantification of mtDNA copy calculated by: 2 x $2^{(\Delta CT)}$ whereby ΔC_T = B2M average C_T – ND1 average C_T. Data from 3 independent experiments are shown. **(C)** 2 x 10^7 cells were incubated in 1 µg/ml doxycyline for 48 hours then harvested. Cells were lysed in ChIP lysis buffer and sonicated to yield chromatin length of average ~ 300 bp. 10 % volume was set aside as input, while the remaining lysates were immunoprecipitated using GFP-conjugated agarose beads. The pull-down material was washed and eluted. The eluent was treated with RNAse A and Proteinase K, then used for qPCR quantification of TOP1mt binding site. The % input was calculated as: 10 x $2^{(\text{adjusted Input CT} - \text{IP CT})}$, whereby adjusted Input C_T = Input C_T –3.32. The % Inputs for each cell line were then normalised against the respective mtDNA copy numbers of the cell line. Data are the mean of 3 independent experiments and error bars represent ±1 S.E.M. *p* values were derived from one-tailed Student's t-test , whereby * = $p < 0.05$ and ** = $p < 0.01$.

6.3.6 TDP1 promotes mitochondrial transcription

Having established the molecular mechanism of TDP1 interaction with TOP1mt, I then investigated whether depletion of TDP1 has an impact on TOP1mt-regulated transcription. Overexpression of TOP1mt led to marked reduction of five of the mitochondrial mRNA transcripts examined by RT-qPCR (**Fig. 6.13C**, ***p < 0*.001**; **Student's t-test**). Depletion of TDP1 led to ~ 50 % reduction of all transcripts tested, which was partially rescued by complementation with human TDP1 (**Fig. 6.18A, *p* < 0.01; Student's t-test**). Interestingly, depletion of TDP1 in cells overexpressing wildtype TOP1mt did not further suppress transcription (**Fig. 6.18B**). In striking contrast to wildtype TOP1mt, overexpression of TOP1mt* led to ~ 2-fold increase in mitochondrial gene transcription, which was largely dependent on TDP1 (**Fig. 6.18C, *p* < 0.05; Student's t-test**). Given the observed role of TDP1 in processing TOP1mt-cc, the increase in transcription could be due to a compensatory upregulation of TDP1 catalytic activity. This is consistent with the ~ 25 % increase in mitochondrial TDP1 activity in cells overexpressing TOP1mt* observed in **Fig. 6.12C&D**. Together, these data suggest a role for TDP1 in promoting mitochondrial gene transcription by resolving TOP1mt-cc. In addition, there appears to be a second distinct mechanism by which TOP1mt suppresses transcription independent of TOP1mt-cc formation or TDP1.

6.3.7 TDP1 promotes proper assembly of the ETC complex

Since transcription of mtDNA-encoded genes is essential for synthesis of major subunits of all the ETC complexes of the OXPHOS system except complex II, I next assessed the abundance of these complexes in purified mitochondria, by probing for the subunits that are particularly labile when the complexes are not correctly assembled (**Fig. 6.19A**). As expected, neither overexpression of TOP1mt or TOP1mt*, nor depletion of TDP1 had a significant effect on the nuclear-encoded complex II subunit, SDHB, at protein (**Fig. 6.19C**) or mRNA levels (**Fig. 6.19G**). Nor was there significant alterations in stability of complexes I, IV or V (**Fig. 6.19B,E,F**). The most

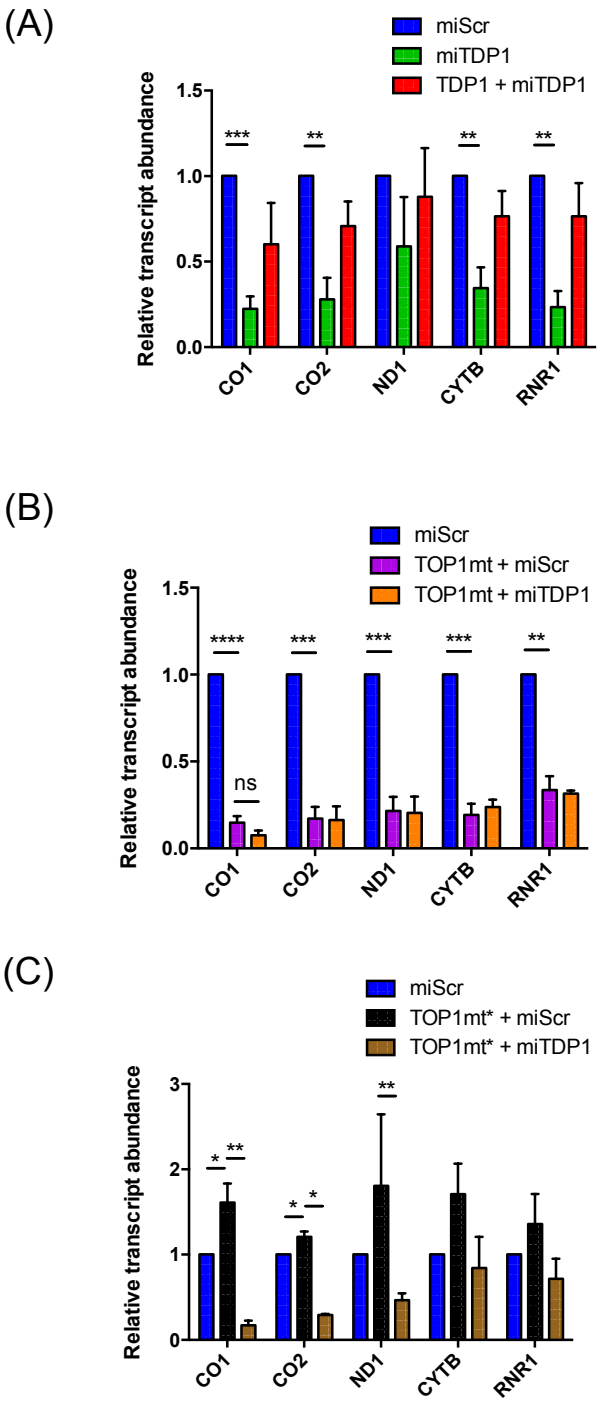

Figure 6.18 TDP1 depletion negatively regulates mitochondrial transcription in a TOP1mt*-dependent manner. 10^6 cells were incubated in 1 µg/ml doxycycline for 48 hours, then harvested. Total RNA was extracted and 5 µg was reverse transcribed. RT-qPCR quantification of transcript abundance of five mitochondrial genes normalised against GAPDH from cells depleted of TDP1 with or without TDP1 complementation **(A),** overexpressing TOP1mt with or without TDP1 depletion **(B),** and overexpressing TOP1mt* with or without TDP1 depletion **(C)**, relative to the abundance of the mitochondrial transcripts in control miScr cells. Data are the mean of 3 independent experiments and error bars represent ±1 S.E.M. *p* values were derived from two-tailed Student's t-test, whereby * denotes $p < 0.05$, ** denotes $p < 0.01$ and *** denotes $p < 0.001$.

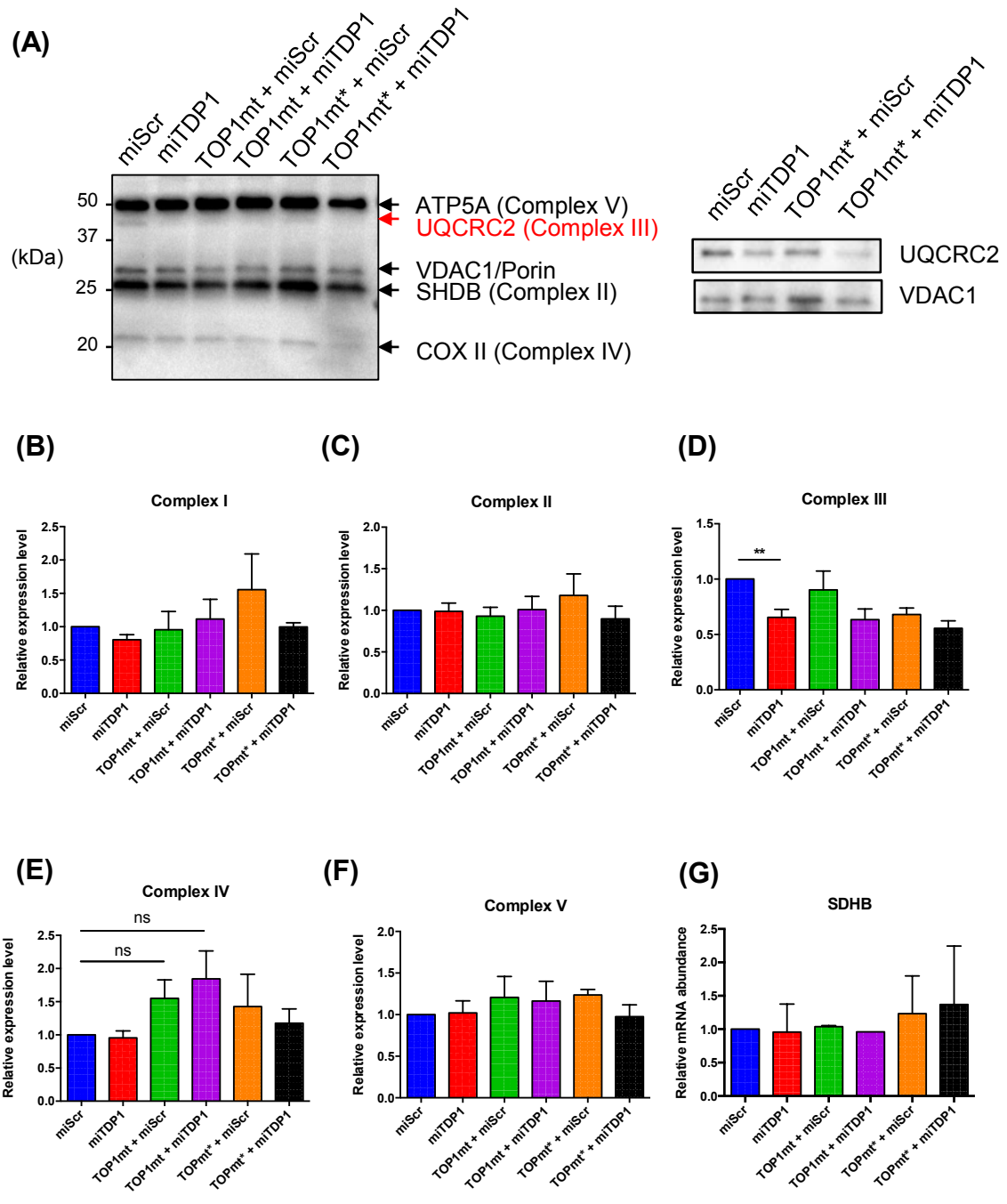

Figure 6.19 TDP1 facilitates assembly of ETC complex III. (A) *Left:* Immunoblotting of mitochondrial lysates from doxycycline-induced Flp-In T-Rex 293 cells using antibody cocktails against human OXPHOS proteins NDUFB8 (complex I), SDHB (complex II), UQCRC2 (complex III), COX-II (complex IV), and ATP5A (complex V). *Right:* Immunoblotting using specific UQCRC2 antibody. **(B-F)** Protein expression levels of the labile subunit from the indicated complexes relative to those of control miScr cells, after normalisation to levels of the mitochondrial loading control, VDAC1. **(G)** RT-qPCR quantification of SDHB transcript abundance using total RNA extracted from cells in (A) and GAPDH as internal control. Expression levels were then normalised to miScr cells. Data are the means of 3 independent experiments and error bars indicate $\pm$1 S.E.M. *p* values were derived from two-tailed Student's t-test. ** = $p < 0.01$ and ns = non-significant.

noticeable difference was detected with complex III. When normalised to the mitochondrial structural protein VDAC1 (porin), the level of UQCRC2 in complex III was reduced by ~ 40 % when TDP1 was depleted (**Fig. 6.19D, *p < 0.01***). Surprisingly, overexpression of TOP1mt in the presence of TDP1 was not associated with complex III instability, despite a marked reduction in mitochondrial transcription (**Fig. 6.18A**). Overexpression of TOP1mt* alone had the same effect as TDP1 depletion, and concomitant TDP1 depletion did not further decrease the protein level (**Fig. 6.19C**). These results suggest that TDP1 plays a role in maintaining the integrity of complex III in TOP1mt-overexpressing cells in the face of lower of mitochondrial encoded ETC subunits. In contrast, TDP1 is unable to compensate for complex III structural instability as a result of excess mitochondrial subunits in TOP1mt*-overexpressing cells.

6.3.8 TDP1 promotes mitochondrial OXPHOS

Next I examined whether dysregulation in mitochondrial transcription and complex III assembly would have an impact on mitochondrial function in terms of OXPHOS and ATP production. Real-time measurement of mitochondrial OCR in response to oligomycin, FCCP, rotenone and antimycin A was performed using the Seahorse bioanalyzer (**Fig. 6.20A**). Under basal condition, mitochondrial respiration rate was ~ 25% lower in TDP1-depleted cells compared to control cells (**Fig. 6.20B, left panel, *p < 0*.01**; **Student's t-test**). Overexpression of TOP1mt reduced basal mitochondrial respiration by ~ 20%, and depletion of TDP1 in these cells further reduced basal respiration by an additional 8%, but this decrease was not statistically significant (**Fig. 6.20B, middle panel**). Overexpression of TOP1mt* reduced basal respiration by ~ 30%, and depletion of TDP1 in these cells had no further effect on basal respiration (**Fig. 6.20B, right panel, *p < 0*.05**; **Student's t-test**). I then examined if the mild basal respiratory defect was due to a switch to non-aerobic respiration by glycolysis, which is accompanied by acidosis. The extracellular acidification rate (ECAR) measured was comparable amongst all the tested cell lines under basal and stressed conditions

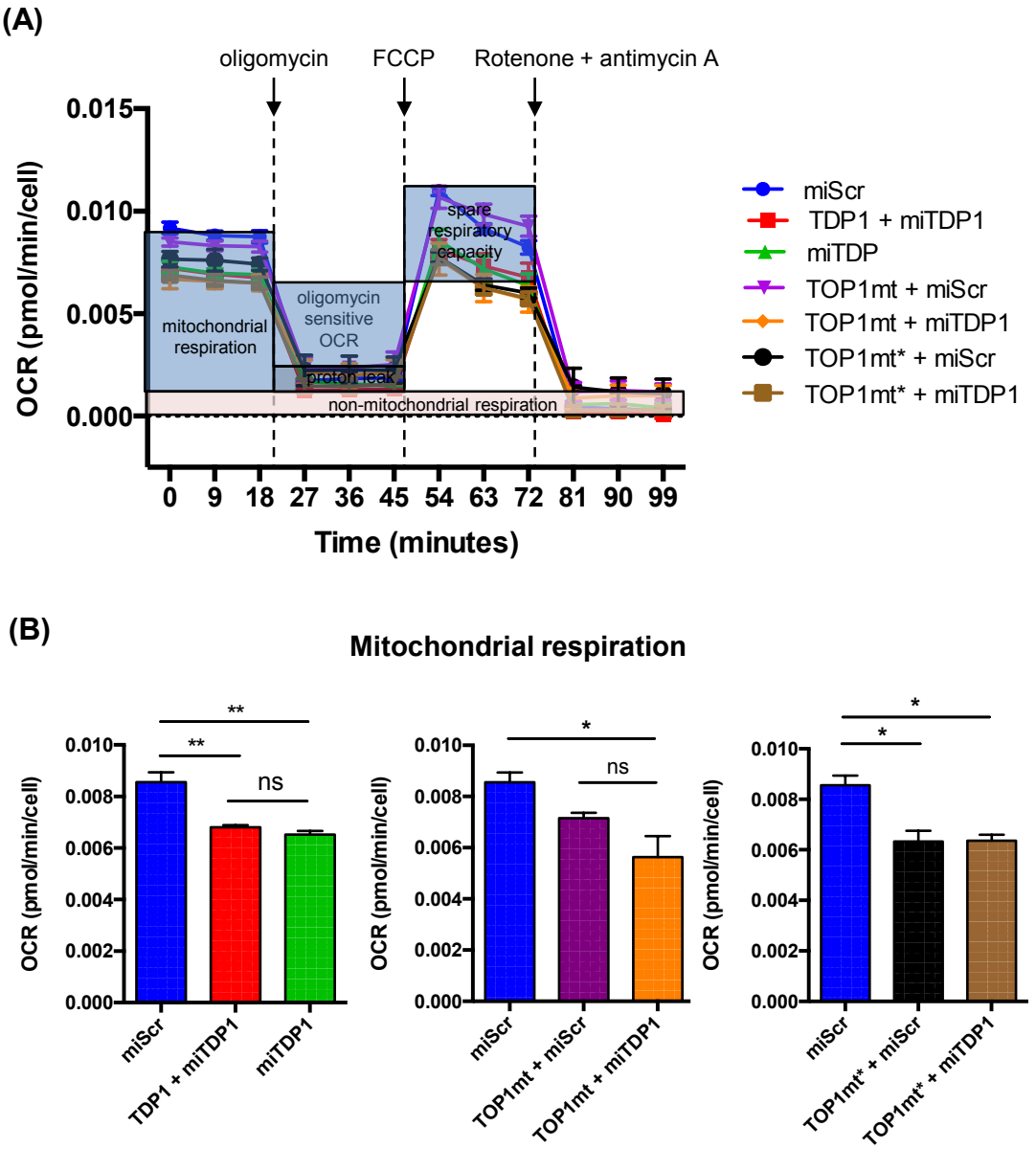

Figure 6.20 TDP1 depletion negatively regulates mitochondrial respiration. (A) 10^6 cells were incubated in 1 µg/ml doxycycline for 48 hours, then harvested. $6.5x10^4$ cells/well were plated in Cell-Tak pre-coated XF24 cell plate in triplicates and three basal readings of oxygen consumption rate ("OCR") were taken. Cells were then subjected to sequential treatments with 1 µM oligomycin, 1 µM FCCP, and 1 µM rotenone and antimycin A during which three repeat OCR readings were taken. **(B)** Mitochondria respiration was calculated by subtracting average rotenone/antimycin A OCR from average basal OCR. Data are the mean of 3 independent experiments and error bars represent ± 1 S.E.M. *p* values were derived from two-tailed Student's t-test. * = $p < 0.05$, ** = $p < 0.01$, and ns = non-significant.

(**Fig. 6.21A&B**). Interestingly, the respiratory (OCR/ECAR) ratio was decreased in TOP1mt+miScr, TOP1mt*+miScr, and TOP1mt*+miTDP1 cells in similar pattern as basal OCR (**Fig. 6.21C**), suggesting that the defect in basal OCR was specific to the OXPHOS pathway. Inhibition of ATP-coupled OXPHOS by oligomycin revealed no significant changes in uncoupled respiration ("proton leak") amongst the cell lines that could account for the lower basal OCR (**Fig. 6.22A**). In contrast, the oligomycin-sensitive OCR (i.e. ATP-coupled respiration) were reduced by ~ 30 % in all cell lines depleted of TDP1 (**Fig. 6.22B, $p < 0.05$**), although in TOP1mt*-overexpressing cells no further reduction was seen by loss of TDP1. Finally, upon induction of maximal respiration by FCCP, mimicking the state of high ATP demand, TDP1-depleted cells showed a ~ 25 % reduction in spare respiratory capacity (SRC) compared to wildtype cells (**Fig. 6.22C, left panel, $p < 0.01$; Student's t-test**). In TOP1mt-overexpressing cells, TDP1 depletion reduced SRC by ~ 50 % (**Fig. 6.22C, middle panel, $p < 0.05$**; **Student's t-test**). Strikingly, TOP1mt*-overexpressing cells had the lowest SRC, at < 10 % compared to wildtype cells (**Fig. 6.22C, right panel, $p < 0.05$**; **Student's t-test**). Depletion of TDP1 partially rescued this defect to ~ 50 % of wildtype level. Taken together, the mitochondrial respiration profiles showed that TDP1 promotes OXPHOS under both basal and high ATP demand conditions. Transient overexpression of wildtype TOP1mt has the mildest OXPHOS degree of dysfunction; while overexpression of TOP1mt* has the worst, with reduction of both basal and maximal respiration in a TDP1 dependent manner. These findings do not entirely correlate with the protein expression data of the ETC complexes, suggesting there are other dynamic factors mediating OXPHOS efficiency.

6.3.9 TDP1 promotes mitochondrial metabolic activity

To find out if the role of TDP1 in resolving TOP1mt-cc and maintaining mitochondrial transcription is important for non-OXPHOS metabolic activity as well, I incubated doxycycline-induced Flp-In cells with CellTiter-Blue (resazurin) reagent, which relies on

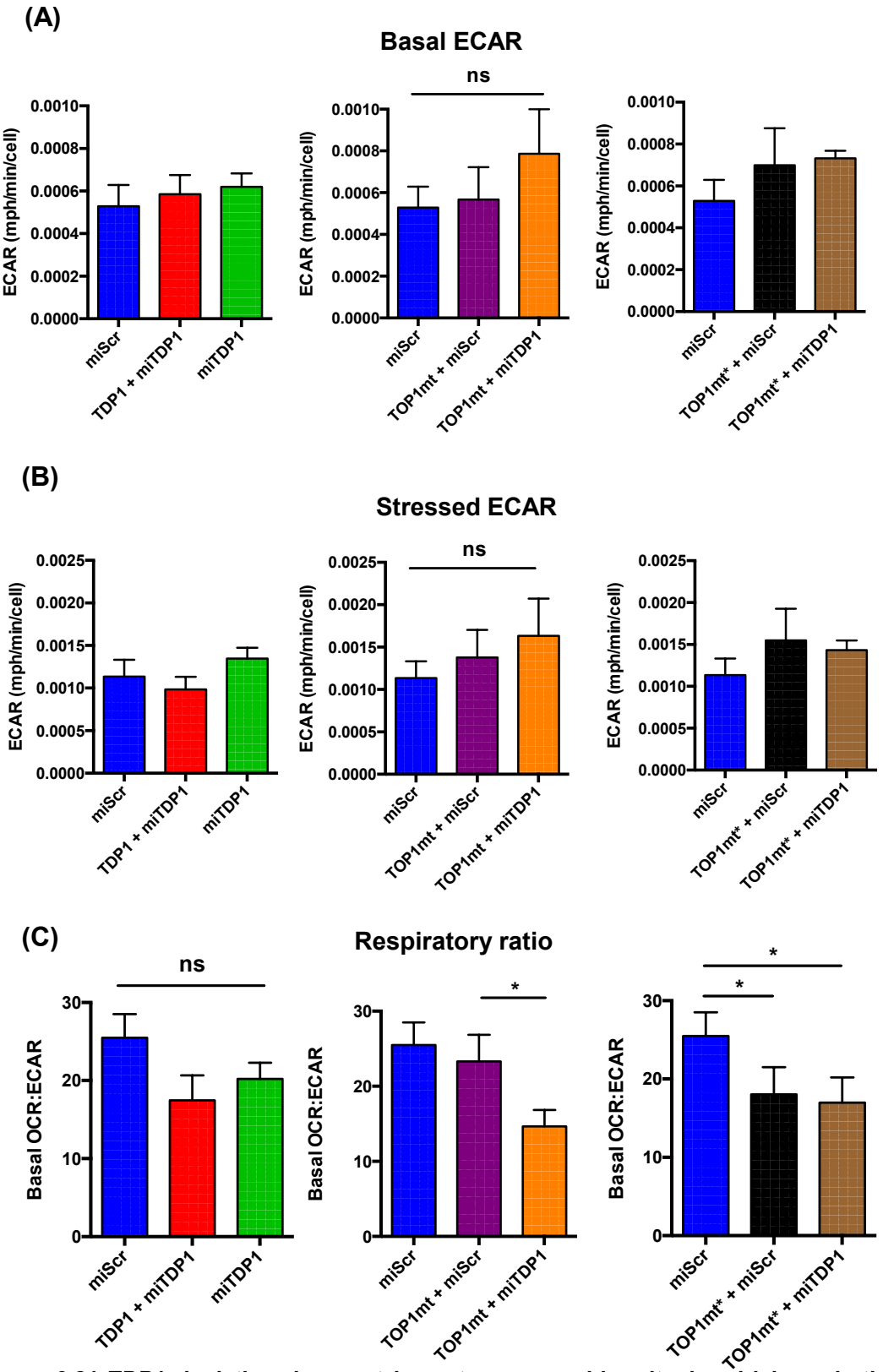

Figure 6.21 TDP1 depletion does not impact on anaerobic mitochondrial respiration. **(A)** Extracellular acidification rate (ECAR) under basal condition in cells from Figure 7.18. **(B)** ECAR after treatments with oligomycin and FCCP. **(C)** Respiratory ratio an indicator of cellular aerobic respiration activity, derived from basal mitochondrial respiration OCR divided by basal ECAR. Data are the mean of 3 independent experiments and error bars represent ±1 S.E.M. *p* values were derived from two-tailed Student's t-test. * = $p < 0.05$, and ns = non-significant.

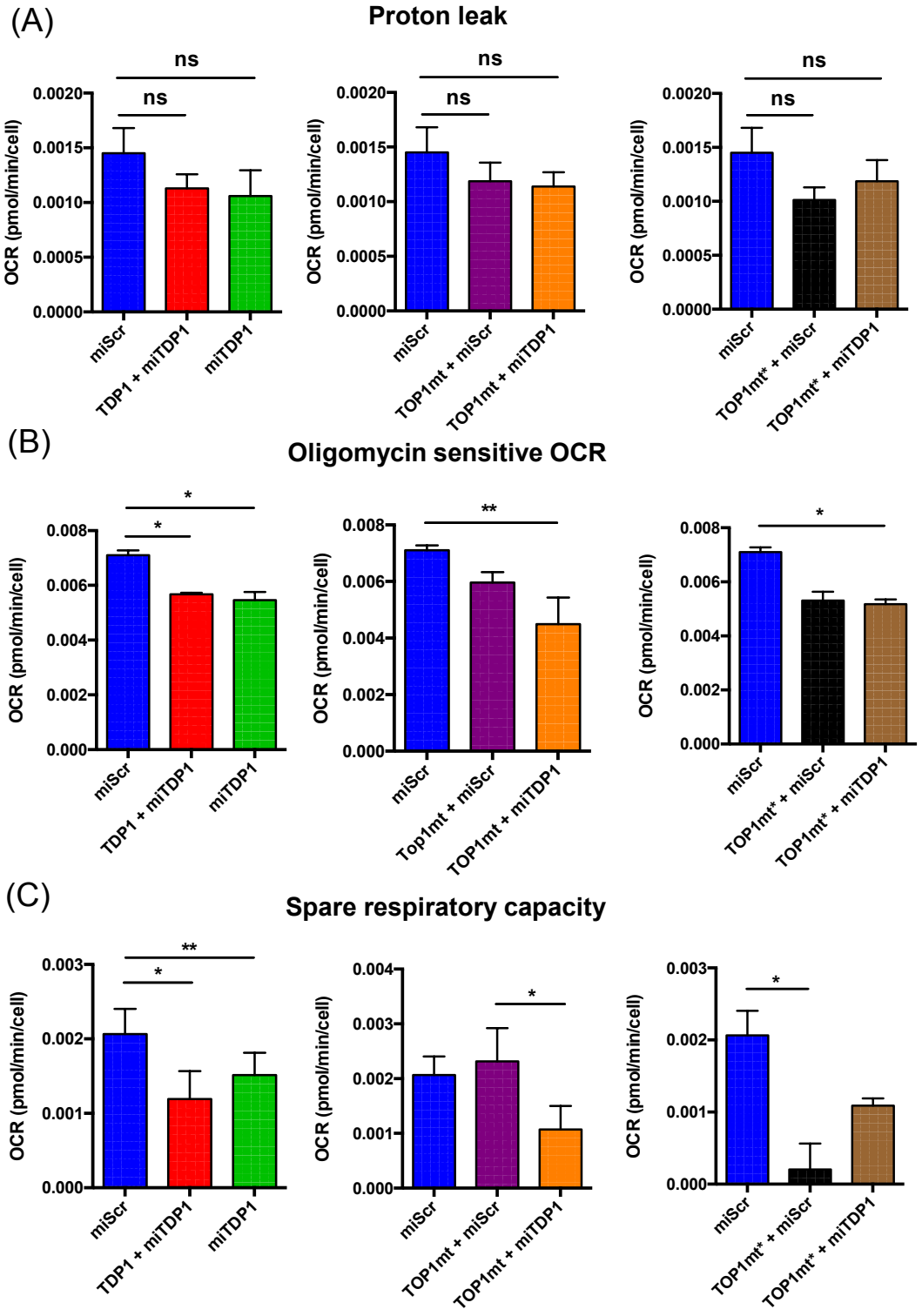

Figure 6.22 TDP1 depletion reduces efficiency of OXPHOS-coupled ATP production. (A) Proton leak calculated by subtracting average oligomycin OCR from average mitochondrial respiration OCR. **(B)** Oligomycin sensitive OCR derived by subtracting average proton leak OCR from average mitochondrial respiration OCR. **(C)** Spare respiratory capacity derived by subtracting average basal OCR from maximum OCR after FCCP. Data are the mean of 3 independent experiments and error bars represent ±1 S.E.M. *p* values were derived from two-tailed Student's t-test. * = $p < 0.05$, ** = $p < 0.01$, and ns = non-significant.

the dehydrogenases in the mitochondria and cytoplasm to be metabolized to a highly fluorescent product, resorufin. The mitochondrial metabolic activity then can be read out as a function of fluorescence intensity normalised to cell numbers. TDP1 depletion reduced the metabolic activity with or without TOP1mt overexpression, while TOP1mt* overexpression alone reduced the metabolic activity, with no further reduction when TDP1 was depleted (**Fig. 6.23, $p < 0.05$**; **Student's t-test**). The results closely reflect the OXPHOS profiles obtained by the Seahorse assay, suggesting TDP1 plays a role in the overall functioning of the mitochondria.

6.3.10 Overexpression of TDP1 in the mitochondria negatively impacts mitochondrial function

Interestingly, TDP1-depleted cells overexpressing RNAi-resistant TDP1 showed a similar pattern of mitochondrial bioenergetics profile (**Fig. 6.19 – 6.22**) and metabolic activity (**Fig. 6.23**) as miTDP1 cells. As TDP1-EmGFP was detectable in the mitochondria by immunoblotting (**Fig. 6.24**) and clearly had an opposing effect on mitochondrial transcription compared to miTDP1 cells (**Fig. 6.18A**), I reasoned the observed defect in mitochondrial respiration could be due to overexpression of exogenous TDP1, possibly explaining the suppression of hTDP1 expression in *Tdp1*$^{-/-}$ MEFs.

6.4 Discussion

In this chapter I have presented data generated from the inducible human Flp-In T-Rex 293 cell lines. First I have demonstrated that the miRNA-mediated TDP1 depletion (**Fig. 6.5**) is specific in terms of its catalytic activity (**Fig. 6.6**) and nuclear DNA repair activity (**Fig. 6.7**, **6.8**). The viability defect after CPT treatment was not statistically significant from the control cells (**Fig. 6.9A**), which was not due to compensatory increase in enzymatic activity of the residual TDP1 expressed (**Fig. 6.6B**), nor inhibition of TDP1 activity in control cells by doxycycline (**Fig. 6.9D**). It was also observed that TDP1 depletion did not cause a viability defect from ROS damage (**Fig. 6.9A**).

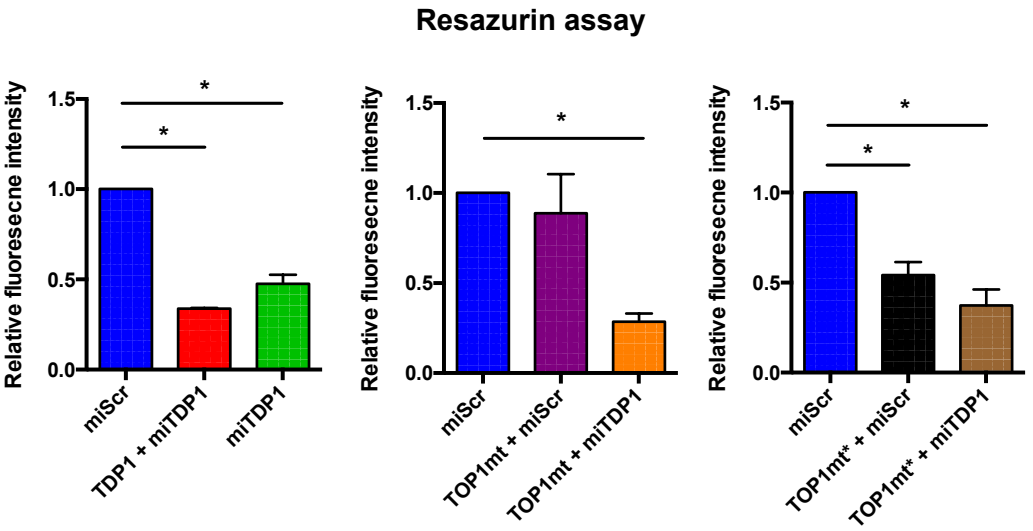

Figure 6.23 TDP1 promotes cellular metabolic activity. 2 x 10^6 Flp-In cells were incubated in 1 µg/ml doxycycline for 48 hours, then re-plated at 10^5 cells/100µl for 72 hours. 20 µl of CellTiter Blue reagent was then added to the cells and incubated at 37°C for 1 hour. The fluorescence intensity emitted by the metabolite resorufein was measured using a fluorescent microplate reader with filters of EX544/EM590-10. Fluorescence intensity was normalised against that of miScr cells. Data are the mean of 3 independent experiments and error bars represent ±1 S.E.M. *p* values were derived from two-tailed Student's t-tests. * = $p < 0.05$.

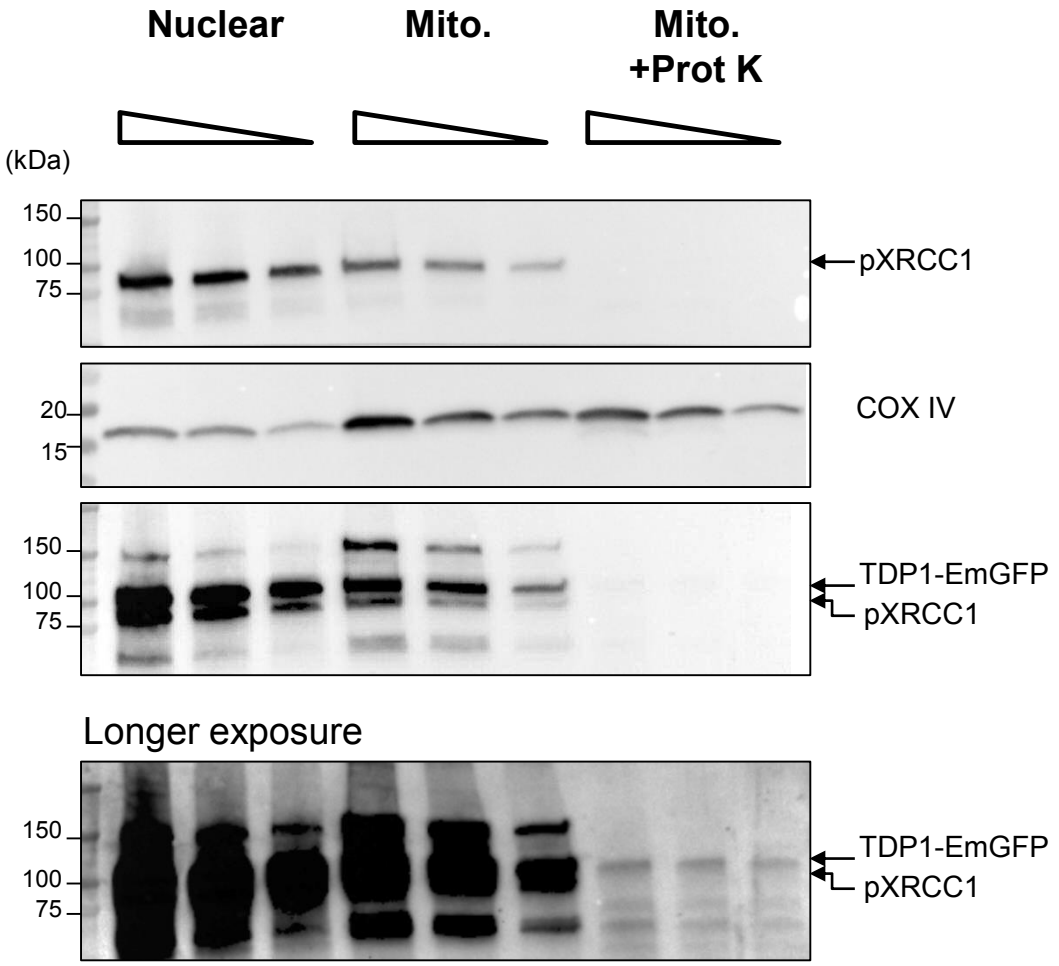

Figure 6.24 TDP1-EmGFP is localised in the mitochondria. 2 x 10^7 Flp-In TDP1 + miTDP1 cells were incubated in 1 µg/ml doxycycline for 48 hours, then harvested. Mitochondria were isolated and quantified using Bradford assay. The mitochondrial pellets were resuspended in homogenisation buffer and treated with or without 20 ng Proteinase K per 5 µg mitochondria on ice for 30 minutes, then washed in homogenisation buffer containing 1 mM phenylmethanesulfonyl fluoride (PMSF) to stop the digestion. The mitochondrial and nuclear fractions were lysed in Laemmli buffer and serially diluted. The nuclear and mitochondrial proteins were then fractionated by SDS-PAGE. The purity of the nuclear ("Nucl.") and mitochondrial ("Mito.") fractions were assessed using antibodies against the nuclear protein phospho-XRCC1(S475, T488), and mitochondrial protein COX IV, respectively, and detected using chemiluminescence. TDP1-EmGFP is detectable inside the mitochondria ("Mito. + Prot K") after long exposure.

As cell viability does not necessarily reflect the amount of DNA damage sustained and the repair capacity of the cells, I quantified these using the alkaline comet and 53BP1 immunofluorescence assays, and confirmed a transient defect in TDP1 depleted cells (**Fig. 6.7**, **6.8**). Alkaline comet assay using H_2O_2 showed similar pattern of early accumulation of chromosomal DNA breaks in TDP1-deficient cells expressing $SOD1^{G93A}$ as observed in MEFs (**Fig. 6.11**), although the expression level of $SOD1^{G93A}$ tolerated in TDP1-deficient Flp-In cells was much lower than in *Tdp1*$^{-/-}$ MEFs. This could point to a higher dependence on TDP1 to reduce $SOD1^{G93A}$-induced toxicity in these cells.

To investigate the functional interaction between TDP1 and TOP1mt, I next induced TOP1mt overexpression in TDP1-proficient and -deficient cells. Interestingly, when TDP1 was depleted, enrichment of a higher molecular weight species (~ 15 kDa) was observed (**Fig. 6.12A**), particularly in the mitochondria (**Fig. 6.12B**). TOP1mt has two isoforms: isoform 1 has a 50 amino acids mitochondrial localisation sequence at the start of the N-terminus, which is cleaved off upon binding the mitochondrial outer membrane, giving rise to isoform 2 (Zhang *et al*., 2001). As the cDNA sequence of isoform 2 was introduced into the host genome, the higher molecular weight species that was also present inside the mitochondria could not be due to isoform 1, but more likely a covalent modification of TOP1mt. Furthermore, the same pattern of enrichment of the higher molecular weight species was also observed when TOP1mt* was overexpressed in TDP1-depleted cells, although at a lower abundance (**Fig. 6.12A**). This could suggest a TDP1-mediated regulation of TOP1mt by post-translational modifications such as de-ubiquitination and de-SUMOylation. The nature of the higher molecular weight species compared to the lower band TOP1mt can be confirmed by mass spectrometric analysis.

The proximity of the mtDNA to the ETC complexes predisposes it to higher levels of oxidative damage (Yakes and Van Houten, 1997) that can stall TOP1mt and disrupt

transcription and replication (Medikayala *et al*., 2011). I confirmed that overexpression of the toxic TOP1mt* mutant indeed generates more TOP1mt-cc detectable by immunoblotting and qPCR (**Fig. 6.16, 6.17**). I also demonstrated that these lesions are dependent on TDP1 for repair. Interestingly, transient (up to 48-hour) overexpression of TOP1mt in TDP1-proficient cells in the absence of topoisomerase poisons does not lead to accumulation of TOP1mt-cc, suggesting there is a fundamental difference in steady-state levels of TOP1mt-cc between cells expressing the two versions of TOP1mt.

As TOP1mt-cc at the NCR region has been implicated in mtDNA replication (Dalla Rosa *et al*., 2014), and *Tdp1*$^{-/-}$ MEFs have reduced mtDNA copy number (**Fig. 5.7**), it would be interesting to examine its role in mitochondrial transcription as well. The measurement of transcript abundance by RT-qPCR usually indicates transcript turnover, which is a product of both transcription rate and transcript stability. In the context of mitochondrial genes, which are translated *in organello*, defective mRNA transportation that can lead to transcript accumulation can be ruled out. In terms of transcription elongation, *Top1mt*$^{-/-}$ MEFs do not appear to accumulate mitochondria transcripts of aberrant lengths (Sobek *et al*., 2013), arguing against an essential role of TOP1mt in transcription elongation. Furthermore, the high concentration of TOP1mt in the NCR containing the two promoter sites strongly suggests its involvement in transcription initiation (Zhang and Pommier, 2008), which is the main rate-limiting factor in determining transcript abundance. Lastly, I analysed multiple sites along the polycistronic heavy chain transcript, from the 5' end *RNR1* gene to the 3' end *CYTB* gene, to allow detection of primary transcripts of different lengths. Taking together these considerations, it is highly likely that in this context, transcript abundance measured by RT-qPCR predominantly reflects the transcription rate.

TOP1mt overexpression in TDP1-proficient cells led to marked reduction of mitochondrial mRNA transcripts, which is consistent with earlier reports (Sobek *et al*.,

2013; Kolesar *et al*., 2013). In contrast, overexpression of TOP1mt* resulted in higher transcript levels. Therefore, it appears that the steady state level of TOP1mt-cc positively correlates with mitochondrial transcription rate. One possible explanation may be through DNA damage mediated retrograde signalling, which can upregulate mitochondrial transcription and biogenesis (Douarre *et al*., 2012; Scarpulla, 2006; Gong *et al*., 1998; Lee *et al*., 2000; Kluza *et al*., 2004; Fu *et al*., 2008). Interestingly, TDP1 activity is also moderately upregulated in our cellular model, tentatively suggesting its involvement in the retrograde signalling response. These data also provide an explanation for the lack of change in mitochondrial mass following TOP1mt* expression in murine cells despite rapid mtDNA depletion (Dalla Rosa *et al*., 2014), further confirming the importance of the mitochondrial TDP1 pathway in repairing TOP1mt-cc and maintaining mitochondrial transcription.

Although translation of mitochondrial-encoded genes occurs *in organello*, assembly of the ETC requires importation of nuclear-encoded subunits. Given that nuclear transcription of ETC subunits is unaffected (**Fig. 6.19C**), changes in levels of the mitochondrial subunits can potentially disrupt the nuclear:mitochondrial stoichiometry resulting in dysfunctional ETC. Intriguingly, although the levels of multiple mitochondrial transcripts are affected by the TOP1mt-TDP1 pathway, only complex III showed particular sensitivity to mis-assembly (**Fig. 6.19D**). Complex III, also known as cytochrome bc_1 complex, is encoded by *CYTB* in the mitochondria, and the remaining 10 subunits are all encoded in the nuclear genome. The cytochrome B subunit is the main transmembrane subunit that anchors the complex, which could explain the disruption of complex III in TDP1 depleted cells with or without TOP1mt* overexpression. However, overexpression of TOP1mt in TDP1-proficient cells does not destabilise complex III, at least within the 48-hour time-frame of the observation. One possible explanation may be that mitochondrial transcription is constitutively suppressed by TOP1mt, and only activated in response to oxidative stress, when

increase in ETC capacity is required. Therefore, even very low level of transcription may be well-tolerated as other compensatory mechanisms such as mitochondrial fusion can facilitate pooling of essential proteins across a large number of mitochondria (Detmer and Chan, 2007; Westermann, 2008). Alternatively, TDP1 may play a yet undefined compensatory role in maintaining ETC assembly. In any case, since complex III plays a crucial role in handling electron transfer, dysfunction of complex III is expected to increase ROS production. The effect of complex III mis-assembly on efficiency of the OXPHOS-ATP system was then examined.

Transient inhibition of transcription by overexpression of TOP1mt-EmGFP minimal effect on mitochondrial respiration by OXPHOS. This is in contrast to the ~ 63 % reduction in oxygen consumption reported in human HT1080 cells constitutively overexpressing YFP-TOP1mt (Dalla Rosa, 2009), which also showed reduction in nuclear-encoded subunits of the ETC complexes. This suggests that transient inhibition of TOP1mt-mediated transcription without accumulation of TOP1mt-cc is not sufficient to alter the efficiency of the ETC system. However, depletion of TDP1 seems to accelerate this process, most likely through accumulation of unresolved TOP1mt-cc. The observation that TDP1 depletion has no further impact on basal mitochondrial respiration in cells overexpressing TOP1mt*, which already show a ~ 25 % reduction compared to control cells, suggests that the effects of TDP1 depletion and TOP1mt* overexpression are epistatic. However, the reduction in SRC in TOP1mt*-overexpressing cells was striking, particularly when it is partially reversed by depletion of TDP1. This could suggest that excessive expression rather than suppression of mitochondrial-encoded proteins without corresponding change in importation of the nuclear-encoded counterparts is more detrimental to cellular bioenergetics, perhaps due to a vicious cycle that consumes ATPs.

Surprisingly, overexpression of targeting-resistant TDP1 in TDP1 depleted cells showed the same mitochondrial respiratory (**Fig. 6.19 – 6.21**) and viability defects

(**Fig. 6.9D**) following the oxidative damage by TBH as TDP1 depleted cells, even though TDP1-EmGFP was detectable in the mitochondria (**Fig. 6.24**) and mitochondrial transcription was not downregulated (**Fig. 6.18B**). Another indicator that overexpression of TDP1 may be detrimental to mitochondrial respiratory function is that in *Tdp1*$^{-/-}$ DT40 cells, the clone that expressed high level of hTDP1 had a higher level of endogenous DNA radicals than the low TDP1-expressing clone (**Fig. 5.4**). If this were true, it could imply that TDP1 expression and importation into the mitochondria could be regulated by mitochondrial OXPHOS homeostasis, similar to TOP1mt (Fam *et al*., 2013a).

Lastly, it is worth noting that although transient overexpression of TOP1mt* did not alter the mtDNA copy number even with depletion of TDP1 (**Fig. 6.17B**), stable overexpression of TOP1mt* in MEFs has been reported to lead to ~ 50 % loss of mtDNA without change in total mitochondrial mass (Dalla Rosa *et al*., 2014). This suggests that, in contrast to mitochondrial transcription, replication stalling and genomic instability were not induced by an acute increase in TOP1mt*-cc. If true, this may have implications for clinical use of TOP1 poisons such as topotecan and TOP1mt poison derivatives (still to be developed) and how these drugs are administered can affect its adverse effects on mitochondrial function over long-term.

CHAPTER 7

General Discussion

7.1 Overview

TDP1 is an important player in the repair of TOP-mediated DNA breaks, is implicated in maintaining cerebellar genome stability, and is a potential therapeutic target in refractory cancers. At the onset of this doctoral project, development of effective novel TDP1 inhibitors had reached a bottleneck; and it became apparent that a detailed understanding of the cellular response to TDP1 inhibition, in terms of compensatory upregulation of TDP1 expression or activity, DNA damage response, and impact on cellular proliferation, was needed.

The main aim of this thesis is to provide insight into the molecular mechanisms of TDP1 functions at the cellular level, which would contribute to a long-term project of investigating TDP1 function (and dysfunction) at a whole organism level, with potential for therapeutic applications.

7.2 Regulation of TDP1 activity by the N-terminus domain impacts cellular resistance to TOP1 poison

TDP1 is conserved across eukaryotes, and the addition of the N-terminus domain (NTD) in higher organisms prompted me to investigate the regulatory role of the NTD in human.

In chapter 3, I described the identification and characterisation of a novel post-translational modification in the NTD, phosphorylation at S81 by the ATM and/or DNA-PK, that promotes TDP1 protein stability, physical interaction with Lig3α, and DNA repair efficiency. This was the first reported post-translational modification of the NTD of human TDP1, and supports the view that regulation of TDP1 expression level plays a significant role in the cellular response to the TOP1 poisons. In chapter 4, I have presented further evidence that the N-terminus domain regulates TDP1 activity through another post-translational modification, SUMOylation at K111. Modification by

SUMO1 at K111 promotes recruitment of TDP1 to sites of DNA damage at transcriptionally active regions of the genome. Neither post-translational modifications affect the catalytic activity *in vitro*, but nevertheless promote repair of TOP1-cc at the cellular level.

7.3 Implications for novel drug combination strategies

These results suggest that, firstly, from a drug discovery point of view, focussing solely on the catalytic activity may not be a reliable indicator for cytotoxicity of TDP1 inhibitors, as the DNA repair capacity can be regulated by the N-terminus domain. Secondly, combination therapy using a TOP1 poison and an existing inhibitor of TDP1 regulatory pathway could be a less time-consuming approach than developing novel TDP1 inhibitors. For example, inhibition of PARP1, a physical interacting partner of TDP1, by veliparib (ABT-888), has recently been shown to reduce TDP1 protein stability and recruitment to DNA damage sites (Das *et al*., 2014; Murai *et al*., 2014). ABT-888 has been used with topotecan in advanced solid tumours and lymphomas in phases I and II clinical trials (Kummar *et al*., 2011; Kunos *et al*., 2015). However, the additive effect of combination therapy was minimal, and haematological toxicity was the main dose-limiting factor. This is likely due to the many TOP1- and TDP1-independent effects of PARP inhibition, such as dysregulation of DNA transcription and replication, DNA repair and apotosis (Weaver and Yang, 2013).

In contrast to PARP1, inhibition of TDP1 by RNA interference and genetic inactivation in mice resulted in few cytotoxic effects in the absence of exogenous DNA damage (Hirano *et al*., 2007; Katyal *et al*., 2007; Guo *et al*., 2014). As an alternative approach that is more TDP1-specific, our lab has been investigating degradation of TDP1 by the ubiquitin-proteasome pathway. As deubiquitinating enzymes (DUBs) regulate protein stability, signalling pathways, cell proliferation and apoptotic response, and are heavily depended on by tumour cells, DUB inhibitors are attractive candidates for anti-cancer

treatments (D'Arcy *et al*., 2015). Identifying and inhibiting specific DUBs that promote TDP1 stability or repair of TOP1-cc by, for example, HR (Orthwein *et al*., 2015), can be potential new avenues to improve efficacy of TOP1 poisons.

The finding that SUMOylated TDP1 promotes repair of transcription-associated SSBs may have implications in cancer therapy as well. Firstly, increasing evidence indicates that the SUMOylation pathway is upregulated in several tumour types (Mo and Moschos, 2005; Mo *et al*., 2005; Moschos *et al*., 2007; Moschos *et al*., 2010; Deng *et al*., 2011). The obligate E2 conjugating enzyme UBC9/UBE2I has been proposed as a cancer therapeutic target, for instance it has been demonstrated that depletion of UBC9 sensitised melanoma-infiltrated lymph nodes to the cytotoxic effect of cisplatin and paclitaxel (Moschos *et al*., 2007). UBC9 polymorphisms that promote TOP1 SUMOylation have also been shown to sensitise NSCLC to irinotecan (Han *et al*., 2010).

7.4 Targeting repair of transcription-mediated DNA damage in quiescent cancer stem cells

Since TOP1 SUMOylation in its catalytic domain at actively transcribed regions promotes recruitment of RNA processing factors and reduces R-loop formation and genome instability (Li *et al*., 2015), targeting UBC9 in tumour cells can potentially be achieved by understanding the molecular mechanisms underlying the specific interactions with TOP1, TDP1 or BRCA1 (Xu *et al*., 2009), and screening for small-molecule inhibitors that disrupt the interaction sites. As TDP1 repairs transcription-dependent protein-linked breaks (PDBs) in non-cycling cells, it could be a potential target in quiescent cancer stem cells (qCSCs), which are often resistant to conventional chemotherapy (Lyle and Moore, 2011). Several current strategies targeting qCSCs involve inhibition of the quiescence process (Essers and Trumpp, 2010), but this process likely also occurs in normal adult stem cells (Li and Bhatia, 2011; Schuettpelz and Link, 2013), therefore this approach runs the risk of depleting

the normal stem cell population (Baldo *et al*., 2010; Sheikh *et al*., 2011; Skoetz *et al*., 2015). Inhibition of TDP1 SUMOylation may therefore be useful in targeting qCSCs, although normal postmitotic tissues such as mature neurons (Hudson *et al*., 2012) and cardiomyocytes may be affected as well. Thus this approach may be most useful as an adjuvant therapy in the paediatric population, who generally have higher tissue regenerative potential.

7.5 Novel anti-oxidant mechanism in vertebrates involving TOP1mt/TDP1 functional interaction

In chapters 5 and 6, I investigated the role of TDP1 in the mitochondria. As organelles implicated in many disease processes including neurodegeneration and tumourigenesis, the observation by several groups that TDP1 is present and active in the mitochondria (Das *et al*., 2010; Fam *et al*., 2013a) warranted further investigation. My findings confirm that TDP1 repairs ROS-induced DNA breaks in the nucleus. I also demonstrated that TDP1 has a direct role on the production of ROS from the mitochondria, namely, by promoting transcription of mitochondria-encoded genes mediated by TOP1mt activity, and thereby maintaining homeostasis of mitochondrial oxidative phosphorylation. This, to the best of my knowledge, is the first report that characterises the functional interaction between human TDP1 and TOP1mt.

7.6 Implications for targeting TOP1mt and mitochondrial TDP1 in cancer cells

TOP1mt has been identified as a modulating factor in several neoplastic diseases, and its expression is upregulated by the proto-oncogene Myc (Goto *et al*., 2006; Zoppoli *et al*., 2011). TOP1mt upregulation and mitochondrial dysfunction have also be observed in an ovarian cancer cell line with acquired resistance to doxorubicin (Chen *et al*., 2014). TOP1mt has therefore been proposed as a novel therapeutic target in doxorubicin-refractory ovarian tumours. However, genetic inactivation of Top1mt in

mice treated with doxorubicin has been shown to exacerbate the cardiotoxicity of doxorubicin and increase the mortality rate (Khiati *et al*., 2014), thus limiting the usefulness of this approach.

On the other hand, lamellarin D, an alkaloid from marine invertebrate with TOP1 poison-like effect (Facompré *et al*., 2003), has been shown to induce TOP1mt-cc (Khiati *et al*., 2014) that promote ROS production and cancer cell death (Ballot *et al*., 2014). Inhibition of TDP1 activity and/or its translocation to the mitochondria would promote accumulation of TOP1mt-cc, and would therefore be a logical combination with TOP1mt poisons like lamellarin D. This approach would likely be particularly deleterious to qCSCs that rely heavily on mitochondrial OXPHOS and have relatively low glycolytic capacity (Lagadinou *et al*., 2013). It is conceivable that the Flp-In TOP1mt/TDP1 cell line or an *in vivo* model such as transgenic zebrafish embryos could be utilised as positive controls in cell-based assays for development of TOP1mt inhibitors.

7.7 Regulation of mitochondrial transcription in non-replicating cells

The finding that TDP1 plays a direct role in maintaining mitochondrial function may also have implications in the fields of aging and neurodegeneration research. In differentiated postmitotic cells, regulation of mitochondrial transcription and translation are likely to be more crucial than mitochondrial DNA replication, as they allow more rapid adaptive response to mitochondrial stress. The TOP1mt-overexpressing Flp-In cell line may serve as a cellular model to investigate the effects of dysregulation of mitochondrial transcription independent of replication (Dalla Rosa, 2009). The Flp-In cells exhibit a high mitochondrial respiration rate both under basal and stressed conditions, which is reminiscent of highly aerobic cell types such as neurons. The tetracycline-inducible system also allows the distinction between short-term

mitochondria-regulated response and longer term retrograde nuclear response (Jazwinski, 2013).

7.8 Future directions

Several questions that arose from this project remain to be addressed:

1. *How does TDP1 SUMOylation promote its accumulation at sites of transcription-mediated DNA damage? Could it be through interaction with SUMOylated TOP1, components of the transcription machinery, or other proteins?* Mass spectroscopic analysis of TDP1 and TDP1^{K111R} interacting proteins in the presence of DNA replication inhibitor aphidicolin could address this question.
2. *How does TDP1 translocate to the mitochondria? Does it rely on a PTM or protein-protein interaction? Is it triggered by endogenous ROS?* TDP1 does not appear to have a known mitochondrial targeting sequence in the NTD or mitochondrial isoform like many mitochondria-targeted DNA repair proteins. Although several groups have shown that TDP1 is present and active in the mitochondria without exogenously induced oxidative stress, its expression and translocation is stimulated by H_2O_2 and menadione in human fibroblasts (Fam *et al.*, 2013). This further supports my findings that TDP1 functions as part of the anti-oxidant response by upregulating OXPHOS efficiency. SOD1^{G93A}-overexpressing MEFs and Flp-In cells can be utilised to study translocation of TDP1 in response to endogenous ROS. Furthermore, since PTMs can regulate mitochondrial translocation of cytoplasmic proteins (Deng *et al*., 2011; Zhang *et al*., 2012; McBride *et al*., 2014), the TDP1^{S81A} and TDP1^{K111R} mutants can be similarly utilised.
3. *Does TDP1 interact with Lig3α in the mitochondria? If so, what role does Lig3 play in the function of TDP1 in the mitochondria?* Our collaborator has previously shown that in Flp-In cells, Flag-TDP1^{S81E} does not physically interact with endogenous Lig3α in the mitochondria (Meagher and Lightowlers, 2014), however the

interaction could be transient or abolished by the phosphomimetic mutation. Functional interaction could be assessed by depletion of Lig3α with or without co-depletion of TDP1 using the Flp-In cells.

4. *Does the TDP1^{H493R} catalytic mutation generate mtPDB's that can contribute to loss of postmitotic neurons in SCAN1 patients?* Flp-In cells complemented with TDP1^{H493R} would be useful for initial assessment of the levels of mtTDP1-cc's and mitochondrial bioenergetics profiles using protocols established in this thesis. Further work can be carried out in neurons reprogrammed from SCAN1 lymphoblastoid cells or TDP1^{H493R} knock-in neuronal cell lines using CRISPR technology.
5. *Does TOP1mt and/or TDP1 regulate mitochondrial transcription via R-loop formation?* R-loop formation, especially at the O_H, is intrinsically linked to regulation of mitochondrial transcription and replication (Brown *et al*., 2008; El Hage *et al*., 2014). Nuclear TOP1 and TDP1 have both been demonstrated to reduce R-loop formation (El Hage *et al*., 2010; Yeo *et al*., 2014). Given the opposing effects of TOP1mt and TOP1mt* on transcription in contrast to nuclear TOP1, it would be interesting to assess the level of mitochondrial R-loops in the Flp-In cell lines overexpressing TOP1mt or TOP1mt* in the presence and absence of TDP1. An increase in R-loops in TOP1mt-overexpressing cells in the absence of TDP1 would support the hypothesis that TOP1mt inhibits transcription through excessive relaxation of the transcription initiation region. It would also be interesting to identify TOP1mt*-binding protein partners at the O_H in the presence or absence of TDP1 using mass spectrometry.

7.9 Conclusions

To conclude, the main findings from this thesis comprise firstly of the identification and characterisation of novel factors involved in the regulation of TDP1 function, which can contribute to the rational design of combination therapies for neoplastic diseases; and

secondly of the characterisation of the protective role of TDP1 against oxidative stress, which can be utilised again in design of combination therapies for cancers, as well as design of novel cellular models to study the process of mitochondrial transcription in postmitotic cells.

REFERENCES

ABDURASHIDOVA, G., RADULESCU, S., SANDOVAL, O., ZAHARIEV, S., DANAILOV, M. B., DEMIDOVICH, A., SANTAMARIA, L., BIAMONTI, G., RIVA, S. & FALASCHI, A. 2007. Functional interactions of DNA topoisomerases with a human replication origin. *The Embo Journal,* 26**,** 998-1009.

ABRAHAM, R. T. 2001. Cell cycle checkpoint signaling through the ATM and ATR kinases. *Genes & Development,* 15**,** 2177-96.

ADACHI, N., SUZUKI, H., IIIZUMI, S. & KOYAMA, H. 2003. Hypersensitivity of nonhomologous DNA end-joining mutants to VP-16 and ICRF-193: Implications for the repair of topoisomerase II-mediated DNA damage. *Journal of Biological Chemistry,* 278**,** 35897-902.

ADAMSON, A. W., BEARDSLEY, D. I., KIM, W.-J., GAO, Y., BASKARAN, R. & BROWN, K. D. 2005. Methylator-induced, mismatch repair-dependent G2 arrest is activated through Chk1 and Chk2. *Molecular biology of the cell,* 16**,** 1513-26.

AGUILERA, A. 2002. The connection between transcription and genomic instability. *The EMBO journal,* 21**,** 195-201.

AGUILERA, A. & GARCÍA-MUSE, T. 2012. R Loops: From Transcription Byproducts to Threats to Genome Stability. *Molecular Cell,* 46**,** 115-24.

AHEL, I., RASS, U., EL-KHAMISY, S. F., KATYAL, S., CLEMENTS, P. M., MCKINNON, P. J., CALDECOTT, K. W. & WEST, S. C. 2006. The neurodegenerative disease protein aprataxin resolves abortive DNA ligation intermediates. *Nature,* 443**,** 713-16.

AHNESORG, P., SMITH, P. & JACKSON, S. P. 2006. XLF interacts with the XRCC4-DNA Ligase IV complex to promote DNA nonhomologous end-joining. *Cell,* 124**,** 301-13.

ALAGOZ, M., CHIANG, S.-C., SHARMA, A. & EL-KHAMISY, S. F. 2013. ATM deficiency results in accumulation of DNA-topoisomerase I covalent intermediates in neural cells. *PLoS ONE,* 8**,** e58239-e39.

ALAGOZ, M., KATSUKI, Y., OGIWARA, H., OGI, T., SHIBATA, A., KAKAROUGKAS, A. & JEGGO, P. 2015. SETDB1, HP1 and SUV39 promote repositioning of 53BP1 to extend resection during homologous recombination in G2 cells. *Nucleic Acids Res,* 43**,** 7931-44.

ALAGOZ, M., WELLS, O. S. & EL-KHAMISY, S. F. 2014. TDP1 deficiency sensitizes human cells to base damage via distinct topoisomerase I and PARP mechanisms with potential applications for cancer therapy. *Nucleic acids research,* 42**,** 3089-103.

ALBERTSON, T. M., OGAWA, M., BUGNI, J. M., HAYS, L. E., CHEN, Y., WANG, Y., TREUTING, P. M., HEDDLE, J. A., GOLDSBY, R. E. & PRESTON, B. D. 2009. DNA polymerase epsilon and delta proofreading suppress discrete mutator and cancer phenotypes in mice. *Proceedings of the National Academy of Sciences of the United States of America,* 106**,** 17101-04.

ALLGAYER, J., KITSERA, N., VON DER LIPPEN, C., EPE, B. & KHOBTA, A. 2013. Modulation of base excision repair of 8-oxoguanine by the nucleotide sequence. *Nucleic Acids Research,* 41**,** 8559-71.

ALLINSON, S. L., DIANOVA, I. I. & DIANOV, G. L. 2001. DNA polymerase beta is the major dRP lyase involved in repair of oxidative base lesions in DNA by mammalian cell extracts. *The EMBO journal,* 20**,** 6919-26.

ALPI, A. F., PACE, P. E., BABU, M. M. & PATEL, K. J. 2008. Mechanistic insight into site-restricted monoubiquitination of FANCD2 by Ube2t, FANCL, and FANCI. *Mol Cell,* 32**,** 767-77.

ANDEGEKO, Y., MOYAL, L., MITTELMAN, L., TSARFATY, I., SHILOH, Y. & ROTMAN, G. 2001. Nuclear retention of ATM at sites of DNA double strand breaks. *The Journal of biological chemistry,* 276**,** 38224-30.

ANDERSEN, P. M., SIMS, K. B., XIN, W. W., KIELY, R., O'NEILL, G., RAVITS, J., PIORO, E., HARATI, Y., BROWER, R. D., LEVINE, J. S., HEINICKE, H. U., SELTZER, W., BOSS, M. & BROWN, R. H., JR. 2003. Sixteen novel mutations in the Cu/Zn superoxide dismutase gene in amyotrophic lateral sclerosis: a decade of discoveries, defects and disputes. *Amyotroph Lateral Scler Other Motor Neuron Disord,* 4**,** 62-73.

ANDERSEN, S. L., BERGSTRALH, D. T., KOHL, K. P., LAROCQUE, J. R., MOORE, C. B. & SEKELSKY, J. 2009. Drosophila MUS312 and the vertebrate ortholog BTBD12 interact with DNA structure-specific endonucleases in DNA repair and recombination. *Mol Cell,* 35**,** 128-35.

ANDERSON, C. W. & LEES-MILLER, S. P. 1992. The nuclear serine/threonine protein kinase DNA-PK. *Critical reviews in eukaryotic gene expression,* 2**,** 283-314.

ANDREWS, A. D., BARRETT, S. F., YODER, F. W. & ROBBINS, J. H. 1978. Cockayne's syndrome fibroblasts have increased sensitivity to ultraviolet light but normal rates of unscheduled DNA synthesis. *The Journal of investigative dermatology,* 70**,** 237-9.

ANDRUS, P. K., FLECK, T. J., GURNEY, M. E. & HALL, E. D. 1998. Protein oxidative damage in a transgenic mouse model of familial amyotrophic lateral sclerosis. *J Neurochem,* 71**,** 2041-8.

ANTOCCIA, A., SAKAMOTO, S., MATSUURA, S., TAUCHI, H. & KOMATSU, K. 2008. NBS1 prevents chromatid-type aberrations through ATM-dependent interactions with SMC1. *Radiation research,* 170**,** 345-52.

ANTONY, S., MARCHAND, C., STEPHEN, A. G., THIBAUT, L., AGAMA, K. K., FISHER, R. J. & POMMIER, Y. 2007. Novel high-throughput electrochemiluminescent assay for identification of human tyrosyl-DNA phosphodiesterase (Tdp1) inhibitors and characterization of furamidine (NSC 305831) as an inhibitor of Tdp1. *Nucleic Acids Research,* 35**,** 4474-84.

ARTUSO, M., ESTEVE, A., BRESIL, H., VUILLAUME, M. & HALL, J. 1995. The role of the Ataxia telangiectasia gene in the p53, WAF1/CIP1(p21)- and GADD45-mediated response to DNA damage produced by ionising radiation. *Oncogene,* 11**,** 1427-35.

ASHOUR, M. E., ATTEYA, R. & EL-KHAMISY, S. F. 2015. Topoisomerase-mediated chromosomal break repair: an emerging player in many games. *Nature reviews. Cancer,* 15**,** 137-51.

AUDEBERT, M., SALLES, B. & CALSOU, P. 2004. Involvement of poly(ADP-ribose) polymerase-1 and XRCC1/DNA ligase III in an alternative route for DNA double-strand breaks rejoining. *The Journal of biological chemistry,* 279**,** 55117-26.

AUDEBERT, M., SALLES, B., WEINFELD, M. & CALSOU, P. 2006. Involvement of polynucleotide kinase in a poly(ADP-ribose) polymerase-1-dependent DNA double-strand breaks rejoining pathway. *Journal of Molecular Biology,* 356**,** 257-65.

BAHMED, K., NITISS, K. C. & NITISS, J. L. 2010. Yeast Tdp1 regulates the fidelity of nonhomologous end joining. *Proceedings of the National Academy of Sciences of the United States of America,* 107**,** 4057-62.

BALDO, P., RUPOLO, M., COMPAGNONI, A., LAZZARINI, R., BEARZ, A., CANNIZZARO, R., SPAZZAPAN, S., TRUCCOLO, I. & MOJA, L. 2010. Interferon-alpha for maintenance of follicular lymphoma. *The Cochrane database of systematic reviews,* 10.1002/14651858.CD004629.pub2**,** CD004629-CD29.

BALL, H. L., MYERS, J. S. & CORTEZ, D. 2005. ATRIP binding to replication protein A-single-stranded DNA promotes ATR-ATRIP localization but is dispensable for Chk1 phosphorylation. *Molecular biology of the cell,* 16**,** 2372-81.

BALLINGER, S. W., PATTERSON, C., YAN, C. N., DOAN, R., BUROW, D. L., YOUNG, C. G., YAKES, F. M., VAN HOUTEN, B., BALLINGER, C. A., FREEMAN, B. A. & RUNGE, M. S. 2000. Hydrogen peroxide- and peroxynitrite-induced mitochondrial DNA damage and dysfunction in vascular endothelial and smooth muscle cells. *Circ Res,* 86**,** 960-6.

BALLINGER, S. W., VAN HOUTEN, B., JIN, G. F., CONKLIN, C. A. & GODLEY, B. F. 1999. Hydrogen peroxide causes significant mitochondrial DNA damage in human RPE cells. *Exp Eye Res,* 68**,** 765-72.

BALLOT, C., MARTORIATI, A., JENDOUBI, M., BUCHE, S. B., FORMSTECHER, P., MORTIER, L., KLUZA, J. R. & MARCHETTI, P. 2014. Another facet to the anticancer response to lamellarin D: Induction

of cellular senescence through inhibition of topoisomerase i and intracellular ros production. *Marine Drugs,* 12**,** 779-98.

BANERJEE, D., MANDAL, S. M., DAS, A., HEGDE, M. L., DAS, S., BHAKAT, K. K., BOLDOGH, I., SARKAR, P. S., MITRA, S. & HAZRA, T. K. 2011. Preferential repair of oxidized base damage in the transcribed genes of mammalian cells. *Journal of Biological Chemistry,* 286**,** 6006-16.

BANNISTER, A. J., GOTTLIEB, T. M., KOUZARIDES, T. & JACKSON, S. P. 1993. c-Jun is phosphorylated by the DNA-dependent protein kinase in vitro; definition of the minimal kinase recognition motif. *Nucleic acids research,* 21**,** 1289-95.

BANNISTER, L. A., PEZZA, R. J., DONALDSON, J. R., DE ROOIJ, D. G., SCHIMENTI, K. J., CAMERINI-OTERO, R. D. & SCHIMENTI, J. C. 2007. A dominant, recombination-defective allele of Dmc1 causing male-specific sterility. *PLoS Biol,* 5**,** e105.

BARANELLO, L., BERTOZZI, D., FOGLI, M. V., POMMIER, Y. & CAPRANICO, G. 2010. DNA topoisomerase I inhibition by camptothecin induces escape of RNA polymerase II from promoter-proximal pause site, antisense transcription and histone acetylation at the human HIF-1alpha gene locus. *Nucleic Acids Res,* 38**,** 159-71.

BARANELLO, L., WOJTOWICZ, D., CUI, K., DEVAIAH, B. N., CHUNG, H. J., CHAN-SALIS, K. Y., GUHA, R., WILSON, K., ZHANG, X., ZHANG, H., PIOTROWSKI, J., THOMAS, C. J., SINGER, D. S., PUGH, B. F., POMMIER, Y., PRZYTYCKA, T. M., KOUZINE, F., LEWIS, B. A., ZHAO, K. & LEVENS, D. 2016. RNA Polymerase II Regulates Topoisomerase 1 Activity to Favor Efficient Transcription. *Cell,* 165**,** 357-71.

BARBOSA, L. F., CERQUEIRA, F. M., MACEDO, A. F., GARCIA, C. C., ANGELI, J. P., SCHUMACHER, R. I., SOGAYAR, M. C., AUGUSTO, O., CARRI, M. T., DI MASCIO, P. & MEDEIROS, M. H. 2010. Increased SOD1 association with chromatin, DNA damage, p53 activation, and apoptosis in a cellular model of SOD1-linked ALS. *Biochim Biophys Acta,* 1802**,** 462-71.

BARTHELMES, H. U., HABERMEYER, M., CHRISTENSEN, M. O., MIELKE, C., INTERTHAL, H., POULIOT, J. J., BOEGE, F. & MARKO, D. 2004. TDP1 overexpression in human cells counteracts DNA damage mediated by topoisomerases I and II. *Journal of Biological Chemistry,* 279**,** 55618-25.

BARZILAY, G. & HICKSON, I. D. 1995. Structure and function of apurinic/apyrimidinic endonucleases. *BioEssays,* 17**,** 713-19.

BASU, A. K., LOECHLER, E. L., LEADON, S. A. & ESSIGMANN, J. M. 1989. Genetic effects of thymine glycol: site-specific mutagenesis and molecular modeling studies. *Proceedings of the National Academy of Sciences of the United States of America,* 86**,** 7677-81.

BAUDAT, F., MANOVA, K., YUEN, J. P., JASIN, M. & KEENEY, S. 2000. Chromosome synapsis defects and sexually dimorphic meiotic progression in mice lacking Spo11. *Mol Cell,* 6**,** 989-98.

BAUER, P. I., BUKI, K. G., COMSTOCK, J. A. & KUN, E. 2000. Activation of topoisomerase I by poly [ADP-ribose] polymerase. *International journal of molecular medicine,* 5**,** 533-40.

BAUERSCHMIDT, C., WOODCOCK, M., STEVENS, D. L., HILL, M. A., ROTHKAMM, K. & HELLEDAY, T. 2011. Cohesin phosphorylation and mobility of SMC1 at ionizing radiation-induced DNA double-strand breaks in human cells. *Experimental cell research,* 317**,** 330-7.

BAXTER, J., SEN, N., MARTÍNEZ, V. L., DE CARANDINI, M. E. M., SCHVARTZMAN, J. B., DIFFLEY, J. F. X. & ARAGÓN, L. 2011. Positive supercoiling of mitotic DNA drives decatenation by topoisomerase II in eukaryotes. *Science (New York, N.Y.),* 331**,** 1328-32.

BEBENEK, K., TISSIER, A., FRANK, E. G., MCDONALD, J. P., PRASAD, R., WILSON, S. H., WOODGATE, R. & KUNKEL, T. A. 2001. 5 '-Deoxyribose phosphate lyase activity of human DNA polymerase iota in vitro. *Science,* 291**,** 2156-59.

BECKER, T. & HAFERKAMP, S. 2013. *Molecular Mechanisms of Cellular Senescence*, InTech, 10.5772/54120.

BECKMAN, K. B. & AMES, B. N. 1997. Oxidative decay of DNA. *J Biol Chem,* 272**,** 19633-6.

BENDIXEN, C., THOMSEN, B., ALSNER, J. & WESTERGAARD, O. 1990. Camptothecin-stabilized topoisomerase I-DNA adducts cause premature termination of transcription. *Biochemistry,* 29**,** 5613-19.

BENEKE, S. 2012. Regulation of chromatin structure by poly(ADP-ribosyl)ation. *Frontiers in Genetics,* 3**,** 169.

BENNARDO, N., CHENG, A., HUANG, N. & STARK, J. M. 2008. Alternative-NHEJ is a mechanistically distinct pathway of mammalian chromosome break repair. *PLoS Genetics,* 4**,** e1000110.

BENZ, R. & MCLAUGHLIN, S. 1983. The molecular mechanism of action of the proton ionophore FCCP (carbonylcyanide p-trifluoromethoxyphenylhydrazone). *Biophysical journal,* 41**,** 381-98.

BERETTA, G. L., GATTI, L., PEREGO, P. & ZAFFARONI, N. 2013. Camptothecin resistance in cancer: insights into the molecular mechanisms of a DNA-damaging drug. *Curr Med Chem,* 20**,** 1541-65.

BERGAMINI, E., CAVALLINI, G., DONATI, A. & GORI, Z. 2007. The role of autophagy in aging: its essential part in the anti-aging mechanism of caloric restriction. *Ann N Y Acad Sci,* 1114**,** 69-78.

BERGINK, S. & JENTSCH, S. 2009. Principles of ubiquitin and SUMO modifications in DNA repair. *Nature,* 458**,** 461-67.

BERNSTEIN, N. K., WILLIAMS, R. S., RAKOVSZKY, M. L., CUI, D., GREEN, R., KARIMI-BUSHERI, F., MANI, R. S., GALICIA, S., KOCH, C. A., CASS, C. E., DUROCHER, D., WEINFELD, M. & GLOVER, J. N. M. 2005. The molecular architecture of the mammalian DNA repair enzyme, polynucleotide kinase. *Molecular Cell,* 17**,** 657-70.

BEUCHER, A., BIRRAUX, J., TCHOUANDONG, L., BARTON, O., SHIBATA, A., CONRAD, S., GOODARZI, A. A., KREMPLER, A., JEGGO, P. A. & LÖBRICH, M. 2009. ATM and Artemis promote homologous recombination of radiation-induced DNA double-strand breaks in G2. *The EMBO journal,* 28**,** 3413-27.

BISHOP, N. A. & GUARENTE, L. 2007. Genetic links between diet and lifespan: shared mechanisms from yeast to humans. *Nature reviews. Genetics,* 8**,** 835-44.

BLASINA, A., PRICE, B. D., TURENNE, G. A. & MCGOWAN, C. H. 1999. Caffeine inhibits the checkpoint kinase ATM. *Current biology : CB,* 9**,** 1135-8.

BOCHAR, D. A., WANG, L., BENIYA, H., KINEV, A., XUE, Y., LANE, W. S., WANG, W., KASHANCHI, F. & SHIEKHATTAR, R. 2000. BRCA1 is associated with a human SWI/SNF-related complex: linking chromatin remodeling to breast cancer. *Cell,* 102**,** 257-65.

BOITEUX, S. & RADICELLA, J. P. 2000. The human OGG1 gene: structure, functions, and its implication in the process of carcinogenesis. *Arch Biochem Biophys,* 377**,** 1-8.

BORDA, M. A., PALMITELLI, M., VERON, G., GONZALEZ-CID, M. & DE CAMPOS NEBEL, M. 2015. Tyrosyl-DNA-phosphodiesterase I (TDP1) participates in the removal and repair of stabilized-Top2alpha cleavage complexes in human cells. *Mutat Res,* 781**,** 37-48.

BOTHMER, A., ROBBIANI, D. F., DI VIRGILIO, M., BUNTING, S. F., KLEIN, I. A., FELDHAHN, N., BARLOW, J., CHEN, H. T., BOSQUE, D., CALLEN, E., NUSSENZWEIG, A. & NUSSENZWEIG, M. C. 2011. Regulation of DNA end joining, resection, and immunoglobulin class switch recombination by 53BP1. *Mol Cell,* 42**,** 319-29.

BRAITHWAITE, E. K., KEDAR, P. S., LAN, L., POLOSINA, Y. Y., ASAGOSHI, K., POLTORATSKY, V. P., HORTON, J. K., MILLER, H., TEEBOR, G. W., YASUI, A. & WILSON, S. H. 2005a. DNA polymerase lambda protects mouse fibroblasts against oxidative DNA damage and is recruited to sites of DNA damage/repair. *The Journal of biological chemistry,* 280**,** 31641-7.

BRAITHWAITE, E. K., PRASAD, R., SHOCK, D. D., HOU, E. W., BEARD, W. A. & WILSON, S. H. 2005b. DNA polymerase lambda mediates a back-up base excision repair activity in extracts of mouse embryonic fibroblasts. *The Journal of biological chemistry,* 280**,** 18469-75.

BRAND, M. D. & NICHOLLS, D. G. 2011. Assessing mitochondrial dysfunction in cells. *Biochem J,* 435**,** 297-312.

BRAS, J., ALONSO, I., BARBOT, C., COSTA, M. M., DARWENT, L., ORME, T., SEQUEIROS, J., HARDY, J., COUTINHO, P. & GUERREIRO, R. 2015. Mutations in PNKP cause recessive ataxia with oculomotor apraxia type 4. *American journal of human genetics,* 96**,** 474-9.

BRILL, S. J., DINARDO, S., VOELKEL-MEIMAN, K. & STERNGLANZ, R. 1987. Need for DNA topoisomerase activity as a swivel for DNA replication for transcription of ribosomal RNA. *Nature,* 326**,** 414-6.

BRODERICK, R., NIEMINUSZCZY, J., BLACKFORD, A. N., WINCZURA, A. & NIEDZWIEDZ, W. 2015. TOPBP1 recruits TOP2A to ultra-fine anaphase bridges to aid in their resolution. *Nature communications,* 6**,** 6572-72.

BROOKS, S. C., ADHIKARY, S., RUBINSON, E. H. & EICHMAN, B. F. 2013. Recent advances in the structural mechanisms of DNA glycosylases. *Biochemica et Biophysica Acta - Proteins and Proteomics,* 1834**,** 247-71.

BROWN, E. J. & BALTIMORE, D. 2003. Essential and dispensable roles of ATR in cell cycle arrest and genome maintenance. *Genes and Development,* 17**,** 615-28.

BROWN, K. D., RATHI, A., KAMATH, R., BEARDSLEY, D. I., ZHAN, Q., MANNINO, J. L. & BASKARAN, R. 2003. The mismatch repair system is required for S-phase checkpoint activation. *Nature genetics,* 33**,** 80-84.

BROWN, T. A., TKACHUK, A. N. & CLAYTON, D. A. 2008. Native R-loops persist throughout the mouse mitochondrial DNA genome. *Journal of Biological Chemistry,* 283**,** 36743-51.

BROWNE, S. E., YANG, L., DIMAURO, J. P., FULLER, S. W., LICATA, S. C. & BEAL, M. F. 2006. Bioenergetic abnormalities in discrete cerebral motor pathways presage spinal cord pathology in the G93A SOD1 mouse model of ALS. *Neurobiol Dis,* 22**,** 599-610.

BRÜCKNER, A., POLGE, C., LENTZE, N., AUERBACH, D. & SCHLATTNER, U. 2009. Yeast two-hybrid, a powerful tool for systems biology. *Int J Mol Sci,* 10**,** 2763-88.

BRUDERER, R., TATHAM, M. H., PLECHANOVOVA, A., MATIC, I., GARG, A. K. & HAY, R. T. 2011. Purification and identification of endogenous polySUMO conjugates. *EMBO reports,* 12**,** 142-48.

BRUGAROLAS, J., MOBERG, K., BOYD, S. D., TAYA, Y., JACKS, T. & LEES, J. A. 1999. Inhibition of cyclin-dependent kinase 2 by p21 is necessary for retinoblastoma protein-mediated G1 arrest after gamma-irradiation. *Proceedings of the National Academy of Sciences of the United States of America,* 96**,** 1002-7.

BUNTING, S. F., CALLEN, E., WONG, N., CHEN, H. T., POLATO, F., GUNN, A., BOTHMER, A., FELDHAHN, N., FERNANDEZ-CAPETILLO, O., CAO, L., XU, X., DENG, C. X., FINKEL, T., NUSSENZWEIG, M., STARK, J. M. & NUSSENZWEIG, A. 2010. 53BP1 inhibits homologous recombination in Brca1-deficient cells by blocking resection of DNA breaks. *Cell,* 141**,** 243-54.

BURKE, T. G. & MI, Z. 1994. The structural basis of camptothecin interactions with human serum albumin: impact on drug stability. *Journal of medicinal chemistry,* 37**,** 40-46.

BURMA, S., CHEN, B. P., MURPHY, M., KURIMASA, A. & CHEN, D. J. 2001. ATM Phosphorylates Histone H2AX in Response to DNA Double-strand Breaks. *Journal of Biological Chemistry,* 276**,** 42462-67.

CALDECOTT, K. W. 2001. Mammalian DNA single-strand break repair: An X-ra(y)ted affair. *BioEssays,* 23**,** 447-55.

CALDECOTT, K. W. 2008. Single-strand break repair and genetic disease. *Nature reviews. Genetics,* 9**,** 619-31.

CALDECOTT, K. W., AOUFOUCHI, S., JOHNSON, P. & SHALL, S. 1996. XRCC1 polypeptide interacts with DNA polymerase beta and possibly poly (ADP-ribose) polymerase, and DNA ligase III is a novel molecular 'nick- sensor' in vitro. *Nucleic acids research,* 24**,** 4387-94.

CALDECOTT, K. W., MCKEOWN, C. K., TUCKER, J. D., LJUNGQUIST, S. & THOMPSON, L. H. 1994. An interaction between the mammalian DNA repair protein XRCC1 and DNA ligase III. *Molecular and cellular biology,* 14**,** 68-76.

CALDECOTT, K. W., TUCKER, J. D., STANKER, L. H. & THOMPSON, L. H. 1995. Characterization of the XRCC1-DNA ligase III complex in vitro and its absence from mutant hamster cells. *Nucleic Acids Research,* 23**,** 4836-43.

CAMPALANS, A., MARSIN, S., NAKABEPPU, Y., O'CONNOR, T. R., BOITEUX, S. & RADICELLA, J. P. 2005. XRCC1 interactions with multiple DNA glycosylases: A model for its recruitment to base excision repair. *DNA Repair,* 4**,** 826-35.

CAMPISI, J. & D'ADDA DI FAGAGNA, F. 2007. Cellular senescence: when bad things happen to good cells. *Nature reviews. Molecular cell biology,* 8**,** 729-40.

CANNAVO, E., MARRA, G., SABATES-BELLVER, J., MENIGATTI, M., LIPKIN, S. M., FISCHER, F., CEJKA, P. & JIRICNY, J. 2005. Expression of the MutL homologue hMLH3 in human cells and its role in DNA mismatch repair. *Cancer Res,* 65**,** 10759-66.

CAPRANICO, G., KOHN, K. W. & POMMIER, Y. 1990. Local sequence requirements for DNA cleavage by mammalian topoisomerase II in the presence of doxorubicin. *Nucleic acids research,* 18**,** 6611-19.

CARREIRA, A., HILARIO, J., AMITANI, I., BASKIN, R. J., SHIVJI, M. K., VENKITARAMAN, A. R. & KOWALCZYKOWSKI, S. C. 2009. The BRC repeats of BRCA2 modulate the DNA-binding selectivity of RAD51. *Cell,* 136**,** 1032-43.

CARROLL, J., PAGE, T. K., CHIANG, S. C., KALMAR, B., BODE, D., GREENSMITH, L., MCKINNON, P. J., THORPE, J. R., HAFEZPARAST, M. & EL-KHAMISY, S. F. 2015. Expression of a pathogenic mutation of SOD1 sensitizes aprataxin-deficient cells and mice to oxidative stress and triggers hallmarks of premature ageing. *Hum Mol Genet,* 24**,** 828-40.

CASONI, F., BASSO, M., MASSIGNAN, T., GIANAZZA, E., CHERONI, C., SALMONA, M., BENDOTTI, C. & BONETTO, V. 2005. Protein nitration in a mouse model of familial amyotrophic lateral sclerosis: possible multifunctional role in the pathogenesis. *J Biol Chem,* 280**,** 16295-304.

CASSINA, P., CASSINA, A., PEHAR, M., CASTELLANOS, R., GANDELMAN, M., DE LEON, A., ROBINSON, K. M., MASON, R. P., BECKMAN, J. S., BARBEITO, L. & RADI, R. 2008. Mitochondrial dysfunction in SOD1G93A-bearing astrocytes promotes motor neuron degeneration: prevention by mitochondrial-targeted antioxidants. *J Neurosci,* 28**,** 4115-22.

CEBRIÁN, J., CASTÁN, A., MARTÍNEZ, V., KADOMATSU-HERMOSA, M. J., PARRA, C., FERNÁNDEZ-NESTOSA, M. J., SCHAERER, C., HERNÁNDEZ, P., KRIMER, D. B. & SCHVARTZMAN, J. B. 2015. Direct Evidence for the Formation of Precatenanes during DNA Replication. *The Journal of biological chemistry,* 290**,** 13725-35.

CEJKA, P., CANNAVO, E., POLACZEK, P., MASUDA-SASA, T., POKHAREL, S., CAMPBELL, J. L. & KOWALCZYKOWSKI, S. C. 2010a. DNA end resection by Dna2-Sgs1-RPA and its stimulation by Top3-Rmi1 and Mre11-Rad50-Xrs2. *Nature,* 467**,** 112-6.

CEJKA, P., PLANK, J. L., BACHRATI, C. Z., HICKSON, I. D. & KOWALCZYKOWSKI, S. C. 2010b. Rmi1 stimulates decatenation of double Holliday junctions during dissolution by Sgs1-Top3. *Nat Struct Mol Biol,* 17**,** 1377-82.

CERRITELLI, S. M., CHON, H. & CROUCH, R. J. 2011. A New Twist for Topoisomerase. *Science,* 332**,** 1510-11.

CHAMPOUX, J. J. 2001. DNA topoisomerases: structure, function, and mechanism. *Annu Rev Biochem,* 70**,** 369-413.

CHAN, S. W. & CHEN, J. Z. 2009. Measuring mtDNA damage using a supercoiling-sensitive qPCR approach. *Methods Mol Biol,* 554**,** 183-97.

CHANG, D. D. & CLAYTON, D. A. 1985. Priming of human mitochondrial DNA replication occurs at the light-strand promoter. *Proceedings of the National Academy of Sciences of the United States of America,* 82**,** 351-55.

CHANG, D. D., HAUSWIRTH, W. W. & CLAYTON, D. A. 1985. Replication priming and transcription initiate from precisely the same site in mouse mitochondrial DNA. *The EMBO Journal,* 4**,** 1559-67.

CHANG, L. Y., SLOT, J. W., GEUZE, H. J. & CRAPO, J. D. 1988. Molecular immunocytochemistry of the CuZn superoxide dismutase in rat hepatocytes. *J Cell Biol,* 107**,** 2169-79.

CHAPMAN, J. R., BARRAL, P., VANNIER, J. B., BOREL, V., STEGER, M., TOMAS-LOBA, A., SARTORI, A. A., ADAMS, I. R., BATISTA, F. D. & BOULTON, S. J. 2013. RIF1 is essential for 53BP1-dependent nonhomologous end joining and suppression of DNA double-strand break resection. *Mol Cell,* 49**,** 858-71.

CHAPMAN, J. R., SOSSICK, A. J., BOULTON, S. J. & JACKSON, S. P. 2012. BRCA1-associated exclusion of 53BP1 from DNA damage sites underlies temporal control of DNA repair. *J Cell Sci,* 125**,** 3529-34.

CHAPPELL, C., HANAKAHI, L. A., KARIMI-BUSHERI, F., WEINFELD, M. & WEST, S. C. 2002. Involvement of human polynucleotide kinase in double-strand break repair by non-homologous end joining. *The EMBO journal,* 21**,** 2827-32.

CHARLET-BERGUERAND, N., FEUERHAHN, S., KONG, S. E., ZISERMAN, H., CONAWAY, J. W., CONAWAY, R. & EGLY, J. M. 2006. RNA polymerase II bypass of oxidative DNA damage is regulated by transcription elongation factors. *The EMBO journal,* 25**,** 5481-91.

CHATTOPADHYAY, M., DURAZO, A., SOHN, S. H., STRONG, C. D., GRALLA, E. B., WHITELEGGE, J. P. & VALENTINE, J. S. 2008. Initiation and elongation in fibrillation of ALS-linked superoxide dismutase. *Proceedings of the National Academy of Sciences of the United States of America,* 105**,** 18663-8.

CHEHAB, N. H., MALIKZAY, A., APPEL, M. & HALAZONETIS, T. D. 2000. Chk2/hCds1 functions as a DNA damage checkpoint in G(1) by stabilizing p53. *Genes Dev,* 14**,** 278-88.

CHEN, D., VOLLMAR, M., ROSSI, M. N., PHILLIPS, C., KRAEHENBUEHL, R., SLADE, D., MEHROTRA, P. V., VON DELFT, F., CROSTHWAITE, S. K., GILEADI, O., DENU, J. M. & AHEL, I. 2011. Identification of macrodomain proteins as novel O-acetyl-ADP-ribose deacetylases. *Journal of Biological Chemistry,* 286**,** 13261-71.

CHEN, J. & SADOWSKI, I. 2005. Identification of the mismatch repair genes PMS2 and MLH1 as p53 target genes by using serial analysis of binding elements. *Proceedings of the National Academy of Sciences of the United States of America,* 102**,** 4813-8.

CHEN, M. S., RYAN, C. E. & PIWNICA-WORMS, H. 2003. Chk1 kinase negatively regulates mitotic function of Cdc25A phosphatase through 14-3-3 binding. *Mol Cell Biol,* 23**,** 7488-97.

CHEN, X., WEI, S., MA, Y., LU, J., NIU, G., XUE, Y., CHEN, X. & YANG, F. 2014. Quantitative proteomics analysis identifies mitochondria as therapeutic targets of multidrug-resistance in ovarian cancer. *Theranostics,* 4**,** 1164-75.

CHEN, X. B., MELCHIONNA, R., DENIS, C. M., GAILLARD, P. H., BLASINA, A., VAN DE WEYER, I., BODDY, M. N., RUSSELL, P., VIALARD, J. & MCGOWAN, C. H. 2001. Human Mus81-associated endonuclease cleaves Holliday junctions in vitro. *Mol Cell,* 8**,** 1117-27.

CHIANG, S.-C. C., CARROLL, J. & EL-KHAMISY, S. F. 2010. TDP1 serine 81 promotes interaction with DNA ligase IIIalpha and facilitates cell survival following DNA damage. *Cell cycle (Georgetown, Tex.),* 9**,** 588-95.

CHRISTENSEN, M. O., KROKOWSKI, R. M., BARTHELMES, H. U., HOCK, R., BOEGE, F. & MIELKE, C. 2004. Distinct effects of topoisomerase I and RNA polymerase I inhibitors suggest a dual mechanism of nucleolar/nucleoplasmic partitioning of topoisomerase I. *The Journal of biological chemistry,* 279**,** 21873-82.

CLARK, A. B., VALLE, F., DROTSCHMANN, K., GARY, R. K. & KUNKEL, T. A. 2000. Functional interaction of proliferating cell nuclear antigen with MSH2-MSH6 and MSH2-MSH3 complexes. *Journal of Biological Chemistry,* 275**,** 36498-501.

CLARK, J. M. & BEARDSLEY, G. P. 1986. Thymlne glycol lesions terminate chain elongation by DNA polymerase I in vitro. *Nucleic Acids Research,* 14**,** 737-49.

CLARK, J. M., PATTABIRAMAN, N., JARVIS, W. & BEARDSLEY, G. P. 1987. Modeling and molecular mechanical studies of the cis-thymine glycol radiation damage lesion in DNA. *Biochemistry,* 26**,** 5404-9.

CLAYTON, D. A. 1991. Replication and transcription of vertebrate mitochondrial DNA. *Annual review of cell biology,* 7**,** 453-78.

CLEAVER, J. E. 1978. DNA repair and its coupling to DNA replication in eukaryotic cells. *Biochimica et biophysica acta,* 516**,** 489-516.

CLEVELAND, D. W. 1999. From Charcot to SOD1: mechanisms of selective motor neuron death in ALS. *Neuron,* 24**,** 515-20.

COELHO, P. A., QUEIROZ-MACHADO, J., CARMO, A. M., MOUTINHO-PEREIRA, S., MAIATO, H. & SUNKEL, C. E. 2008. Dual role of topoisomerase II in centromere resolution and aurora B activity. *PLoS Biology,* 6**,** 1758-77.

COIN, F., OKSENYCH, V. & EGLY, J. M. 2007. Distinct Roles for the XPB/p52 and XPD/p44 Subcomplexes of TFIIH in Damaged DNA Opening during Nucleotide Excision Repair. *Molecular Cell,* 26**,** 245-56.

COIN, F., OKSENYCH, V., MOCQUET, V., GROH, S., BLATTNER, C. & EGLY, J. M. 2008. Nucleotide Excision Repair Driven by the Dissociation of CAK from TFIIH. *Molecular Cell,* 31**,** 9-20.

COLLINS, I., WEBER, A. & LEVENS, D. 2001. Transcriptional consequences of topoisomerase inhibition. *Molecular and cellular biology,* 21**,** 8437-51.

COLLIS, S. J., CICCIA, A., DEANS, A. J., HOREJSI, Z., MARTIN, J. S., MASLEN, S. L., SKEHEL, J. M., ELLEDGE, S. J., WEST, S. C. & BOULTON, S. J. 2008. FANCM and FAAP24 function in ATR-mediated checkpoint signaling independently of the Fanconi anemia core complex. *Mol Cell,* 32**,** 313-24.

CONSTANTINOU, A., CHEN, X. B., MCGOWAN, C. H. & WEST, S. C. 2002. Holliday junction resolution in human cells: two junction endonucleases with distinct substrate specificities. *EMBO J,* 21**,** 5577-85.

COOKE, M. S., EVANS, M. D., DIZDAROGLU, M. & LUNEC, J. 2003. Oxidative DNA damage: mechanisms, mutation, and disease. *The FASEB Journal,* 17**,** 1195-214.

COOPER, P. K., NOUSPIKEL, T., CLARKSON, S. G. & LEADON, S. A. 1997. Defective transcription-coupled repair of oxidative base damage in Cockayne syndrome patients from XP group G. *Science (New York, N.Y.),* 275**,** 990-3.

CORTES LEDESMA, F., EL KHAMISY, S. F., ZUMA, M. C., OSBORN, K. & CALDECOTT, K. W. 2009. A human 5'-tyrosyl DNA phosphodiesterase that repairs topoisomerase-mediated DNA damage. *Nature,* 461**,** 674-8.

CORTEZ, D., GUNTUKU, S., QIN, J. & ELLEDGE, S. J. 2001. ATR and ATRIP: partners in checkpoint signaling. *Science (New York, N.Y.),* 294**,** 1713-16.

CORTEZ, D., WANG, Y., QIN, J. & ELLEDGE, S. J. 1999. Requirement of ATM-dependent phosphorylation of brca1 in the DNA damage response to double-strand breaks. *Science (New York, N.Y.),* 286**,** 1162-66.

COSTANTINI, S., WOODBINE, L., ANDREOLI, L., JEGGO, P. A. & VINDIGNI, A. 2007. Interaction of the Ku heterodimer with the DNA ligase IV/Xrcc4 complex and its regulation by DNA-PK. *DNA repair,* 6**,** 712-22.

CRAPO, J. D., OURY, T., RABOUILLE, C., SLOT, J. W. & CHANG, L. Y. 1992. Copper,zinc superoxide dismutase is primarily a cytosolic protein in human cells. *Proc Natl Acad Sci U S A,* 89**,** 10405-9.

CRITCHLOW, S. E., BOWATER, R. P. & JACKSON, S. P. 1997. Mammalian DNA double-strand break repair protein XRCC4 interacts with DNA ligase IV. *Current biology : CB,* 7**,** 588-98.

CUERVO, A. M. 2004. Autophagy: Many paths to the same end. *Molecular and Cellular Biochemistry,* 263**,** 55-72.

CZABOTAR, P. E., LESSENE, G., STRASSER, A. & ADAMS, J. M. 2014. Control of apoptosis by the BCL-2 protein family: implications for physiology and therapy. *Nature reviews. Molecular cell biology,* 15**,** 49-63.

D'AMOURS, D., DESNOYERS, S., D'SILVA, I. & POIRIER, G. G. 1999. Poly(ADP-ribosyl)ation reactions in the regulation of nuclear functions. *Biochem J,* 342 (Pt 2)**,** 249-68.

D'AMOURS, D. & JACKSON, S. P. 2002. The Mre11 complex: at the crossroads of dna repair and checkpoint signalling. *Nature reviews. Molecular cell biology,* 3**,** 317-27.

D'ARCY, P., WANG, X. & LINDER, S. 2015. Deubiquitinase inhibition as a cancer therapeutic strategy. *Pharmacology & therapeutics,* 147**,** 32-54.

DALAL, S. N., YAFFE, M. B. & DECAPRIO, J. A. 2004. 14-3-3 family members act coordinately to regulate mitotic progression. *Cell Cycle,* 3**,** 672-7.

DALLA ROSA, I. 2009. *Role of DNA-topoisomerase I in mtDNA maintenance: Relevance of a distinct, mitochondria-targeted enzyme version in vertebrates.* Dr. rer. nat., Universität Düsseldorf.

DALLA ROSA, I., HUANG, S. Y. N., AGAMA, K., KHIATI, S., ZHANG, H. & POMMIER, Y. 2014. Mapping topoisomerase sites in mitochondrial DNA with a poisonous mitochondrial topoisomerase I (Top1mt). *Journal of Biological Chemistry,* 289**,** 18595-602.

DAMIANO, M., STARKOV, A. A., PETRI, S., KIPIANI, K., KIAEI, M., MATTIAZZI, M., FLINT BEAL, M. & MANFREDI, G. 2006. Neural mitochondrial Ca2+ capacity impairment precedes the onset of motor symptoms in G93A Cu/Zn-superoxide dismutase mutant mice. *J Neurochem,* 96**,** 1349-61.

DAROUI, P., DESAI, S. D., LI, T. K., LIU, A. A. & LIU, L. F. 2004. Hydrogen peroxide induces topoisomerase I-mediated DNA damage and cell death. *J Biol Chem,* 279**,** 14587-94.

DAS, B. B., ANTONY, S., GUPTA, S., DEXHEIMER, T. S., REDON, C. E., GARFIELD, S., SHILOH, Y. & POMMIER, Y. 2009. Optimal function of the DNA repair enzyme TDP1 requires its phosphorylation by ATM and/or DNA-PK. *The EMBO journal,* 28**,** 3667-80.

DAS, B. B., DEXHEIMER, T. S., MADDALI, K. & POMMIER, Y. 2010. Role of tyrosyl-DNA phosphodiesterase (TDP1) in mitochondria. *Proc Natl Acad Sci U S A,* 107**,** 19790-5.

DAS, B. B., HUANG, S. N., MURAI, J., REHMAN, I., AM, J. C., SENGUPTA, S., DAS, S. K., MAJUMDAR, P., ZHANG, H., BIARD, D., MAJUMDER, H. K., SCHREIBER, V. V. R., POMMIER, Y., AMÉ, J. C., SENGUPTA, S., DAS, S. K., MAJUMDAR, P., ZHANG, H., BIARD, D., MAJUMDER, H. K., SCHREIBER, V. V. R. & POMMIER, Y. 2014. PARP1-TDP1 coupling for the repair of topoisomerase I-induced DNA damage. *Nucleic Acids Research,* 42**,** 4435-49.

DATE, H., ONODERA, O., TANAKA, H., IWABUCHI, K., UEKAWA, K., IGARASHI, S., KOIKE, R., HIROI, T., YUASA, T., AWAYA, Y., SAKAI, T., TAKAHASHI, T., NAGATOMO, H., SEKIJIMA, Y., KAWACHI, I., TAKIYAMA, Y., NISHIZAWA, M., FUKUHARA, N., SAITO, K., SUGANO, S. & TSUJI, S. 2001. Early-onset ataxia with ocular motor apraxia and hypoalbuminemia is caused by mutations in a new HIT superfamily gene. *Nature genetics,* 29**,** 184-88.

DAVIDOVIC, L., VODENICHAROV, M., AFFAR, E. B. & POIRIER, G. G. 2001. Importance of poly(ADP-ribose) glycohydrolase in the control of poly(ADP-ribose) metabolism. *Experimental cell research,* 268**,** 7-13.

DAVIES, A. A., HUTTNER, D., DAIGAKU, Y., CHEN, S. & ULRICH, H. D. 2008. Activation of ubiquitin-dependent DNA damage bypass is mediated by replication protein a. *Mol Cell,* 29**,** 625-36.

DAVIES, D. R., INTERTHAL, H., CHAMPOUX, J. J. & HOL, W. G. J. 2002. The Crystal Structure of Human Tyrosyl-DNA Phosphodiesterase, Tdp1. *Structure,* 10**,** 237-48.

DAVIES, D. R., INTERTHAL, H., CHAMPOUX, J. J. & HOL, W. G. J. 2003. Crystal structure of a transition state mimic for Tdp1 assembled from vanadate, DNA, and a topoisomerase I-derived peptide. *Chemistry & biology,* 10**,** 139-47.

DAVIES, D. R., INTERTHAL, H., CHAMPOUX, J. J. & HOL, W. G. J. 2004. Explorations of Peptide and Oligonucleotide Binding Sites of Tyrosyl-DNA Phosphodiesterase Using Vanadate Complexes. *Journal of Medicinal Chemistry,* 47**,** 829-37.

DE LAAT, W. L., APPELDOORN, E., SUGASAWA, K., WETERINGS, E., JASPERS, N. G. J. & HOEIJMAKERS, J. H. J. 1998. DNA-binding polarity of human replication protein A positions nucleases in nucleotide excision repair. *Genes and Development,* 12**,** 2598-609.

DE MELO, J. T. A., DE SOUZA TIMOTEO, A. R., LAJUS, T. B. P., BRANDÃO, J. A., DE SOUZA-PINTO, N. C., MENCK, C. F. M., CAMPALANS, A., RADICELLA, J. P., VESSONI, A. T., MUOTRI, A. R. & AGNEZ-LIMA, L. F. 2016. XPC deficiency is related to APE1 and OGG1 expression and function. *Mutation Research/Fundamental and Molecular Mechanisms of Mutagenesis,* 784-785**,** 25-33.

DE SILVA, I. U., MCHUGH, P. J., CLINGEN, P. H. & HARTLEY, J. A. 2000. Defining the roles of nucleotide excision repair and recombination in the repair of DNA interstrand cross-links in mammalian cells. *Mol Cell Biol,* 20**,** 7980-90.

DEBÉTHUNE, L., KOHLHAGEN, G., GRANDAS, A. & POMMIER, Y. 2002. Processing of nucleopeptides mimicking the topoisomerase I-DNA covalent complex by tyrosyl-DNA phosphodiesterase. *Nucleic acids research,* 30**,** 1198-204.

DEFAZIO, L. G., STANSEL, R. M., GRIFFITH, J. D. & CHU, G. 2002. Synapsis of DNA ends by DNA-dependent protein kinase. *EMBO Journal,* 21**,** 3192-200.

DEL MAESTRO, R. & MCDONALD, W. 1989. Subcellular localization of superoxide dismutases, glutathione peroxidase and catalase in developing rat cerebral cortex. *Mech Ageing Dev,* 48**,** 15-31.

DELANEY, C. A., WANG, L. Z., KYLE, S., WHITE, A. W., CALVERT, A. H., CURTIN, N. J., DURKACZ, B. W., HOSTOMSKY, Z. & NEWELL, D. R. 2000. Potentiation of temozolomide and topotecan growth inhibition and cytotoxicity by novel poly(adenosine diphosphoribose) polymerase inhibitors in a panel of human tumor cell lines. *Clin Cancer Res,* 6**,** 2860-67.

DELLA-MARIA, J., ZHOU, Y., TSAI, M. S., KUHNLEIN, J., CARNEY, J. P., PAULL, T. T. & TOMKINSON, A. E. 2011. Human Mre11/human Rad50/Nbs1 and DNA ligase IIIalpha/XRCC1 protein complexes act together in an alternative nonhomologous end joining pathway. *J Biol Chem,* 286**,** 33845-53.

DEMPLE, B. & HARRISON, L. 1994. Repair of oxidative damage to DNA: enzymology and biology. *Annual review of biochemistry,* 63**,** 915-48.

DEMPLE, B., HERMAN, T. & CHEN, D. S. 1991. Cloning and expression of APE, the cDNA encoding the major human apurinic endonuclease: definition of a family of DNA repair enzymes. *Proceedings of the National Academy of Sciences of the United States of America,* 88**,** 11450-4.

DEMPLE, B. & SUNG, J. S. 2005. Molecular and biological roles of Ape1 protein in mammalian base excision repair. *DNA Repair (Amst),* 4**,** 1442-9.

DENG, C., BROWN, J. A. M., YOU, D. & BROWN, J. A. M. 2005. Multiple endonucleases function to repair covalent topoisomerase I complexes in Saccharomyces cerevisiae. *Genetics,* 170**,** 591-600.

DENG, N., ZHANG, J., ZONG, C., WANG, Y., LU, H., YANG, P., WANG, W., YOUNG, G. W., WANG, Y., KORGE, P., LOTZ, C., DORAN, P., LIEM, D. A., APWEILER, R., WEISS, J. N., DUAN, H. & PING, P. 2011. Phosphoproteome analysis reveals regulatory sites in major pathways of cardiac mitochondria. *Mol Cell Proteomics,* 10**,** M110 000117.

DERIANO, L., STRACKER, T. H., BAKER, A., PETRINI, J. H. J. & ROTH, D. B. 2009. Roles for NBS1 in Alternative Nonhomologous End-Joining of V(D)J Recombination Intermediates. *Molecular Cell,* 34**,** 13-25.

DESAI, S., ZHANG, H., RODRIGUEZ-BAUMAN, A., YANG, J., WU, X., GOUNDER, M., RUBIN, E. & LIU, L. F. 2003. Transcription-dependent degradation of topoisomerase I-DNA covalent complexes. *Molecular and cellular biology,* 23**,** 2341-50.

DETMER, S. A. & CHAN, D. C. 2007. Functions and dysfunctions of mitochondrial dynamics. *Nature reviews. Molecular cell biology,* 8**,** 870-79.

DEXHEIMER, T. S., GEDIYA, L. K., STEPHEN, A. G., WEIDLICH, I., ANTONY, S., MARCHAND, C., INTERTHAL, H., NICKLAUS, M., FISHER, R. J., NJAR, V. C. & POMMIER, Y. 2009. 4-Pregnen-21-ol-3,20-dione-21-(4-bromobenzenesulfonate) (NSC 88915) and related novel steroid derivatives as tyrosyl-DNA phosphodiesterase (Tdp1) inhibitors. *Journal of medicinal chemistry,* 52**,** 7122-31.

DEXHEIMER, T. S., STEPHEN, A. G., FIVASH, M. J., FISHER, R. J. & POMMIER, Y. 2010. The DNA binding and 3'-end preferential activity of human tyrosyl-DNA phosphodiesterase. *Nucleic acids research,* 38**,** 2444-52.

DI VIRGILIO, M., CALLEN, E., YAMANE, A., ZHANG, W., JANKOVIC, M., GITLIN, A. D., FELDHAHN, N., RESCH, W., OLIVEIRA, T. Y., CHAIT, B. T., NUSSENZWEIG, A., CASELLAS, R., ROBBIANI, D. F. & NUSSENZWEIG, M. C. 2013. Rif1 prevents resection of DNA breaks and promotes immunoglobulin class switching. *Science,* 339**,** 711-5.

DIANOV, G., BISCHOFF, C., SUNESEN, M. & BOHR, V. A. 1999. Repair of 8-oxoguanine in DNA is deficient in Cockayne syndrome group B cells. *Nucleic Acids Research,* 27**,** 1365-68.

DIBIASE, S. J., ZENG, Z. C., CHEN, R., HYSLOP, T., CURRAN, W. J. & ILIAKIS, G. 2000. DNA-dependent protein kinase stimulates an independently active, nonhomologous, end-joining apparatus. *Cancer Research,* 60**,** 1245-53.

DIDERICH, K., ALANAZI, M. & HOEIJMAKERS, J. H. 2011. Premature aging and cancer in nucleotide excision repair-disorders. *DNA Repair (Amst),* 10**,** 772-80.

DIGATE, R. J. & MARIANS, K. J. 1988. Identification of a potent decatenating enzyme from Escherichia coli. *Journal of Biological Chemistry,* 263**,** 13366-73.

DOHMEN, R. J. 2004. SUMO protein modification. *Biochim Biophys Acta,* 1695**,** 113-31.

DOIL, C., MAILAND, N., BEKKER-JENSEN, S., MENARD, P., LARSEN, D. H., PEPPERKOK, R., ELLENBERG, J., PANIER, S., DUROCHER, D., BARTEK, J., LUKAS, J. & LUKAS, C. 2009. RNF168 binds and amplifies ubiquitin conjugates on damaged chromosomes to allow accumulation of repair proteins. *Cell,* 136**,** 435-46.

DONALDSON, A. D. & BLOW, J. J. 1999. The regulation of replication origin activation. *Curr Opin Genet Dev,* 9**,** 62-8.

DOU, H., HUANG, C., VAN NGUYEN, T., LU, L. S. & YEH, E. T. 2011. SUMOylation and de-SUMOylation in response to DNA damage. *FEBS Lett,* 585**,** 2891-6.

DOUARRE, C., SOURBIER, C., DALLA ROSA, I., BRATA DAS, B., REDON, C. E., ZHANG, H., NECKERS, L. & POMMIER, Y. 2012. Mitochondrial topoisomerase I is critical for mitochondrial integrity and cellular energy metabolism. *PLoS ONE,* 7**,** e41094.

DRAY, E., ETCHIN, J., WIESE, C., SARO, D., WILLIAMS, G. J., HAMMEL, M., YU, X., GALKIN, V. E., LIU, D., TSAI, M. S., SY, S. M., SCHILD, D., EGELMAN, E., CHEN, J. & SUNG, P. 2010. Enhancement of RAD51 recombinase activity by the tumor suppressor PALB2. *Nat Struct Mol Biol,* 17**,** 1255-9.

DRUMMOND, J. T., LI, G. M., LONGLEY, M. J. & MODRICH, P. 1995. Isolation of an hMSH2-p160 heterodimer that restores DNA mismatch repair to tumor cells. *Science (New York, N.Y.),* 268**,** 1909-12.

DUDLEY, D. D., CHAUDHURI, J., BASSING, C. H. & ALT, F. W. 2005. Mechanism and control of V(D)J recombination versus class switch recombination: Similarities and differences. *Advances in Immunology,* 86**,** 43-112.

DUMAZ, N. & MEEK, D. W. 1999. Serine15 phosphorylation stimulates p53 transactivation but does not directly influence interaction with HDM2. *EMBO J,* 18**,** 7002-10.

DUNCAN, B. K. & MILLER, J. H. 1980. Mutagenic deamination of cytosine residues in DNA. *Nature,* 287**,** 560-61.

DURAND-DUBIEF, M., SVENSSON, J. P., PERSSON, J. & EKWALL, K. 2011. Topoisomerases, chromatin and transcription termination. *Transcription,* 2**,** 66-70.

DYKHUIZEN, E. C., HARGREAVES, D. C., MILLER, E. L., CUI, K., KORSHUNOV, A., KOOL, M., PFISTER, S., CHO, Y.-J., ZHAO, K. & CRABTREE, G. R. 2013. BAF complexes facilitate decatenation of DNA by topoisomerase IIα. *Nature,* 497**,** 624-7.

EDGERTON, H., JOHANSSON, M., KEIFENHEIM, D., MUKHERJEE, S., CHACÓN, J. M., BACHANT, J., GARDNER, M. K. & CLARKE, D. J. 2016. A noncatalytic function of the topoisomerase II CTD in Aurora B recruitment to inner centromeres during mitosis. *The Journal of cell biology,* 213**,** 651-64.

EKSTRAND, M. I., FALKENBERG, M., RANTANEN, A., PARK, C. B., GASPARI, M., HULTENBY, K., RUSTIN, P., GUSTAFSSON, C. M. & LARSSON, N.-G. 2004. Mitochondrial transcription factor A regulates mtDNA copy number in mammals. *Human molecular genetics,* 13**,** 935-44.

EL HAGE, A., FRENCH, S. L., BEYER, A. L. & TOLLERVEY, D. 2010. Loss of Topoisomerase I leads to R-loop-mediated transcriptional blocks during ribosomal RNA synthesis. *Genes and Development,* 24**,** 1546-58.

EL HAGE, A., WEBB, S., KERR, A. & TOLLERVEY, D. 2014. Genome-Wide Distribution of RNA-DNA Hybrids Identifies RNase H Targets in tRNA Genes, Retrotransposons and Mitochondria. *PLoS Genetics,* 10**,** e1004716.

EL-DEIRY, W. S., HARPER, J. W., O'CONNOR, P. M., VELCULESCU, V. E., CANMAN, C. E., JACKMAN, J., PIETENPOL, J. A., BURRELL, M., HILL, D. E. & WANG, Y. 1994. WAF1/CIP1 is induced in p53-mediated G1 arrest and apoptosis. *Cancer research,* 54**,** 1169-74.

EL-KHAMISY, S. F. & CALDECOTT, K. W. 2007. DNA single-strand break repair and spinocerebellar ataxia with axonal neuropathy-1. *Neuroscience,* 145**,** 1260-66.

EL-KHAMISY, S. F., KATYAL, S., PATEL, P., JU, L., MCKINNON, P. J. & CALDECOTT, K. W. 2009. Synergistic decrease of DNA single-strand break repair rates in mouse neural cells lacking both Tdp1 and aprataxin. *DNA Repair,* 8**,** 760-66.

EL-KHAMISY, S. F., MASUTANI, M., SUZUKI, H. & CALDECOTT, K. W. 2003. A requirement for PARP-1 for the assembly or stability of XRCC1 nuclear foci at sites of oxidative DNA damage. *Nucleic Acids Research,* 31**,** 5526-33.

EL-KHAMISY, S. F., SAIFI, G. M., WEINFELD, M., JOHANSSON, F., HELLEDAY, T., LUPSKI, J. R. & CALDECOTT, K. W. 2005. Defective DNA single-strand break repair in spinocerebellar ataxia with axonal neuropathy-1. *Nature,* 434**,** 108-13.

ELDER, R. H., JANSEN, J. G., WEEKS, R. J., WILLINGTON, M. A., DEANS, B., WATSON, A. J., MYNETT, K. J., BAILEY, J. A., COOPER, D. P., RAFFERTY, J. A., HEERAN, M. C., WIJNHOVEN, S. W., VAN ZEELAND, A. A. & MARGISON, G. P. 1998. Alkylpurine-DNA-N-glycosylase knockout mice show increased susceptibility to induction of mutations by methyl methanesulfonate. *Molecular and Cellular Biology,* 18**,** 5828-37.

ELSAYED, W., EL-SHAFIE, L., HASSAN, M. K., FARAG, M. A. & EL-KHAMISY, S. F. 2016. Isoeugenol is a selective potentiator of camptothecin cytotoxicity in vertebrate cells lacking TDP1. *Sci Rep,* 6**,** 26626.

ERRICO, M. D., PARLANTI, E., TESON, M., DE, B. M. B., DEGAN, P., CALCAGNILE, A., CRESCENZI, M., PEDRINI, A. M. A. M., EGLY, J.-M., ZAMBRUNO, G., STEFANINI, M., DIZDAROGLU, M., DOGLIOTTI, E., D'ERRICO, M., DE JESUS, B. M. B. B. M. B., JARUGA, P., BJØRÅS, M. & OTHERS 2006. New functions of XPC in the protection of human skin cells from oxidative damage. *The EMBO journal,* 25**,** 4305-05.

ESCRIBANO-DIAZ, C., ORTHWEIN, A., FRADET-TURCOTTE, A., XING, M., YOUNG, J. T., TKAC, J., COOK, M. A., ROSEBROCK, A. P., MUNRO, M., CANNY, M. D., XU, D. & DUROCHER, D. 2013. A cell cycle-dependent regulatory circuit composed of 53BP1-RIF1 and BRCA1-CtIP controls DNA repair pathway choice. *Mol Cell,* 49**,** 872-83.

ESSERS, M. A. G. & TRUMPP, A. 2010. Targeting leukemic stem cells by breaking their dormancy. *Molecular oncology,* 4**,** 443-50.

EVANS, E., MOGGS, J. G., HWANG, J. R., EGLY, J. M. & WOOD, R. D. 1997. Mechanism of open complex and dual incision formation by human nucleotide excision repair factors. *The EMBO journal,* 16**,** 6559-73.

EVANS, M. D., DIZDAROGLU, M. & COOKE, M. S. 2004. Oxidative DNA damage and disease: Induction, repair and significance. *Mutation Research - Reviews in Mutation Research,* 567**,** 1-61.

FACOMPRÉ, M., TARDY, C., BAL-MAHIEU, C., COLSON, P., PEREZ, C., MANZANARES, I., CUEVAS, C. & BAILLY, C. 2003. Lamellarin D: a novel potent inhibitor of topoisomerase I. *Cancer research,* 63**,** 7392-9.

FAGBEMI, A. F., ORELLI, B. & SCHÄRER, O. D. 2011. Regulation of endonuclease activity in human nucleotide excision repair. *DNA repair,* 10**,** 722-29.

FALASCHI, A. 2009. Binding of DNA topoisomerases I and II to replication origins. *Methods in molecular biology (Clifton, N.J.),* 582**,** 131-43.

FALASCHI, A., ABDURASHIDOVA, G., SANDOVAL, O., RADULESCU, S., BIAMONTI, G. & RIVA, S. 2007. Molecular and structural transactions at human DNA replication origins. *Cell Cycle,* 6**,** 1705-12.

FALCK, J., MAILAND, N., SYLJUÅSEN, R. G., BARTEK, J. & LUKAS, J. 2001. The ATM-Chk2-Cdc25A checkpoint pathway guards against radioresistant DNA synthesis. *Nature,* 410**,** 842-47.

FALCK, J., PETRINI, J. H. J., WILLIAMS, B. R., LUKAS, J. & BARTEK, J. 2002. The DNA damage-dependent intra-S phase checkpoint is regulated by parallel pathways. *Nature genetics,* 30**,** 290-94.

FALKENBERG, M., GASPARI, M., RANTANEN, A., TRIFUNOVIC, A., LARSSON, N.-G. & GUSTAFSSON, C. M. 2002. Mitochondrial transcription factors B1 and B2 activate transcription of human mtDNA. *Nat. Genet,* 31**,** 289-94.

FALKENBERG, M., LARSSON, N.-G. & GUSTAFSSON, C. M. 2007. DNA replication and transcription in mammalian mitochondria. *Annual review of biochemistry,* 76**,** 679-99.

FAM, H. K., CHOWDHURY, M. K., WALTON, C., CHOI, K., BOERKOEL, C. F. & HENDSON, G. 2013a. Expression profile and mitochondrial colocalization of Tdp1 in peripheral human tissues. *J Mol Histol,* 44**,** 481-94.

FAM, H. K., WALTON, C., MITRA, S. A., CHOWDHURY, M., OSBORNE, N., CHOI, K., SUN, G., WONG, P. C. W., O'SULLIVAN, M. J., TURASHVILI, G., APARICIO, S., TRICHE, T. J., BOND, M., PALLEN, C. J. & BOERKOEL, C. F. 2013b. TDP1 and PARP1 deficiency are cytotoxic to rhabdomyosarcoma cells. *Molecular cancer research : MCR,* 11**,** 1179-92.

FARR, C. J., ANTONIOU-KOUROUNIOTI, M., MIMMACK, M. L., VOLKOV, A. & PORTER, A. C. G. 2014. The α isoform of topoisomerase II is required for hypercompaction of mitotic chromosomes in human cells. *Nucleic Acids Research,* 42**,** 4414-26.

FEKAIRI, S., SCAGLIONE, S., CHAHWAN, C., TAYLOR, E. R., TISSIER, A., COULON, S., DONG, M. Q., RUSE, C., YATES, J. R., 3RD, RUSSELL, P., FUCHS, R. P., MCGOWAN, C. H. & GAILLARD, P. H. 2009. Human SLX4 is a Holliday junction resolvase subunit that binds multiple DNA repair/recombination endonucleases. *Cell,* 138**,** 78-89.

FENG, L., FONG, K. W., WANG, J., WANG, W. & CHEN, J. 2013. RIF1 counteracts BRCA1-mediated end resection during DNA repair. *J Biol Chem,* 288**,** 11135-43.

FERRANTE, R. J., SHINOBU, L. A., SCHULZ, J. B., MATTHEWS, R. T., THOMAS, C. E., KOWALL, N. W., GURNEY, M. E. & BEAL, M. F. 1997. Increased 3-nitrotyrosine and oxidative damage in mice with a human copper/zinc superoxide dismutase mutation. *Ann Neurol,* 42**,** 326-34.

FIELDS, S. & SONG, O. 1989. A novel genetic system to detect protein-protein interactions. *Nature,* 340**,** 245-6.

FILOMENI, G., ZIO, D. D., CECCONI, F., DE ZIO, D. & CECCONI, F. 2015. Oxidative stress and autophagy: the clash between damage and metabolic needs. *Cell Death and Differentiation,* 22**,** 377-88.

FISHER, A. E. O., HOCHEGGER, H., TAKEDA, S. & CALDECOTT, K. W. 2007. Poly(ADP-ribose) polymerase 1 accelerates single-strand break repair in concert with poly(ADP-ribose) glycohydrolase. *Molecular and cellular biology,* 27**,** 5597-605.

FLATTEN, K., DAI, N. T., VROMAN, B. T., LOEGERING, D., ERLICHMAN, C., KARNITZ, L. M. & KAUFMANN, S. H. 2005. The role of checkpoint kinase 1 in sensitivity to topoisomerase I poisons. *Journal of Biological Chemistry,* 280**,** 14349-55.

FLOHR, C., BÜRKE, A., RADICELLA, J. P. & EPE, B. 2003. Poly(ADP-ribosyl)ation accelerates DNA repair in a pathway dependent on Cockayne syndrome B protein. *Nucleic Acids Research,* 31**,** 5332-37.

FLORES-ROZAS, H., CLARK, D. & KOLODNER, R. D. 2000. Proliferating cell nuclear antigen and Msh2p-Msh6p interact to form an active mispair recognition complex. *Nature genetics,* 26**,** 375-8.

FORREST, A. & GABRIELLI, B. 2001. Cdc25B activity is regulated by 14-3-3. *Oncogene,* 20**,** 4393-401.

FORTERRE, P., GRIBALDO, S., GADELLE, D. & SERRE, M.-C. 2007. Origin and evolution of DNA topoisomerases. *Biochimie,* 89**,** 427-46.

FOUSTERI, M., VERMEULEN, W., VAN ZEELAND, A. A. & MULLENDERS, L. H. F. 2006. Cockayne Syndrome A and B Proteins Differentially Regulate Recruitment of Chromatin Remodeling and Repair Factors to Stalled RNA Polymerase II In Vivo. *Molecular Cell,* 23**,** 471-82.

FRANKEN, N. A., RODERMOND, H. M., STAP, J., HAVEMAN, J. & VAN BREE, C. 2006. Clonogenic assay of cells in vitro. *Nat Protoc,* 1**,** 2315-19.

FRENCH, S. L., SIKES, M. L., HONTZ, R. D., OSHEIM, Y. N., LAMBERT, T. E., EL HAGE, A., SMITH, M. M., TOLLERVEY, D., SMITH, J. S. & BEYER, A. L. 2011. Distinguishing the roles of Topoisomerases I and II in relief of transcription-induced torsional stress in yeast rRNA genes. *Mol Cell Biol,* 31**,** 482-94.

FRESE-SCHAPER, M., KEIL, A., STEINER, S. K., GUGGER, M., KORNER, M., KOCHER, G. J., SCHIFFER, L., ANDERS, H. J., HUYNH-DO, U., SCHMID, R. A. & FRESE, S. 2014. Low-dose irinotecan

improves advanced lupus nephritis in mice potentially by changing DNA relaxation and anti-double-stranded DNA binding. *Arthritis Rheumatol,* 66**,** 2259-69.

FRIDOVICH, I. 1986. Superoxide dismutases. *Advances in enzymology and related areas of molecular biology,* 58**,** 61-97.

FRIEDBERG, E. C., WALKER, G. C., SIEDE, W., WOOD, R. D., SCHULTZ, R. A. & ELLENBURGER, T. 2006. *DNA repair and mutagenesis*, ASM Press, 10.1097/01.shk.0000232588.61871.ff.

FRIEDMAN, J. R. & NUNNARI, J. 2014. Mitochondrial form and function. *Nature,* 505**,** 335-43.

FU, D., CALVO, J. A. & SAMSON, L. D. 2012. Balancing repair and tolerance of DNA damage caused by alkylating agents. *Nature reviews. Cancer,* 12**,** 104-20.

FU, X., WAN, S., LYU, Y. L., LIU, L. F. & QI, H. 2008. Etoposide induces ATM-dependent mitochondrial biogenesis through AMPK activation. *PLoS ONE,* 3**,** e2009.

FURUKAWA, Y., KANEKO, K., YAMANAKA, K., O'HALLORAN, T. V. & NUKINA, N. 2008. Complete loss of post-translational modifications triggers fibrillar aggregation of SOD1 in the familial form of amyotrophic lateral sclerosis. *Journal of Biological Chemistry,* 283**,** 24167-76.

GAGGIOLI, V., LE VIET, B., GERME, T. & HYRIEN, O. 2013. DNA topoisomerase II?? controls replication origin cluster licensing and firing time in Xenopus egg extracts. *Nucleic Acids Research,* 41**,** 7313-31.

GALISSON, F., MAHROUCHE, L., COURCELLES, M., BONNEIL, E., MELOCHE, S., CHELBI-ALIX, M. K. & THIBAULT, P. 2011. A novel proteomics approach to identify SUMOylated proteins and their modification sites in human cells. *Mol Cell Proteomics,* 10**,** M110 004796.

GAO, H., COYLE, D. L., MEYER-FICCA, M. L., MEYER, R. G., JACOBSON, E. L., WANG, Z. Q. & JACOBSON, M. K. 2007. Altered poly(ADP-ribose) metabolism impairs cellular responses to genotoxic stress in a hypomorphic mutant of poly(ADP-ribose) glycohydrolase. *Experimental Cell Research,* 313**,** 984-96.

GAO, R., DAS, B. B., CHATTERJEE, R., ABAAN, O. D., AGAMA, K., MATUO, R., VINSON, C., MELTZER, P. S. & POMMIER, Y. 2014. Epigenetic and genetic inactivation of tyrosyl-DNA-phosphodiesterase 1 (TDP1) in human lung cancer cells from the NCI-60 panel. *DNA repair,* 13**,** 1-9.

GAO, Y., KATYAL, S., LEE, Y., ZHAO, J., REHG, J. E., RUSSELL, H. R. & MCKINNON, P. J. 2011. DNA ligase III is critical for mtDNA integrity but not Xrcc1-mediated nuclear DNA repair. *Nature,* 471**,** 240-4.

GARCÍA-DÍAZ, M., BEBENEK, K., KUNKEL, T. A. & BLANCO, L. 2001. Identification of an intrinsic 5'-deoxyribose-5-phosphate lyase activity in human DNA polymerase lambda: a possible role in base excision repair. *The Journal of biological chemistry,* 276**,** 34659-63.

GARCIA-DOMINGUEZ, M. 2013. *SUMO Tasks in Chromatin Remodeling*, InTech, 10.5772/55395.

GATEI, M., SCOTT, S. P., FILIPPOVITCH, I., SORONIKA, N., LAVIN, M. F., WEBER, B. & KHANNA, K. K. 2000a. Role for ATM in DNA damage-induced phosphorylation of BRCA1. *Cancer Research,* 60**,** 3299-304.

GATEI, M., YOUNG, D., CEROSALETTI, K. M., DESAI-MEHTA, A., SPRING, K., KOZLOV, S., LAVIN, M. F., GATTI, R. A., CONCANNON, P. & KHANNA, K. 2000b. ATM-dependent phosphorylation of nibrin in response to radiation exposure. *Nature genetics,* 25**,** 115-19.

GAVIN, I., HORN, P. J. & PETERSON, C. L. 2001. SWI/SNF chromatin remodeling requires changes in DNA topology. *Molecular Cell,* 7**,** 97-104.

GERSON, S. L. 2004. MGMT: its role in cancer aetiology and cancer therapeutics. *Nature reviews. Cancer,* 4**,** 296-307.

GERTZ, B., WONG, M. & MARTIN, L. J. 2012. Nuclear localization of human SOD1 and mutant SOD1-specific disruption of survival motor neuron protein complex in transgenic amyotrophic lateral sclerosis mice. *J Neuropathol Exp Neurol,* 71**,** 162-77.

GEUTING, V., REUL, C. & LÖBRICH, M. 2013. ATM Release at Resected Double-Strand Breaks Provides Heterochromatin Reconstitution to Facilitate Homologous Recombination. *PLoS Genetics,* 9**,** e1003667.

GILLET, L. C. J. & SCHÄRER, O. D. 2006. Molecular mechanisms of mammalian global genome nucleotide excision repair. *Chemical reviews,* 106**,** 253-76.

GOCKE, C. B., YU, H. & KANG, J. 2005. Systematic identification and analysis of mammalian small ubiquitin-like modifier substrates. *Journal of Biological Chemistry,* 280**,** 5004-12.

GOETZ, J. D., MOTYCKA, T. A., HAN, M., JASIN, M. & TOMKINSON, A. E. 2005. Reduced repair of DNA double-strand breaks by homologous recombination in a DNA ligase I-deficient human cell line. *DNA Repair (Amst),* 4**,** 649-54.

GOLDSBY, R. E., HAYS, L. E., CHEN, X., OLMSTED, E. A., SLAYTON, W. B., SPANGRUDE, G. J. & PRESTON, B. D. 2002. High incidence of epithelial cancers in mice deficient for DNA polymerase delta proofreading. *Proceedings of the National Academy of Sciences of the United States of America,* 99**,** 15560-5.

GOLDSTEIN, S., MEYERSTEIN, D. & CZAPSKI, G. 1993. The Fenton reagents. *Free Radical Biology and Medicine,* 15**,** 435-45.

GÓMEZ-HERREROS, F., ROMERO-GRANADOS, R., ZENG, Z., ALVAREZ-QUILÓN, A., QUINTERO, C., JU, L., UMANS, L., VERMEIRE, L., HUYLEBROECK, D., CALDECOTT, K. W. & CORTÉS-LEDESMA, F. 2013. TDP2-dependent non-homologous end-joining protects against topoisomerase II-induced DNA breaks and genome instability in cells and in vivo. *PLoS genetics,* 9**,** e1003226-e26.

GONG, B., CHEN, Q. & ALMASAN, A. 1998. Ionizing radiation stimulates mitochondrial gene expression and activity. *Radiation research,* 150**,** 505-12.

GONZALEZ, R. E., LIM, C.-U., COLE, K., BIANCHINI, C. H., SCHOOLS, G. P., DAVIS, B. E., WADA, I., RONINSON, I. B. & BROUDE, E. V. 2011. Effects of conditional depletion of topoisomerase II on cell cycle progression in mammalian cells. *Cell cycle (Georgetown, Tex.),* 10**,** 3505-14.

GOODARZI, A. A., KURKA, T. & JEGGO, P. A. 2011. KAP-1 phosphorylation regulates CHD3 nucleosome remodeling during the DNA double-strand break response. *Nat Struct Mol Biol,* 18**,** 831-9.

GOTO, Y., HAYASHI, R., KANG, D. & YOSHIDA, K. 2006. Acute loss of transcription factor E2F1 induces mitochondrial biogenesis in HeLa cells. *J Cell Physiol,* 209**,** 923-34.

GOTTLIEB, T. M. & JACKSON, S. P. 1993. The DNA-dependent protein kinase: Requirement for DNA ends and association with Ku antigen. *Cell,* 72**,** 131-42.

GRAVEL, S., CHAPMAN, J. R., MAGILL, C. & JACKSON, S. P. 2008. DNA helicases Sgs1 and BLM promote DNA double-strand break resection. *Genes Dev,* 22**,** 2767-72.

GRAWUNDER, U., WILM, M., WU, X., KULESZA, P., WILSON, T. E., MANN, M. & LIEBER, M. R. 1997. Activity of DNA ligase IV stimulated by complex formation with XRCC4 protein in mammalian cells. *Nature,* 388**,** 492-95.

GRAWUNDER, U., ZIMMER, D. & LIEBER, M. R. 1998. DNA ligase IV binds to XRCC4 via a motif located between rather than within its BRCT domains. *Current Biology,* 8**,** 873-79.

GRUNDY, G. J., RULTEN, S. L., ZENG, Z., ARRIBAS-BOSACOMA, R., ILES, N., MANLEY, K., OLIVER, A. & CALDECOTT, K. W. 2013. APLF promotes the assembly and activity of non-homologous end joining protein complexes. *EMBO J,* 32**,** 112-25.

GU, L., HONG, Y., MCCULLOCH, S., WATANABE, H. & LI, G. M. 1998. ATP-dependent interaction of human mismatch repair proteins and dual role of PCNA in mismatch repair. *Nucleic Acids Research,* 26**,** 1173-78.

GUDNASON, H., DUFVA, M., BANG, D. D. & WOLFF, A. 2007. Comparison of multiple DNA dyes for real-time PCR: effects of dye concentration and sequence composition on DNA amplification and melting temperature. *Nucleic Acids Res,* 35**,** e127.

GUILLET, M. & BOITEUX, S. 2002. Endogenous DNA abasic sites cause cell death in the absence of Apn1, Apn2 and Rad1/Rad10 in Saccharomyces cerevisiae. *The EMBO journal,* 21**,** 2833-41.

GUO, D., DEXHEIMER, T. S., POMMIER, Y. & NASH, H. A. 2014. Neuroprotection and repair of 3'-blocking DNA ends by glaikit (gkt) encoding Drosophila tyrosyl-DNA phosphodiesterase 1 (TDP1). *Proc Natl Acad Sci U S A,* 111**,** 15816-20.

GUO, J., HANAWALT, P. C. & SPIVAK, G. 2013. Comet-FISH with strand-specific probes reveals transcription-coupled repair of 8-oxoGuanine in human cells. *Nucleic Acids Research,* 41**,** 7700-12.

GUO, S., PRESNELL, S. R., YUAN, F., ZHANG, Y., GU, L. & LI, G. M. 2004. Differential Requirement for Proliferating Cell Nuclear Antigen in 5??? and 3??? Nick-directed Excision in Human Mismatch Repair. *Journal of Biological Chemistry,* 279**,** 16912-17.

GUO, S., ZHANG, Y., YUAN, F., GAO, Y., GU, L., WONG, I. & LI, G.-M. 2006. Regulation of replication protein A functions in DNA mismatch repair by phosphorylation. *The Journal of biological chemistry,* 281**,** 21607-16.

GURNEY, M. E., PU, H., CHIU, A. Y., DAL CANTO, M. C., POLCHOW, C. Y., ALEXANDER, D. D., CALIENDO, J., HENTATI, A., KWON, Y. W., DENG, H.-X., CHEN, W., ZHAI, P., SUFIT, R. L. & SIDDIQUE, T. 1994. Motor neuron degeneration in mice that express a human Cu,Zn superoxide dismutase mutation. *Science,* 264**,** 1772-75.

HABER, F. & WEISS, J. 1934. The Catalytic Decomposition of Hydrogen Peroxide by Iron Salts. *Proceedings of the Royal Society A: Mathematical, Physical and Engineering Sciences,* 147**,** 332-51.

HABRAKEN, Y. & VERLY, W. G. 1988. Further purification and characterization of the DNA 3'-phosphatase from rat-liver chromatin which is also a polynuclotide 5'-hydroxyl kinase. *European Journal of Biochemistry,* 171**,** 59-66.

HAFFNER, M. C., ARYEE, M. J., TOUBAJI, A., ESOPI, D. M., ALBADINE, R., GUREL, B., ISAACS, W. B., BOVA, G. S., LIU, W., XU, J., MEEKER, A. K., NETTO, G., DE MARZO, A. M., NELSON, W. G. & YEGNASUBRAMANIAN, S. 2010. Androgen-induced TOP2B-mediated double-strand breaks and prostate cancer gene rearrangements. *Nature genetics,* 42**,** 668-75.

HAFFNER, M. C., DE MARZO, A. M., MEEKER, A. K., NELSON, W. G. & YEGNASUBRAMANIAN, S. 2011. Transcription-induced DNA double strand breaks: both oncogenic force and potential therapeutic target? *Clinical cancer research : an official journal of the American Association for Cancer Research,* 17**,** 3858-64.

HALL-JACKSON, C. A., CROSS, D. A., MORRICE, N. & SMYTHE, C. 1999. ATR is a caffeine-sensitive, DNA-activated protein kinase with a substrate specificity distinct from DNA-PK. *Oncogene,* 18**,** 6707-13.

HAMILTON, N. K. & MAIZELS, N. 2010. MRE11 function in response to topoisomerase poisons is independent of its function in double-strand break repair in Saccharomyces cerevisiae. *PLoS ONE,* 5**,** e15387.

HAN, J.-Y., LEE, G. K., YOO, S. Y., YOON, S. J., CHO, E. Y., KIM, H. T. & LEE, J. S. 2010. Association of SUMO1 and UBC9 genotypes with tumor response in non-small-cell lung cancer treated with irinotecan-based chemotherapy. *The pharmacogenomics journal,* 10**,** 86-93.

HANAWALT, P. C. & SPIVAK, G. 2008. Transcription-coupled DNA repair: two decades of progress and surprises. *Nature reviews. Molecular cell biology,* 9**,** 958-70.

HANCE, N., EKSTRAND, M. I. & TRIFUNOVIC, A. 2005. Mitochondrial DNA polymerase gamma is essential for mammalian embryogenesis. *Human Molecular Genetics,* 14**,** 1775-83.

HARDELAND, U., BENTELE, M., JIRICNY, J. & SCHAR, P. 2000. Separating substrate recognition from base hydrolysis in human thymine DNA glycosylase by mutational analysis. *Journal of Biological Chemistry,* 275**,** 33449-56.

HARRIGAN, J. A., FAN, J., MOMAND, J., PERRINO, F. W., BOHR, V. A. & WILSON, D. M. 2007. WRN exonuclease activity is blocked by DNA termini harboring 3′ obstructive groups. *Mechanisms of Ageing and Development,* 128**,** 259-66.

HARTLERODE, A. J. & SCULLY, R. 2009. Mechanisms of double-strand break repair in somatic mammalian cells. *Biochem J,* 423**,** 157-68.

HARTSUIKER, E. 2011. Detection of covalent DNA-bound Spo11 and topoisomerase complexes. *Methods in molecular biology (Clifton, N.J.),* 745**,** 65-77.

HARTSUIKER, E., MIZUNO, K., MOLNAR, M., KOHLI, J., OHTA, K. & CARR, A. M. 2009. Ctp1CtIP and Rad32Mre11 nuclease activity are required for Rec12Spo11 removal, but Rec12Spo11 removal is dispensable for other MRN-dependent meiotic functions. *Molecular and cellular biology,* 29**,** 1671-81.

HARTUNG, F., SUER, S., KNOLL, A., WURZ-WILDERSINN, R. & PUCHTA, H. 2008. Topoisomerase 3alpha and RMI1 suppress somatic crossovers and are essential for resolution of meiotic recombination intermediates in Arabidopsis thaliana. *PLoS genetics,* 4**,** e1000285-e85.

HATEFI, Y. 1985. The mitochondrial electron transport and oxidative phosphorylation system. *Annual review of biochemistry,* 54**,** 1015-69.

HAUPT, S., BERGER, M., GOLDBERG, Z. & HAUPT, Y. 2003. Apoptosis - the p53 network. *Journal of cell science,* 116**,** 4077-85.

HAWKINS, A. J., SUBLER, M. A., AKOPIANTS, K., WILEY, J. L., TAYLOR, S. M., RICE, A. C., WINDLE, J. J., VALERIE, K. & POVIRK, L. F. 2009. In vitro complementation of Tdp1 deficiency indicates a stabilized enzyme-DNA adduct from tyrosyl but not glycolate lesions as a consequence of the SCAN1 mutation. *DNA repair,* 8**,** 654-63.

HAYWOOD, R., ANDRADY, C., KASSOUF, N. & SHEPPARD, N. 2011. Intensity-dependent direct solar radiation- and UVA-induced radical damage to human skin and DNA, lipids and proteins. *Photochemistry and Photobiology,* 87**,** 117-30.

HAYWOOD, R., ROGGE, F. & LEE, M. 2008. Protein, lipid, and DNA radicals to measure skin UVA damage and modulation by melanin. *Free radical biology & medicine,* 44**,** 990-1000.

HEIDEKER, J., PRUDDEN, J., PERRY, J. J., TAINER, J. A. & BODDY, M. N. 2011. SUMO-targeted ubiquitin ligase, Rad60, and Nse2 SUMO ligase suppress spontaneous Top1-mediated DNA damage and genome instability. *PLoS Genet,* 7**,** e1001320.

HEKMAT-NEJAD, M., YOU, Z., YEE, M.-C., NEWPORT, J. W. & CIMPRICH, K. A. 2000. Xenopus ATR is a replication-dependent chromatin-binding protein required for the DNA replication checkpoint. *Current Biology,* 10**,** 1565-73.

HELLEDAY, T. 2011. The underlying mechanism for the PARP and BRCA synthetic lethality: clearing up the misunderstandings. *Molecular oncology,* 5**,** 387-93.

HENNING, K. A., LI, L., IYER, N., MCDANIEL, L. D., REAGAN, M. S., LEGERSKI, R., SCHULTZ, R. A., STEFANINI, M., LEHMANN, A. R., MAYNE, L. V. & FRIEDBERG, E. C. 1995. The Cockayne syndrome group A gene encodes a WD repeat protein that interacts with CSB protein and a subunit of RNA polymerase II TFIIH. *Cell,* 82**,** 555-64.

HEO, J., LI, J., SUMMERLIN, M., HAYS, A., KATYAL, S., MCKINNON, P. J., NITISS, K. C., NITISS, J. L. & HANAKAHI, L. A. 2015. TDP1 promotes assembly of non-homologous end joining protein complexes on DNA. *DNA repair,* 30**,** 28-37.

HERMANSON-MILLER, I. L. & TURCHI, J. J. 2002. Strand-specific binding of RPA and XPA to damaged duplex DNA. *Biochemistry,* 41**,** 2402-08.

HERMEKING, H., LENGAUER, C., POLYAK, K., HE, T. C., ZHANG, L., THIAGALINGAM, S., KINZLER, K. W. & VOGELSTEIN, B. 1997. 14-3-3 sigma is a p53-regulated inhibitor of G2/M progression. *Molecular cell,* 1**,** 3-11.

HICKSON, I. D. & MANKOURI, H. W. 2011. Processing of homologous recombination repair intermediates by the Sgs1-Top3-Rmi1 and Mus81-Mms4 complexes. *Cell Cycle,* 10**,** 3078-85.

HILL, J. W., HAZRA, T. K., IZUMI, T. & MITRA, S. 2001. Stimulation of human 8-oxoguanine-DNA glycosylase by AP-endonuclease: potential coordination of the initial steps in base excision repair. *Nucleic acids research,* 29**,** 430-38.

HINZ, J. M. 2010. Role of homologous recombination in DNA interstrand crosslink repair. *Environ Mol Mutagen,* 51**,** 582-603.

HIRANO, R., INTERTHAL, H., HUANG, C., NAKAMURA, T., DEGUCHI, K., CHOI, K., BHATTACHARJEE, M. B., ARIMURA, K., UMEHARA, F., IZUMO, S., NORTHROP, J. L., SALIH, M. A. M., INOUE, K., ARMSTRONG, D. L., CHAMPOUX, J. J., TAKASHIMA, H. & BOERKOEL, C. F. 2007. Spinocerebellar ataxia with axonal neuropathy: consequence of a Tdp1 recessive neomorphic mutation? *The EMBO journal,* 26**,** 4732-43.

HIRANO, T. & MITCHISON, T. J. 1993. Topoisomerase II does not play a scaffolding role in the organization of mitotic chromosomes assembled in Xenopus egg extracts. *The Journal of cell biology,* 120**,** 601-12.

HIRAO, A., KONG, Y. Y., MATSUOKA, S., WAKEHAM, A., RULAND, J., YOSHIDA, H., LIU, D., ELLEDGE, S. J. & MAK, T. W. 2000. DNA damage-induced activation of p53 by the checkpoint kinase Chk2. *Science,* 287**,** 1824-7.

HOEGE, C., PFANDER, B., MOLDOVAN, G. L., PYROWOLAKIS, G. & JENTSCH, S. 2002. RAD6-dependent DNA repair is linked to modification of PCNA by ubiquitin and SUMO. *Nature,* 419**,** 135-41.

HOEIJMAKERS, J. H. 2001. Genome maintenance mechanisms for preventing cancer. *Nature,* 411**,** 366-74.

HOLM, C., GOTO, T., WANG, J. C. & BOTSTEIN, D. 1985. DNA topoisomerase II is required at the time of mitosis in yeast. *Cell,* 41**,** 553-63.

HOLTHAUSEN, J. T., WYMAN, C. & KANAAR, R. 2010. Regulation of DNA strand exchange in homologous recombination. *DNA Repair (Amst),* 9**,** 1264-72.

HORI, A., YOSHIDA, M., SHIBATA, T. & LING, F. 2009. Reactive oxygen species regulate DNA copy number in isolated yeast mitochondria by triggering recombination-mediated replication. *Nucleic Acids Res,* 37**,** 749-61.

HORIE, K., TOMIDA, A., SUGIMOTO, Y., YASUGI, T., YOSHIKAWA, H., TAKETANI, Y. & TSURUO, T. 2002. SUMO-1 conjugation to intact DNA topoisomerase I amplifies cleavable complex formation induced by camptothecin. *Oncogene,* 21**,** 7913-22.

HOUSE, N. C. M., KOCH, M. R. & FREUDENREICH, C. H. 2014. Chromatin modifications and DNA repair: Beyond double-strand breaks. *Frontiers in Genetics,* 5**,** 296.

HØYER-HANSEN, M. & JÄÄTTELÄ, M. 2007. Connecting endoplasmic reticulum stress to autophagy by unfolded protein response and calcium. *Cell death and differentiation,* 14**,** 1576-82.

HU, H.-G., BAACK, M. & KNIPPERS, R. 2009. Proteins of the origin recognition complex (ORC) and DNA topoisomerases on mammalian chromatin. *BMC molecular biology,* 10**,** 36-36.

HU, Y. F., HAO, Z. L. & LI, R. 1999. Chromatin remodeling and activation of chromosomal DNA replication by an acidic transcriptional activation domain from BRCA1. *Genes Dev,* 13**,** 637-42.

HUANG, M., KIM, J. M., SHIOTANI, B., YANG, K., ZOU, L. & D'ANDREA, A. D. 2010. The FANCM/FAAP24 complex is required for the DNA interstrand crosslink-induced checkpoint response. *Mol Cell,* 39**,** 259-68.

HUANG, S.-Y. N., POMMIER, Y. & MARCHAND, C. 2011. Tyrosyl-DNA Phosphodiesterase 1 (Tdp1) inhibitors. *Expert opinion on therapeutic patents,* 21**,** 1285-92.

HUANG, S. Y. N., MURAI, J., DALLA ROSA, I., DEXHEIMER, T. S., NAUMOVA, A., GMEINER, W. H. & POMMIER, Y. 2013. TDP1 repairs nuclear and mitochondrial DNA damage induced by chain-terminating anticancer and antiviral nucleoside analogs. *Nucleic Acids Research,* 41**,** 7793-803.

HUANG, Y., QURESHI, I. A. & CHEN, H. 1999. Effects of phosphatidylinositol 4,5-bisphosphate and neomycin on phospholipase D: Kinetic studies. *Molecular and Cellular Biochemistry,* 197**,** 195-201.

HUDSON, J. J., CHIANG, S. C., WELLS, O. S., ROOKYARD, C. & EL-KHAMISY, S. 2012. SUMO modification of the neuroprotective protein TDP1 facilitates chromosomal single-strand break repair. *Nature Communications,* 3**,** 713-33.

HULETSKY, A., DE MURCIA, G., MULLER, S., HENGARTNER, M., MENARD, L., LAMARRE, D. & POIRIER, G. G. 1989. The effect of poly(ADP-ribosyl)ation on native and H1-depleted chromatin. A role of poly(ADP-ribosyl)ation on core nucleosome structure. *J. Biol. Chem.,* 264**,** 8878-86.

HUSAIN, A., BEGUM, N. A., TANIGUCHI, T., TANIGUCHI, H., KOBAYASHI, M. & HONJO, T. 2016. Chromatin remodeller SMARCA4 recruits topoisomerase 1 and suppresses transcription-associated genomic instability. *Nature communications,* 7**,** 10549-49.

IDE, H., KOW, Y. W. & WALLACE, S. S. 1985. Thymine glycols and urea residues in M13 DNA constitute replicative blocks in vitro. *Nucleic Acids Research,* 13**,** 8035-52.

IKEHATA, H. & ONO, T. 2011. The mechanisms of UV mutagenesis. *J Radiat Res,* 52**,** 115-25.

ILIAKIS, G., WANG, H., PERRAULT, A. R., BOECKER, W., ROSIDI, B., WINDHOFER, F., WU, W., GUAN, J., TERZOUDI, G. & PANTELIAS, G. 2004. Mechanisms of DNA double strand break repair and chromosome aberration formation. *Cytogenet Genome Res,* 104**,** 14-20.

IMPENS, F., RADOSHEVICH, L., COSSART, P. & RIBET, D. 2014. Mapping of SUMO sites and analysis of SUMOylation changes induced by external stimuli. *Proc Natl Acad Sci U S A,* 111**,** 12432-7.

INAMDAR, K. V., POULIOT, J. J., ZHOU, T., LEES-MILLER, S. P., RASOULI-NIA, A. & POVIRK, L. F. 2002. Conversion of phosphoglycolate to phosphate termini on 3' overhangs of DNA double strand breaks by the human tyrosyl-DNA phosphodiesterase hTdp1. *The Journal of biological chemistry,* 277**,** 27162-8.

INTERTHAL, H. & CHAMPOUX, J. J. 2011. Effects of DNA and protein size on substrate cleavage by human tyrosyl-DNA phosphodiesterase 1. *The Biochemical journal,* 436**,** 559-66.

INTERTHAL, H., CHEN, H. J. & CHAMPOUX, J. J. 2005a. Human Tdp1 cleaves a broad spectrum of substrates, including phosphoamide linkages. *The Journal of biological chemistry,* 280**,** 36518-28.

INTERTHAL, H., CHEN, H. J., KEHL-FIE, T. E., ZOTZMANN, J., LEPPARD, J. B. & CHAMPOUX, J. J. 2005b. SCAN1 mutant Tdp1 accumulates the enzyme--DNA intermediate and causes camptothecin hypersensitivity. *The EMBO journal,* 24**,** 2224-33.

INTERTHAL, H., POULIOT, J. J. & CHAMPOUX, J. J. 2001. The tyrosyl-DNA phosphodiesterase Tdp1 is a member of the phospholipase D superfamily. *Proceedings of the National Academy of Sciences,* 98**,** 12009-14.

IOANOVICIU, A., ANTONY, S., POMMIER, Y., STAKER, B. L., STEWART, L. & CUSHMAN, M. 2005. Synthesis and mechanism of action studies of a series of norindenoisoquinoline topoisomerase I poisons reveal an inhibitor with a flipped orientation in the ternary DNA-enzyme-inhibitor complex as determined by X-ray crystallographic analysis. *J Med Chem,* 48**,** 4803-14.

IRA, G., MALKOVA, A., LIBERI, G., FOIANI, M. & HABER, J. E. 2003. Srs2 and Sgs1-Top3 suppress crossovers during double-strand break repair in yeast. *Cell,* 115**,** 401-11.

IZUMI, T., HAZRA, T. K., BOLDOGH, I., TOMKINSON, A. E., PARK, M. S., IKEDA, S. & MITRA, S. 2000. Requirement for human AP endonuclease 1 for repair of 3'-blocking damage at DNA single-strand breaks induced by reactive oxygen species. *Carcinogenesis,* 21**,** 1329-34.

JACKSON, S. P. 2002. Sensing and repairing DNA double-strand breaks. *Carcinogenesis,* 23**,** 687-96.

JACKSON, S. P. & BARTEK, J. 2009. The DNA-damage response in human biology and disease. *Nature,* 461**,** 1071-8.

JACOBS, A. L. & SCHÄR, P. 2012. DNA glycosylases: In DNA repair and beyond. *Chromosoma,* 121**,** 1-20.

JACQUIAU, H. R., VAN WAARDENBURG, R. C., REID, R. J., WOO, M. H., GUO, H., JOHNSON, E. S. & BJORNSTI, M. A. 2005. Defects in SUMO (small ubiquitin-related modifier) conjugation and deconjugation alter cell sensitivity to DNA topoisomerase I-induced DNA damage. *J Biol Chem,* 280**,** 23566-75.

JAISWAL, M. K. & KELLER, B. U. 2009. Cu/Zn superoxide dismutase typical for familial amyotrophic lateral sclerosis increases the vulnerability of mitochondria and perturbs Ca2+ homeostasis in SOD1G93A mice. *Mol Pharmacol,* 75**,** 478-89.

JAISWAL, M. K., ZECH, W. D., GOOS, M., LEUTBECHER, C., FERRI, A., ZIPPELIUS, A., CARRI, M. T., NAU, R. & KELLER, B. U. 2009. Impairment of mitochondrial calcium handling in a mtSOD1 cell culture model of motoneuron disease. *BMC Neurosci,* 10**,** 64.

JAKOBSEN, A.-K., LAURIDSEN, K. L., SAMUEL, E. B., PROSZEK, J., KNUDSEN, B. R., HAGER, H. & STOUGAARD, M. 2015. Correlation between topoisomerase I and tyrosyl-DNA phosphodiesterase 1 activities in non-small cell lung cancer tissue. *Experimental and Molecular Pathology,* 99**,** 56-64.

JANSSENS, S. & TSCHOPP, J. 2006. Signals from within: the DNA-damage-induced NF-kappaB response. *Cell death and differentiation,* 13**,** 773-84.

JAXEL, C., CAPRANICO, G., KERRIGAN, D., KOHN, K. W. & POMMIER, Y. 1991. Effect of local DNA sequence on topoisomerase I cleavage in the presence or absence of camptothecin. *J Biol Chem,* 266**,** 20418-23.

JAZWINSKI, S. M. 2013. The retrograde response: when mitochondrial quality control is not enough. *Biochimica et biophysica acta,* 1833**,** 400-9.

JENSEN, R. B., CARREIRA, A. & KOWALCZYKOWSKI, S. C. 2010. Purified human BRCA2 stimulates RAD51-mediated recombination. *Nature,* 467**,** 678-83.

JILANI, A., RAMOTAR, D., SLACK, C., ONG, C., YANG, X. M., SCHERER, S. W. & LASKO, D. D. 1999. Molecular cloning of the human gene, PNKP, encoding a polynucleotide kinase 3'-phosphatase and evidence for its role in repair of DNA strand breaks caused by oxidative damage. *The Journal of biological chemistry,* 274**,** 24176-86.

JIN, G. F., HURST, J. S. & GODLEY, B. F. 2001. Rod outer segments mediate mitochondrial DNA damage and apoptosis in human retinal pigment epithelium. *Curr Eye Res,* 23**,** 11-9.

JIN, S., KHARBANDA, S., MAYER, B., KUFE, D. & WEAVER, D. T. 1997. Binding of Ku and c-Abl at the kinase homology region of DNA-dependent protein kinase catalytic subunit. *Journal of Biological Chemistry,* 272**,** 24763-66.

JIN, S., TONG, T., FAN, W., FAN, F., ANTINORE, M. J., ZHU, X., MAZZACURATI, L., LI, X., PETRIK, K. L., RAJASEKARAN, B., WU, M. & ZHAN, Q. 2002. GADD45-induced cell cycle G2-M arrest associates with altered subcellular distribution of cyclin B1 and is independent of p38 kinase activity. *Oncogene,* 21**,** 8696-704.

JOHNSON, R. E., KONDRATICK, C. M., PRAKASH, S. & PRAKASH, L. 1999. hRAD30 mutations in the variant form of xeroderma pigmentosum. *Science,* 285**,** 263-65.

JONES, R. E., CHAPMAN, J. R., PULIGILLA, C., MURRAY, J. M., CAR, A. M., FORD, C. C. & LINDSAY, H. D. 2003. XRad17 is required for the activation of XChk1 but not XCds1 during checkpoint signaling in Xenopus. *Molecular biology of the cell,* 14**,** 3898-910.

JU, B.-G., LUNYAK, V. V., PERISSI, V., GARCIA-BASSETS, I., ROSE, D. W., GLASS, C. K. & ROSENFELD, M. G. 2006. A topoisomerase IIbeta-mediated dsDNA break required for regulated transcription. *Science (New York, N.Y.),* 312**,** 1798-802.

JUNG, C., HIGGINS, C. M. & XU, Z. 2002. Mitochondrial electron transport chain complex dysfunction in a transgenic mouse model for amyotrophic lateral sclerosis. *J Neurochem,* 83**,** 535-45.

KABOTYANSKI, E. B., GOMELSKY, L., HAN, J.-O., STAMATO, T. D. & ROTH, D. B. 1998. Double-strand break repair in Ku86- and XRCC4-deficient cells. *Nucleic Acids Research,* 26**,** 5333-42.

KADYROV, F. A., DZANTIEV, L., CONSTANTIN, N. & MODRICH, P. 2006. Endonucleolytic function of MutLalpha in human mismatch repair. *Cell,* 126**,** 297-308.

KAGUNI, J. M. & KORNBERG, A. 1984. Replication initiated at the origin (oriC) of the E. coli chromosome reconstituted with purified enzymes. *Cell,* 38**,** 183-90.

KAKAROUGKAS, A., ISMAIL, A., KLEMENT, K., GOODARZI, A. A., CONRAD, S., FREIRE, R., SHIBATA, A., LOBRICH, M. & JEGGO, P. A. 2013. Opposing roles for 53BP1 during homologous recombination. *Nucleic Acids Res,* 41**,** 9719-31.

KANNOUCHE, P. L., WING, J. & LEHMANN, A. R. 2004. Interaction of human DNA polymerase eta with monoubiquitinated PCNA: a possible mechanism for the polymerase switch in response to DNA damage. *Mol Cell,* 14**,** 491-500.

KARIMI-BUSHERI, F., LEE, J., TOMKINSON, A. E. & WEINFELD, M. 1998. Repair of DNA strand gaps and nicks containing 3'-phosphate and 5'-hydroxyl termini by purified mammalian enzymes. *Nucleic Acids Research,* 26**,** 4395-400.

KARIMI-BUSHERI, F., RASOULI-NIA, A., ALLALUNIS-TURNER, J. & WEINFELD, M. 2007. Human polynucleotide kinase participates in repair of DNA double-strand breaks by nonhomologous end joining but not homologous recombination. *Cancer Research,* 67**,** 6619-25.

KASPAREK, T. R. & HUMPHREY, T. C. 2011. DNA double-strand break repair pathways, chromosomal rearrangements and cancer. *Seminars in cell & developmental biology,* 22**,** 886-97.

KASSAM, S. N. & RAINBOW, A. J. 2007. Deficient base excision repair of oxidative DNA damage induced by methylene blue plus visible light in xeroderma pigmentosum group C fibroblasts. *Biochemical and Biophysical Research Communications,* 359**,** 1004-09.

KASTAN, M. B. & LIM, D. S. 2000. The many substrates and functions of ATM. *Nature reviews. Molecular cell biology,* 1**,** 179-86.

KATYAL, S., EL-KHAMISY, S. F., RUSSELL, H. R., LI, Y., JU, L., CALDECOTT, K. W. & MCKINNON, P. J. 2007. TDP1 facilitates chromosomal single-strand break repair in neurons and is neuroprotective in vivo. *The EMBO journal,* 26**,** 4720-31.

KATYAL, S., LEE, Y., NITISS, K. C., DOWNING, S. M., LI, Y., SHIMADA, M., ZHAO, J., RUSSELL, H. R., PETRINI, J. H. J., NITISS, J. L. & MCKINNON, P. J. 2014. Aberrant topoisomerase-1 DNA lesions are pathogenic in neurodegenerative genome instability syndromes. *Nature neuroscience,* 17**,** 813-21.

KAUR, H., DEMUYT, A. & LICHTEN, M. 2015. Top3-Rmi1 DNA single-strand decatenase is integral to the formation and resolution of meiotic recombination intermediates. *Molecular Cell,* 57**,** 583-94.

KAWAMATA, H. & MANFREDI, G. 2008. Different regulation of wild-type and mutant Cu,Zn superoxide dismutase localization in mammalian mitochondria. *Hum Mol Genet,* 17**,** 3303-17.

KAZAK, L., REYES, A. & HOLT, I. J. 2012. Minimizing the damage: repair pathways keep mitochondrial DNA intact. *Nat Rev Mol Cell Biol,* 13**,** 659-71.

KEENEY, S. 2008. Spo11 and the formation of DNA double-strand breaks in meiosis. *Genome Dynamics and Stability,* 2**,** 81-123.

KEENEY, S. & NEALE, M. J. 2006. Initiation of meiotic recombination by formation of DNA double-strand breaks: mechanism and regulation. *Biochemical Society transactions,* 34**,** 523-5.

KEIL, A., FRESE-SCHAPER, M., STEINER, S. K., KÖRNER, M., SCHMID, R. A. & FRESE, S. 2015. The Topoisomerase I Inhibitor Irinotecan and the Tyrosyl-DNA Phosphodiesterase 1 Inhibitor Furamidine Synergistically Suppress Murine Lupus Nephritis. *Arthritis & rheumatology (Hoboken, N.J.),* 67**,** 1858-67.

KELLER, G. A., WARNER, T. G., STEIMER, K. S. & HALLEWELL, R. A. 1991. Cu,Zn superoxide dismutase is a peroxisomal enzyme in human fibroblasts and hepatoma cells. *Proc Natl Acad Sci U S A,* 88**,** 7381-5.

KELLEY, M. R., KOW, Y. W. & WILSON, D. M. 2003. Disparity between DNA base excision repair in yeast and mammals: Translational implications. *Cancer Research,* 63**,** 549-54.

KERZENDORFER, C., WHIBLEY, A., CARPENTER, G., OUTWIN, E., CHIANG, S.-C., TURNER, G., SCHWARTZ, C., EL-KHAMISY, S., RAYMOND, F. L. & O'DRISCOLL, M. 2010. Mutations in Cullin 4B result in a human syndrome associated with increased camptothecin-induced topoisomerase I-dependent DNA breaks. *Human molecular genetics,* 19**,** 1324-34.

KHIATI, S., BAECHLER, S. A., FACTOR, V. M., ZHANG, H., HUANG, S. Y., DALLA ROSA, I., SOURBIER, C., NECKERS, L., THORGEIRSSON, S. S. & POMMIER, Y. 2015. Lack of mitochondrial topoisomerase I (TOP1mt) impairs liver regeneration. *Proc Natl Acad Sci U S A,* 112**,** 11282-7.

KHIATI, S., DALLA ROSA, I., SOURBIER, C., MA, X., RAO, V. A., NECKERS, L. M., ZHANG, H. & POMMIER, Y. 2014. Mitochondrial topoisomerase I (top1mt) is a novel limiting factor of doxorubicin cardiotoxicity. *Clin Cancer Res,* 20**,** 4873-81.

KHOBTA, A., FERRI, F., LOTITO, L., MONTECUCCO, A., ROSSI, R. & CAPRANICO, G. 2006. Early effects of topoisomerase I inhibition on RNA polymerase II along transcribed genes in human cells. *J Mol Biol,* 357**,** 127-38.

KIERAN, D., WOODS, I., VILLUNGER, A., STRASSER, A. & PREHN, J. H. 2007. Deletion of the BH3-only protein puma protects motoneurons from ER stress-induced apoptosis and delays motoneuron loss in ALS mice. *Proc Natl Acad Sci U S A,* 104**,** 20606-11.

KIM, J. M., KEE, Y., GURTAN, A. & D'ANDREA, A. D. 2008. Cell cycle-dependent chromatin loading of the Fanconi anemia core complex by FANCM/FAAP24. *Blood,* 111**,** 5215-22.

KIM, R. A. & WANG, J. C. 1989. Function of DNA topoisomerases as replication swivels in Saccharomyces cerevisiae. *Journal of Molecular Biology,* 208**,** 257-67.

KIM, S. T., LIM, D. S., CANMAN, C. E. & KASTAN, M. B. 1999. Substrate specificities and identification of putative substrates of ATM kinase family members. *Journal of Biological Chemistry,* 274**,** 37538-43.

KIM, Y., SPITZ, G. S., VETURI, U., LACH, F. P., AUERBACH, A. D. & SMOGORZEWSKA, A. 2013. Regulation of multiple DNA repair pathways by the Fanconi anemia protein SLX4. *Blood,* 121**,** 54-63.

KIM, S. T., XU, B. & KASTAN, M. B. 2002. Involvement of the cohesin protein, Smc1, in Atm-dependent and independent responses to DNA damage. *Genes and Development,* 16**,** 560-70.

KIRKEGAARD, K. & WANG, J. C. 1985. Bacterial DNA topoisomerase I can relax positively supercoiled DNA containing a single-stranded loop. *J Mol Biol,* 185**,** 625-37.

KIRKINEZOS, I. G., BACMAN, S. R., HERNANDEZ, D., OCA-COSSIO, J., ARIAS, L. J., PEREZ-PINZON, M. A., BRADLEY, W. G. & MORAES, C. T. 2005. Cytochrome c association with the inner mitochondrial membrane is impaired in the CNS of G93A-SOD1 mice. *J Neurosci,* 25**,** 164-72.

KITAGAWA, R., BAKKENIST, C. J., MCKINNON, P. J. & KASTAN, M. B. 2004. Phosphorylation of SMC1 is a critical downstream event in the ATM-NBS1-BRCA1 pathway. *Genes and Development,* 18**,** 1423-38.

KITAGAWA, R. & KASTAN, M. B. The ATM-dependent DNA damage signaling pathway. Cold Spring Harbor Symposia on QUantitative Biology, 2005 2005. 99-109.

KITAMURA, T., KOSHINO, Y., SHIBATA, F., OKI, T., NAKAJIMA, H., NOSAKA, T. & KUMAGAI, H. 2003. Retrovirus-mediated gene transfer and expression cloning: Powerful tools in functional genomics. *Experimental Hematology,* 31**,** 1007-14.

KLINGENBERG, M. 2008. The ADP and ATP transport in mitochondria and its carrier. *Biochemica et Biophysica Acta - Biomembranes,* 1778**,** 1978-2021.

KLIONSKY, D. J., CUERVO, A. M., DUNN, W. A., LEVINE, B., VAN DER KLEI, I. & SEGLEN, P. O. 2007. How shall i eat thee? *Autophagy,* 3**,** 413-16.

KLUNGLAND, A., H??SS, M., GUNZ, D., CONSTANTINOU, A., CLARKSON, S. G., DOETSCH, P. W., BOLTON, P. H., WOOD, R. D. & LINDAHL, T. 1999. Base excision repair of oxidative DNA damage activated by XPG protein. *Molecular Cell,* 3**,** 33-42.

KLUZA, J., MARCHETTI, P., GALLEGO, M.-A., LANCEL, S., FOURNIER, C., LOYENS, A., BEAUVILLAIN, J.-C. & BAILLY, C. 2004. Mitochondrial proliferation during apoptosis induced by anticancer agents: effects of doxorubicin and mitoxantrone on cancer and cardiac cells. *Oncogene,* 23**,** 7018-30.

KOCH, C. A., AGYEI, R., GALICIA, S., METALNIKOV, P., O'DONNELL, P., STAROSTINE, A., WEINFELD, M. & DUROCHER, D. 2004. Xrcc4 physically links DNA end processing by polynucleotide kinase to DNA ligation by DNA ligase IV. *The EMBO journal,* 23**,** 3874-85.

KOLESAR, J. E., WANG, C. Y., TAGUCHI, Y. V., CHOU, S. H. & KAUFMAN, B. A. 2013. Two-dimensional intact mitochondrial DNA agarose electrophoresis reveals the structural complexity of the mammalian mitochondrial genome. *Nucleic Acids Res,* 41**,** e58.

KONDO, T., WAKAYAMA, T., NAIKI, T., MATSUMOTO, K. & SUGIMOTO, K. 2001. Recruitment of Mec1 and Ddc1 checkpoint proteins to double-strand breaks through distinct mechanisms. *Science (New York, N.Y.),* 294**,** 867-70.

KORHONEN, J. A., PHAM, X. H., PELLEGRINI, M. & FALKENBERG, M. 2004. Reconstitution of a minimal mtDNA replisome in vitro. *The EMBO Journal,* 23**,** 2423-29.

KRATZ, K., SCHOPF, B., KADEN, S., SENDOEL, A., EBERHARD, R., LADEMANN, C., CANNAVO, E., SARTORI, A. A., HENGARTNER, M. O. & JIRICNY, J. 2010. Deficiency of FANCD2-associated nuclease KIAA1018/FAN1 sensitizes cells to interstrand crosslinking agents. *Cell,* 142**,** 77-88.

KRAUS, W. L. & LIS, J. T. 2003. PARP goes transcription. *Cell,* 113**,** 677-83.

KRETZSCHMAR, M., MEISTERERNST, M. & ROEDER, R. G. 1993. Identification of human DNA topoisomerase I as a cofactor for activator-dependent transcription by RNA polymerase II. *Proc Natl Acad Sci U S A,* 90**,** 11508-12.

KRISHNAKUMAR, R., GAMBLE, M. J., FRIZZELL, K. M., BERROCAL, J. G., KININIS, M. & KRAUS, W. L. 2008. Reciprocal binding of PARP-1 and histone H1 at promoters specifies transcriptional outcomes. *Science (New York, NY),* 319**,** 819-21.

KUMAGAI, A. & DUNPHY, W. G. 1999. Binding of 14-3-3 proteins and nuclear export control the intracellular localization of the mitotic inducer Cdc25. *Genes & Development,* 13**,** 1067-72.

KUMMAR, S., CHEN, A., JI, J., ZHANG, Y., REID, J. M., AMES, M., JIA, L., WEIL, M., SPERANZA, G., MURGO, A. J., KINDERS, R., WANG, L., PARCHMENT, R. E., CARTER, J., STOTLER, H., RUBINSTEIN, L., HOLLINGSHEAD, M., MELILLO, G., POMMIER, Y., BONNER, W., TOMASZEWSKI, J. E. & DOROSHOW, J. H. 2011. Phase I study of PARP inhibitor ABT-888 in combination with topotecan in adults with refractory solid tumors and lymphomas. *Cancer Res,* 71**,** 5626-34.

KUNOS, C., DENG, W., DAWSON, D., LEA, J. S., ZANOTTI, K. M., GRAY, H. J., BENDER, D. P., GUAGLIANONE, P. P., CARTER, J. S. & MOORE, K. N. 2015. A phase I-II evaluation of veliparib (NSC #737664), topotecan, and filgrastim or pegfilgrastim in the treatment of persistent or recurrent carcinoma of the uterine cervix: an NRG Oncology/Gynecologic Oncology Group study. *Int J Gynecol Cancer,* 25**,** 484-92.

KURAOKA, I., KOBERTZ, W. R., ARIZA, R. R., BIGGERSTAFF, M., ESSIGMANN, J. M. & WOOD, R. D. 2000. Repair of an interstrand DNA cross-link initiated by ERCC1-XPF repair/recombination nuclease. *J Biol Chem,* 275**,** 26632-6.

LAGADINOU, E. D., SACH, A., CALLAHAN, K., ROSSI, R. M., NEERING, S. J., MINHAJUDDIN, M., ASHTON, J. M., PEI, S., GROSE, V., O'DWYER, K. M., LIESVELD, J. L., BROOKES, P. S., BECKER, M. W. & JORDAN, C. T. 2013. BCL-2 inhibition targets oxidative phosphorylation and selectively eradicates quiescent human leukemia stem cells. *Cell stem cell,* 12**,** 329-41.

LANE, D. P. 1992. Cancer. p53, guardian of the genome. *Nature,* 358**,** 15-16.

LAU, P. J. & KOLODNER, R. D. 2003. Transfer of the MSH2.MSH6 complex from proliferating cell nuclear antigen to mispaired bases in DNA. *The Journal of biological chemistry,* 278**,** 14-7.

LAX, N. Z., HEPPLEWHITE, P. D., REEVE, A. K., NESBITT, V., MCFARLAND, R., JAROS, E., TAYLOR, R. W. & TURNBULL, D. M. 2012. Cerebellar ataxia in patients with mitochondrial DNA disease: a molecular clinicopathological study. *J Neuropathol Exp Neurol,* 71**,** 148-61.

LE PAGE, F., GENTIL, A. & SARASIN, A. 1999. Repair and mutagenesis survey of 8-hydroxyguanine in bacteria and human cells. *Biochimie,* 81**,** 147-53.

LEBEDEVA, N. A., ANARBAEV, R. O., SUKHANOVA, M., VASIL'EVA, I. A., RECHKUNOVA, N. I. & LAVRIK, O. I. 2015. Poly(ADP-ribose)polymerase 1 stimulates the AP-site cleavage activity of tyrosyl-DNA phosphodiesterase 1. *Bioscience reports,* 35**,** e00230.

LEBEDEVA, N. A., RECHKUNOVA, N. I. & LAVRIK, O. I. 2011. AP-site cleavage activity of tyrosyl-DNA phosphodiesterase 1. *FEBS letters,* 585**,** 683-6.

LEE, H. C., YIN, P. H., LU, C. Y., CHI, C. W. & WEI, Y. H. 2000. Increase of mitochondria and mitochondrial DNA in response to oxidative stress in human cells. *Biochem J,* 348 Pt 2**,** 425-32.

LEE, J.-H. & PAULL, T. T. 2004. Direct activation of the ATM protein kinase by the Mre11/Rad50/Nbs1 complex. *Science (New York, N.Y.),* 304**,** 93-96.

LEE, J.-H. & PAULL, T. T. 2005. ATM activation by DNA double-strand breaks through the Mre11-Rad50-Nbs1 complex. *Science (New York, NY),* 308**,** 551-54.

LEE, K. & SANG, E. L. 2007. Saccharomyces cerevisiae Sae2- and Tel1-dependent single-strand DNA formation at DNA break promotes microhomology-mediated end joining. *Genetics,* 176**,** 2003-14.

LEE, K.-B., WANG, D., LIPPARD, S. J. & SHARP, P. A. 2002. Transcription-coupled and DNA damage-dependent ubiquitination of RNA polymerase II in vitro. *Proceedings of the National Academy of Sciences,* 99**,** 4239-44.

LEE-THEILEN, M., MATTHEWS, A. J., KELLY, D., ZHENG, S. & CHAUDHURI, J. 2010. CtIP promotes microhomology-mediated alternative end joining during class-switch recombination. *Nature Structural & Molecular Biology,* 18**,** 75-79.

LEHMANN, A. R. 2003. DNA repair-deficient diseases, xeroderma pigmentosum, Cockayne syndrome and trichothiodystrophy. *Biochimie,* 85**,** 1101-11.

LEMARIE, A. & GRIMM, S. 2011. Mitochondrial respiratory chain complexes: apoptosis sensors mutated in cancer? *Oncogene,* 30**,** 3985-4003.

LEVINE, B. & YUAN, J. 2005. Autophagy in cell death: An innocent convict? *Journal of Clinical Investigation,* 115**,** 2679-88.

LI, G.-M. 2008. Mechanisms and functions of DNA mismatch repair. *Cell research,* 18**,** 85-98.

LI, G. M. & MODRICH, P. 1995. Restoration of mismatch repair to nuclear extracts of H6 colorectal tumor cells by a heterodimer of human MutL homologs. *Proceedings of the National Academy of Sciences of the United States of America,* 92**,** 1950-54.

LI, L. & BHATIA, R. 2011. Stem cell quiescence. *Clinical cancer research,* 17**,** 4936-41.

LI, M., POKHAREL, S., WANG, J.-T., XU, X. & LIU, Y. 2015. RECQ5-dependent SUMOylation of DNA topoisomerase I prevents transcription-associated genome instability. *Nature communications,* 6**,** 6720-20.

LI, S., CHANG, H. H., NIEWOLIK, D., HEDRICK, M. P., PINKERTON, A. B., HASSIG, C. A., SCHWARZ, K. & LIEBER, M. R. 2014. Evidence that the DNA endonuclease ARTEMIS also has intrinsic 5′-exonuclease activity. *Journal of Biological Chemistry,* 289**,** 7825-34.

LI, W. & MA, H. 2006. Double-stranded DNA breaks and gene functions in recombination and meiosis. *Cell research,* 16**,** 402-12.

LI, X. & HEYER, W. D. 2009. RAD54 controls access to the invading 3'-OH end after RAD51-mediated DNA strand invasion in homologous recombination in Saccharomyces cerevisiae. *Nucleic Acids Res,* 37**,** 638-46.

LI, X. & MANLEY, J. L. 2006. Cotranscriptional processes and their influence on genome stability. *Genes & Development,* 20**,** 1838-47.

LIANG, L., DENG, L., NGUYEN, S. C., ZHAO, X., MAULION, C. D., SHAO, C. & TISCHFIELD, J. A. 2008. Human DNA ligases I and III, but not ligase IV, are required for microhomology-mediated end joining of DNA double-strand breaks. *Nucleic Acids Research,* 36**,** 3297-310.

LIAO, S., TOCZYLOWSKI, T. & YAN, H. 2008. Identification of the Xenopus DNA2 protein as a major nuclease for the 5'->3' strand-specific processing of DNA ends. *Nucleic Acids Res,* 36**,** 6091-100.

LIAO, Z., THIBAUT, L., JOBSON, A. & POMMIER, Y. 2006. Inhibition of human tyrosyl-DNA phosphodiesterase by aminoglycoside antibiotics and ribosome inhibitors. *Molecular pharmacology,* 70**,** 366-72.

LIEBER, M. R. 2010. The mechanism of double-strand DNA break repair by the nonhomologous DNA end-joining pathway. *Annual review of biochemistry,* 79**,** 181-211.

LIEBER, M. R. & KARANJAWALA, Z. E. 2004. Ageing, repetitive genomes and DNA damage. *Nat Rev Mol Cell Biol,* 5**,** 69-75.

LIEBER, M. R., MA, Y., PANNICKE, U. & SCHWARZ, K. 2003. Mechanism and regulation of human non-homologous DNA end-joining. *Nature reviews. Molecular cell biology,* 4**,** 712-20.

LIM, D. S., KIM, S. T., XU, B., MASER, R. S., LIN, J., PETRINI, J. H. & KASTAN, M. B. 2000. ATM phosphorylates p95/nbs1 in an S-phase checkpoint pathway. *Nature,* 404**,** 613-7.

LIN, C.-P., BAN, Y., LYU, Y. L. & LIU, L. F. 2009. Proteasome-dependent processing of topoisomerase I-DNA adducts into DNA double strand breaks at arrested replication forks. *The Journal of biological chemistry,* 284**,** 28084-92.

LIN, C. P., BAN, Y., LYU, Y. L., DESAI, S. D. & LIU, L. F. 2008. A ubiquitin-proteasome pathway for the repair of topoisomerase I-DNA covalent complexes. *Journal of Biological Chemistry,* 283**,** 21074-83.

LIN, W., AMÉ, J. C., ABOUL-ELA, N., JACOBSON, E. L. & JACOBSON, M. K. 1997. Isolation and characterization of the cDNA encoding bovine poly(ADP-ribose) glycohydrolase. *The Journal of biological chemistry,* 272**,** 11895-901.

LINDAHL, T. 1993. Instability and decay of the primary structure of DNA. *Nature,* 362**,** 709-15.

LINDAHL, T. & KARLSTRÖM, O. 1973. Heat-induced depyrimidination of deoxyribonucleic acid in neutral solution. *Biochemistry,* 12**,** 5151-54.

LINDAHL, T. & NYBERG, B. 1972. Rate of depurination of native deoxyribonucleic acid. *Biochemistry,* 11**,** 3610-18.

LINDAHL, T. & WOOD, R. D. 1999. Quality control by DNA repair. *Science,* 286**,** 1897-905.

LIU, C., ZHOU, S., BEGUM, S., SIDRANSKY, D., WESTRA, W. H., BROCK, M. & CALIFANO, J. A. 2007. Increased expression and activity of repair genes TDP1 and XPF in non-small cell lung cancer. *Lung cancer (Amsterdam, Netherlands),* 55**,** 303-11.

LIU, J., DOTY, T., GIBSON, B. & HEYER, W. D. 2010. Human BRCA2 protein promotes RAD51 filament formation on RPA-covered single-stranded DNA. *Nat Struct Mol Biol,* 17**,** 1260-2.

LIU, L. F., DUANN, P., LIN, C. T., D'ARPA, P., WU, J., DESAI, S. D., LI, T. K., MAO, Y., SUN, M. & SIM, S. P. 2000. Mechanism of action of camptothecin. *Ann N Y Acad Sci,* 922**,** 1-10.

LIU, L. F. & WANG, J. C. 1987. Supercoiling of the DNA template during transcription. *Proceedings of the National Academy of Sciences of the United States of America,* 84**,** 7024-27.

LIU, M. & SCHATZ, D. G. 2009. Balancing AID and DNA repair during somatic hypermutation. *Trends in Immunology,* 30**,** 173-81.

LIU, R., ALTHAUS, J. S., ELLERBROCK, B. R., BECKER, D. A. & GURNEY, M. E. 1998. Enhanced oxygen radical production in a transgenic mouse model of familial amyotrophic lateral sclerosis. *Ann Neurol,* 44**,** 763-70.

LIU, Y., BEARD, W. A., SHOCK, D. D., PRASAD, R., HOU, E. W. & WILSON, S. H. 2005. DNA polymerase beta and flap endonuclease 1 enzymatic specificities sustain DNA synthesis for long patch base excision repair. *J Biol Chem,* 280**,** 3665-74.

LJUNGMAN, M. & HANAWALT, P. C. 1996. The anti-cancer drug camptothecin inhibits elongation but stimulates initiation of RNA polymerase II transcription. *Carcinogenesis,* 17**,** 31-35.

LOEB, L. A., PRESTON, B. D., SNOW, E. T. & SCHAAPER, R. M. 1986. Apurinic sites as common intermediates in mutagenesis. *Basic Life Sci,* 38**,** 341-47.

LONGERICH, S., SAN FILIPPO, J., LIU, D. & SUNG, P. 2009. FANCI binds branched DNA and is monoubiquitinated by UBE2T-FANCL. *J Biol Chem,* 284**,** 23182-6.

LORUSSO, P. M., LI, J., BURGER, A., HEILBRUN, L. K., SAUSVILLE, E. A., BOERNER, S. A., SMITH, D., PILAT, M. J., ZHANG, J., TOLANEY, S. M., CLEARY, J. M., CHEN, A. P., RUBINSTEIN, L., BOERNER, J. L., BOWDITCH, A., CAI, D., BELL, T., WOLANSKI, A., MARRERO, A. M., ZHANG, Y., JI, J., FERRY-GALOW, K., KINDERS, R. J., PARCHMENT, R. E. & SHAPIRO, G. I. 2016. Phase I Safety, Pharmacokinetic, and Pharmacodynamic Study of the Poly(ADP-ribose) Polymerase (PARP) Inhibitor Veliparib (ABT-888) in Combination with Irinotecan in Patients with Advanced Solid Tumors. *Clin Cancer Res,* 22**,** 3227-37.

LOWNDES, N. F. & MURGUIA, J. R. 2000. Sensing and responding to DNA damage. *Current Opinion in Genetics and Development,* 10**,** 17-25.

LU, B., LEE, J., NIE, X., LI, M., MOROZOV, Y. I., VENKATESH, S., BOGENHAGEN, D. F., TEMIAKOV, D. & SUZUKI, C. K. 2013. Phosphorylation of human TFAM in mitochondria impairs DNA binding and promotes degradation by the AAA+ Lon protease. *Molecular cell,* 49**,** 121-32.

LUCAS, I., GERME, T., CHEVRIER-MILLER, M. & HYRIEN, O. 2001. Topoisomerase II can unlink replicating DNA by precatenane removal. *EMBO Journal,* 20**,** 6509-19.

LUM, J. J., BAUER, D. E., KONG, M., HARRIS, M. H., LI, C., LINDSTEN, T. & THOMPSON, C. B. 2005. Growth factor regulation of autophagy and cell survival in the absence of apoptosis. *Cell,* 120**,** 237-48.

LYLE, S. & MOORE, N. 2011. Quiescent, slow-cycling stem cell populations in cancer: A review of the evidence and discussion of significance. *Journal of Oncology,* 10.1155/2011/396076.

LYNCH, M., SUNG, W., MORRIS, K., COFFEY, N., R.LANDRY, C., B.DOPMAN, E., DICKINSON, W. J., OKAMOTO, K., KULKARNI, S., L.HARTL, D. & THOMAS, W. K. 2008. A genome-wide view of the spectrumof spontaneous mutations in yeast. *National Academy of Sciences of the United States of America,* 105**,** 9272-77.

MA, J.-L., KIM, E. M., HABER, J. E. & LEE, S. E. 2003. Yeast Mre11 and Rad1 Proteins Define a Ku-Independent Mechanism To Repair Double-Strand Breaks Lacking Overlapping End Sequences. *MOLECULAR AND CELLULAR BIOLOGY,* 23**,** 8820-28.

MA, Y., PANNICKE, U., SCHWARZ, K. & LIEBER, M. R. 2002. Hairpin opening and overhang processing by an Artemis/DNA-dependent protein kinase complex in nonhomologous end joining and V(D)J recombination. *Cell,* 108**,** 781-94.

MA, Y., SCHWARZ, K. & LIEBER, M. R. 2005. The Artemis:DNA-PKcs endonuclease cleaves DNA loops, flaps, and gaps. *DNA Repair,* 4**,** 845-51.

MAALØE, O. 1966. *Control of macromolecular synthesis a study of DNA, RNA, and protein synthesis in bacteria,* New York, W.A. Benjamin

MACKAY, C., DECLAIS, A. C., LUNDIN, C., AGOSTINHO, A., DEANS, A. J., MACARTNEY, T. J., HOFMANN, K., GARTNER, A., WEST, S. C., HELLEDAY, T., LILLEY, D. M. & ROUSE, J. 2010. Identification of KIAA1018/FAN1, a DNA repair nuclease recruited to DNA damage by monoubiquitinated FANCD2. *Cell,* 142**,** 65-76.

MADABHUSHI, R., GAO, F., PFENNING, A. R., PAN, L., YAMAKAWA, S., SEO, J., RUEDA, R., PHAN, T. X., YAMAKAWA, H., PAO, P. C., STOTT, R. T., GJONESKA, E., NOTT, A., CHO, S., KELLIS, M. & TSAI, L. H. 2015. Activity-Induced DNA Breaks Govern the Expression of Neuronal Early-Response Genes. *Cell,* 161**,** 1592-605.

MAGRANE, J. & MANFREDI, G. 2009. Mitochondrial function, morphology, and axonal transport in amyotrophic lateral sclerosis. *Antioxid Redox Signal,* 11**,** 1615-26.

MAILLARD, O., SOLYOM, S. & NAEGELI, H. 2007. An aromatic sensor with aversion to damaged strands confers versatility to DNA repair. *PLoS Biology,* 5**,** 717-28.

MAIURI, M. C., ZALCKVAR, E., KIMCHI, A. & KROEMER, G. 2007. Self-eating and self-killing: crosstalk between autophagy and apoptosis. *Nature reviews. Molecular cell biology,* 8**,** 741-52.

MAKI, H. & SEKIGUCHI, M. 1992. MutT protein specifically hydrolyses a potent mutagenic substrate for DNA synthesis. *Nature,* 355**,** 273-75.

MAKINEN, P. L. 1985. Biochemical studies on a novel vanadate- and molybdate-sensitive acid phosphatase from human epidermis. *J Invest Dermatol,* 85**,** 118-24.

MANDAVILLI, B. S., ALI, S. F. & VAN HOUTEN, B. 2000. DNA damage in brain mitochondria caused by aging and MPTP treatment. *Brain Res,* 885**,** 45-52.

MANI, R. S., YU, Y., FANG, S., LU, M., FANTA, M., ZOLNER, A. E., TAHBAZ, N., RAMSDEN, D. A., LITCHFIELD, D. W., LEES-MILLER, S. P. & WEINFELD, M. 2010. Dual modes of interaction between XRCC4 and polynucleotide kinase/phosphatase: implications for nonhomologous end joining. *The Journal of biological chemistry,* 285**,** 37619-29.

MAO, Y., SUN, M., DESAI, S. D. & LIU, L. F. 2000. SUMO-1 conjugation to topoisomerase I: A possible repair response to topoisomerase-mediated DNA damage. *Proceedings of the National Academy of Sciences of the United States of America,* 97**,** 4046-51.

MARCHAND, C., ANTONY, S., KOHN, K. W., CUSHMAN, M., IOANOVICIU, A., STAKER, B. L., BURGIN, A. B., STEWART, L. & POMMIER, Y. 2006. A novel norindenoisoquinoline structure reveals a common interfacial inhibitor paradigm for ternary trapping of the topoisomerase I-DNA covalent complex. *Mol Cancer Ther,* 5**,** 287-95.

MARCHAND, C., HUANG, S.-Y. N., DEXHEIMER, T. S., LEA, W. A., MOTT, B. T., CHERGUI, A., NAUMOVA, A., STEPHEN, A. G., ROSENTHAL, A. S., RAI, G., MURAI, J., GAO, R., MALONEY, D. J., JADHAV, A., JORGENSEN, W. L., SIMEONOV, A. & POMMIER, Y. 2014. Biochemical Assays for the Discovery of TDP1 Inhibitors. *Molecular cancer therapeutics,* 13**,** 2116-26.

MARCHAND, C., LEA, W. A., JADHAV, A., DEXHEIMER, T. S., AUSTIN, C. P., INGLESE, J., POMMIER, Y. & SIMEONOV, A. 2009. Identification of phosphotyrosine mimetic inhibitors of human tyrosyl-DNA phosphodiesterase I by a novel AlphaScreen high-throughput assay. *Molecular cancer therapeutics,* 8**,** 240-8.

MARGISON, G. P., SANTIBÁÑEZ KOREF, M. F. & POVEY, A. C. 2002. Mechanisms of carcinogenicity/chemotherapy by O6-methylguanine. *Mutagenesis,* 17**,** 483-7.

MARSIN, S., VIDAL, A. E., SOSSOU, M., MÉNISSIER-DE MURCIA, J., LE PAGE, F., BOITEUX, S., DE MURCIA, G. & RADICELLA, J. P. 2003. Role of XRCC1 in the Coordination and Stimulation of Oxidative DNA Damage Repair Initiated by the DNA Glycosylase hOGG1. *Journal of Biological Chemistry,* 278**,** 44068-74.

MARTIN, A. & SCHARFF, M. D. 2002. AID and mismatch repair in antibody diversification. *Nature Reviews: Immunology,* 2**,** 605-14.

MARTIN, G. M., SMITH, A. C., KETTERER, D. J., OGBURN, C. E. & DISTECHE, C. M. 1985. Increased chromosomal aberrations in first metaphases of cells isolated from the kidneys of aged mice. *Israel journal of medical sciences,* 21**,** 296-301.

MARTIN, L. J., LIU, Z., CHEN, K., PRICE, A. C., PAN, Y., SWABY, J. A. & GOLDEN, W. C. 2007. Motor neuron degeneration in amyotrophic lateral sclerosis mutant superoxide dismutase-1 transgenic mice: mechanisms of mitochondriopathy and cell death. *J Comp Neurol,* 500**,** 20-46.

MASSON, M., NIEDERGANG, C., SCHREIBER, V., MULLER, S., MENISSIER-DE MURCIA, J. & DE MURCIA, G. 1998. XRCC1 is specifically associated with poly(ADP-ribose) polymerase and negatively regulates its activity following DNA damage. *Molecular and cellular biology,* 18**,** 3563-71.

MASUTANI, C., KUSUMOTO, R., YAMADA, A., DOHMAE, N., YOKOI, M., YUASA, M., ARAKI, M., IWAI, S., TAKIO, K. & HANAOKA, F. 1999. The XPV (xeroderma pigmentosum variant) gene encodes human DNA polymerase eta. *Nature,* 399**,** 700-04.

MASUTANI, C., SUGASAWA, K., YANAGISAWA, J., SONOYAMA, T., UI, M., ENOMOTO, T., TAKIO, K., TANAKA, K., VAN DER SPEK, P. J. & BOOTSMA, D. 1994. Purification and cloning of a nucleotide excision repair complex involving the xeroderma pigmentosum group C protein and a human homologue of yeast RAD23. *The EMBO journal,* 13**,** 1831-43.

MATHIEU, N., KACZMAREK, N. & NAEGELI, H. 2010. Strand- and site-specific DNA lesion demarcation by the xeroderma pigmentosum group D helicase. *Proceedings of the National Academy of Sciences of the United States of America,* 107**,** 17545-50.

MATSUMOTO, G., KIM, S. & MORIMOTO, R. I. 2006. Huntingtin and mutant SOD1 form aggregate structures with distinct molecular properties in human cells. *Journal of Biological Chemistry,* 281**,** 4477-85.

MATSUMOTO, G., STOJANOVIC, A., HOLMBERG, C. I., KIM, S. & MORIMOTO, R. I. 2005. Structural properties and neuronal toxicity of amyotrophic lateral sclerosis-associated Cu/Zn superoxide dismutase 1 aggregates. *The Journal of cell biology,* 171**,** 75-85.

MATTIAZZI, M., D'AURELIO, M., GAJEWSKI, C. D., MARTUSHOVA, K., KIAEI, M., BEAL, M. F. & MANFREDI, G. 2002. Mutated human SOD1 causes dysfunction of oxidative phosphorylation in mitochondria of transgenic mice. *J Biol Chem,* 277**,** 29626-33.

MAYA, R., BALASS, M., KIM, S. T., SHKEDY, D., MARTINEZ LEAL, J. F., SHIFMAN, O., MOAS, M., BUSCHMANN, T., RONAI, Z. E., SHILOH, Y., KASTAN, M. B., KATZIR, E. & OREN, M. 2001. ATM-dependent phosphorylation of Mdm2 on serine 395: Role in p53 activation by DNA damage. *Genes and Development,* 15**,** 1067-77.

MAYNARD, S., SCHURMAN, S. H., HARBOE, C., DE SOUZA-PINTO, N. C. & BOHR, V. A. 2009. Base excision repair of oxidative DNA damage and association with cancer and aging. *Carcinogenesis,* 30**,** 2-10.

MAYNE, L. V. & LEHMANN, A. R. 1982. Failure of RNA synthesis to recover after UV irradiation: An early defect in cells from individuals with Cockayne's syndrome and xeroderma pigmentosum. *Cancer Research,* 42**,** 1473-78.

MAZUMDER, A., GERLT, J. A., ABSALON, M. J., STUBBE, J., CUNNINGHAM, R. P., WITHKA, J. & BOLTON, P. H. 1991. Stereochemical Studies of the P-Elimination Reactions at Aldehydic Abasic Sites in DNA: Endonuclease III from Escherichia coli, Sodium Hydroxide, and Lys-Trp-Lys. *Biochemistry,* 30**,** 1119-26.

MCBRIDE, H., ZUNINO, R. & GOYON, V. 2014. Mitochondrial SUMOylation as a critical regulator of proliferation and death (349.3). *FASEB J,* 28**,** 349.3--49.3-.

MCCULLOCH, V., SEIDEL-ROGOL, B. L. & SHADEL, G. S. 2002. A human mitochondrial transcription factor is related to RNA adenine methyltransferases and binds S-adenosylmethionine. *Molecular and cellular biology,* 22**,** 1116-25.

MEAGHER, M. & LIGHTOWLERS, R. N. 2014. The role of TDP1 and APTX in mitochondrial DNA repair. *Biochimie,* 100**,** 121-24.

MEDIKAYALA, S., PITEO, B., ZHAO, X. & EDWARDS, J. G. 2011. Chronically elevated glucose compromises myocardial mitochondrial DNA integrity by alteration of mitochondrial topoisomerase function. *American Journal of Physiology- Cell Physiology,* 300**,** C338--48.

MEI, H., SUN, S., BAI, Y., CHEN, Y., CHAI, R. & LI, H. 2015. Reduced mtDNA copy number increases the sensitivity of tumor cells to chemotherapeutic drugs. *Cell Death Dis,* 6**,** e1710.

MEISENBERG, C., GILBERT, D. C., CHALMERS, A., HALEY, V., GOLLINS, S., WARD, S. E. & EL-KHAMISY, S. F. 2014a. Clinical and Cellular Roles for TDP1 and TOP1 in Modulating Colorectal Cancer Response to Irinotecan. *Molecular Cancer Therapeutics,* 14**,** 575-85.

MEISENBERG, C., WARD, S. E., SCHMID, P. & EL-KHAMISY, S. F. 2014b. TDP1/TOP1 Ratio as a Promising Indicator for the Response of Small Cell Lung Cancer to Topotecan. *Journal of cancer science & therapy,* 6**,** 258-67.

MELIS, J. P. M., LUIJTEN, M., MULLENDERS, L. H. F. & VAN STEEG, H. 2011. The role of XPC: implications in cancer and oxidative DNA damage. *Mutation research,* 728**,** 107-17.

MELO, J. A., COHEN, J. & TOCZYSKI, D. P. 2001. Two checkpoint complexes are independently recruited to sites of DNA damage in vivo. *Genes and Development,* 15**,** 2809-21.

MERINO, A., MADDEN, K. R., LANE, W. S., CHAMPOUX, J. J. & REINBERG, D. 1993. DNA topoisomerase I is involved in both repression and activation of transcription. *Nature,* 365**,** 227-32.

MIAO, Z. H., AGAMA, K., SORDET, O., POVIRK, L., KOHN, K. W. & POMMIER, Y. 2006. Hereditary ataxia SCAN1 cells are defective for the repair of transcription-dependent topoisomerase I cleavage complexes. *DNA Repair,* 5**,** 1489-94.

MIELKE, C., TÜMMLER, M., SCHÜBELER, D., VON HOEGEN, I. & HAUSER, H. 2000. Stabilized, long-term expression of heterodimeric proteins from tricistronic mRNA. *Gene,* 254**,** 1-8.

MIMITOU, E. P. & SYMINGTON, L. S. 2009. Nucleases and helicases take center stage in homologous recombination. *Trends Biochem Sci,* 34**,** 264-72.

MIMITOU, E. P. & SYMINGTON, L. S. 2010. Ku prevents Exo1 and Sgs1-dependent resection of DNA ends in the absence of a functional MRX complex or Sae2. *The EMBO journal,* 29**,** 3358-69.

MIN, J.-H. & PAVLETICH, N. P. 2007. Recognition of DNA damage by the Rad4 nucleotide excision repair protein. *Nature,* 449**,** 570-5.

MO, Y. Y. & MOSCHOS, S. J. 2005. Targeting Ubc9 for cancer therapy. *Expert Opin Ther Targets,* 9**,** 1203-16.

MO, Y. Y., YU, Y., EE, P. L. & BECK, W. T. 2004. Overexpression of a dominant-negative mutant Ubc9 is associated with increased sensitivity to anticancer drugs. *Cancer Res,* 64**,** 2793-8.

MO, Y. Y., YU, Y., SHEN, Z. & BECK, W. T. 2002. Nucleolar delocalization of human topoisomerase I in response to topotecan correlates with sumoylation of the protein. *J Biol Chem,* 277**,** 2958-64.

MO, Y. Y., YU, Y., THEODOSIOU, E., EE, P. L. & BECK, W. T. 2005. A role for Ubc9 in tumorigenesis. *Oncogene,* 24**,** 2677-83.

MOCQUET, V., LAINÉ, J. P., RIEDL, T., YAJIN, Z., LEE, M. Y. & EGLY, J. M. 2008. Sequential recruitment of the repair factors during NER: the role of XPG in initiating the resynthesis step. *The EMBO journal,* 27**,** 155-67.

MOERTEL, C. G., SCHUTT, A. J., REITEMEIER, R. J. & HAHN, R. G. 1972. Phase II study of camptothecin (NSC-100880) in the treatment of advanced gastrointestinal cancer. *Cancer chemotherapy reports,* 56**,** 95-101.

MOHAN, V. & MADHUSUDAN, S. 2013. DNA Base Excision Repair : Evolving Biomarkers for Personalized Therapies in Cancer. InTech.

MOLDOVAN, G. L. & D'ANDREA, A. D. 2009. How the fanconi anemia pathway guards the genome. *Annu Rev Genet,* 43**,** 223-49.

MÖRCK, C. & PILON, M. 2007. Caloric restriction and autophagy in Caenorhabditis elegans. *Autophagy,* 3**,** 51-53.

MOREIRA, M.-C., BARBOT, C., TACHI, N., KOZUKA, N., UCHIDA, E., GIBSON, T., MENDONÇA, P., COSTA, M., BARROS, J., YANAGISAWA, T., WATANABE, M., IKEDA, Y., AOKI, M., NAGATA, T., COUTINHO, P., SEQUEIROS, J. & KOENIG, M. 2001. The gene mutated in ataxia-ocular apraxia 1 encodes the new HIT/Zn-finger protein aprataxin. *Nature genetics,* 29**,** 189-93.

MORTUSEWICZ, O., ROTHBAUER, U., CARDOSO, M. C. & LEONHARDT, H. 2006. Differential recruitment of DNA ligase I and III to DNA repair sites. *Nucleic Acids Research,* 34**,** 3523-32.

MOSCHOS, S. J., JUKIC, D. M., ATHANASSIOU, C., BHARGAVA, R., DACIC, S., WANG, X., KUAN, S.-F., FAYEWICZ, S. L., GALAMBOS, C., ACQUAFONDATA, M., DHIR, R. & BECKER, D. 2010. Expression analysis of Ubc9, the single small ubiquitin-like modifier (SUMO) E2 conjugating enzyme, in normal and malignant tissues. *Human pathology,* 41**,** 1286-98.

MOSCHOS, S. J., SMITH, A. P., MANDIC, M., ATHANASSIOU, C., WATSON-HURST, K., JUKIC, D. M., EDINGTON, H. D., KIRKWOOD, J. M. & BECKER, D. 2007. SAGE and antibody array analysis of melanoma-infiltrated lymph nodes: identification of Ubc9 as an important molecule in advanced-stage melanomas. *Oncogene,* 26**,** 4216-25.

MOSER, J., KOOL, H., GIAKZIDIS, I., CALDECOTT, K., MULLENDERS, L. H. F. & FOUSTERI, M. I. 2007. Sealing of Chromosomal DNA Nicks during Nucleotide Excision Repair Requires XRCC1 and DNA Ligase III?? in a Cell-Cycle-Specific Manner. *Molecular Cell,* 27**,** 311-23.

MU, J. J., WANG, Y., LUO, H., LENG, M., ZHANG, J., YANG, T., BESUSSO, D., JUNG, S. Y. & QIN, J. 2007. A proteomic analysis of ataxia telangiectasia-mutated (ATM)/ATM-Rad3-related (ATR) substrates identifies the ubiquitin-proteasome system as a regulator for DNA damage checkpoints. *J Biol Chem,* 282**,** 17330-34.

MUGGIA, F. M., CREAVEN, P. J., HANSEN, H. H., COHEN, M. H. & SELAWRY, O. S. 1972. Phase I clinical trial of weekly and daily treatment with camptothecin (NSC-100880): correlation with preclinical studies. *Cancer chemotherapy reports. Part 1,* 56**,** 515-21.

MUKHOPADHYAY, D. & DASSO, M. 2007. Modification in reverse: the SUMO proteases. *Trends Biochem Sci,* 32**,** 286-95.

MUNOZ, I. M., HAIN, K., DECLAIS, A. C., GARDINER, M., TOH, G. W., SANCHEZ-PULIDO, L., HEUCKMANN, J. M., TOTH, R., MACARTNEY, T., EPPINK, B., KANAAR, R., PONTING, C. P., LILLEY, D. M. J., ROUSE, J., MUÑOZ, I. M., HAIN, K., DÉCLAIS, A.-C., GARDINER, M., TOH, G. W., SANCHEZ-PULIDO, L., HEUCKMANN, J. M., TOTH, R., MACARTNEY, T., EPPINK, B., KANAAR, R., PONTING, C. P., LILLEY, D. M. J. & ROUSE, J. 2009. Coordination of structure-specific nucleases by human SLX4/BTBD12 is required for DNA repair. *Mol Cell,* 35**,** 116-27.

MURAI, J., HUANG, S.-Y. N., DAS, B. B., DEXHEIMER, T. S., TAKEDA, S. & POMMIER, Y. 2012. Tyrosyl-DNA phosphodiesterase 1 (TDP1) repairs DNA damage induced by topoisomerases I and II and base alkylation in vertebrate cells. *The Journal of biological chemistry,* 287**,** 12848-57.

MURAI, J., MARCHAND, C., SHAHANE, S. A., SUN, H., HUANG, R., ZHANG, Y., CHERGUI, A., JI, J., DOROSHOW, J. H., JADHAV, A., TAKEDA, S., XIA, M. & POMMIER, Y. 2014. Identification of novel PARP inhibitors using a cell-based TDP1 inhibitory assay in a quantitative high-throughput screening platform. *DNA Repair,* 21**,** 177-82.

NAKAMURA, J., LA, D. K. & SWENBERG, J. A. 2000. 5'-nicked apurinic/apyrimidinic sites are resistant to beta-elimination by beta-polymerase and are persistent in human cultured cells after oxidative stress. *The Journal of biological chemistry,* 275**,** 5323-8.

NASH, H. M., LU, R., LANE, W. S. & VERDINE, G. L. 1997. The critical active-site amine of the human 8-oxoguanine DNA glycosylase, hOgg1: direct identification, ablation and chemical reconstitution. *Chemistry & biology,* 4**,** 693-702.

NEALE, M. J., PAN, J. & KEENEY, S. 2005. Endonucleolytic processing of covalent protein-linked DNA double-strand breaks. *Nature,* 436**,** 1053-7.

NEVELING, K., ENDT, D., HOEHN, H. & SCHINDLER, D. 2009. Genotype-phenotype correlations in Fanconi anemia. *Mutat Res,* 668**,** 73-91.

NIEDERNHOFER, L. J., ODIJK, H., BUDZOWSKA, M., VAN DRUNEN, E., MAAS, A., THEIL, A. F., DE WIT, J., JASPERS, N. G., BEVERLOO, H. B., HOEIJMAKERS, J. H. & KANAAR, R. 2004. The structure-specific endonuclease Ercc1-Xpf is required to resolve DNA interstrand cross-link-induced double-strand breaks. *Mol Cell Biol,* 24**,** 5776-87.

NIELSEN, C. F., HUTTNER, D., BIZARD, A. H., HIRANO, S., LI, T.-N., PALMAI-PALLAG, T., BJERREGAARD, V. A., LIU, Y., NIGG, E. A., WANG, L. H.-C. & HICKSON, I. D. 2015. PICH promotes sister chromatid disjunction and co-operates with topoisomerase II in mitosis. *Nature communications,* 6**,** 8962-62.

NIMONKAR, A. V., GENSCHEL, J., KINOSHITA, E., POLACZEK, P., CAMPBELL, J. L., WYMAN, C., MODRICH, P. & KOWALCZYKOWSKI, S. C. 2011. BLM-DNA2-RPA-MRN and EXO1-BLM-RPA-MRN constitute two DNA end resection machineries for human DNA break repair. *Genes Dev,* 25**,** 350-62.

NIMONKAR, A. V., OZSOY, A. Z., GENSCHEL, J., MODRICH, P. & KOWALCZYKOWSKI, S. C. 2008. Human exonuclease 1 and BLM helicase interact to resect DNA and initiate DNA repair. *Proc Natl Acad Sci U S A,* 105**,** 16906-11.

NISHI, R., OKUDA, Y., WATANABE, E., MORI, T., IWAI, S., MASUTANI, C., SUGASAWA, K. & HANAOKA, F. 2005. Centrin 2 stimulates nucleotide excision repair by interacting with xeroderma pigmentosum group C protein. *Molecular and cellular biology,* 25**,** 5664-74.

NISHITOH, H., KADOWAKI, H., NAGAI, A., MARUYAMA, T., YOKOTA, T., FUKUTOMI, H., NOGUCHI, T., MATSUZAWA, A., TAKEDA, K. & ICHIJO, H. 2008. ALS-linked mutant SOD1 induces ER stress- and ASK1-dependent motor neuron death by targeting Derlin-1. *Genes Dev,* 22**,** 1451-64.

NITISS, J. L. 2009. DNA topoisomerase II and its growing repertoire of biological functions. *Nature reviews. Cancer,* 9**,** 327-37.

NITISS, K. C., MALIK, M., HE, X., WHITE, S. W. & NITISS, J. L. 2006. Tyrosyl-DNA phosphodiesterase (Tdp1) participates in the repair of Top2-mediated DNA damage. *Proceedings of the National Academy of Sciences of the United States of America,* 103**,** 8953-58.

NIVENS, M. C., FELDER, T., GALLOWAY, A. H., PENA, M. M. O., POULIOT, J. J. & SPENCER, H. T. 2004. Engineered resistance to camptothecin and antifolates by retroviral coexpression of tyrosyl DNA phosphodiesterase-I and thymidylate synthase. *Cancer Chemotherapy and Pharmacology,* 53**,** 107-15.

NOON, A. T., SHIBATA, A., RIEF, N., LOBRICH, M., STEWART, G. S., JEGGO, P. A. & GOODARZI, A. A. 2010. 53BP1-dependent robust localized KAP-1 phosphorylation is essential for heterochromatic DNA double-strand break repair. *Nat Cell Biol,* 12**,** 177-84.

NORBURY, C. & NURSE, P. 1992. Animal cell cycles and their control. *Annual review of biochemistry,* 61**,** 441-70.

NURSE, P., LEVINE, C., HASSING, H. & MARIANS, K. J. 2003. Topoisomerase III can serve as the cellular decatenase in Escherichia coli. *Journal of Biological Chemistry,* 278**,** 8653-60.

O'DRISCOLL, M. & JEGGO, P. A. 2006. The role of double-strand break repair - insights from human genetics. *Nature reviews. Genetics,* 7**,** 45-54.

O'GORMAN, S., FOX, D. T. & WAHL, G. M. 1991. Recombinase-mediated gene activation and site-specific integration in mammalian cells. *Science,* 251**,** 1351-5.

OGATA, M., HINO, S.-I., SAITO, A., MORIKAWA, K., KONDO, S., KANEMOTO, S., MURAKAMI, T., TANIGUCHI, M., TANII, I., YOSHINAGA, K., SHIOSAKA, S., HAMMARBACK, J. A., URANO, F. & IMAIZUMI, K. 2006. Autophagy is activated for cell survival after endoplasmic reticulum stress. *Molecular and cellular biology,* 26**,** 9220-31.

OGATA, N., UEDA, K., KAWAICHI, M. & HAYAISHI, O. 1981. Poly(ADP-ribose) synthetase, a main acceptor of poly(ADP-ribose) in isolated nuclei. *J. Biol. Chem.,* 256**,** 4135-37.

OGI, T. & LEHMANN, A. R. 2006. The Y-family DNA polymerase kappa (pol kappa) functions in mammalian nucleotide-excision repair. *Nature cell biology,* 8**,** 640-2.

OGI, T., LIMSIRICHAIKUL, S., OVERMEER, R. M., VOLKER, M., TAKENAKA, K., CLONEY, R., NAKAZAWA, Y., NIIMI, A., MIKI, Y., JASPERS, N. G., MULLENDERS, L. H. F., YAMASHITA, S., FOUSTERI, M. I. & LEHMANN, A. R. 2010. Three DNA Polymerases, Recruited by Different Mechanisms, Carry Out NER Repair Synthesis in Human Cells. *Molecular Cell,* 37**,** 714-27.

OKA, J., UEDA, K., HAYAISHI, O., KOMURA, H. & NAKANISHI, K. 1984. ADP-ribosyl protein lyase. Purification, properties, and identification of the product. *Journal of Biological Chemistry,* 259**,** 986-95.

OKADO-MATSUMOTO, A. & FRIDOVICH, I. 2001. Subcellular distribution of superoxide dismutases (SOD) in rat liver: Cu,Zn-SOD in mitochondria. *J Biol Chem,* 276**,** 38388-93.

OKANO, S., LAN, L., CALDECOTT, K. W., MORI, T. & YASUI, A. 2003. Spatial and temporal cellular responses to single-strand breaks in human cells. *Molecular and cellular biology,* 23**,** 3974-81.

OKSENYCH, V., DE JESUS, B. B., ZHOVMER, A., EGLY, J.-M. & COIN, F. 2009. Molecular insights into the recruitment of TFIIH to sites of DNA damage. *The EMBO journal,* 28**,** 2971-80.

OLIVE, P. L. & BANÁTH, J. P. 2006. The comet assay: a method to measure DNA damage in individual cells. *Nat. Protoc.,* 1**,** 23-29.

OLIVE, P. L., BANÁTH, J. P. & DURAND, R. E. 1990. Heterogeneity in radiation-induced DNA damage and repair in tumor and normal cells measured using the "comet" assay. *Radiation research,* 122**,** 86-94.

ORTHWEIN, A., NOORDERMEER, S. M., WILSON, M. D., LANDRY, S., ENCHEV, R. I., SHERKER, A., MUNRO, M., PINDER, J., SALSMAN, J., DELLAIRE, G., XIA, B., PETER, M. & DUROCHER, D. 2015. A mechanism for the suppression of homologous recombination in G1 cells. *Nature,* 528**,** 422-26.

OSTLING, O. & JOHANSON, K. J. 1984. Microelectrophoretic study of radiation-induced DNA damages in individual mammalian cells. *Biochemical and biophysical research communications,* 123**,** 291-8.

PALOMBO, F., GALLINARI, P., IACCARINO, I., LETTIERI, T., HUGHES, M., D'ARRIGO, A., TRUONG, O., HSUAN, J. J. & JIRICNY, J. 1995. GTBP, a 160-kilodalton protein essential for mismatch-binding activity in human cells. *Science (New York, N.Y.),* 268**,** 1912-14.

PALOMBO, F., IACCARINO, I., NAKAJIMA, E., IKEJIMA, M., SHIMADA, T. & JIRICNY, J. 1996. hMutS??, a heterodimer of hMSH2 and hMSH3, binds to insertion/deletion loops in DNA. *Current Biology,* 6**,** 1181-84.

PANDITA, T. K., LIEBERMAN, H. B., LIM, D. S., DHAR, S., ZHENG, W., TAYA, Y. & KASTAN, M. B. 2000. Ionizing radiation activates the ATM kinase throughout the cell cycle. *Oncogene,* 19**,** 1386-91.

PAPA, S., MARTINO, P. L., CAPITANIO, G., GABALLO, A., DE RASMO, D., SIGNORILE, A. & PETRUZZELLA, V. 2012. The oxidative phosphorylation system in mammalian mitochondria. *Advances in Experimental Medicine and Biology,* 942**,** 1-37.

PAPATHANASIOU, M. A., KERR, N. C., ROBBINS, J. H., MCBRIDE, O. W., ALAMO, I., BARRETT, S. F., HICKSON, I. D. & FORNACE, A. J. 1991. Induction by ionizing radiation of the gadd45 gene in cultured human cells: lack of mediation by protein kinase C. *Molecular and cellular biology,* 11**,** 1009-16.

PÂQUES, F., HABER, J. E., PAQUES, F. & HABER, J. E. 1999. Multiple pathways of recombination induced by double-strand breaks in Saccharomyces cerevisiae. *Microbiol Mol Biol Rev,* 63**,** 349-404.

PARIKH, S. S., MOL, C. D., SLUPPHAUG, G., BHARATI, S., KROKAN, H. E. & TAINER, J. A. 1998. Base excision repair initiation revealed by crystal structures and binding kinetics of human uracil-DNA glycosylase with DNA. *The EMBO journal,* 17**,** 5214-26.

PARK, J. W. & AMES, B. N. 1988. 7-Methylguanine adducts in DNA are normally present at high levels and increase on aging: analysis by HPLC with electrochemical detection. *Proceedings of the National Academy of Sciences of the United States of America,* 85**,** 7467-70.

PARSONS, J. L., DIANOVA, I. I., ALLINSON, S. L. & DIANOV, G. L. 2005. Poly(ADP-ribose) polymerase-1 protects excessive DNA strand breaks from deterioration during repair in human cell extracts. *FEBS Journal,* 272**,** 2012-21.

PARSONS, J. L., DIANOVA, I. I. & DIANOV, G. L. 2004. APE1 is the major 3???-phosphoglycolate activity in human cell extracts. *Nucleic Acids Research,* 32**,** 3531-36.

PASINELLI, P., BELFORD, M. E., LENNON, N., BACSKAI, B. J., HYMAN, B. T., TROTTI, D. & BROWN, R. H. 2004. Amyotrophic lateral sclerosis-associated SOD1 mutant proteins bind and aggregate with Bcl-2 in spinal cord mitochondria. *Neuron,* 43**,** 19-30.

PATEL, A. G., FLATTEN, K. S., SCHNEIDER, P. A., DAI, N. T., MCDONALD, J. S., POIRIER, G. G. & KAUFMANN, S. H. 2012. Enhanced killing of cancer cells by poly(ADP-ribose) polymerase inhibitors and topoisomerase I inhibitors reflects poisoning of both enzymes. *J Biol Chem,* 287**,** 4198-210.

PAUL, K., WANG, M., MLADENOV, E., BENCSIK-THEILEN, A., BEDNAR, T., WU, W., ARAKAWA, H. & ILIAKIS, G. 2013. DNA Ligases I and III Cooperate in Alternative Non-Homologous End-Joining in Vertebrates. *PLoS ONE,* 8**,** e59505.

PAUL-KONIETZKO, K., THOMALE, J., ARAKAWA, H. & ILIAKIS, G. 2015. DNA Ligases I and III Support Nucleotide Excision Repair in DT40 Cells with Similar Efficiency. *Photochem Photobiol,* 91**,** 1173-80.

PEDRINI, S., SAU, D., GUARESCHI, S., BOGUSH, M., BROWN, R. H., JR., NANICHE, N., KIA, A., TROTTI, D. & PASINELLI, P. 2010. ALS-linked mutant SOD1 damages mitochondria by promoting conformational changes in Bcl-2. *Hum Mol Genet,* 19**,** 2974-86.

PELLEGRINI, L., YU, D. S., LO, T., ANAND, S., LEE, M., BLUNDELL, T. L. & VENKITARAMAN, A. R. 2002. Insights into DNA recombination from the structure of a RAD51-BRCA2 complex. *Nature,* 420**,** 287-93.

PETER, B. J., ULLSPERGER, C., HIASA, H., MARIANS, K. J. & COZZARELLI, N. R. 1998. The structure of supercoiled intermediates in DNA replication. *Cell,* 94**,** 819-27.

PETRINI, J. H., MASER, R. S. & BRESSAN, D. A. 2001. The Mre11-Rad50 complex. *In:* HOEKSTRA, M. F. (ed.). Totowa, NJ: Humana Press.

PETUKHOVA, G., STRATTON, S. & SUNG, P. 1998. Catalysis of homologous DNA pairing by yeast Rad51 and Rad54 proteins. *Nature,* 393**,** 91-4.

PETUKHOVA, G., VAN KOMEN, S., VERGANO, S., KLEIN, H. & SUNG, P. 1999. Yeast Rad54 promotes Rad51-dependent homologous DNA pairing via ATP hydrolysis-driven change in DNA double helix conformation. *J Biol Chem,* 274**,** 29453-62.

PFEIFER, G. P. 1997. Formation and processing of UV photoproducts: effects of DNA sequence and chromatin environment. *Photochemistry and photobiology,* 65**,** 270-83.

PFEIFFER, P., GOEDECKE, W. & OBE, G. 2000. Mechanisms of DNA double-strand break repair and their potential to induce chromosomal aberrations. *Mutagenesis,* 15**,** 289-302.

PICHIERRI, P. & ROSSELLI, F. 2004. Fanconi anemia proteins and the s phase checkpoint. *Cell Cycle,* 3**,** 698-700.

PLANK, J. L., CHU, S. H., POHLHAUS, J. R., WILSON-SALI, T. & HSIEH, T. S. 2005. Drosophila melanogaster topoisomerase IIIalpha preferentially relaxes a positively or negatively supercoiled bubble substrate and is essential during development. *J Biol Chem,* 280**,** 3564-73.

PLANK, J. L., WU, J. & HSIEH, T.-S. 2006. Topoisomerase IIIalpha and Bloom's helicase can resolve a mobile double Holliday junction substrate through convergent branch migration. *Proceedings of the National Academy of Sciences of the United States of America,* 103**,** 11118-23.

PLESCHKE, J. M., KLECZKOWSKA, H. E., STROHM, M. & ALTHAUS, F. R. 2000. Poly(ADP-ribose) binds to specific domains in DNA damage checkpoint proteins. *Journal of Biological Chemistry,* 275**,** 40974-80.

PLO, I., LIAO, Z. Y., BARCELÓ, J. M., KOHLHAGEN, G., CALDECOTT, K. W., WEINFELD, M. & POMMIER, Y. 2003. Association of XRCC1 and tyrosyl DNA phosphodiesterase (Tdp1) for the repair of topoisomerase I-mediated DNA lesions. *DNA Repair,* 2**,** 1087-100.

PLUCIENNIK, A., DZANTIEV, L., IYER, R. R., CONSTANTIN, N., KADYROV, F. A. & MODRICH, P. 2010. PCNA function in the activation and strand direction of MutLα endonuclease in mismatch repair. *Proceedings of the National Academy of Sciences of the United States of America,* 107**,** 16066-71.

PODLUTSKY, A. J., DIANOVA, I. I., PODUST, V. N., BOHR, V. A. & DIANOV, G. L. 2001. Human DNA polymerase ?? initiates DNA synthesis during long-patch repair of reduced AP sites in DNA. *EMBO Journal,* 20**,** 1477-82.

POHJOISMÄKI, J. L. O., WANROOIJ, S., HYVÄRINEN, A. K., GOFFART, S., HOLT, I. J., SPELBRINK, J. N. & JACOBS, H. T. 2006. Alterations to the expression level of mitochondrial transcription factor A, TFAM, modify the mode of mitochondrial DNA replication in cultured human cells. *Nucleic acids research,* 34**,** 5815-28.

POMMIER, Y. 2006. Topoisomerase I inhibitors: camptothecins and beyond. *Nature reviews. Cancer,* 6**,** 789-802.

POMMIER, Y., BARCELO, J. M., RAO, V. A., SORDET, O., JOBSON, A. G., THIBAUT, L., MIAO, Z. H., SEILER, J. A., ZHANG, H., MARCHAND, C., AGAMA, K., NITISS, J. L. & REDON, C. 2006. Repair of topoisomerase I-mediated DNA damage. *Prog Nucleic Acid Res Mol Biol,* 81**,** 179-229.

POMMIER, Y., REDON, C., RAO, V. A., SEILER, J. A., SORDET, O., TAKEMURA, H., ANTONY, S., MENG, L., LIAO, Z., KOHLHAGEN, G., ZHANG, H. & KOHN, K. W. 2003. Repair of and checkpoint response to topoisomerase I-mediated DNA damage. *Mutation Research - Fundamental and Molecular Mechanisms of Mutagenesis,* 532**,** 173-203.

POMMIER, Y., SORDET, O., RAO, V. A., ZHANG, H. & KOHN, K. W. 2005. Targeting chk2 kinase: molecular interaction maps and therapeutic rationale. *Curr Pharm Des,* 11**,** 2855-72.

POMMIER, Y., SUN, Y., HUANG, S. N. & NITISS, J. L. 2016. Roles of eukaryotic topoisomerases in transcription, replication and genomic stability. *Nat Rev Mol Cell Biol,* 17**,** 703-721.

POON, H. F., HENSLEY, K., THONGBOONKERD, V., MERCHANT, M. L., LYNN, B. C., PIERCE, W. M., KLEIN, J. B., CALABRESE, V. & BUTTERFIELD, D. A. 2005. Redox proteomics analysis of oxidatively modified proteins in G93A-SOD1 transgenic mice--a model of familial amyotrophic lateral sclerosis. *Free Radic Biol Med,* 39**,** 453-62.

POPE, M. A., PORELLO, S. L. & DAVID, S. S. 2002. Escherichia coli apurinic-apyrimidinic endonucleases enhance the turnover of the adenine glycosylase MutY with G:A substrates. *Journal of Biological Chemistry,* 277**,** 22605-15.

PORTER, S. E. & CHAMPOUX, J. J. 1989. The basis for camptothecin enhancement of DNA breakage by eukaryotic topoisomerase I. *Nucleic Acids Research,* 17**,** 8521-32.

POULIOT, J. J., ROBERTSON, C. A. & NASH, H. A. 2001. Pathways for repair of topoisomerase I covalent complexes in Saccharomyces cerevisiae. *Genes to Cells,* 6**,** 677-87.

POULIOT, J. J., YAO, K. C., ROBERTSON, C. A. & NASH, H. A. 1999. Yeast gene for a Tyr-DNA phosphodiesterase that repairs topoisomerase I complexes. *Science,* 286**,** 552-55.

POULTON, C., OEGEMA, R., HEIJSMAN, D., HOOGEBOOM, J., SCHOT, R., STROINK, H., WILLEMSEN, M. A., VERHEIJEN, F. W., VAN DE SPEK, P., KREMER, A. & MANCINI, G. M. S. 2013. Progressive cerebellar atrophy and polyneuropathy: expanding the spectrum of PNKP mutations. *Neurogenetics,* 14**,** 43-51.

POURQUIER, P. & POMMIER, Y. 2001. Topoisomerase I-mediated DNA damage. *Adv Cancer Res,* 80**,** 189-216.

POVIRK, L. F., ZHOU, T., ZHOU, R., COWAN, M. J. & YANNONE, S. M. 2007. Processing of 3'-phosphoglycolate-terminated DNA double strand breaks by Artemis nuclease. *J Biol Chem,* 282**,** 3547-58.

PRASAD, R., DIANOV, G. L., BOHR, V. A. & WILSON, S. H. 2000. FEN1 stimulation of DNA polymerase ?? mediates an excision step in mammalian long patch base excision repair. *Journal of Biological Chemistry,* 275**,** 4460-66.

PUC, J., KOZBIAL, P., AGGARWAL, A. K., ROSENFELD, M. G., LI, W., TAN, Y., LIU, Z., SUTER, T., OHGI, K. A. & ZHANG, J. 2015. Ligand-Dependent Enhancer Activation Regulated by Topoisomerase-I Activity Article Ligand-Dependent Enhancer Activation Regulated by Topoisomerase-I Activity. *Cell,* 160**,** 367-80.

PUCK, T. T. & MARCUS, P. I. 1956. Action of x-rays on mammalian cells. *The Journal of experimental medicine,* 103**,** 653-66.

PUEBLA-OSORIO, N., LACEY, D. B., ALT, F. W. & ZHU, C. 2006. Early embryonic lethality due to targeted inactivation of DNA ligase III. *Mol Cell Biol,* 26**,** 3935-41.

RALLABHANDI, P., HASHIMOTO, K., MO, Y. Y., BECK, W. T., MOITRA, P. K. & D'ARPA, P. 2002. Sumoylation of topoisomerase I is involved in its partitioning between nucleoli and nucleoplasm and its clearing from nucleoli in response to camptothecin. *J Biol Chem,* 277**,** 40020-26.

RAMADAN, S., TERRINONI, A., CATANI, M. V., SAYAN, A. E., KNIGHT, R. A., MUELLER, M., KRAMMER, P. H., MELINO, G. & CANDI, E. 2005. p73 induces apoptosis by different mechanisms. *Biochemical and biophysical research communications,* 331**,** 713-7.

RAMILO, C., GU, L., GUO, S., ZHANG, X., PATRICK, S. M., TURCHI, J. J. & LI, G. M. 2002. Partial Reconstitution of Human DNA Mismatch Repair In Vitro: Characterization of the Role of Human Replication Protein A. *Molecular and Cellular Biology,* 22**,** 2037-46.

RAMPAKAKIS, E., GKOGKAS, C., DI PAOLA, D. & ZANNIS-HADJOPOULOS, M. 2010. Replication initiation and DNA topology: The twisted life of the origin. *Journal of Cellular Biochemistry,* 110**,** 35-43.

RAMPAKAKIS, E. & ZANNIS-HADJOPOULOS, M. 2009. Transient dsDNA breaks during pre-replication complex assembly. *Nucleic Acids Research,* 37**,** 5714-24.

RÄSCHLE, M., MARRA, G., NYSTRÖM-LAHTI, M., SCHÄR, P. & JIRICNY, J. 1999. Identification of hMutLbeta, a heterodimer of hMLH1 and hPMS1. *The Journal of biological chemistry,* 274**,** 32368-75.

RASS, E., GRABARZ, A., PLO, I., GAUTIER, J., BERTRAND, P. & LOPEZ, B. S. 2009. Role of Mre11 in chromosomal nonhomologous end joining in mammalian cells. *Nature Structural & Molecular Biology,* 16**,** 819-24.

RASS, U., AHEL, I. & WEST, S. C. 2007. Actions of aprataxin in multiple DNA repair pathways. *The Journal of biological chemistry,* 282**,** 9469-74.

RATHBUN, G. A., ZIV, Y., LAI, J. H., HILL, D., ABRAHAM, R. H., SHILOH, Y. & CANTLEY, L. C. 1999. ATM and lymphoid malignancies; use of oriented peptide libraries to identify novel substrates of ATM critical in downstream signaling pathways. *Current topics in microbiology and immunology,* 246**,** 267-73; discussion 74.

RATNER, J. N., BALASUBRAMANIAN, B., CORDEN, J., WARREN, S. L. & BREGMAN, D. B. 1998. Ultraviolet Radiation-induced Ubiquitination and Proteasomal Degradation of the Large Subunit of RNA Polymerase II. *J. Biol. Chem.,* 273**,** 5184-89.

RAYMOND, A. C., STAKER, B. L. & BURGIN, A. B. 2005. Substrate specificity of tyrosyl-DNA phosphodiesterase I (Tdp1). *Journal of Biological Chemistry,* 280**,** 22029-35.

REARDON, J. T., BESSHO, T., KUNG, H. C., BOLTON, P. H. & SANCAR, A. 1997. +"repair of 8-OH-G is excision" In vitro repair of oxidative DNA damage by human nucleotide excision repair system: possible explanation for neurodegeneration in xeroderma pigmentosum patients. *Proc Natl Acad Sci U S A,* 94**,** 9463-68.

REDON, C., PILCH, D. R., ROGAKOU, E. P., ORR, A. H., LOWNDES, N. F. & BONNER, W. M. 2003. Yeast histone 2A serine 129 is essential for the efficient repair of checkpoint-blind DNA damage. *EMBO reports,* 4**,** 678-84.

REGAIRAZ, M., ZHANG, Y. W., FU, H., AGAMA, K. K., TATA, N., AGRAWAL, S., ALADJEM, M. I. & POMMIER, Y. 2011. Mus81-mediated DNA cleavage resolves replication forks stalled by topoisomerase I-DNA complexes. *J Cell Biol,* 195**,** 739-49.

REYNOLDS, J. J., WALKER, A. K., GILMORE, E. C., WALSH, C. A. & CALDECOTT, K. W. 2012. Impact of PNKP mutations associated with microcephaly, seizures and developmental delay on enzyme activity and DNA strand break repair. *Nucleic Acids Research,* 40**,** 6608-19.

RIBALLO, E., KÜHNE, M., RIEF, N., DOHERTY, A., SMITH, G. C. M., RECIO, M.-J., REIS, C., DAHM, K., FRICKE, A., KREMPLER, A., PARKER, A. R., JACKSON, S. P., GENNERY, A., JEGGO, P. A. & LÖBRICH, M. 2004. A pathway of double-strand break rejoining dependent upon ATM, Artemis, and proteins locating to gamma-H2AX foci. *Molecular cell,* 16**,** 715-24.

RIBALLO, E., WOODBINE, L., STIFF, T., WALKER, S. A., GOODARZI, A. A. & JEGGO, P. A. 2009. XLF-Cernunnos promotes DNA ligase IV-XRCC4 re-adenylation following ligation. *Nucleic Acids Research,* 37**,** 482-92.

RILEY, P. A. 1994. Free radicals in biology: Oxidative stress and the effects of ionizing radiation. *International Journal of Radiation Biology,* 65**,** 27-33.

ROBBERECHT, W. 2000. Oxidative stress in amyotrophic lateral sclerosis. *Journal of neurology,* 247 Suppl**,** I1-6.

ROBSON, C. N. & HICKSON, I. D. 1991. Isolation of cDNA clones encoding a human apurinic/apyrimidinic endonuclease that corrects DNA repair and mutagenesis defects in E. coli xth (exonuclease III) mutants. *Nucleic Acids Res.,* 19**,** 5519-23.

ROGAKOU, E. P., PILCH, D. R., ORR, A. H., IVANOVA, V. S. & BONNER, W. M. 1998. DNA double-stranded breaks induce histone H2AX phosphorylation on serine 139. *Journal of Biological Chemistry,* 273**,** 5858-68.

ROOS-MATTJUS, P., HOPKINS, K. M., OESTREICH, A. J., VROMAN, B. T., JOHNSON, K. L., NAYLOR, S., LIEBERMAN, H. B. & KARNITZ, L. M. 2003. Phosphorylation of Human Rad9 Is Required for Genotoxin-activated Checkpoint Signaling. *Journal of Biological Chemistry,* 278**,** 24428-37.

ROSA, I. D., GOFFART, S., WURM, M., WIEK, C., ESSMANN, F., SOBEK, S., SCHROEDER, P., ZHANG, H., KRUTMANN, J., HANENBERG, H., SCHULZE-OSTHOFF, K., MIELKE, C., POMMIER, Y., BOEGE, F. & CHRISTENSEN, M. O. 2009. Adaptation of topoisomerase I paralogs to nuclear and mitochondrial DNA. *Nucleic Acids Research,* 37**,** 6414-28.

ROSSI, F., LABOURIER, E., FORNE, T., DIVITA, G., DERANCOURT, J., RIOU, J. F., ANTOINE, E., CATHALA, G., BRUNEL, C. & TAZI, J. 1996. Specific phosphorylation of SR proteins by mammalian DNA topoisomerase I. *Nature,* 381**,** 80-82.

RULTEN, S. L., FISHER, A. E., ROBERT, I., ZUMA, M. C., ROULEAU, M., JU, L., POIRIER, G., REINA-SAN-MARTIN, B. & CALDECOTT, K. W. 2011. PARP-3 and APLF function together to accelerate nonhomologous end-joining. *Mol Cell,* 41**,** 33-45.

RYDBERG, B. & LINDAHL, T. 1982. Nonenzymatic methylation of DNA by the intracellular methyl group donor S-adenosyl-L-methionine is a potentially mutagenic reaction. *The EMBO journal,* 1**,** 211-16.

SACHO, E. J. & MAIZELS, N. 2011. DNA repair factor MRE11/RAD50 cleaves 3'-phosphotyrosyl bonds and resects DNA to repair damage caused by topoisomerase 1 poisons. *The Journal of biological chemistry,* 286**,** 44945-51.

SAITOH, H. & HINCHEY, J. 2000. Functional heterogeneity of small ubiquitin-related protein modifiers SUMO-1 versus SUMO-2/3. *The Journal of biological chemistry,* 275**,** 6252-8.

SALAZAR, J. J. & VAN HOUTEN, B. 1997. Preferential mitochondrial DNA injury caused by glucose oxidase as a steady generator of hydrogen peroxide in human fibroblasts. *Mutat Res,* 385**,** 139-49.

SAMBROOK, J. & W RUSSELL, D. 2001. Molecular Cloning: A Laboratory Manual. *Cold Spring Harbor Laboratory Press, Cold Spring Harbor, NY***,** 999-99.

SAMOL, J., RANSON, M., SCOTT, E., MACPHERSON, E., CARMICHAEL, J., THOMAS, A. & CASSIDY, J. 2012. Safety and tolerability of the poly(ADP-ribose) polymerase (PARP) inhibitor, olaparib (AZD2281) in combination with topotecan for the treatment of patients with advanced solid tumors: a phase I study. *Invest New Drugs,* 30**,** 1493-500.

SAN FILIPPO, J., CHI, P., SEHORN, M. G., ETCHIN, J., KREJCI, L., SUNG, P., FILIPPO, J. S., CHI, P., SEHORN, M. G., ETCHIN, J., KREJCI, L. & SUNG, P. 2006. Recombination mediator and Rad51 targeting activities of a human BRCA2 polypeptide. *J Biol Chem,* 281**,** 11649-57.

SANCHEZ, Y., WONG, C., THOMA, R. S., RICHMAN, R., WU, Z., PIWNICA-WORMS, H. & ELLEDGE, S. J. 1997. Conservation of the Chk1 checkpoint pathway in mammals: linkage of DNA damage to Cdk regulation through Cdc25. *Science (New York, N.Y.),* 277**,** 1497-501.

SARKARIA, J. N., BUSBY, E. C., TIBBETTS, R. S., ROOS, P., TAYA, Y., KARNITZ, L. M. & ABRAHAM, R. T. 1999. Inhibition of ATM and ATR kinase activities by the radiosensitizing agent, caffeine. *Cancer Research,* 59**,** 4375-82.

SAU, D., RUSMINI, P., CRIPPA, V., ONESTO, E., BOLZONI, E., RATTI, A. & POLETTI, A. 2011. Dysregulation of axonal transport and motorneuron diseases. *Biol Cell,* 103**,** 87-107.

SAWYER, D. E., ROMAN, S. D. & AITKEN, R. J. 2001. Relative susceptibilities of mitochondrial and nuclear DNA to damage induced by hydrogen peroxide in two mouse germ cell lines. *Redox Rep,* 6**,** 182-4.

SCARPULLA, R. C. 2006. Nuclear control of respiratory gene expression in mammalian cells. *Journal of Cellular Biochemistry,* 97**,** 673-83.

SCHAR, P., HERRMANN, G., DALY, G. & LINDAHL, T. 1997. A newly identified DNA ligase of Saccharomyces cerevisiae involved in RAD52-independent repair of DNA double-strand breaks. *Genes Dev,* 11**,** 1912-24.

SCHÄRER, O. D. 2007. Achieving Broad Substrate Specificity in Damage Recognition by Binding Accessible Nondamaged DNA. *Molecular Cell,* 28**,** 184-86.

SCHMICKEL, R. D., CHU, E. H., TROSKO, J. E. & CHANG, C. C. 1977. Cockayne syndrome: a cellular sensitivity to ultraviolet light. *Pediatrics,* 60**,** 135-9.

SCHUETTPELZ, L. G. & LINK, D. C. 2013. Regulation of hematopoietic stem cell activity by inflammation. *Frontiers in Immunology,* 4**,** 204.

SCHWAB, R. A., BLACKFORD, A. N. & NIEDZWIEDZ, W. 2010. ATR activation and replication fork restart are defective in FANCM-deficient cells. *Embo J,* 29**,** 806-18.

SCLAFANI, R. A. & HOLZEN, T. M. 2007. Cell cycle regulation of DNA replication. *Annual review of genetics,* 41**,** 237-80.

SEDGWICK, B., ROBINS, P. & LINDAHL, T. 2006. Direct Removal of Alkylation Damage from DNA by AlkB and Related DNA Dioxygenases. *Methods in enzymology,* 408**,** 108-20.

SEGAL-RAZ, H., MASS, G., BARANES-BACHAR, K., LERENTHAL, Y., WANG, S.-Y., CHUNG, Y. M., ZIV-LEHRMAN, S., STRÖM, C. E., HELLEDAY, T., HU, M. C. T., CHEN, D. J. & SHILOH, Y. 2011. ATM-mediated phosphorylation of polynucleotide kinase/phosphatase is required for effective DNA double-strand break repair. *EMBO reports,* 12**,** 713-9.

SEKI, S., OHZEKI, M., UCHIDA, A., HIRANO, S., MATSUSHITA, N., KITAO, H., ODA, T., YAMASHITA, T., KASHIHARA, N., TSUBAHARA, A., TAKATA, M. & ISHIAI, M. 2007. A requirement of FancL and FancD2 monoubiquitination in DNA repair. *Genes Cells,* 12**,** 299-310.

SHAO, R. G., CAO, C. X., SHIMIZU, T., O'CONNOR, P. M., KOHN, K. W. & POMMIER, Y. 1997. Abrogation of an S-phase checkpoint and potentiation of camptothecin cytotoxicity by 7-hydroxystaurosporine (UCN-01) in human cancer cell lines, possibly influenced by p53 function. *Cancer Res,* 57**,** 4029-35.

SHARAN, S. K., MORIMATSU, M., ALBRECHT, U., LIM, D. S., REGEL, E., DINH, C., SANDS, A., EICHELE, G., HASTY, P. & BRADLEY, A. 1997. Embryonic lethality and radiation hypersensitivity mediated by Rad51 in mice lacking Brca2. *Nature,* 386**,** 804-10.

SHEIKH, H., COLACO, R., LORIGAN, P., BLACKHALL, F., CALIFANO, R., ASHCROFT, L., TAYLOR, P., THATCHER, N. & FAIVRE-FINN, C. 2011. Use of G-CSF during concurrent chemotherapy and thoracic radiotherapy in patients with limited-stage small-cell lung cancer safety data from a phase II trial. *Lung cancer (Amsterdam, Netherlands),* 74**,** 75-9.

SHEN, J., GILMORE, E. C., MARSHALL, C. A., HADDADIN, M., REYNOLDS, J. J., EYAID, W., BODELL, A., BARRY, B., GLEASON, D., ALLEN, K., GANESH, V. S., CHANG, B. S., GRIX, A., HILL, R. S., TOPCU, M., CALDECOTT, K. W., BARKOVICH, A. J. & WALSH, C. A. 2010. Mutations in PNKP cause microcephaly, seizures and defects in DNA repair. *Nature genetics,* 42**,** 245-9.

SHIBATA, A., BARTON, O., NOON, A. T., DAHM, K., DECKBAR, D., GOODARZI, A. A., LOBRICH, M. & JEGGO, P. A. 2010. Role of ATM and the damage response mediator proteins 53BP1 and MDC1 in the maintenance of G(2)/M checkpoint arrest. *Mol Cell Biol,* 30**,** 3371-83.

SHIBATA, N. 2001. Transgenic mouse model for familial amyotrophic lateral sclerosis with superoxide dismutase-1 mutation. *Neuropathology,* 21**,** 82-92.

SHIBUTANI, S., TAKESHITA, M. & GROLLMAN, A. P. 1991. Insertion of specific bases during DNA synthesis past the oxidation-damaged base 8-oxodG. *Nature,* 349**,** 431-34.

SHIEH, S. Y., AHN, J., TAMAI, K., TAYA, Y. & PRIVES, C. 2000. The human homologs of checkpoint kinases Chk1 and Cds1 (Chk2) phosphorylate p53 at multiple DNA damage-inducible sites. *Genes Dev,* 14**,** 289-300.

SHILOH, Y. 2003. ATM and related protein kinases: safeguarding genome integrity. *Nature reviews. Cancer,* 3**,** 155-68.

SHIMIZU, S., KANASEKI, T., MIZUSHIMA, N., MIZUTA, T., ARAKAWA-KOBAYASHI, S., THOMPSON, C. B. & TSUJIMOTO, Y. 2004. Role of Bcl-2 family proteins in a non-apoptotic programmed cell death dependent on autophagy genes. *Nature cell biology,* 6**,** 1221-28.

SHIMODAIRA, H., YOSHIOKA-YAMASHITA, A., KOLODNER, R. D. & WANG, J. Y. J. 2003. Interaction of mismatch repair protein PMS2 and the p53-related transcription factor p73 in apoptosis response to cisplatin. *Proceedings of the National Academy of Sciences of the United States of America,* 100**,** 2420-5.

SHINTOMI, K., TAKAHASHI, T. S. & HIRANO, T. 2015. Reconstitution of mitotic chromatids with a minimum set of purified factors. *Nature Cell Biology,* 17**,** 1014-23.

SHIVJI, M. K., EKER, A. P. & WOOD, R. D. 1994. DNA repair defect in xeroderma pigmentosum group C and complementing factor from HeLa cells. *The Journal of biological chemistry,* 269**,** 22749-57.

SHYKIND, B. M., KIM, J., STEWART, L., CHAMPOUX, J. J. & SHARP, P. A. 1997. Topoisomerase I enhances TFIID-TFIIA complex assembly during activation of transcription. *Genes Dev,* 11**,** 397-407.

SIJMONS, R. H. & HOFSTRA, R. M. W. 2016. Review: Clinical aspects of hereditary DNA Mismatch repair gene mutations. *DNA repair,* 38**,** 155-62.

SIMSEK, D., BRUNET, E., WONG, S. Y. W., KATYAL, S., GAO, Y., MCKINNON, P. J., LOU, J., ZHANG, L., LI, J., REBAR, E. J., GREGORY, P. D., HOLMES, M. C. & JASIN, M. 2011. DNA ligase III promotes alternative nonhomologous end-joining during chromosomal translocation formation. *PLoS Genetics,* 7**,** e1002080.

SINGH, N. P., MCCOY, M. T., TICE, R. R. & SCHNEIDER, E. L. 1988. A simple technique for quantitation of low levels of DNA damage in individual cells. *Experimental Cell Research,* 175**,** 184-91.

SKOETZ, N., BOHLIUS, J., ENGERT, A., MONSEF, I., BLANK, O. & VEHRESCHILD, J.-J. 2015. Prophylactic antibiotics or G(M)-CSF for the prevention of infections and improvement of survival in cancer patients receiving myelotoxic chemotherapy. *The Cochrane database of systematic reviews,* 12**,** CD007107-CD07.

SLADE, D., DUNSTAN, M. S., BARKAUSKAITE, E., WESTON, R., LAFITE, P., DIXON, N., AHEL, M., LEYS, D. & AHEL, I. 2011. The structure and catalytic mechanism of a poly(ADP-ribose) glycohydrolase. *Nature,* 477**,** 616-20.

SMOGORZEWSKA, A., DESETTY, R., SAITO, T. T., SCHLABACH, M., LACH, F. P., SOWA, M. E., CLARK, A. B., KUNKEL, T. A., HARPER, J. W., COLAIACOVO, M. P. & ELLEDGE, S. J. 2010. A genetic screen identifies FAN1, a Fanconi anemia-associated nuclease necessary for DNA interstrand crosslink repair. *Mol Cell,* 39**,** 36-47.

SOBEK, S. & BOEGE, F. 2014. DNA topoisomerases in mtDNA maintenance and ageing. *Experimental Gerontology,* 56**,** 135-41.

SOBEK, S., DALLA ROSA, I., POMMIER, Y., BORNHOLZ, B., KALFALAH, F., ZHANG, H., WIESNER, R. J., VON KLEIST-RETZOW, J.-C., HILLEBRAND, F., SCHAAL, H., MIELKE, C., CHRISTENSEN, M. O. & BOEGE, F. 2013. Negative regulation of mitochondrial transcription by mitochondrial topoisomerase I. *Nucleic acids research,* 41**,** 9848-57.

SOEJIMA, H., ZHAO, W. & MUKAI, T. 2005. Epigenetic silencing of the MGMT gene in cancer. *Biochemistry and cell biology = Biochimie et biologie cellulaire,* 83**,** 429-37.

SOLIER, S., LANSIAUX, A., LOGETTE, E., WU, J., SORET, J., TAZI, J., BAILLY, C., DESOCHE, L., SOLARY, E. & CORCOS, L. 2004. Topoisomerase I and II inhibitors control caspase-2 pre-messenger RNA splicing in human cells. *Mol Cancer Res,* 2**,** 53-61.

SOLIER, S., RYAN, M. C., MARTIN, S. E., VARMA, S., KOHN, K. W., LIU, H., ZEEBERG, B. R. & POMMIER, Y. 2013. Transcription poisoning by topoisomerase i is controlled by gene length, splice sites, and miR-142-3p. *Cancer Research,* 73**,** 4830-39.

SOLIER, S. P., BARB, J., ZEEBERG, B. R., VARMA, S., RYAN, M. C., KOHN, K. W., WEINSTEIN, J. N., MUNSON, P. J. & POMMIER, Y. 2010. Genome-wide analysis of novel splice variants induced by topoisomerase i poisoning shows preferential occurrence in genes encoding splicing factors. *Cancer Research,* 70**,** 8055-65.

SOLINGER, J. A., KIIANITSA, K. & HEYER, W. D. 2002. Rad54, a Swi2/Snf2-like recombinational repair protein, disassembles Rad51:dsDNA filaments. *Mol Cell,* 10**,** 1175-88.

SORDET, O., KHAN, Q. A., KOHN, K. W. & POMMIER, Y. 2003. Apoptosis induced by topoisomerase inhibitors. *Curr Med Chem Anti-Canc Agents,* 3**,** 271-90.

SORDET, O., REDON, C. E., GUIROUILH-BARBAT, J., SMITH, S., SOLIER, S., DOUARRE, C., CONTI, C., NAKAMURA, A. J., DAS, B. B., NICOLAS, E., KOHN, K. W., BONNER, W. M. & POMMIER, Y. 2009. Ataxia telangiectasia mutated activation by transcription- and topoisomerase I-induced DNA double-strand breaks. *EMBO reports,* 10**,** 887-93.

SOTELO-SILVEIRA, J. R., LEPANTO, P., ELIZONDO, V., HORJALES, S., PALACIOS, F., MARTINEZ-PALMA, L., MARIN, M., BECKMAN, J. S. & BARBEITO, L. 2009. Axonal mitochondrial clusters containing mutant SOD1 in transgenic models of ALS. *Antioxid Redox Signal,* 11**,** 1535-45.

SPELBRINK, J. N. 2010. Functional organization of mammalian mitochondrial DNA in nucleoids: History, recent developments, and future challenges. *IUBMB life,* 62**,** 19-32.

SPITZNER, J. R. & MULLER, M. T. 1988. A consensus sequence for cleavage by vertebrate DNA topoisomerase II. *Nucleic Acids Research,* 16**,** 5533-56.

SRIVENUGOPAL, K. S., LOCKSHON, D. & MORRIS, D. R. 1984. Escherichia coli DNA topoisomerase III: purification and characterization of a new type I enzyme. *Biochemistry,* 23**,** 1899-906.

STAKER, B. L., FEESE, M. D., CUSHMAN, M., POMMIER, Y., ZEMBOWER, D., STEWART, L. & BURGIN, A. B. 2005. Structures of three classes of anticancer agents bound to the human topoisomerase I-DNA covalent complex. *J Med Chem,* 48**,** 2336-45.

STAKER, B. L., HJERRILD, K., FEESE, M. D., BEHNKE, C. A., BURGIN, A. B. & STEWART, L. 2002. The mechanism of topoisomerase I poisoning by a camptothecin analog. *Proceedings of the National Academy of Sciences of the United States of America,* 99**,** 15387-92; DOI: 10.1073/pnas.242259599.

STANKIEWICZ, P. J. & GRESSER, M. J. 1988. Inhibition of phosphatase and sulfatase by transition-state analogues. *Biochemistry,* 27**,** 206-12.

STEFANINI, M., LAGOMARSINI, P., GILIANI, S., NARDO, T., BOTTA, E., PESERICO, A., KLEIJER, W. J., LEHMANN, A. R. & SARASIN, A. 1993a. Genetic heterogeneity of the excision repair defect associated with trichothiodystrophy. *Carcinogenesis,* 14**,** 1101-05.

STEFANINI, M., VERMEULEN, W., WEEDA, G., GILIANI, S., NARDO, T., MEZZINA, M., SARASIN, A., HARPER, J. I., ARLETT, C. F. & HOEIJMAKERS, J. H. 1993b. A new nucleotide-excision-repair gene associated with the disorder trichothiodystrophy. *American journal of human genetics,* 53**,** 817-21.

STELTER, P. & ULRICH, H. D. 2003. Control of spontaneous and damage-induced mutagenesis by SUMO and ubiquitin conjugation. *Nature,* 425**,** 188-91.

STEVNSNER, T., MUFTUOGLU, M., AAMANN, M. D. & BOHR, V. A. 2008. The role of Cockayne Syndrome group B (CSB) protein in base excision repair and aging. *Mech Ageing Dev,* 129**,** 441-8.

STEVNSNER, T., NYAGA, S., DE SOUZA-PINTO, N. C., VAN DER HORST, G. T. J., GORGELS, T. G. M. F., HOGUE, B. A., THORSLUND, T. & BOHR, V. A. 2002. Mitochondrial repair of 8-oxoguanine is deficient in Cockayne syndrome group B. *Oncogene,* 21**,** 8675-82.

STEWART, G. S., PANIER, S., TOWNSEND, K., AL-HAKIM, A. K., KOLAS, N. K., MILLER, E. S., NAKADA, S., YLANKO, J., OLIVARIUS, S., MENDEZ, M., OLDREIVE, C., WILDENHAIN, J., TAGLIAFERRO, A., PELLETIER, L., TAUBENHEIM, N., DURANDY, A., BYRD, P. J., STANKOVIC, T., TAYLOR, A. M. & DUROCHER, D. 2009. The RIDDLE syndrome protein mediates a ubiquitin-dependent signaling cascade at sites of DNA damage. *Cell,* 136**,** 420-34.

STRUMBERG, D., PILON, A. A., SMITH, M., HICKEY, R., MALKAS, L. & POMMIER, Y. 2000. Conversion of topoisomerase I cleavage complexes on the leading strand of ribosomal DNA into 5'-phosphorylated DNA double-strand breaks by replication runoff. *Molecular and Cellular Biology,* 20**,** 3977-87.

STURTZ, L. A., DIEKERT, K., JENSEN, L. T., LILL, R. & CULOTTA, V. C. 2001. A fraction of yeast Cu,Zn-superoxide dismutase and its metallochaperone, CCS, localize to the intermembrane space of mitochondria. A physiological role for SOD1 in guarding against mitochondrial oxidative damage. *J Biol Chem,* 276**,** 38084-9.

STURZENEGGER, A., BURDOVA, K., KANAGARAJ, R., LEVIKOVA, M., PINTO, C., CEJKA, P. & JANSCAK, P. 2014. DNA2 cooperates with the WRN and BLM RecQ helicases to mediate long-range DNA end resection in human cells. *J Biol Chem,* 289**,** 27314-26.

SUGASAWA, K., NG, J. M., MASUTANI, C., IWAI, S., VAN DER SPEK, P. J., EKER, A. P., HANAOKA, F., BOOTSMA, D. & HOEIJMAKERS, J. H. 1998. Xeroderma pigmentosum group C protein complex is the initiator of global genome nucleotide excision repair. *Molecular cell,* 2**,** 223-32.

SUGIOKA, K., NAKANO, M., TOTSUNE-NAKANO, H., MINAKAMI, H., TERO-KUBOTA, S. & IKEGAMI, Y. 1988. Mechanism of O2- generation in reduction and oxidation cycle of ubiquinones in a model of mitochondrial electron transport systems. *Biochimica et biophysica acta,* 936**,** 377-85.

SUH, D., WILSON, D. M. & POVIRK, L. F. 1997. 3 ′ -Phosphodiesterase activity of human apurinic / apyrimidinic endonuclease at DNA double-strand break ends. *Nucleic Acids Res.,* 25**,** 2495-500.

SUN, B., LATHAM, K. A., DODSON, M. L. & LLOYD, R. S. 1995. Studies on the catalytic mechanism of five DNA glycosylases: Probing for enzyme-DNA imino intermediates. *Journal of Biological Chemistry,* 270**,** 19501-08.

SUNG, P. & KLEIN, H. 2006. Mechanism of homologous recombination: mediators and helicases take on regulatory functions. *Nat Rev Mol Cell Biol,* 7**,** 739-50.

SUSKI, C. & MARIANS, K. J. 2008. Resolution of Converging Replication Forks by RecQ and Topoisomerase III. *Molecular Cell,* 30**,** 779-89.

SUWA, A., HIRAKATA, M., TAKEDA, Y., JESCH, S. A., MIMORI, T. & HARDIN, J. A. 1994. DNA-dependent protein kinase (Ku protein-p350 complex) assembles on double-stranded DNA. *Proceedings of the National Academy of Sciences of the United States of America,* 91**,** 6904-08.

SVENDSEN, J. M., SMOGORZEWSKA, A., SOWA, M. E., O'CONNELL, B. C., GYGI, S. P., ELLEDGE, S. J. & HARPER, J. W. 2009. Mammalian BTBD12/SLX4 assembles a Holliday junction resolvase and is required for DNA repair. *Cell,* 138**,** 63-77.

SY, S. M., HUEN, M. S. & CHEN, J. 2009. PALB2 is an integral component of the BRCA complex required for homologous recombination repair. *Proc Natl Acad Sci U S A,* 106**,** 7155-60.

SYKORA, P., WILSON, D. M., 3RD & BOHR, V. A. 2012. Repair of persistent strand breaks in the mitochondrial genome. *Mech Ageing Dev,* 133**,** 169-75.

SYMINGTON, L. S. & GAUTIER, J. 2011. Double-Strand Break End Resection and Repair Pathway Choice. *Annual Review of Genetics,* 45**,** 247-71.

TADA, K., KOBAYASHI, M., TAKIUCHI, Y., IWAI, F., SAKAMOTO, T., NAGATA, K., SHINOHARA, M., IO, K., SHIRAKAWA, K., HISHIZAWA, M., SHINDO, K., KADOWAKI, N., HIROTA, K., YAMAMOTO, J., IWAI, S., SASANUMA, H., TAKEDA, S. & TAKAORI-KONDO, A. 2015. Abacavir, an anti–HIV-1 drug, targets TDP1-deficient adult T cell leukemia. *Science Advances,* 1**,** e140020.

TAKAHATA, C., MASUDA, Y., TAKEDACHI, A., TANAKA, K., IWAI, S. & KURAOKA, I. 2015. Repair synthesis step involving ERCC1-XPF participates in DNA repair of the Top1-DNA damage complex. *Carcinogenesis,* 36**,** 841-51.

TAKAMATSU, C., UMEDA, S., OHSATO, T., OHNO, T., ABE, Y., FUKUOH, A., SHINAGAWA, H., HAMASAKI, N. & KANG, D. 2002. Regulation of mitochondrial D-loops by transcription factor A and single-stranded DNA-binding protein. *EMBO reports,* 3**,** 451-6.

TAKAO, M., KANNO, S. I., KOBAYASHI, K., ZHANG, Q. M., YONEI, S., VAN DER HORST, G. T. J. & YASUI, A. 2002. A back-up glycosylase in Nth1 knock-out mice is a functional Nei (endonuclease VIII) homologue. *Journal of Biological Chemistry,* 277**,** 42205-13.

TAKASHIMA, H., BOERKOEL, C. F., JOHN, J., SAIFI, G. M., SALIH, M. A., ARMSTRONG, D., MAO, Y., QUIOCHO, F. A., ROA, B. B., NAKAGAWA, M., STOCKTON, D. W. & LUPSKI, J. R. 2002. Mutation of TDP1, encoding a topoisomerase I-dependent DNA damage repair enzyme, in spinocerebellar ataxia with axonal neuropathy. *Nat Genet,* 32**,** 267-72.

TAN, W., NANICHE, N., BOGUSH, A., PEDRINI, S., TROTTI, D. & PASINELLI, P. 2013. Small peptides against the mutant SOD1/Bcl-2 toxic mitochondrial complex restore mitochondrial function and cell viability in mutant SOD1-mediated ALS. *The Journal of neuroscience : the official journal of the Society for Neuroscience,* 33**,** 11588-98.

TANIGUCHI, T., GARCIA-HIGUERA, I., XU, B., ANDREASSEN, P. R., GREGORY, R. C., KIM, S. T., LANE, W. S., KASTAN, M. B. & D'ANDREA, A. D. 2002. Convergence of the fanconi anemia and ataxia telangiectasia signaling pathways. *Cell,* 109**,** 459-72.

TAUCHI, H., MATSUURA, S., KOBAYASHI, J., SAKAMOTO, S. & KOMATSU, K. 2002. Nijmegen breakage syndrome gene, NBS1, and molecular links to factors for genome stability. *Oncogene,* 21**,** 8967-80.

TEO, S. H. & JACKSON, S. P. 1997. Identification of saccharomyces cerevisiae DNA ligase IV: Involvement in DNA double-strand break repair. *EMBO Journal,* 16**,** 4788-95.

TERZOUDI, G. I., SINGH, S. K., PANTELIAS, G. E. & ILIAKIS, G. 2008. Premature chromosome condensation reveals DNA-PK independent pathways of chromosome break repair. *International Journal of Oncology,* 33**,** 871-79.

THOMAS, H. D., CALABRESE, C. R., BATEY, M. A., CANAN, S., HOSTOMSKY, Z., KYLE, S., MAEGLEY, K. A., NEWELL, D. R., SKALITZKY, D., WANG, L. Z., WEBBER, S. E. & CURTIN, N. J. 2007. Preclinical selection of a novel poly(ADP-ribose) polymerase inhibitor for clinical trial. *Mol Cancer Ther,* 6**,** 945-56.

THORSLUND, T., MCILWRAITH, M. J., COMPTON, S. A., LEKOMTSEV, S., PETRONCZKI, M., GRIFFITH, J. D. & WEST, S. C. 2010. The breast cancer tumor suppressor BRCA2 promotes the specific targeting of RAD51 to single-stranded DNA. *Nat Struct Mol Biol,* 17**,** 1263-65.

THORSLUND, T., VON KOBBE, C., HARRIGAN, J. A., INDIG, F. E., CHRISTIANSEN, M., STEVNSNER, T. & BOHR, V. A. 2005. Cooperation of the Cockayne Syndrome Group B Protein and Poly(ADP-Ribose) Polymerase 1 in the Response to Oxidative Stress. *MOLECULAR AND CELLULAR BIOLOGY,* 25**,** 7625-36.

THUITA, J. K., WANG, M. Z., KAGIRA, J. M., DENTON, C. L., PAINE, M. F., MDACHI, R. E., MURILLA, G. A., CHING, S., BOYKIN, D. W., TIDWELL, R. R., HALL, J. E. & BRUN, R. 2012. Pharmacology of DB844, an orally active aza analogue of pafuramidine, in a monkey model of second stage human African trypanosomiasis. *PLoS Negl Trop Dis,* 6**,** e1734-e34.

TOLEDO, L. I., MURGA, M., GUTIERREZ-MARTINEZ, P., SORIA, R. & FERNANDEZ-CAPETILLO, O. 2008. ATR signaling can drive cells into senescence in the absence of DNA breaks. *Genes Dev,* 22**,** 297-302.

TOMKINSON, A. E., VIJAYAKUMAR, S., PASCAL, J. M. & ELLENBERGER, T. 2006. DNA ligases: structure, reaction mechanism, and function. *Chem. Rev.,* 106**,** 687-99.

TORNALETTI, S. 2005. Transcription arrest at DNA damage sites. *Fundamental and Molecular Mechanisms of Mutagenesis,* 577**,** 131-45.

TROTTER, K. W., KING, H. A. & ARCHER, T. K. 2015. Glucocorticoid Receptor Transcriptional Activation via the BRG1-Dependent Recruitment of TOP2β and Ku70/86. *Molecular and cellular biology,* 35**,** 2799-817.

TSANG, C. K., LIU, Y., THOMAS, J., ZHANG, Y. & ZHENG, X. F. 2014. Superoxide dismutase 1 acts as a nuclear transcription factor to regulate oxidative stress resistance. *Nat Commun,* 5**,** 3446.

TSE, A. N. & SCHWARTZ, G. K. 2004. Potentiation of cytotoxicity of topoisomerase i poison by concurrent and sequential treatment with the checkpoint inhibitor UCN-01 involves disparate mechanisms resulting in either p53-independent clonogenic suppression or p53-dependent mitotic catastroph. *Cancer Res,* 64**,** 6635-44.

TUDURI, S., CRABBE, L., CONTI, C., TOURRIERE, H., HOLTGREVE-GREZ, H., JAUCH, A., PANTESCO, V., DE VOS, J., THOMAS, A., THEILLET, C., POMMIER, Y., TAZI, J., COQUELLE, A. & PASERO, P. 2009. Topoisomerase I suppresses genomic instability by preventing interference between replication and transcription. *Nat Cell Biol,* 11**,** 1315-24.

TURRENS, J. F. & BOVERIS, A. 1980. Generation of superoxide anion by the NADH dehydrogenase of bovine heart mitochondria. *Biochemical Journal,* 191**,** 421-27.

TYYNISMAA, H., SEMBONGI, H., BOKORI-BROWN, M., GRANYCOME, C., ASHLEY, N., POULTON, J., JALANKO, A., SPELBRINK, J. N., HOLT, I. J. & SUOMALAINEN, A. 2004. Twinkle helicase is essential for mtDNA maintenance and regulates mtDNA copy number. *Human Molecular Genetics,* 13**,** 3219-27.

UCHIMURA, A., HIDAKA, Y., HIRABAYASHI, T., HIRABAYASHI, M. & YAGI, T. 2009. DNA polymerase delta is required for early mammalian embryogenesis. *PloS one,* 4**,** e4184-e84.

UEMATSU, N., WETERINGS, E., YANO, K. I., MOROTOMI-YANO, K., JAKOB, B., TAUCHER-SCHOLZ, G., MARI, P. O., VAN GENT, D. C., CHEN, B. P. C. & CHEN, D. J. 2007. Autophosphorylation of DNA-PKCS regulates its dynamics at DNA double-strand breaks. *Journal of Cell Biology,* 177**,** 219-29.

UEMURA, T. & YANAGIDA, M. 1986. Mitotic spindle pulls but fails to separate chromosomes in type II DNA topoisomerase mutants: uncoordinated mitosis. *The EMBO journal,* 5**,** 1003-10.

UMAR, A., BUERMEYER, A. B., SIMON, J. A., THOMAS, D. C., CLARK, A. B., LISKAY, R. M. & KUNKEL, T. A. 1996. Requirement for PCNA in DNA mismatch repair at a step preceding DNA resynthesis. *Cell,* 87**,** 65-73.

UNSAL-KAÇMAZ, K., MAKHOV, A. M., GRIFFITH, J. D. & SANCAR, A. 2002. Preferential binding of ATR protein to UV-damaged DNA. *Proceedings of the National Academy of Sciences of the United States of America,* 99**,** 6673-78.

UNSAL-KAÇMAZ, K. & SANCAR, A. 2004. Quaternary structure of ATR and effects of ATRIP and replication protein A on its DNA binding and kinase activities. *Molecular and cellular biology,* 24**,** 1292-300.

UZIEL, T., LERENTHAL, Y., MOYAL, L., ANDEGEKO, Y., MITTELMAN, L. & SHILOH, Y. 2003. Requirement of the MRN complex for ATM activation by DNA damage. *EMBO Journal,* 22**,** 5612-21.

VALENTINE, J. S., DOUCETTE, P. A. & ZITTIN POTTER, S. 2005. Copper-zinc superoxide dismutase and amyotrophic lateral sclerosis. *Annu Rev Biochem,* 74**,** 563-93.

VAN CRIEKINGE, W. & BEYAERT, R. 1999. Yeast Two-Hybrid: State of the Art. *Biological procedures online,* 2**,** 1-38.

VAN GOOL, A. J., CITTERIO, E., RADEMAKERS, S., VAN OS, R., VERMEULEN, W., CONSTANTINOU, A., EGLY, J. M., BOOTSMA, D. & HOEIJMAKERS, J. H. J. 1997. The Cockayne syndrome B protein, involved in transcription-coupled DNA repair, resides in an RNA polymerase II-containing complex. *EMBO Journal,* 16**,** 5955-65.

VAN HEEMST, D., DEN REIJER, P. M. & WESTENDORP, R. G. J. 2007. Ageing or cancer: A review. On the role of caretakers and gatekeepers. *European Journal of Cancer,* 43**,** 2144-52.

VANCE, J. R. & WILSON, T. E. 2002. Yeast Tdp1 and Rad1-Rad10 function as redundant pathways for repairing Top1 replicative damage. *Proceedings of the National Academy of Sciences of the United States of America,* 99**,** 13669-74.

VENEMA, J., MULLENDERS, L. H., NATARAJAN, A. T., VAN ZEELAND, A. A. & MAYNE, L. V. 1990. The genetic defect in Cockayne syndrome is associated with a defect in repair of UV-induced DNA damage in transcriptionally active DNA. *Proceedings of the National Academy of Sciences of the United States of America,* 87**,** 4707-11.

VERMEULEN, K., VAN BOCKSTAELE, D. R. & BERNEMAN, Z. N. 2003. The cell cycle: A review of regulation, deregulation and therapeutic targets in cancer. 10.1046/j.1365-2184.2003.00266.x.

VERMEULEN, W., VAN VUUREN, A. J., CHIPOULET, M., SCHAEFFER, L., APPELDOORN, E., WEEDA, G., JASPERS, N. G. J., PRIESTLEY, A., ARLETT, C. F., LEHMANN, A. R., STEFANINI, M., MEZZINA, M., SARASIN, A., BOOTSMA, D., EGLY, J. M. & HOEIJMAKERS, J. H. J. 1994. Three unusual repair deficiencies associated with transcription factor BTF2(TFIIH): Evidence for the existence of a transcription syndrome. *Cold Spring Harbor Symposia on Quantitative Biology,* 59**,** 317-29.

VERTEGAAL, A. C., ANDERSEN, J. S., OGG, S. C., HAY, R. T., MANN, M. & LAMOND, A. I. 2006. Distinct and overlapping sets of SUMO-1 and SUMO-2 target proteins revealed by quantitative proteomics. *Mol Cell Proteomics,* 5**,** 2298-310.

VIJAYVERGIYA, C., BEAL, M. F., BUCK, J. & MANFREDI, G. 2005. Mutant superoxide dismutase 1 forms aggregates in the brain mitochondrial matrix of amyotrophic lateral sclerosis mice. *The Journal of neuroscience : the official journal of the Society for Neuroscience,* 25**,** 2463-70.

VREDENBURGH, J. J., DESJARDINS, A., REARDON, D. A. & FRIEDMAN, H. S. 2009. Experience with irinotecan for the treatment of malignant glioma. *Neuro Oncol,* 11**,** 80-91.

WAGA, S., HANNON, G. J., BEACH, D. & STILLMAN, B. 1994. The p21 inhibitor of cyclin-dependent kinases controls DNA replication by interaction with PCNA. *Nature,* 369**,** 574-8.

WAKEMAN, T. P., KIM, W.-J., CALLENS, S., CHIU, A., BROWN, K. D. & XU, B. 2004. The ATM-SMC1 pathway is essential for activation of the chromium[VI]-induced S-phase checkpoint. *Mutation research,* 554**,** 241-51.

WALKER, J. R., CORPINA, R. A. & GOLDBERG, J. 2001. Structure of the Ku heterodimer bound to DNA and its implications for double-strand break repair. *Nature,* 412**,** 607-14.

WALKER, S., MEISENBERG, C., BIBBY, R. A., ASKWITH, T., WILLIAMS, G., RININSLAND, F. H., PEARL, L. H., OLIVER, A. W., EL-KHAMISY, S., WARD, S. & ATACK, J. R. 2014. Development of an oligonucleotide-based fluorescence assay for the identification of tyrosyl-DNA phosphodiesterase 1 (TDP1) inhibitors. *Analytical biochemistry*, 454, 17-22.

WALL, M. E. & WANI, M. C. 1995. Camptothecin and taxol: discovery to clinic--thirteenth Bruce F. Cain Memorial Award Lecture. *Cancer Res,* 55**,** 753-60.

WANG, H., PERRAULT, A. R., TAKEDA, Y., QIN, W., WANG, H. & ILIAKIS, G. 2003. Biochemical evidence for Ku-independent backup pathways of NHEJ. *Nucleic Acids Research,* 31**,** 5377-88.

WANG, H., ROSIDI, B., PERRAULT, R., WANG, M., ZHANG, L., WINDHOFER, F. & ILIAKIS, G. 2005. DNA ligase III as a candidate component of backup pathways of nonhomologous end joining. *Cancer Research,* 65**,** 4020-30.

WANG, J., FARR, G. W., HALL, D. H., LI, F., FURTAK, K., DREIER, L. & HORWICH, A. L. 2009. An ALS-linked mutant SOD1 produces a locomotor defect associated with aggregation and synaptic dysfunction when expressed in neurons of Caenorhabditis elegans. *PLoS Genetics,* 5**,** e1000350.

WANG, J. C. 1971. Interaction between DNA and an Escherichia coli protein omega. 10.1016/0022-2836(71)90334-2.

WANG, J. C. 2002. Cellular roles of DNA topoisomerases: a molecular perspective. *Nature reviews. Molecular cell biology,* 3**,** 430-40.

WANG, M., WU, W., WU, W., ROSIDI, B., ZHANG, L., WANG, H. & ILIAKIS, G. 2006. PARP-1 and Ku compete for repair of DNA double strand breaks by distinct NHEJ pathways. *Nucleic Acids Research,* 34**,** 6170-82.

WANG, X. W., ZHAN, Q., COURSEN, J. D., KHAN, M. A., KONTNY, H. U., YU, L., HOLLANDER, M. C., O'CONNOR, P. M., FORNACE, A. J. & HARRIS, C. C. 1999. GADD45 induction of a G2/M cell cycle checkpoint. *Proceedings of the National Academy of Sciences of the United States of America,* 96**,** 3706-11.

WANG, Y., LEUNG, J. W., JIANG, Y., LOWERY, M. G., DO, H., VASQUEZ, K. M., CHEN, J., WANG, W. & LI, L. 2013. FANCM and FAAP24 maintain genome stability via cooperative as well as unique functions. *Mol Cell,* 49**,** 997-1009.

WANG, Y. & QIN, J. 2003. MSH2 and ATR form a signaling module and regulate two branches of the damage response to DNA methylation. *Proceedings of the National Academy of Sciences of the United States of America,* 100**,** 15387-92.

WANROOIJ, S., FUSTÉ, J. M., FARGE, G., SHI, Y., GUSTAFSSON, C. M. & FALKENBERG, M. 2008. Human mitochondrial RNA polymerase primes lagging-strand DNA synthesis in vitro. *Proceedings of the National Academy of Sciences of the United States of America,* 105**,** 11122-27.

WARD, J. F. 1990. The yield of DNA double-strand breaks produced intracellularly by ionizing radiation: a review. *International Journal of Radiation Biology,* 57**,** 1141-50.

WARD, J. F. 1998. Nature of Lesions Formed by Ionizing Radiation. 10.1007/978-1-59259-455-9_5**,** 65-84.

WARITA, H., ITOYAMA, Y. & ABE, K. 1999. Selective impairment of fast anterograde axonal transport in the peripheral nerves of asymptomatic transgenic mice with a G93A mutant SOD1 gene. *Brain Res,* 819**,** 120-31.

WATERS, L. S., MINESINGER, B. K., WILTROUT, M. E., D'SOUZA, S., WOODRUFF, R. V. & WALKER, G. C. 2009. Eukaryotic translesion polymerases and their roles and regulation in DNA damage tolerance. *Microbiol Mol Biol Rev,* 73**,** 134-54.

WATERS, T. R., GALLINARI, P., JIRICNYL, J. & SWANN, P. F. 1999. Human thymine DNA glycosylase binds to apurinic sites in DNA but is displaced by human apurinic endonuclease 1. *Journal of Biological Chemistry,* 274**,** 67-74.

WEAVER, A. N. & YANG, E. S. 2013. Beyond DNA Repair: Additional Functions of PARP-1 in Cancer. *Frontiers in oncology,* 3**,** 290-90.

WEBER, A. R., SCHUERMANN, D. & SCHAR, P. 2014. Versatile recombinant SUMOylation system for the production of SUMO-modified protein. *PLoS One,* 9**,** e102157.

WEBER, S. 2005. Light-driven enzymatic catalysis of DNA repair: A review of recent biophysical studies on photolyase. *Biochemica et Biophysica Acta - Bioenergetics,* 1707**,** 1-23.

WECHSLER, T., NEWMAN, S. & WEST, S. C. 2011. Aberrant chromosome morphology in human cells defective for Holliday junction resolution. *Nature,* 471**,** 642-6.

WEISBERG, S. J., LYAKHOVETSKY, R., WERDIGER, A. C., GITLER, A. D., SOEN, Y. & KAGANOVICH, D. 2012. Compartmentalization of superoxide dismutase 1 (SOD1G93A) aggregates determines their toxicity. *Proceedings of the National Academy of Sciences,* 109**,** 15811-16.

WEISIGER, R. A. & FRIDOVICH, I. 1973. Mitochondrial superoxide simutase. Site of synthesis and intramitochondrial localization. *J Biol Chem,* 248**,** 4793-6.

WEISS, R. S., MATSUOKA, S., ELLEDGE, S. J. & LEDER, P. 2002. Hus1 acts upstream of Chk1 in a mammalian DNA damage response pathway. *Current Biology,* 12**,** 73-77.

WELLS, O. S. 2014. *Cellular and biochemical analyses of TDP1 mediated chromosomal break repair.* DPhil Biochemistry, University of Sussex.

WESTERMANN, B. 2008. Molecular machinery of mitochondrial fusion and fission. 10.1074/jbc.R800011200.

WIEDAU-PAZOS, M., GOTO, J. J., RABIZADEH, S., GRALLA, E. B., ROE, J. A., LEE, M. K., VALENTINE, J. S. & BREDESEN, D. E. 1996. Altered reactivity of superoxide dismutase in familial amyotrophic lateral sclerosis. *Science,* 271**,** 515-8.

WIEDERHOLD, L., LEPPARD, J. B., KEDAR, P., KARIMI-BUSHERI, F., RASOULI-NIA, A., WEINFELD, M., TOMKINSON, A. E., IZUMI, T., PRASAD, R., WILSON, S. H., MITRA, S. & HAZRA, T. K. 2004. AP endonuclease-independent DNA base excision repair in human cells. *Molecular Cell,* 15**,** 209-20.

WILLIAMSON, L. M. & LEES-MILLER, S. P. 2011. Estrogen receptor alpha-mediated transcription induces cell cycle-dependent DNA double-strand breaks. *Carcinogenesis,* 32**,** 279-85.

WILSON, D. M. & BOHR, V. A. 2007. The mechanics of base excision repair, and its relationship to aging and disease. *DNA Repair,* 6**,** 544-59.

WILSON, T. E., GRAWUNDER, U. & LIEBER, M. R. 1997. Yeast DNA ligase IV mediates non-homologous DNA end joining. *Nature,* 388**,** 495-98.

WILSON, T. M., CHEN, A. D. & HSIEH, T. 2000. Cloning and characterization of Drosophila topoisomerase IIIbeta. Relaxation of hypernegatively supercoiled DNA. *The Journal of biological chemistry,* 275**,** 1533-40.

WONG, A. K., PERO, R., ORMONDE, P. A., TAVTIGIAN, S. V. & BARTEL, P. L. 1997. RAD51 interacts with the evolutionarily conserved BRC motifs in the human breast cancer susceptibility gene brca2. *J Biol Chem,* 272**,** 31941-4.

WONG, H. K., MUFTUOGLU, M., BECK, G., IMAM, S. Z., BOHR, V. A. & WILSON, D. M. 2007. Cockayne syndrome B protein stimulates apurinic endonuclease 1 activity and protects against agents that introduce base excision repair intermediates. *Nucleic Acids Research,* 35**,** 4103-13.

WONG, R. H. F., CHANG, I., HUDAK, C. S. S., HYUN, S., KWAN, H. Y. & SUL, H. S. 2009. A Role of DNA-PK for the Metabolic Gene Regulation in Response to Insulin. *Cell,* 136**,** 1056-72.

WOOD, R. D. 1999. DNA damage recognition during nucleotide excision repair in mammalian cells. *Biochimie,* 81**,** 39-44.

WRIGHT, J. A., KEEGAN, K. S., HERENDEEN, D. R., BENTLEY, N. J., CARR, A. M., HOEKSTRA, M. F. & CONCANNON, P. 1998. Protein kinase mutants of human ATR increase sensitivity to UV and ionizing radiation and abrogate cell cycle checkpoint control. *Proceedings of the National Academy of Sciences of the United States of America,* 95**,** 7445-50.

WRIGHT, W. D. & HEYER, W. D. 2014. Rad54 functions as a heteroduplex DNA pump modulated by its DNA substrates and Rad51 during D loop formation. *Mol Cell,* 53**,** 420-32.

WU, J. & LIU, L. F. 1997. Processing of topoisomerase I cleavable complexes into DNA damage by transcription. *Nucleic Acids Research,* 25**,** 4181-86.

WU, L., BACHRATI, C. Z., OU, J., XU, C., YIN, J., CHANG, M., WANG, W., LI, L., BROWN, G. W. & HICKSON, I. D. 2006. BLAP75/RMI1 promotes the BLM-dependent dissolution of homologous recombination intermediates. *Proceedings of the National Academy of Sciences of the United States of America,* 103**,** 4068-73.

WU, L. & HICKSON, I. D. 2003. The Bloom's syndrome helicase suppresses crossing over during homologous recombination. *Nature,* 426**,** 870-74.

WU, X., RANGANATHAN, V., WEISMAN, D. S., HEINE, W. F., CICCONE, D. N., O'NEILL, T. B., CRICK, K. E., PIERCE, K. A., LANE, W. S., RATHBUN, G., LIVINGSTON, D. M. & WEAVER, D. T. 2000. ATM phosphorylation of Nijmegen breakage syndrome protein is required in a DNA damage response. *Nature,* 405**,** 477-82.

XIE, A., KWOK, A. & SCULLY, R. 2009. Role of mammalian Mre11 in classical and alternative nonhomologous end joining. *Nature structural & molecular biology,* 16**,** 814-8.

XIONG, Y., HANNON, G. J., ZHANG, H., CASSO, D., KOBAYASHI, R. & BEACH, D. 1993. p21 is a universal inhibitor of cyclin kinases. *Nature,* 366**,** 701-4.

XU, B. O., KIM, S.-T. & KASTAN, M. B. 2001. Involvement of Brca1 in S-Phase and G 2 -Phase Checkpoints after Ionizing Irradiation Involvement of Brca1 in S-Phase and G 2 -Phase Checkpoints after Ionizing Irradiation. *Molecular and cellular biology,* 21**,** 3445-50.

XU, J., WATKINS, T., REDDY, A., REDDY, E. S. P. & RAO, V. N. 2009. A novel mechanism whereby BRCA1/1a/1b fine tunes the dynamic complex interplay between SUMO-dependent/independent activities of Ubc9 on E2-induced ERalpha activation/repression and degradation in breast cancer cells. *International journal of oncology,* 34**,** 939-49.

XU, Y. & HER, C. 2015. Inhibition of Topoisomerase (DNA) I (TOP1): DNA Damage Repair and Anticancer Therapy. *Biomolecules,* 5**,** 1652-70.

XU, Z., ZAN, H., PONE, E. J., MAI, T. & CASALI, P. 2012. Immunoglobulin class-switch DNA recombination: induction, targeting and beyond. *Nat Rev Immunol,* 12**,** 517-31.

YAKES, F. M. & VAN HOUTEN, B. 1997. Mitochondrial DNA damage is more extensive and persists longer than nuclear DNA damage in human cells following oxidative stress. *Proceedings of the National Academy of Sciences of the United States of America,* 94**,** 514-9.

YANG, M., HSU, C. T., TING, C. Y., LIU, L. F. & HWANG, J. 2006. Assembly of a polymeric chain of SUMO1 on human topoisomerase I in vitro. *J Biol Chem,* 281**,** 8264-74.

YANG, S. W., BURGIN, A. B., HUIZENGA, B. N., ROBERTSON, C. A., YAO, K. C. & NASH, H. A. 1996. A eukaryotic enzyme that can disjoin dead-end covalent complexes between DNA and type I topoisomerases. *Proceedings of the National Academy of Sciences of the United States of America,* 93**,** 11534-9.

YARDEN, R. I., PARDO-REOYO, S., SGAGIAS, M., COWAN, K. H. & BRODY, L. C. 2002. BRCA1 regulates the G2/M checkpoint by activating Chk1 kinase upon DNA damage. *Nature genetics,* 30**,** 285-9.

YAZDI, P. T., WANG, Y., ZHAO, S., PATEL, N., LEE, E. Y. H. P. & QIN, J. 2002. SMC1 is a downstream effector in the ATM/NBS1 branch of the human S-phase checkpoint. *Genes & development,* 16**,** 571-82.

YE, Q., HU, Y. F., ZHONG, H., NYE, A. C., BELMONT, A. S. & LI, R. 2001. BRCA1-induced large-scale chromatin unfolding and allele-specific effects of cancer-predisposing mutations. *The Journal of cell biology,* 155**,** 911-21.

YEH, E. T. 2009. SUMOylation and De-SUMOylation: wrestling with life's processes. *J Biol Chem,* 284**,** 8223-7.

YEO, A. J., BECHEREL, O. J., LUFF, J. E., CULLEN, J. K., WONGSURAWAT, T., JENJAROENPOON, P., KUZNETSOV, V. A., MCKINNON, P. J. & LAVIN, M. F. 2014. R-Loops in proliferating cells but not in the brain: Implications for AOA2 and other autosomal recessive ataxias. *PLoS ONE,* 9**,** e105258.

YOO, S. & DYNAN, W. S. 1999. Geometry of a complex formed by double strand break repair proteins at a single DNA end: recruitment of DNA-PKcs induces inward translocation of Ku protein. *Nucleic acids research,* 27**,** 4679-86.

YORIMITSU, T., NAIR, U., YANG, Z. & KLIONSKY, D. J. 2006. Endoplasmic reticulum stress triggers autophagy. *Journal of Biological Chemistry,* 281**,** 30299-304.

YOU, Z., CHAHWAN, C., BAILIS, J., HUNTER, T. & RUSSELL, P. 2005. ATM activation and its recruitment to damaged DNA require binding to the C terminus of Nbs1. *Mol Cell Biol,* 25**,** 5363-79.

YU, A., FAN, H. Y., LIAO, D., BAILEY, A. D. & WEINER, A. M. 2000. Activation of p53 or loss of the Cockayne syndrome group B repair protein causes metaphase fragility of human U1, U2, and 5S genes. *Molecular Cell,* 5**,** 801-10.

YU, S.-L., LEE, S.-K., JOHNSON, R. E., PRAKASH, L. & PRAKASH, S. 2003. The stalling of transcription at abasic sites is highly mutagenic. *Molecular and cellular biology,* 23**,** 382-88.

YUN, M. H. & HIOM, K. 2009. CtIP-BRCA1 modulates the choice of DNA double-strand-break repair pathway throughout the cell cycle. *Nature,* 459**,** 460-3.

ZAHRADKA, P. & EBISUZAKI, K. 1982. A shuttle mechanism for DNA-protein interactions. The regulation of poly(ADP-ribose) polymerase. *European Journal of Biochemistry,* 127**,** 579-85.

ZAJA, R., MIKOČ, A., BARKAUSKAITE, E. & AHEL, I. 2012. Molecular Insights into Poly(ADP-ribose) Recognition and Processing. *Biomolecules,* 3**,** 1-17.

ZANDER, S. A., KERSBERGEN, A., VAN DER BURG, E., DE WATER, N., VAN TELLINGEN, O., GUNNARSDOTTIR, S., JASPERS, J. E., PAJIC, M., NYGREN, A. O., JONKERS, J., BORST, P. & ROTTENBERG, S. 2010. Sensitivity and acquired resistance of BRCA1;p53-deficient mouse mammary tumors to the topoisomerase I inhibitor topotecan. *Cancer Res,* 70**,** 1700-10.

ZHAN, Q., ANTINORE, M. J., WANG, X. W., CARRIER, F., SMITH, M. L., HARRIS, C. C. & FORNACE, A. J., JR. 1999. Association with Cdc2 and inhibition of Cdc2/Cyclin B1 kinase activity by the p53-regulated protein Gadd45. *Oncogene,* 18**,** 2892-900.

ZHANG, H., BARCELÓ, J. M., LEE, B., KOHLHAGEN, G., ZIMONJIC, D. B., POPESCU, N. C. & POMMIER, Y. 2001. Human mitochondrial topoisomerase I. *Proceedings of the National Academy of Sciences of the United States of America,* 98**,** 10608-13.

ZHANG, H., LIU, H., CHEN, Y., YANG, X., WANG, P., LIU, T., DENG, M., QIN, B., CORREIA, C., LEE, S., KIM, J., SPARKS, M., NAIR, A. A., EVANS, D. L., KALARI, K. R., ZHANG, P., WANG, L., YOU, Z., KAUFMANN, S. H., LOU, Z. & PEI, H. 2016. A cell cycle-dependent BRCA1-UHRF1 cascade regulates DNA double-strand break repair pathway choice. *Nat Commun,* 7**,** 10201.

ZHANG, H., MENG, L. H. & POMMIER, Y. 2007. Mitochondrial topoisomerases and alternative splicing of the human TOP1mt gene. *Biochimie,* 89**,** 474-81.

ZHANG, H., MENG, L. H., ZIMONJIC, D. B., POPESCU, N. C. & POMMIER, Y. 2004a. Thirteen-exon-motif signature for vertebrate nuclear and mitochondrial type IB topoisomerases. *Nucleic Acids Research,* 32**,** 2087-92.

ZHANG, H. & POMMIER, Y. 2008. Mitochondrial topoisomerase I sites in the regulatory D-loop region of mitochondrial DNA. *Biochemistry,* 47**,** 11196-203.

ZHANG, H., ZHANG, Y.-W., YASUKAWA, T., DALLA ROSA, I., KHIATI, S. & POMMIER, Y. 2014. Increased negative supercoiling of mtDNA in TOP1mt knockout mice and presence of topoisomerases IIα and IIβ in vertebrate mitochondria. *Nucleic acids research,* 42**,** 7259-67.

ZHANG, H. F., TOMIDA, A., KOSHIMIZU, R., OGISO, Y., LEI, S. & TSURUO, T. 2004b. Cullin 3 promotes proteasomal degradation of the topoisomerase I-DNA covalent complex. *Cancer Res,* 64**,** 1114-21.

ZHANG, J., LIN, A., POWERS, J., LAM, M. P., LOTZ, C., LIEM, D., LAU, E., WANG, D., DENG, N., KORGE, P., ZONG, N. C., CAI, H., WEISS, J. & PING, P. 2012. Perspectives on: SGP symposium on mitochondrial physiology and medicine: mitochondrial proteome design: from molecular identity to pathophysiological regulation. *J Gen Physiol,* 139**,** 395-406.

ZHANG, Y. & JASIN, M. 2011. An essential role for CtIP in chromosomal translocation formation through an alternative end-joining pathway. *Nature structural & molecular biology,* 18**,** 80-4.

ZHANG, Y., YUAN, F., PRESNELL, S. R., TIAN, K., GAO, Y., TOMKINSON, A. E., GU, L. & LI, G. M. 2005. Reconstitution of 5???-directed human mismatch repair in a purified system. *Cell,* 122**,** 693-705.

ZHAO, H. & PIWNICA-WORMS, H. 2001. ATR-mediated checkpoint pathways regulate phosphorylation and activation of human Chk1. *Molecular and cellular biology,* 21**,** 4129-39.

ZHAO, H., WATKINS, J. L. & PIWNICA-WORMS, H. 2002. Disruption of the checkpoint kinase 1/cell division cycle 25A pathway abrogates ionizing radiation-induced S and G2 checkpoints. *Proceedings of the National Academy of Sciences of the United States of America,* 99**,** 14795-800.

ZHOU, B. B., CHATURVEDI, P., SPRING, K., SCOTT, S. P., JOHANSON, R. A., MISHRA, R., MATTERN, M. R., WINKLER, J. D. & KHANNA, K. K. 2000. Caffeine abolishes the mammalian G(2)/M DNA damage checkpoint by inhibiting ataxia-telangiectasia-mutated kinase activity. *The Journal of biological chemistry,* 275**,** 10342-8.

ZHOU, T., AKOPIANTS, K., MOHAPATRA, S., LIN, P.-S., VALERIE, K., RAMSDEN, D. A., LEES-MILLER, S. P. & POVIRK, L. F. 2009. Tyrosyl-DNA phosphodiesterase and the repair of 3'-phosphoglycolate-terminated DNA double-strand breaks. *DNA repair,* 8**,** 901-11.

ZHOU, T., LEE, J. W., TATAVARTHI, H., LUPSKI, J. R., VALERIE, K. & POVIRK, L. F. 2005. Deficiency in 3'-phosphoglycolate processing in human cells with a hereditary mutation in tyrosyl-DNA phosphodiesterase (TDP1). *Nucleic Acids Res,* 33**,** 289-97.

ZHU, W. & DUTTA, A. 2006. An ATR- and BRCA1-mediated Fanconi anemia pathway is required for activating the G2/M checkpoint and DNA damage repair upon rereplication. *Mol Cell Biol,* 26**,** 4601-11.

ZHU, Z., CHUNG, W. H., SHIM, E. Y., LEE, S. E. & IRA, G. 2008. Sgs1 helicase and two nucleases Dna2 and Exo1 resect DNA double-strand break ends. *Cell,* 134**,** 981-94.

ZHUANG, J., JIANG, G., WILLERS, H. & XIA, F. 2009. Exonuclease function of human Mre11 promotes deletional nonhomologous end joining. *Journal of Biological Chemistry,* 284**,** 30565-73.

ZIMMERMANN, M., LOTTERSBERGER, F., BUONOMO, S. B., SFEIR, A. & DE LANGE, T. 2013. 53BP1 regulates DSB repair using Rif1 to control 5' end resection. *Science,* 339**,** 700-4.

ZOPPOLI, G., DOUARRE, C., DALLA ROSA, I., LIU, H., REINHOLD, W. & POMMIER, Y. 2011. Coordinated regulation of mitochondrial topoisomerase IB with mitochondrial nuclear encoded genes and MYC. *Nucleic Acids Res,* 39**,** 6620-32.

ZOU, L., CORTEZ, D. & ELLEDGE, S. J. 2002. Regulation of ATR substrate selection by Rad17-dependent loading of Rad9 complexes onto chromatin. *Genes and Development,* 16**,** 198-208.

ZOU, L. & ELLEDGE, S. J. 2003. Sensing DNA damage through ATRIP recognition of RPA-ssDNA complexes. *Science (New York, N.Y.),* 300**,** 1542-48.

APPENDIX

List of publications:

Chiang, S.-C., Carroll, J., & El-Khamisy, S. F. 2010. TDP1 serine 81 promotes interaction with DNA ligase IIIα and facilitates cell survival following DNA damage. *Cell Cycle*, 9, 588-595. http://doi.org/10.4161/cc.9.3.10598

Hudson, J. J., Chiang, S. C., Wells, O. S., Rookyard, C., & El-Khamisy, S. 2012. SUMO modification of the neuroprotective protein TDP1 facilitates chromosomal single-strand break repair. *Nature Communications*, 3, 713-3. http://doi.org/10.1038/ncomms1739

Chiang, S-C, Meagher, M., Kassouf, N., Hafezparast, M., McKinnon, P., Haywood, R., El-Khamisy, S. 2017. Mitochondrial protein-linked DNA breaks perturb mitochondrial gene transcription and trigger free radical induced DNA damage. *Science Advances*, 3:e1602506. http://doi.org/10.1126/sciadv.1602506